frontiers | Research Topics

Deep brain stimulation think tank: Updates in neurotechnology and neuromodulation, volume III

Edited by
Michael S. Okun, James J. Giordano, Adolfo Ramirez-Zamora and Joshua K. Wong

Published in
Frontiers in Human Neuroscience

ISSN 1664-8714
ISBN 978-2-83251-307-1
DOI 10.3389/978-2-83251-307-1

About Frontiers

Frontiers is more than just an open access publisher of scholarly articles: it is a pioneering approach to the world of academia, radically improving the way scholarly research is managed. The grand vision of Frontiers is a world where all people have an equal opportunity to seek, share and generate knowledge. Frontiers provides immediate and permanent online open access to all its publications, but this alone is not enough to realize our grand goals.

Frontiers journal series

The Frontiers journal series is a multi-tier and interdisciplinary set of open-access, online journals, promising a paradigm shift from the current review, selection and dissemination processes in academic publishing. All Frontiers journals are driven by researchers for researchers; therefore, they constitute a service to the scholarly community. At the same time, the *Frontiers journal series* operates on a revolutionary invention, the tiered publishing system, initially addressing specific communities of scholars, and gradually climbing up to broader public understanding, thus serving the interests of the lay society, too.

Dedication to quality

Each Frontiers article is a landmark of the highest quality, thanks to genuinely collaborative interactions between authors and review editors, who include some of the world's best academicians. Research must be certified by peers before entering a stream of knowledge that may eventually reach the public - and shape society; therefore, Frontiers only applies the most rigorous and unbiased reviews. Frontiers revolutionizes research publishing by freely delivering the most outstanding research, evaluated with no bias from both the academic and social point of view. By applying the most advanced information technologies, Frontiers is catapulting scholarly publishing into a new generation.

What are Frontiers Research Topics?

Frontiers Research Topics are very popular trademarks of the *Frontiers journals series*: they are collections of at least ten articles, all centered on a particular subject. With their unique mix of varied contributions from Original Research to Review Articles, Frontiers Research Topics unify the most influential researchers, the latest key findings and historical advances in a hot research area.

Find out more on how to host your own Frontiers Research Topic or contribute to one as an author by contacting the Frontiers editorial office: frontiersin.org/about/contact

Deep brain stimulation think tank: Updates in neurotechnology and neuromodulation, volume III

Topic editors

Michael S. Okun — University of Florida, United States
James J. Giordano — Georgetown University, United States
Adolfo Ramirez-Zamora — University of Florida, United States
Joshua K. Wong — University of Florida, United States

Citation

Okun, M. S., Giordano, J. J., Ramirez-Zamora, A., Wong, J. K., eds. (2023). *Deep brain stimulation think tank: Updates in neurotechnology and neuromodulation, volume III*. Lausanne: Frontiers Media SA. doi: 10.3389/978-2-83251-307-1

Table of contents

frontiers in Human Neuroscience

ORIGINAL RESEARCH
published: 22 February 2022
doi: 10.3389/fnhum.2022.829198

Quantitative Analysis for the Delineation of the Subthalamic Nuclei on Three-Dimensional Stereotactic MRI Before Deep Brain Stimulation Surgery for Medication-Refractory Parkinson's Disease

*Chun-Yu Su[1,2], Alex Mun-Ching Wong[1,2,3], Chih-Chen Chang[1,2], Po-Hsun Tu[2,4], Chiung Chu Chen[2,5,6] and Chih-Hua Yeh[1,2]**

[1] Department of Medical Imaging and Intervention, Chang Gung Memorial Hospital, Linkou, Taiwan, [2] College of Medicine, Chang Gung University, Taoyuan, Taiwan, [3] Department of Diagnostic Radiology, Chang Gung Memorial Hospital, Keelung, Taiwan, [4] Department of Neurosurgery, Chang Gung Memorial Hospital, Linkou, Taiwan, [5] Department of Neurology, Chang Gung Memorial Hospital, Linkou, Taiwan, [6] Neuroscience Research Center, Chang Gung Memorial Hospital, Linkou, Taiwan

Delineation of the subthalamic nuclei (STN) on MRI is critical for deep brain stimulation (DBS) surgery in patients with Parkinson's disease (PD). We propose this retrospective cohort study for quantitative analysis of MR signal-to-noise ratio (SNR), contrast, and signal difference-to-noise ratio (SDNR) of the STN on pre-operative three-dimensional (3D) stereotactic MRI in patients with medication-refractory PD. Forty-five consecutive patients with medication-refractory PD who underwent STN-DBS surgery in our hospital from January 2018 to June 2021 were included in this study. All patients had whole-brain 3D MRI, including T2-weighted imaging (T2WI), T2-weighted fluid-attenuated inversion recovery (FLAIR), and susceptibility-weighted imaging (SWI), at 3.0 T scanner for stereotactic navigation. The signal intensities of the STN, corona radiata, and background noise were obtained after placing regions of interest (ROIs) on corresponding structures. Quantitative comparisons of SNR, contrast, and SDNR of the STN between MR pulse sequences, including the T2WI, FLAIR, and SWI. Subgroup analysis regarding patients' sex, age, and duration of treatment. We used one-way repeated measures analysis of variance for quantitative comparisons of SNR, contrast, and SDNR of the STN between different MR pulse sequences, and we also used the dependent *t*-test for the *post hoc* tests. In addition, we used Mann–Whitney U test for subgroup analyses. Both the contrast (0.33 ± 0.07) and SDNR (98.65 ± 51.37) were highest on FLAIR (all $p < 0.001$). The SNR was highest on SWI (276.16 ± 115.5), and both the SNR (94.23 ± 31.63) and SDNR (32.14 ± 17.23) were lowest on T2WI.

OPEN ACCESS

Edited by:
Joshua K. Wong, University of Florida Health, United States

Reviewed by:
Satoshi Maesawa, Nagoya University Graduate School of Medicine, Japan
Sepehr Sani, Rush University, United States

***Correspondence:**
Chih-Hua Yeh
chih.hua.yeh@gmail.com

Specialty section:
This article was submitted to Brain Imaging and Stimulation, a section of the journal Frontiers in Human Neuroscience

Received: *05 December 2021*
Accepted: *19 January 2022*
Published: *22 February 2022*

Citation:
Su C-Y, Wong AM-C, Chang C-C, Tu P-H, Chen CC and Yeh C-H (2022) Quantitative Analysis for the Delineation of the Subthalamic Nuclei on Three-Dimensional Stereotactic MRI Before Deep Brain Stimulation Surgery for Medication-Refractory Parkinson's Disease. Front. Hum. Neurosci. 16:829198. doi: 10.3389/fnhum.2022.829198

Subgroup analyses demonstrated significantly lower SDNR on SWI for patients receiving medication treatment for ≥13 years (p = 0.003). In conclusion, on 3D stereotactic MRI of medication-refractory PD patients, the contrast and SDNR for the STN are highest on FLAIR, suggesting the optimal delineation of STN on FLAIR.

Keywords: subthalamic nuclei, Parkinson's disease, deep brain stimulation, signal-to-noise ratio, contrast, signal difference-to-contrast ratio

INTRODUCTION

Most patients with Parkinson's disease (PD) are treated with medication, and a multitude of dopamine-enhancing agents is available as the therapeutic option (Armstrong and Okun, 2020). However, deep brain stimulation (DBS) has been successfully used to treat PD among patients who do not adequately respond to pharmacologic treatment, or who have intolerable medication-induced complications, which may be more severe than the motor impairment of the disease itself (Perestelo-Perez et al., 2014). Subthalamic nuclei (STN) are the most used targets of electrode implantation in patients with PD (Vizcarra et al., 2019). Because the STN are indiscernible on CT images and conventional MR images at 1.5 T, STN targeting has conventionally been performed indirectly by predicting the location of the STN according to coordinates derived from atlases (Tu et al., 2018). The drawback of the indirect targeting method, however, is that STN sizes, shapes, and positions vary between patients (Chandran et al., 2016).

With the advancement of MRI imaging techniques, delineation of the deep brain nuclei became possible on MRI at 3.0 T. Currently, the direct targeting method, which involves attempting to locate the STN in each patient, has become the mainstream targeting technique for DBS surgery (Larson et al., 2012). Compared with the adjacent white matter structures, the STN is relatively hypointense on T2-weighted imaging (T2WI), T2-weighted fluid-attenuated inversion recovery (FLAIR), and susceptibility-weighted imaging (SWI). STN is typically 3 mm lateral to the lateral border of the red nucleus, and 2 mm inferior to the superior border of the red nuclei (Andrade-Souza et al., 2008); however, the STN remain difficult to image because of their biconvex shape, small size, and its oblique spatial orientation (Ashkan et al., 2007). In our hospital, whole-brain three-dimensional (3D) stereotactic MR with T1-weighted imaging (T1WI), T2WI, FLAIR, and SWI are obtained for trajectory planning before DBS surgery (Chandran et al., 2016). Delineating the STN on MRI is vital for the direct targeting method employed in the DBS surgery. The signal intensities (SIs) of the STN and surrounding white matter structures, however, vary on by MR pulse sequences, which may influence the ability to differentiate between these structures (Wolff and Balaban, 1997).

In the field of diagnostic imaging, the quality of images and the ability to demonstrate the target lesion are crucial. The MR imaging quality depends on both the signal intensity (SI) of the human body structures and the noise caused by the thermally driven Brownian motion of electrons within the body's conducting tissue and within the receiving coil itself (Kaufman et al., 1989). Signal-to-noise ratio (SNR) is one of the standardized parameters for quantitative measurement and comparison of image quality. Contrast is the ratio of the difference in SI between two regions, which can reflect the human eyes' ability to differentiate between these two regions (Wolff and Balaban, 1997). Furthermore, signal difference-to-noise ratio (SDNR) is calculated by dividing the difference in SI by noise and is a display-independent parameter that reflects the contrast-generating ability of a pulse sequence (Wolff and Balaban, 1997; Pijl et al., 2004). Contrast and SDNR are both commonly used to measure the ability to delineate a structure on MR pulse sequences.

In this retrospective cohort study, we compared the delineation of the STN on multiple MR pulse sequences. Additionally, studies of STN delineation on MRI have had limited sample sizes or were based on MRI of healthy participants (Ashkan et al., 2007; O'Gorman et al., 2011). Therefore, the purpose of this study was to propose a quantitative analysis of SNR, contrast, and SDNR for STN on 3D stereotactic MRI before DBS surgery in patients with medication-refractory PD.

MATERIALS AND METHODS

Patients

This study was approved by our institution's institutional review board (IRB NO: 202101300B0). We retrospectively included 45 consecutive patients with medication-refractory PD who underwent STN DBS surgery in our hospital from January 2018 to June 2021. The following clinical data were collected through medical chart review: basic demographics, duration of medication treatment, history of other chronic diseases, and report of dopamine scan.

MRI Technique and Deep Brain Stimulation Trajectory Planning

MRI was performed on a 3.0 T MR system (Ingenia, Philips Medical Systems, Best, Netherlands) with the patient in the supine position. Whole-brain 3D turbo spin-echo T1WI, T2WI, and FLAIR were performed using a 15-channel head coil (dStream HeadSpine coil, Philips Medical Systems, Best, Netherlands). A total of 160 slices of axial sections without intersection gap in the orientation parallel to the AC–PC line orientation were obtained. Axial SWI with the same coverage was also performed. The detailed parameters of the MR pulse sequences are listed in **Table 1**. Immediately before the STN-DBS surgery, a whole-brain stereotactic non-enhanced CT in

TABLE 1 | Detailed parameters of MR pulse sequence for three-dimensional stereotactic MRI for preoperative evaluation of deep brain stimulation surgery.

	T1WI	T2WI	FLAIR	SWI
TR (msec)	6.1	2000	4800	30
TE (msec)	2.8	136	268	7.2
Flip angle (deg)	8	90	40	17
Slices	160	160	160	160
Thickness (mm)	1	1	1	2
Gap (mm)	0	0	0	-1
Bandwidth (Hz)	334	890	890	254
Field of view (mm)	240 × 200	240 × 200	240 × 200	230 × 179
Matrix size	240 × 200	240 × 200	240 × 200	328 × 257
Scan time (min:sec)	04:06	05:26	07:41	05:07

T2WI, T2-weighted imaging; T1WI, T1-weighted imaging; FLAIR, fluid-attenuated inversion recovery; SWI, susceptibility-weighted imaging.

TABLE 2 | Signal intensity measurements for regions of interest (ROI) locations in 45 patients with medication-refractory Parkinson's disease.

	Signal intensity		
	T2WI	FLAIR	SWI
Target structures			
STN	314.78 ± 49.33	659.25 ± 210.71	720.97 ± 122.43
Surround structure			
Corona radiata	420.62 ± 54.38	986.29 ± 301.77	886.02 ± 141.8
Background area			
Background noise	2.41 ± 0.53	0.86 ± 0.53	1.28 ± 1.22

T2WI, T2-weighted imaging; FLAIR, fluid-attenuated inversion recovery; SWI, susceptibility-weighted imaging; STN, Subthalamic nucleus. Data are presented as mean ± SD.

TABLE 3 | SNR, contrast, and SDNR for subthalamic nucleus in 45 patients with medication-refractory Parkinson's disease.

	T2WI	FLAIR	SWI	*p*
SNR	94.23 ± 31.63	196.18 ± 86.45	276.16 ± 115.5	*<0.001*
Contrast	0.25 ± 0.09	0.33 ± 0.07	0.18 ± 0.08	*<0.001*
SDNR	32.14 ± 17.23	98.65 ± 51.37	62.68 ± 38.55	*<0.001*

T2WI, T2-weighted imaging; FLAIR, fluid-attenuated inversion recovery; SWI, susceptibility-weighted imaging; SNR, signal-to-noise ratio; SDNR, signal difference-to-contrast ratio. Data are presented as mean ± SD.

1-mm slice thickness was also performed after application of the Cosman-Roberts-Wells frame (Integra Radionics, Burlington, MA, United States). Images of the 3D MRI and stereotactic CT were both transferred to a stereotactic workstation (BrainLab AG, Munich, Germany) for imaging fusion and target planning.

Data Postprocessing

All MR images were analyzed on a postprocessing workstation (IntelliSpace Portal, Philips Medical Systems, Best, Netherlands). First, the level of axial MR image with the optimal visualization of both STN and red nuclei was selected after a review of the T2WI, FLAIR, and SWI (**Figure 1**). Oblique coronal and sagittal reformation images were rechecked to ensure that the substantia nigra was not covered on the selected image (**Figure 2**). On the selected images, regions of interest (ROIs) were placed on bilateral STN and adjacent corona radiata. A rectangular ROI of the background area with a long axis perpendicular to the phase-encoding direction and with an area greater than 10.0 cm^2 was placed on the right aspect of the images. Two radiologists with experience in neuroimaging for more than 10 years independently reviewed the images and determined ROIs for all patients. **Figure 3** illustrates a representative example of the ROI placed on the FLAIR image.

In the next step, we calculated the SNR, contrast, and SDNR using the following formulas (Wolff and Balaban, 1997; Pijl et al., 2004).

$$SNR = \frac{mean\ signal\ intensity\ (SI)\ of\ STN}{standard\ deviation\ (SD)\ of\ background\ noise}$$

$$Contrast = \frac{mean\ SI\ of\ corona\ radiata\ -\ mean\ SI\ of\ STN}{mean\ SI\ of\ corona\ radiata}$$

$$SDNR = \frac{mean\ SI\ of\ corona\ radiata -\ mean\ SI\ of\ STN}{SD\ of\ background\ noise}$$

Evaluation for Subthalamic Nuclei Border Delineation

Along the trajectory of STN-DBS electrodes, we reconstructed the oblique sagittal images on different MR pulse sequences. We also reconstructed the oblique axial images perpendicularly to the trajectory at the level of the STN (**Figure 4**). On the oblique sagittal images, we evaluate the delineation between STN and substantia nigra. On the oblique axial images, we evaluate the delineation of the lateral border of STN. A fixed-points scale was used for qualitative evaluation of the STN delineation (Score 1: delineation not visible. Score 2: delineation barely visible with highly blurred margin. Score 3: visible delineation with moderately blurred margin. Score 4: delineation with slightly blurred margin. Score 5: delineation with excellent shapely defined margin.). The two neuroradiologists evaluated these images independently. And discrepancy in scoring was solved by consensus.

Statistical Analyses

Intraclass correlation coefficient (ICC) was calculated to represent the interobserver agreement. One-way repeated measures analysis of variance (ANOVA; Mishra et al., 2019) was used to compare the SNR, contrast, and SDNR for STN between multiple MR pulse sequences. Dependent *t*-tests were used for the *post hoc* tests of one-way repeated measures ANOVA. Subgroup analyses were performed according to the sex, mean age (<65 years vs. ≥65 years), and mean duration of medication treatment (<13 years vs. ≥13 years) of these 45 patients. The Mann–Whitney U test was used for non-parametric comparisons in subgroup analyses. A *p-value* of <0.05 indicated statistically significant differences, and the *p*-values were adjusted using the Bonferroni multiple testing correction for multiple comparisons in the *post hoc* tests and subgroup analyses. We also calculated the Cramer's V coefficient to represent the correlations of STN

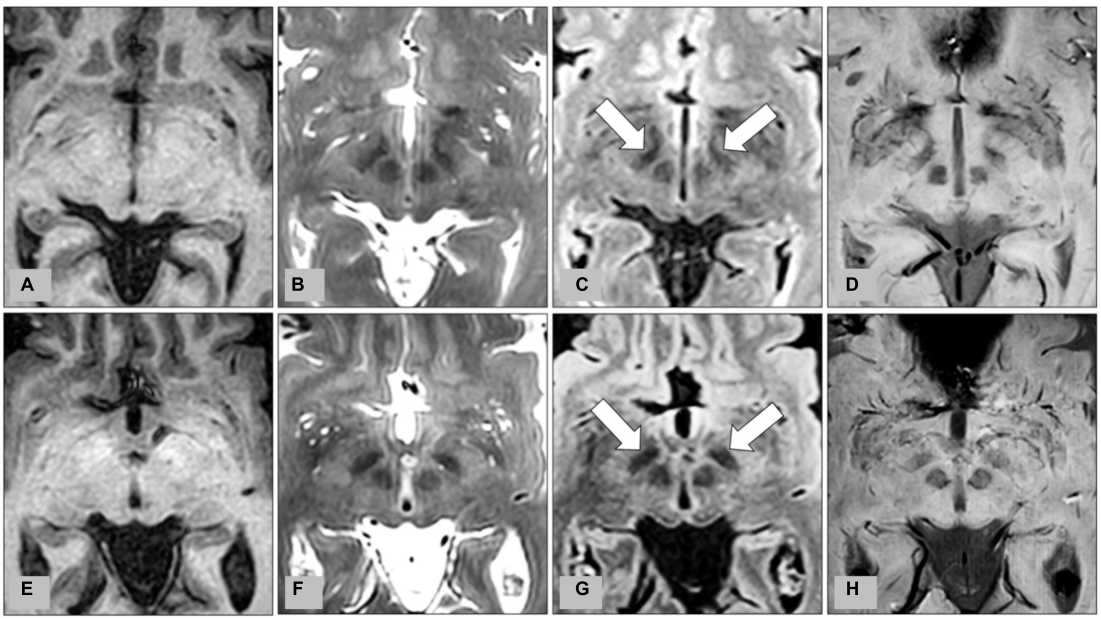

FIGURE 1 | Representative images from preoperative MRI of two patients with medication-refractory Parkinson's disease at the level of the subthalamic nucleus (STN). **(A)** T1-weighted imaging (T1WI), **(B)** T2-weighted imaging (T2WI), **(C)** fluid-attenuated inversion recovery (FLAIR), and **(D)** susceptibility-weighted imaging (SWI) from MRI of a 56-year-old male patient, and corresponding **(E)** T1WI, **(F)** T2WI, **(G)** FLAIR, and **(H)** SWI from MRI of a 62-year-old male patient. Bilateral STN are indicated by arrows on FLAIR **(C,G)**.

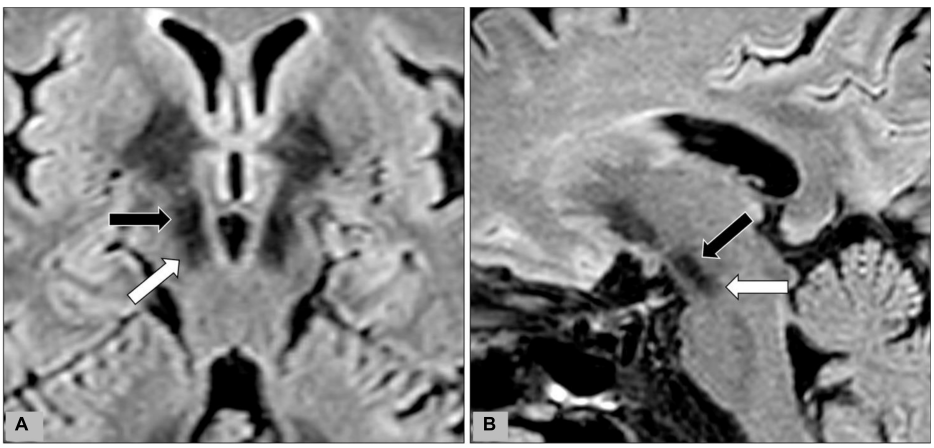

FIGURE 2 | During data-postprocessing, we selected the level of axial image with the optimal visualization of subthalamic nuclei (black arrows) after a review of the T2WI, FLAIR, and SWI images. Oblique coronal **(A)** and sagittal **(B)** reformation images were rechecked to ensure that the substantia nigra (white arrow) was not covered on the selected image.

delineation between different MR pulse sequences. All statistical analyses were performed using RStudio software (version 1.4.0, Boston, MA, United States) (Hackenberger, 2020).

RESULTS

Patients

This retrospective cohort included 45 patients with medication-refractory PD. Fourteen patients were women, and 31 patients were men. The mean age of these patients was 62.09 ± 9.17 (mean ± SD, range = 38–73) years. The mean duration of medication treatment for PD was 13.09 ± 4.69 (range = 6–25) years. Five patients had diabetes, and 15 patients had hypertension. None of the patients had other major systemic disorders. From the dopamine scan, 19 patients were determined to have a right-side predominant disease, 11 patients had the left-side predominant disease, and the other 15 patients had the bilateral symmetric disease.

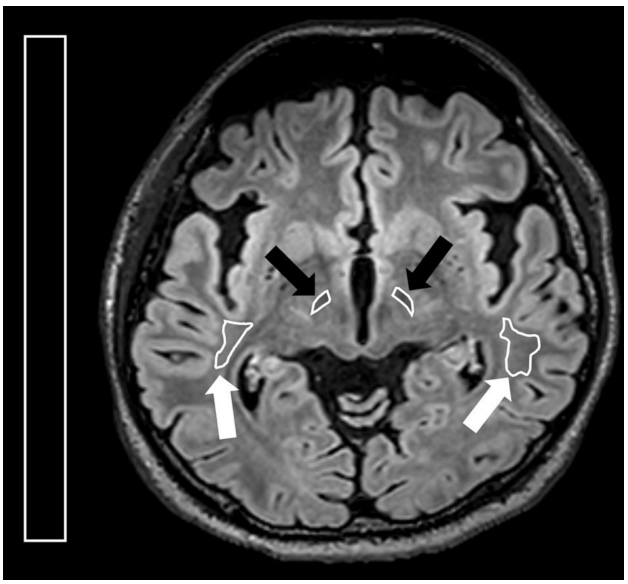

FIGURE 3 | Illustration for regions of interest (ROIs) placed on the axial FLAIR image. On the axial image with the optimal visualization of both subthalamic nucleus, ROIs were placed at bilateral STN (black arrows) and corona radiata (white arrows). A rectangular ROI of the background area with an area greater than 10.0 cm^2 was placed on the right side of the image.

Signal Intensity and Interobserver Agreement

The mean SIs of STN and corona radiata were normally distributed on Q–Q plots. The ICC between the SIs of the STN measured by two observers was 0.796 on T2WI, 0.899 on FLAIR, and 0.877 on SWI. The ICC for corona radiata was 0.751 on T2WI, 0.856 on FLAIR, and 0.854 on SWI. These results suggested satisfactory interobserver agreement. The SI of the STN was 314.78 ± 49.33 on T2WI, 659.25 ± 210.71 on FLAIR, and 720.97 ± 122.43 on SWI (**Table 2**). The SI of the corona radiata was highest on FLAIR (986.29 ± 301.77), followed by the SI on SWI (886.02 ± 141.8) and SI on T2WI (420.62 ± 54.38). Background noise was relatively low on all three pulse sequences. Mean noise was largest on T2WI (2.41 ± 0.53) and smallest on FLAIR (0.86 ± 0.53), but the variation of the background noise was largest on SWI (1.28 ± 1.22).

Signal-To-Noise Ratio

The SNR of STN was also highest on SWI (276.16 ± 115.5), followed by that on FLAIR (196.18 ± 86.45). Because the lowest STN SI was observed on T2WI, the SNR was also lowest on T2WI (94.23 ± 31.63). Repeated measures ANOVA (**Figure 5A**) revealed significant differences between the SNR of these three pulse sequences ($p < 0.001$). *Post hoc* tests using a dependent *t*-test also demonstrated significant differences between T2WI and FLAIR, between FLAIR and SWI, and between T2WI and SWI (all $p < 0.001$).

Contrast and Signal Difference-To-Noise Ratio

Both the contrast and the SDNR of the STN were highest on FLAIR (contrast: 0.33 ± 0.07; SDNR: 98.65 ± 51.37). The contrast of the STN was smallest on SWI (0.18 ± 0.08), but the SDNR was smallest on T2WI (32.14 ± 17.23; **Table 3**). Significant differences of contrast were noted between the three pulse sequences on repeated measures ANOVA ($p < 0.001$) and *post hoc* tests (all $p < 0.001$; **Figure 5B**). For the SDNR (**Figure 5C**), significant differences were also noted on repeated measures ANOVA and *post hoc* tests (all $p < 0.001$).

Subgroup Analyses

No significant difference in SNR, contrast or SDNR of the STN on the three pulse sequences were noted between patients of different sex (14 women and 31 men) or age [<65 years ($n = 23$) and ≥65 years ($n = 22$); **Table 4**]. However, after Bonferroni correction, the SDNR on SWI was significantly lower among the 25 patients who had been treated with medication for ≥13 years (mean = 46.83) than it was among the 20 patients who had been treated with medication for <13 years (mean = 82.50, $p = 0.003$). The SDNR on FLAIR ($p = 0.032$) and T2WI ($p = 0.207$) also trended lower in patients with a longer history of medication treatment, but the difference was non-significant.

Evaluation for Subthalamic Nuclei Border Delineation

Results of the fixed-points scale for delineation between the STN and the substantia nigra, and the scoring for the lateral border of STN were summarized in **Table 5**. There are "relatively strong" interobserver agreements according to Cramer's V coefficients. The delineation between STN and substantia nigra was good on both FLAIR and T2WI with a score of 4 or 5 for 81 STNs on FLAIR and 74 STNs on T2WI. But the scoring on SWI was relatively lower with a score of 4 or 5 in less than half STNs ($n = 36$). The Cramer's V coefficient is 0.406 between FLAIR and T2WI, 0.298 between T2WI and SWI, and 0.193 between FLAIR and SWI. For the lateral border of the STN, the Cramer's V coefficient is 0.448 between FLAIR and T2WI, 0.221 between T2WI and SWI, and 0.234 between FLAIR and SWI.

DISCUSSION

Indirect targeting of the STN with CT coordinates for stereotactic localization is rapid (Spiegelmann and Friedman, 1991); however, anatomic details of the STN on CT are poor when compared with MRI (Lemaire et al., 1999). On the contrary, although good for visualization of the target structure, 3D reformation, and trajectory planning on conventional 2D MRI is difficult due to the large slice thickness and the non-negligible gap between images. The CT-MR images fusion procedure combines the stereotactic accuracy of CT and the precise anatomical definition of 3D MRI with distortions less than 1 mm except at the tissue-air interface (Kooy et al., 1994). In our institution, we primarily used the direct targeting method with CT-MRI image fusion

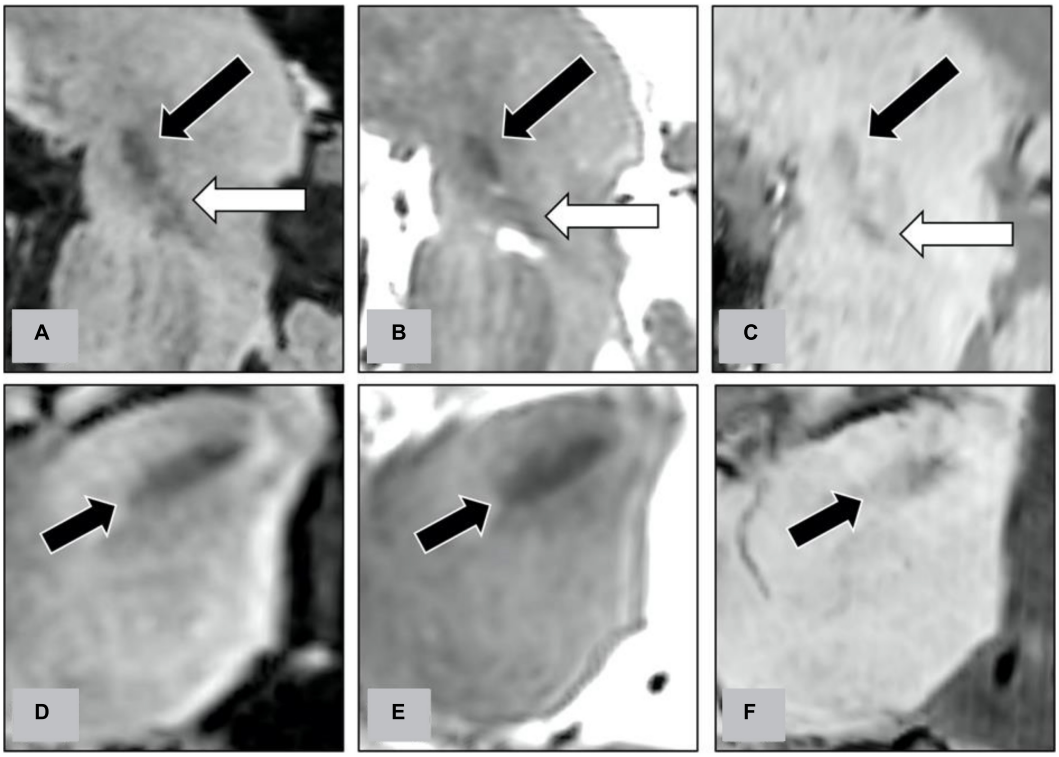

FIGURE 4 | Along the trajectory of STN-DBS electrodes, we reconstructed the oblique sagittal images on FLAIR **(A)**, T2WI **(B)**, and SWI **(C)**. On the oblique sagittal images, we evaluate the delineation between STN (indicated by black arrows on figures) and substantia nigra (indicated by white arrows). We also reconstructed the oblique axial images perpendicularly to the trajectory at the level of the STN on FLAIR **(D)**, T2WI **(E)**, and SWI **(F)**. On the oblique axial images, we evaluate the delineation of the lateral border of STN (indicated by black arrows).

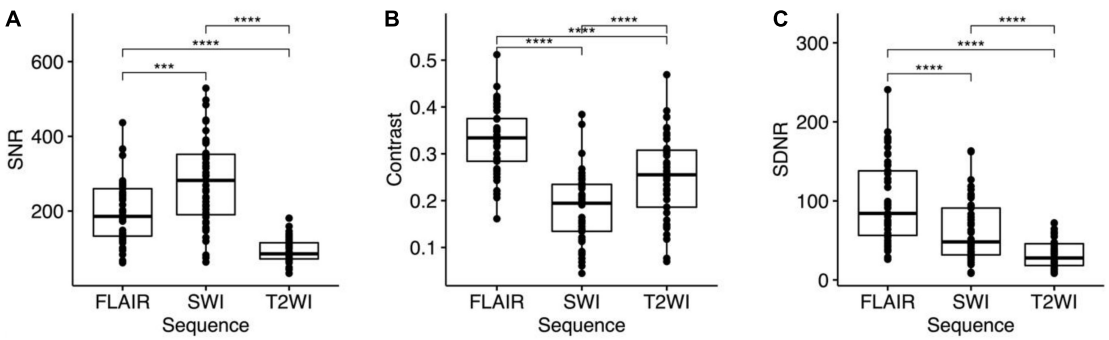

FIGURE 5 | One-way repeated measures analysis of variance (ANOVA) and *post hoc* tests for **(A)** signal-to-noise ratio (SNR), **(B)** contrast, and **(C)** signal difference-to-noise ratio (SDNR) the STN on FLAIR, SWI, and T2WI. Bonferroni multiple testing correction for multiple comparisons in the *post hoc* tests. All the $p < 0.001$ for ANOVA and *post hoc* tests of SNR, contrasts, and SDNR. ***$p \leq 0.001$ and ****$p \leq 0.0001$.

for STN-DBS surgery. **Figure 6** demonstrates the delineation of STN on different MR pulse sequences along the trajectory of DBS electrodes.

In our study, the contrast and the SDNR of the STN were both highest on FLAIR, suggesting the optimal visualization of the STN. FLAIR is one of the inversion recovery sequences used to enhance contrast by selective suppression of water signals. Because the characteristic hypointense SIs of the STN on T2-weighted MR pulse sequences, reflecting the shortened T2 relaxation time by the high intrinsic iron content high in STN, T2WI, and FLAIR are commonly used to target the STN (Dormont et al., 2004). Previous studies reported optimal demonstration of the STN on 3D T2WI at both 1.5 T and 3.0 T (Dormont et al., 2004; Slavin et al., 2006). One previous study compared two-dimensional (2D) T2WI and 3D FLAIR images for the visualization of brain stem anatomy (Kitajima et al., 2012). Another study compared 3D FLAIR with 2D T2-turbo-spin-echo (TSE) and 2D T2*-fast-field echo for the delineation

TABLE 4 | Subgroup comparison of SNR, contrast, and SDNR for STN in 45 patients with medication-refractory Parkinson's disease.

	Sex			Age (years)			Medication treatment (years)		
	Woman (*n* = 14)	Man (*n* = 31)	*p*	<65 (*n* = 23)	≧65 (*n* = 22)	*p*	<13 (*n* = 20)	≧13 (*n* = 25)	*p*
SNR									
T2WI	95.52	93.65	*0.952*	88.16	100.57	*0.194*	103.38	86.91	*0.199*
FLAIR	227.96	181.83	*0.362*	172.08	221.38	*0.115*	200.32	192.87	*0.883*
SWI	253.63	286.34	*0.313*	273.06	279.42	*0.813*	317.75	242.90	*0.042*
Contrast									
T2WI	0.27	0.24	*0.375*	0.26	0.24	*0.464*	0.27	0.23	*0.191*
FLAIR	0.32	0.33	*0.913*	0.34	0.32	*0.350*	0.35	0.31	*0.124*
SWI	0.19	0.18	*0.637*	0.19	0.18	*0.218*	0.20	0.17	*0.136*
SDNR									
T2WI	36.24	30.30	*0.325*	31.77	32.54	*0.937*	38.13	27.35	*0.032*
FLAIR	108.10	94.38	*0.672*	91.16	106.48	*0.437*	111.15	88.65	*0.207*
SWI	65.37	61.47	*0.781*	66.03	59.18	*0.361*	82.50	46.83	*0.003**

*T2WI, T2-weighted imaging; FLAIR, fluid-attenuated inversion recovery; SWI, susceptibility-weighted imaging; SNR, signal-to-noise ratio; SDNR, signal difference-to-noise ratio. Bonferroni multiple testing correction for p-value = 0.0166. *p ≤ 0.05.*

TABLE 5 | Results of the fixed-points scale scores for delineation between the STN and the substantia nigra, and the scoring for the lateral border of the STN.

		The delineation between the STN and the substantia nigra					Delineation of the lateral border of the STN				
Score		**1**	**2**	**3**	**4**	**5**	**1**	**2**	**3**	**4**	**5**
FLAIR											
Right	(*n* = 45)	0	1	5	22	17	0	1	6	21	17
Left	(*n* = 45)	0	1	2	22	20	0	2	7	23	13
Total	(*n* = 90)	0	2	7	44	37	0	3	13	44	30
T2WI											
Right	(*n* = 45)	0	2	7	29	7	0	2	14	22	7
Left	(*n* = 45)	1	1	5	30	8	1	5	15	18	6
Total	(*n* = 90)	1	3	12	59	15	1	7	29	40	13
SWI											
Right	(*n* = 45)	1	5	20	19	0	3	9	17	13	3
Left	(*n* = 45)	1	6	21	17	0	2	11	16	12	4
Total	(*n* = 90)	2	11	41	36	0	5	20	33	25	7

of the STN (Heo et al., 2015), but to our knowledge, no study has yet compared 3D FLAIR with 3D T2WI or 3D SWI for the visualization of the STN in such a large group of patients with medication-refractory PD. It is generally accepted that 3D FLAIR provides high spatial resolution and a high SNR (Li et al., 2020). 3D FLAIR also emphasizes the T2-weighted contrast effect compared with the T2-TSE pulse sequence because of the longer time-to-echo, higher turbo factor number, and longer echo train length (Kitajima et al., 2012). In addition, 3D MR images with whole-brain coverage and thin slice thickness are more suitable for image co-registration than using 2D MR images.

Susceptibility-weighted imaging is a combination of phase and magnitude images with enhanced contrast that is sensitive to hemorrhage, calcium, iron storage, and slow venous blood (Beriault et al., 2014). The high iron concentration of the STN corresponds to increased susceptibility and the hypointense signal on SWI (Dormont et al., 2004). SWI has been reported to be more accurate than T2WI for visualization of the STN at both 1.5 T and 3.0 T field strength (O'Gorman et al., 2011; Kerl et al., 2012; Liu et al., 2013). A previous study reported a higher contrast-to-noise ratio on SWI than that on FLAIR images at 3.0 T (Kerl et al., 2012). However, a 2D axial FLAIR sequence with thick slice thickness (4 mm) was used in that study, and only nine healthy volunteers and one patient with PD were included. Our study also demonstrated a higher SDNR on SWI than that on T2WI. The enhanced visualization of cerebral veins is another benefit of SWI for preoperative planning of DBS lead trajectory. However, the non-local susceptibility effect, also known as blooming artifact, is a notable drawback of SWI. This means that on SWI, the STN may also appear to originate from surrounding non-STN tissue (Li et al., 2012). This blooming artifact, therefore, requires quantification and correction before the accurate direct targeting of the STN.

In our study, the SDNR on SWI was significantly lower among patients who had been on a medication treatment regimen for ≥13 years. The SDNR also trended lower in patients with longer medication treatment on FLAIR and T2WI, but the difference was non-significant. The effect of tissue iron

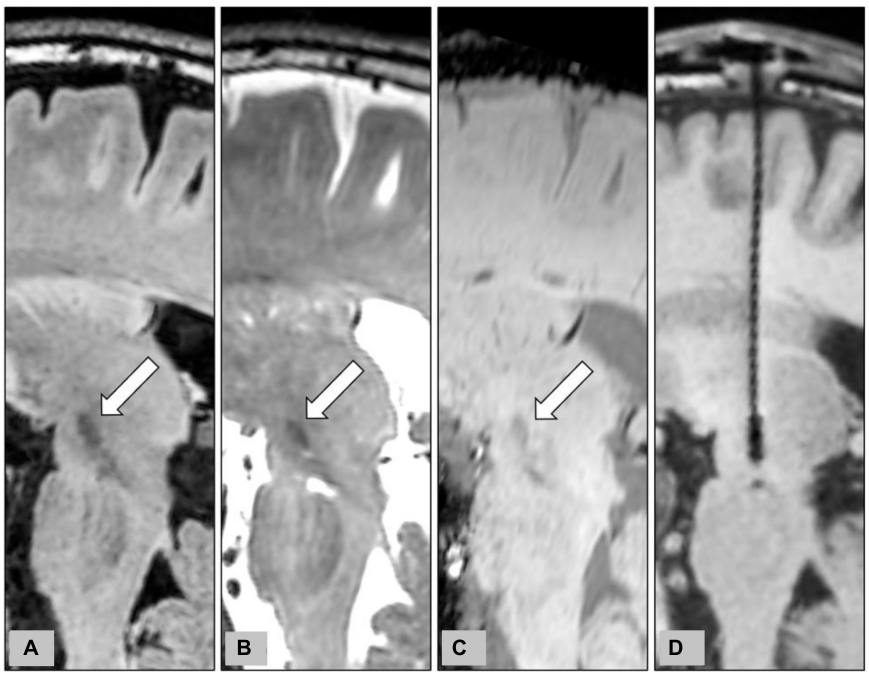

FIGURE 6 | Representative case to show the delineation of STN on different MR pulse sequences for the planning of STN-DBS surgery. The planned trajectory for the right STN-DBS lead was demonstrated on the oblique sagittal reconstruction of pre-operative 3D FLAIR **(A)**, T2WI **(B)**, and SWI **(C)**. The target structures, the STN, were indicated by white arrows on pre-operative images. The final position of the electrode was also shown on the oblique sagittal reconstruction of post-operative T1WI **(D)**.

concentration on MR SI is well known, but the exact relationship between iron accumulation and long-term medication treatment in patients with PD remains unclear (Jellinger, 2012). These results in our study suggest a possible change of tissue iron concentration in STN after long-term dopamine-enhancing agent therapy. However, further histopathology study or quantitative measurement by non-invasive imaging is required to verify this postulation.

The delineation between STN and substantia nigra, and the visualization of the lateral border of the STN on different MR pulse sequences were evaluated using a fix-point scale modified from similar research (Suther et al., 2018). The ordinal fixed-point scales, which are composed of ordered quantitative features ranging from "totally disagree" to "totally agree", are commonly used in subjective image quality assessment for diagnostic images (Bourdel et al., 2015). For the total 90 STNs in 45 patients, scoring for the delineation between STN and substantia nigra was good on both FLAIR and T2WI. The Cramer's V coefficient suggested a "relatively strong" association between FLAIR and T2WI. But the scoring on SWI was relatively lower, and was only "weakly" associated with FLAIR, and "moderately" associated with T2WI according to Cramer's V coefficient. These results suggested an inferior ability to delineate between STN and substantia nigra on SWI. For the visualization of the lateral border of the STN, our results also showed a similar disadvantage of SWI.

This study has several limitations. First, we used standardized procedures of ROI placement and SI measurement by two neuroradiologists in this study. However, some errors during ROI placement are still possible. Second, the SNR, contrast, and SDNR are commonly used quantitative parameters for MR image quality and contrast-generating ability. These parameters, however, cannot completely reflect the subjective delineation of STN by the human eyes on MRI. Third, MR image distortion is another challenge for stereotactic surgery and is not covered in this study. Fusion of MRI and stereotactic CT with a metallic frame was performed to overcome the MR image distortion in our hospital. Furthermore, a recent study has suggested that the error of measurement on MRI was random and did not appear to move in any predictable manner (Simon et al., 2005). MR images distortion may not be as significant as it was postulated to be. In addition, this study was based on quantitative analyses of the signal intensity measured on 3D MRI. The STN-DBS surgery is a minimally invasive procedure and relies on stereotactic navigation and multichannel microelectrode recording (MER). Unlike conventional open surgery, the target structures are not directly visualized during operation. In the absence of a golden standard reference, it is difficult to evaluate the clinical accuracy and reliability of STN delineation on different MR pulse sequences.

In conclusion, we reported a retrospective cohort that included preoperative MRI in 45 patients with medication-refractory PD. The contrast and SDNR for the STN are highest on FLAIR, suggesting the optimal ability for delineating STN on MRI. These results can contribute to facilitating the STN delineation during preoperative planning and enhanced electrodes placement accuracy during surgery.

DATA AVAILABILITY STATEMENT

The datasets presented in this study can be found in online repositories. The names of the repository/repositories and accession number(s) can be found below: https://drive.google.com/file/d/1K8Y_0OkJYrHDWhjz Say Bbg10_MVzF8qz/view?usp=sharing.

ETHICS STATEMENT

The studies involving human participants were reviewed and approved by Chang Gung Medical Foundation Institutional Review Board RB No. 202101300B0. Written informed consent for participation was not required for this study in accordance with the national legislation and the institutional requirements.

AUTHOR CONTRIBUTIONS

C-YS, AW, and C-HY contributed to the conception and design of the study and performed the data post-processing. C-YS organized the database and wrote the first draft of the manuscript. C-HY performed the statistical analysis. AW, C-CC, P-HT, and CCC wrote sections of the manuscript. All authors contributed to manuscript revision, read, and approved the submitted version.

REFERENCES

Andrade-Souza, Y. M., Schwalb, J. M., Hamani, C., Eltahawy, H., Hoque, T., Saint-Cyr, J., et al. (2008). Comparison of three methods of targeting the subthalamic nucleus for chronic stimulation in Parkinson's disease. *Neurosurgery* 62 Suppl 2, 875–883. doi: 10.1227/01.neu.0000316289.75736.55

Armstrong, M. J., and Okun, M. S. (2020). Diagnosis and treatment of Parkinson disease: a review. *JAMA* 323, 548–560. doi: 10.1001/jama.2019.22360

Ashkan, K., Blomstedt, P., Zrinzo, L., Tisch, S., Yousry, T., Limousin-Dowsey, P., et al. (2007). Variability of the subthalamic nucleus: the case for direct MRI guided targeting. *Br. J. Neurosurg.* 21, 197–200. doi: 10.1080/02688690701272240

Beriault, S., Sadikot, A. F., Alsubaie, F., Drouin, S., Collins, D. L., and Pike, G. B. (2014). Neuronavigation using susceptibility-weighted venography: application to deep brain stimulation and comparison with gadolinium contrast. *J. Neurosurg.* 121, 131–141. doi: 10.3171/2014.3.JNS131860

Bourdel, N., Alves, J., Pickering, G., Ramilo, I., Roman, H., and Canis, M. (2015). Systematic review of endometriosis pain assessment: how to choose a scale? *Hum. Reprod. Update* 21, 136–152. doi: 10.1093/humupd/dmu046

Chandran, A. S., Bynevelt, M., and Lind, C. R. (2016). Magnetic resonance imaging of the subthalamic nucleus for deep brain stimulation. *J. Neurosurg.* 124, 96–105. doi: 10.3171/2015.1.JNS142066

Dormont, D., Ricciardi, K. G., Tande, D., Parain, K., Menuel, C., Galanaud, D., et al. (2004). Is the subthalamic nucleus hypointense on T2-weighted images? A correlation study using MR imaging and stereotactic atlas data. *AJNR Am. J. Neuroradiol.* 25, 1516–1523.

Hackenberger, B. K. (2020). R software: unfriendly but probably the best. *Croat. Med. J.* 61, 66–68. doi: 10.3325/cmj.2020.61.66

Heo, Y. J., Kim, S. J., Kim, H. S., Choi, C. G., Jung, S. C., Lee, J. K., et al. (2015). Three-dimensional fluid-attenuated inversion recovery sequence for visualization of subthalamic nucleus for deep brain stimulation in Parkinson's disease. *Neuroradiology* 57, 929–935. doi: 10.1007/s00234-015-1555-z

Jellinger, K. A. (2012). Neuropathology of sporadic Parkinson's disease: evaluation and changes of concepts. *Mov. Disord.* 27, 8–30. doi: 10.1002/mds.23795

Kaufman, L., Kramer, D. M., Crooks, L. E., and Ortendahl, D. A. (1989). Measuring signal-to-noise ratios in MR imaging. *Radiology* 173, 265–267. doi: 10.1148/radiology.173.1.2781018

Kerl, H. U., Gerigk, L., Pechlivanis, I., Al-Zghloul, M., Groden, C., and Nolte, I. (2012). The subthalamic nucleus at 3.0 Tesla: choice of optimal sequence and orientation for deep brain stimulation using a standard installation protocol: clinical article. *J. Neurosurg.* 117, 1155–1165. doi: 10.3171/2012.8.JNS111930

Kitajima, M., Hirai, T., Shigematsu, Y., Uetani, H., Iwashita, K., Morita, K., et al. (2012). Comparison of 3D FLAIR, 2D FLAIR, and 2D T2-weighted MR imaging of brain stem anatomy. *AJNR Am. J. Neuroradiol.* 33, 922–927. doi: 10.3174/ajnr.A2874

Kooy, H. M., van Herk, M., Barnes, P. D., Alexander, E. III, Dunbar, S. F., Tarbell, N. J., et al. (1994). Image fusion for stereotactic radiotherapy and radiosurgery treatment planning. *Int. J. Radiat. Oncol. Biol. Phys.* 28, 1229–1234. doi: 10.1016/0360-3016(94)90499-5

Larson, P. S., Starr, P. A., Bates, G., Tansey, L., Richardson, R. M., and Martin, A. J. (2012). An optimized system for interventional magnetic resonance imaging-guided stereotactic surgery: preliminary evaluation of targeting accuracy. *Neurosurgery* 70(Issue suppl_1), ons95–ons103. doi: 10.1227/NEU.0b013e31822f4a91

Lemaire, J. J., Durif, F., Boire, J. Y., Debilly, B., Irthum, B., and Chazal, J. (1999). Direct stereotactic MRI location in the globus pallidus for chronic stimulation in Parkinson's disease. *Acta Neurochir. (Wien.)* 141(7), 759–765. discussion 766, doi: 10.1007/s007010050372

Li, J., Chang, S., Liu, T., Wang, Q., Cui, D., Chen, X., et al. (2012). Reducing the object orientation dependence of susceptibility effects in gradient echo MRI through quantitative susceptibility mapping. *Magn. Reson. Med.* 68, 1563–1569. doi: 10.1002/mrm.24135

Li, Z., Pipe, J. G., Ooi, M. B., Kuwabara, M., and Karis, J. P. (2020). Improving the image quality of 3D FLAIR with a spiral MRI technique. *Magn. Reson. Med.* 83, 170–177. doi: 10.1002/mrm.27911

Liu, T., Eskreis-Winkler, S., Schweitzer, A. D., Chen, W., Kaplitt, M. G., Tsiouris, A. J., et al. (2013). Improved subthalamic nucleus depiction with quantitative susceptibility mapping. *Radiology* 269, 216–223. doi: 10.1148/radiol.13121991

Mishra, P., Singh, U., Pandey, C. M., Mishra, P., and Pandey, G. (2019). Application of student's t-test, analysis of variance, and covariance. *Ann. Card. Anaesth.* 22, 407–411. doi: 10.4103/aca.ACA_94_19

O'Gorman, R. L., Shmueli, K., Ashkan, K., Samuel, M., Lythgoe, D. J., Shahidiani, A., et al. (2011). Optimal MRI methods for direct stereotactic targeting of the subthalamic nucleus and globus pallidus. *Eur. Radiol.* 21, 130–136. doi: 10.1007/s00330-010-1885-5

Perestelo-Perez, L., Rivero-Santana, A., Perez-Ramos, J., Serrano-Perez, P., Panetta, J., and Hilarion, P. (2014). Deep brain stimulation in Parkinson's disease: meta-analysis of randomized controlled trials. *J. Neurol.* 261, 2051–2060. doi: 10.1007/s00415-014-7254-6

Pijl, M. E., Doornbos, J., Wasser, M. N., van Houwelingen, H. C., Tollenaar, R. A., and Bloem, J. L. (2004). Quantitative analysis of focal masses at MR imaging: a plea for standardization. *Radiology* 231, 737–744. doi: 10.1148/radiol.2313030173

Simon, S. L., Douglas, P., Baltuch, G. H., and Jaggi, J. L. (2005). Error analysis of MRI and leksell stereotactic frame target localization in deep brain stimulation surgery. *Stereotact. Funct. Neurosurg.* 83, 1–5. doi: 10.1159/000083861

Slavin, K. V., Thulborn, K. R., Wess, C., and Nersesyan, H. (2006). Direct visualization of the human subthalamic nucleus with 3T MR imaging. *AJNR Am. J. Neuroradiol.* 27, 80–84.

Spiegelmann, R., and Friedman, W. A. (1991). Rapid determination of thalamic CT-stereotactic coordinates: a method. *Acta Neurochir. (Wien.)* 110, 77–81. doi: 10.1007/BF01402051

Suther, K. R., Hopp, E., Smevik, B., Fiane, A. E., Lindberg, H. L., Larsen, S., et al. (2018). Can visual analogue scale be used in radiologic subjective image quality assessment? *Pediatr. Radiol.* 48, 1567–1575. doi: 10.1007/s00247-018-4187-8

Tu, P. H., Liu, Z. H., Chen, C. C., Lin, W. Y., Bowes, A. L., Lu, C. S., et al. (2018). Indirect targeting of subthalamic deep brain stimulation guided by stereotactic computed tomography and microelectrode recordings in patients with Parkinson's disease. *Front. Hum. Neurosci.* 12:470. doi: 10.3389/fnhum.2018.00470

Vizcarra, J. A., Situ-Kcomt, M., Artusi, C. A., Duker, A. P., Lopiano, L., Okun, M. S., et al. (2019). Subthalamic deep brain stimulation and levodopa in Parkinson's disease: a meta-analysis of combined effects. *J. Neurol.* 266, 289–297. doi: 10.1007/s00415-018-8936-2

Wolff, S. D., and Balaban, R. S. (1997). Assessing contrast on MR images. *Radiology* 202, 25–29. doi: 10.1148/radiology.202.1.8988186

Conflict of Interest: The authors declare that the research was conducted in the absence of any commercial or financial relationships that could be construed as a potential conflict of interest.

frontiers in Human Neuroscience

PERSPECTIVE
published: 04 March 2022
doi: 10.3389/fnhum.2022.813387

OPEN ACCESS

Edited by:
Karsten Mueller, Max Planck Institute for Human Cognitive and Brain Sciences, Germany

Reviewed by:
Josef Vymazal, Na Homolce Hospital, Czechia

***Correspondence:**
Joshua K. Wong
joshua.wong@neurology.ufl.edu

Specialty section:
This article was submitted to Brain Imaging and Stimulation, a section of the journal Frontiers in Human Neuroscience

Received: *11 November 2021*
Accepted: *11 January 2022*
Published: *04 March 2022*

Citation:
Wong JK, Deuschl G, Wolke R, Bergman H, Muthuraman M, Groppa S, Sheth SA, Bronte-Stewart HM, Wilkins KB, Petrucci MN, Lambert E, Kehnemouyi Y, Starr PA, Little S, Anso J, Gilron R, Poree L, Kalamangalam GP, Worrell GA, Miller KJ, Schiff ND, Butson CR, Henderson JM, Judy JW, Ramirez-Zamora A, Foote KD, Silburn PA, Li L, Oyama G, Kamo H, Sekimoto S, Hattori N, Giordano JJ, DiEuliis D, Shook JR, Doughtery DD, Widge AS, Mayberg HS, Cha J, Choi K, Heisig S, Obatusin M, Opri E, Kaufman SB, Shirvalkar P, Rozell CJ, Alagapan S, Raike RS, Bokil H, Green D and Okun MS (2022) Proceedings of the Ninth Annual Deep Brain Stimulation Think Tank: Advances in Cutting Edge Technologies, Artificial Intelligence, Neuromodulation, Neuroethics, Pain, Interventional Psychiatry, Epilepsy, and Traumatic Brain Injury. Front. Hum. Neurosci. 16:813387. doi: 10.3389/fnhum.2022.813387

Proceedings of the Ninth Annual Deep Brain Stimulation Think Tank: Advances in Cutting Edge Technologies, Artificial Intelligence, Neuromodulation, Neuroethics, Pain, Interventional Psychiatry, Epilepsy, and Traumatic Brain Injury

Joshua K. Wong[1]*, Günther Deuschl[2], Robin Wolke[2], Hagai Bergman[3], Muthuraman Muthuraman[4], Sergiu Groppa[4], Sameer A. Sheth[5], Helen M. Bronte-Stewart[6], Kevin B. Wilkins[6], Matthew N. Petrucci[6], Emilia Lambert[6], Yasmine Kehnemouyi[6], Philip A. Starr[7], Simon Little[7], Juan Anso[7], Ro'ee Gilron[7], Lawrence Poree[8], Giridhar P. Kalamangalam[9], Gregory A. Worrell[10], Kai J. Miller[11], Nicholas D. Schiff[12], Christopher R. Butson[1], Jaimie M. Henderson[13], Jack W. Judy[14], Adolfo Ramirez-Zamora[1], Kelly D. Foote[15], Peter A. Silburn[16], Luming Li[17], Genko Oyama[18], Hikaru Kamo[18], Satoko Sekimoto[18], Nobutaka Hattori[18], James J. Giordano[19], Diane DiEuliis[20], John R. Shook[21], Darin D. Doughtery[22], Alik S. Widge[23], Helen S. Mayberg[24], Jungho Cha[24], Kisueng Choi[24], Stephen Heisig[24], Mosadolu Obatusin[24], Enrico Opri[25], Scott B. Kaufman[26], Prasad Shirvalkar[6,27], Christopher J. Rozell[28], Sankaraleengam Alagapan[28], Robert S. Raike[29], Hemant Bokil[30], David Green[31] and Michael S. Okun[1]

[1] Department of Neurology, Fixel Institute for Neurological Diseases, University of Florida, Gainesville, FL, United States, [2] Department of Neurology, Christian-Albrechts-University, Kiel, Germany, [3] Department of Medical Neurobiology (Physiology), Institute of Medical Research Israel-Canada, Hebrew University of Jerusalem, Jerusalem, Israel, [4] Biomedical Statistics and Multimodal Signal Processing Unit, Section of Movement Disorders and Neurostimulation, Focus Program Translational Neuroscience, Department of Neurology, University Medical Center of the Johannes Gutenberg-University Mainz, Mainz, Germany, [5] Department of Neurological Surgery, Baylor College of Medicine, Houston, TX, United States, [6] The Human Motor Control and Neuromodulation Laboratory, Department of Neurology and Neurological Sciences, Stanford University School of Medicine, Stanford University, Stanford, CA, United States, [7] Department of Neurological Surgery, Kavli Institute for Fundamental Neuroscience, University of California, San Francisco, San Francisco, CA, United States, [8] Department of Anesthesia, University of California, San Francisco, San Francisco, CA, United States, [9] Department of Neurology, Wilder Center for Epilepsy Research, University of Florida, Gainesville, FL, United States, [10] Department of Neurology, Mayo Clinic, Rochester, NY, United States, [11] Department of Neurosurgery, Mayo Clinic, Rochester, NY, United States, [12] Department of Neurology, Weill Cornell Brain and Spine Institute, Weill Cornell Medicine, New York, NY, United States, [13] Department of Neurosurgery, Stanford University, Stanford, CA, United States, [14] Department of Electrical and Computer Engineering, University of Florida, Gainesville, FL, United States, [15] Department of Neurosurgery, Fixel Institute for Neurological Diseases, University of Florida, Gainesville, FL, United States, [16] Queensland Brain Institute, University of Queensland and Saint Andrews War Memorial Hospital, Brisbane, QLD, Australia, [17] National Engineering Laboratory for Neuromodulation, School of Aerospace Engineering, Tsinghua University, Beijing, China, [18] Department of Neurology, Faculty of Medicine, Juntendo University, Tokyo, Japan, [19] Neuroethics Studies Program, Department of Neurology, Georgetown University Medical Center, Washington, DC, United States, [20] US Department of Defense Fort Lesley J. McNair, National Defense University, Washington, DC, United States, [21] Department of Philosophy and Science Education, University of Buffalo, Buffalo, NY, United States, [22] Department of Psychiatry, Massachusetts General Hospital

and Harvard Medical School, Boston, MA, United States, [23] Department of Psychiatry, University of Minnesota, Minneapolis, MN, United States, [24] Department of Neurology and Neurosurgery, Icahn School of Medicine at Mount Sinai, New York, NY, United States, [25] Department of Neurology, Emory University, Atlanta, GA, United States, [26] Department of Psychology, Columbia University, New York, NY, United States, [27] Department of Anesthesiology (Pain Management) and Neurology, University of California, San Francisco, San Francisco, CA, United States, [28] School of Electrical and Computer Engineering, Georgia Institute of Technology, Atlanta, GA, United States, [29] Restorative Therapies Group Implantables, Research and Core Technology, Medtronic Inc., Minneapolis, MN, United States, [30] Boston Scientific Neuromodulation Corporation, Valencia, CA, United States, [31] NeuroPace, Inc., Mountain View, CA, United States

DBS Think Tank IX was held on August 25–27, 2021 in Orlando FL with US based participants largely in person and overseas participants joining by video conferencing technology. The DBS Think Tank was founded in 2012 and provides an open platform where clinicians, engineers and researchers (from industry and academia) can freely discuss current and emerging deep brain stimulation (DBS) technologies as well as the logistical and ethical issues facing the field. The consensus among the DBS Think Tank IX speakers was that DBS expanded in its scope and has been applied to multiple brain disorders in an effort to modulate neural circuitry. After collectively sharing our experiences, it was estimated that globally more than 230,000 DBS devices have been implanted for neurological and neuropsychiatric disorders. As such, this year's meeting was focused on advances in the following areas: neuromodulation in Europe, Asia and Australia; cutting-edge technologies, neuroethics, interventional psychiatry, adaptive DBS, neuromodulation for pain, network neuromodulation for epilepsy and neuromodulation for traumatic brain injury.

Keywords: deep brain stimulation, artificial intelligence, neuroethics, pain, interventional psychiatry, adaptive DBS, epilepsy, traumatic brain injury

INTRODUCTION

The DBS Think Tank IX presenters pooled data and determined that DBS expanded in its scope and has been applied to multiple brain disorders in an effort to modulate neural circuitry. It was estimated that globally more than 230,000 deep brain stimulation (DBS) devices have been implanted for neurological and neuropsychiatric disorders. The DBS Think Tank was founded in 2012 and it provides an open platform where clinicians, engineers and researchers (from industry and academia) can freely discuss current and emerging DBS technologies as well as the logistical and ethical issues facing the field. The emphasis of the DBS Think Tank is on cutting edge research and collaboration with the potential to advance the DBS field. The DBS Think Tank IX was held on August 25–27 in Orlando FL with US based participants largely in person and overseas participants joining by video conferencing technology. The meeting was focused on advances in the following areas: neuromodulation in Europe, Asia and Australia; cutting-edge technologies, neuroethics, interventional psychiatry, adaptive DBS, neuromodulation for pain, network neuromodulation for epilepsy and neuromodulation for traumatic brain injury. The DBS Think Tank discussed Maslow's theories and a path to transcendence both for patients as well as for DBS practitioners. The attendees also participated in a DBS Think Tank survey, which documented the expansion of DBS into several indications such as movement disorders, psychiatric disorders, and pain disorders. This proceeding summarizes the advances discussed at the DBS Think Tank IX.

INTERNATIONAL NEUROMODULATION TRENDS FROM EUROPE, ASIA AND AUSTRALIA

Clinical Predictors of the Deep Brain Stimulation Effect on Parkinson's Disease

Individualization of treatment for persons with Parkinson's disease (PD) is among the main objectives of neurology. The response to treatment is heterogenous and critically depends on our ability to predict the response of a particular patient to different interventions. For DBS we take for granted that the response of a patient to levodopa best predicts the response to stimulation (Charles et al., 2002). But while we can confirm this in our cohort (n = 334 patients; R: 0.58; R^2: 0.35; $p < 2.2e^{-16}$) the response of the individual patient can vary considerably (**Figure 1**). Two approaches may address the variability: (1) First is the application of new statistical machine learning technique(s). Generalized linear models using clinical and medical history data can be used. Following appropriate cross validation, the prediction improves to a maximum mean-R^2 of 0.358. When outcomes are dichotomized (e.g., UPDRS III-score

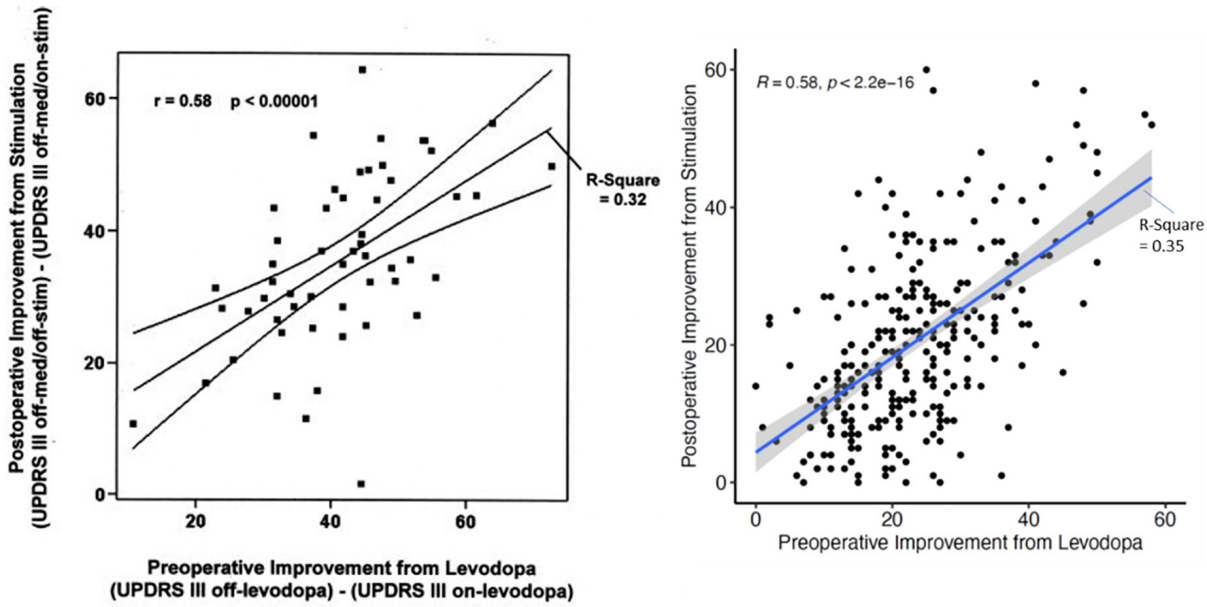

FIGURE 1 | The relation of the UPDRS III-improvement during the preoperative L-dopa-test and the postoperative improvement of the UPDRS III-score due to stimulation only for the first description in 2002 (Charles et al.; *n* = 56 patients) and current data from Kiel (*n* = 334 patients) with almost the same statistical relations. Nevertheless, the dispersion for individual patients is very large.

improvement > 33%) and advanced modeling and machine learning is applied, the best discriminators approximated an AUC of 0.65. Better fits could be obtained with restricted criteria (Habets et al., 2020). Although promising, much larger, pooled patient cohorts will be required to determine the limits of this methodology (Habets et al., 2020). The second approach will be to use more specific and dichotomized outcomes (e.g., tremor severity, quality of life, freezing) for prediction. This approach leads to improvement in the AUC of 0.86 for freezing or balance and improvement to 0.75 for quality of life (Gavriliuc et al., 2021; Jost et al., 2021; Yin et al., 2021). The second approach has more latitude for improvement.

Optimizing the Asleep Deep Brain Stimulation Surgical Procedure

DBS is currently a standard procedure for advanced PD. DBS is not only used for PD patients but can be applied for patients with other movement disorders including dystonia, essential tremor (ET) and psychiatric disorders. The wide range of applications suggests that enhancement of this technique could be far reaching. Many centers employ awake physiological navigation and stimulation assessments to optimize DBS localization and outcome. However, many patients remain fearful of the awake brain surgery, leaving a wide gap for therapeutic improvement.

To enable DBS under sedation, asleep DBS, we characterized the cortico-basal ganglia neuronal network of two non-human primates under propofol, ketamine and interleaved propofol-ketamine (IPK) sedation (Guang et al., 2021). Further, we compared these sedation states in the healthy and Parkinsonian condition to those of healthy sleep.

We found in polysomnography and neuronal activity recordings in animals treated with ketamine increases high-frequency power and synchronization while propofol increases low-frequency power and synchronization (**Figure 2**). Thus, ketamine does not mask the low-frequency oscillations used for physiological navigation toward basal ganglia DBS targets. The brain spectral state under ketamine and propofol mimicked rapid eye movement (REM) and non-REM (NREM) sleep activity, respectively, and the IPK protocol resembled the fast dynamics of the NREM-REM sleep cycle.

These promising results in animal models may be the first step toward asleep DBS with non-distorted physiological navigation. The clinical outcome and the subjective evaluation of the patients under the IPK sedation protocol should be tested in open and then prospective double-blind studies.

Fusing Electrophysiology and Neuroimaging for Optimal Deep Brain Stimulation

The identification of functional predictors using brain imaging and electrophysiological techniques is essential for improving direct planning of DBS implantation, but also for advancing developments in neuromodulation. One way to achieve this goal will be through the development of the fusion of multimodal imaging and advanced data analyses techniques from electrophysiological pre- and intraoperative recordings, that support electrode placement during the stereotactic procedure and the postoperative programming (Gonzalez-Escamilla et al., 2020; Muthuraman et al., 2020). This is particularly relevant when considering electrophysiological data in tremor patients,

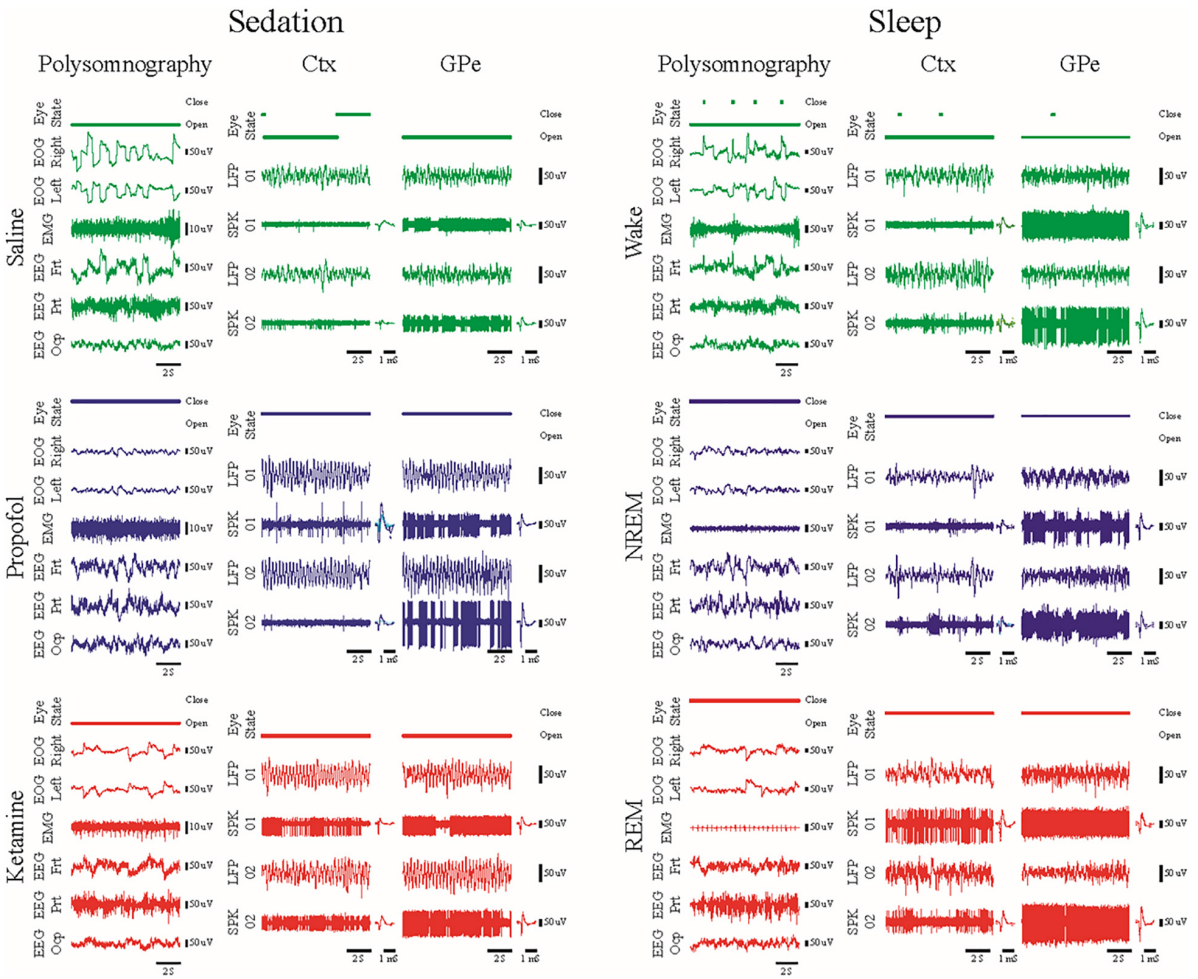

FIGURE 2 | Examples of 10 s traces of polysomnography (eye open/close state, EOG, EMG and EEG), local field potential and spiking activity (LFP/SPK) recorded in the frontal cortex and the external segment of the globus pallidus (Ctx/GPe) during sedation sessions (left, saline baseline—upper, green; propofol—center, blue; and ketamine—lower, red) and during the awake-sleep cycle (right, wake—upper, green; NREM—center, blue; and REM—lower, red). Modified with permission from Guang et-al 2021 (Guang et al., 2021).

using peripheral signals namely electromyography (EMG) and accelerometer (ACC) as vital techniques to assess the suitability for DBS treatment. We started by looking at the mean harmonic power of the accelerometer recordings in tremor patients carrying out a holding condition. We were able to distinguish between PD and ET patients with 94% accuracy and proposed this measure as a new diagnostic test (Muthuraman et al., 2011). Recently, we have developed measures like the tremor stability index and we compared them with the mean harmonic power and some new measures like cross frequency coupling between two EMG or ACC signals from different muscles (di Biase et al., 2017). To identify direct electrophysiological signatures which relate to these findings from the periphery, simultaneous measurement of electroencephalography (EEG) will be required. However, EEG recorded in patients receiving DBS induces artifacts in the frequency domain of the signals, namely at the frequency of the stimulation (130 or 160 Hz) and subsequent harmonics. To examine the frequency signatures, first the artifact needs to be removed. Instead of a simple low pass filter which takes all the information above the cut-off frequency, we were able to develop a method which takes into account both time and frequency domain dynamics (Santillán-Guzmán et al., 2013). Once the artifacts were removed, the oscillatory features could be estimated from the EEG signals, or local field potentials (LFP), which our group (Muthuraman et al., 2018; Tamás et al., 2018) and many other groups have shown as robust predictors (Litvak et al., 2021). We applied microelectrode recording and looked at the optimal predictor for subthalamic nucleus (STN) targeting and optimal trajectories and we were able to show both beta and gamma oscillatory activity as good predictors (Koirala et al., 2020). After identifying robust predictors, further work to translate the predictors to the clinical setting is ongoing. This process is outlined in **Figure 3**. We see a clear need for the multimodal integration of distinct features and models to tune and to understand the pathophysiological DBS mechanisms. In addition, models

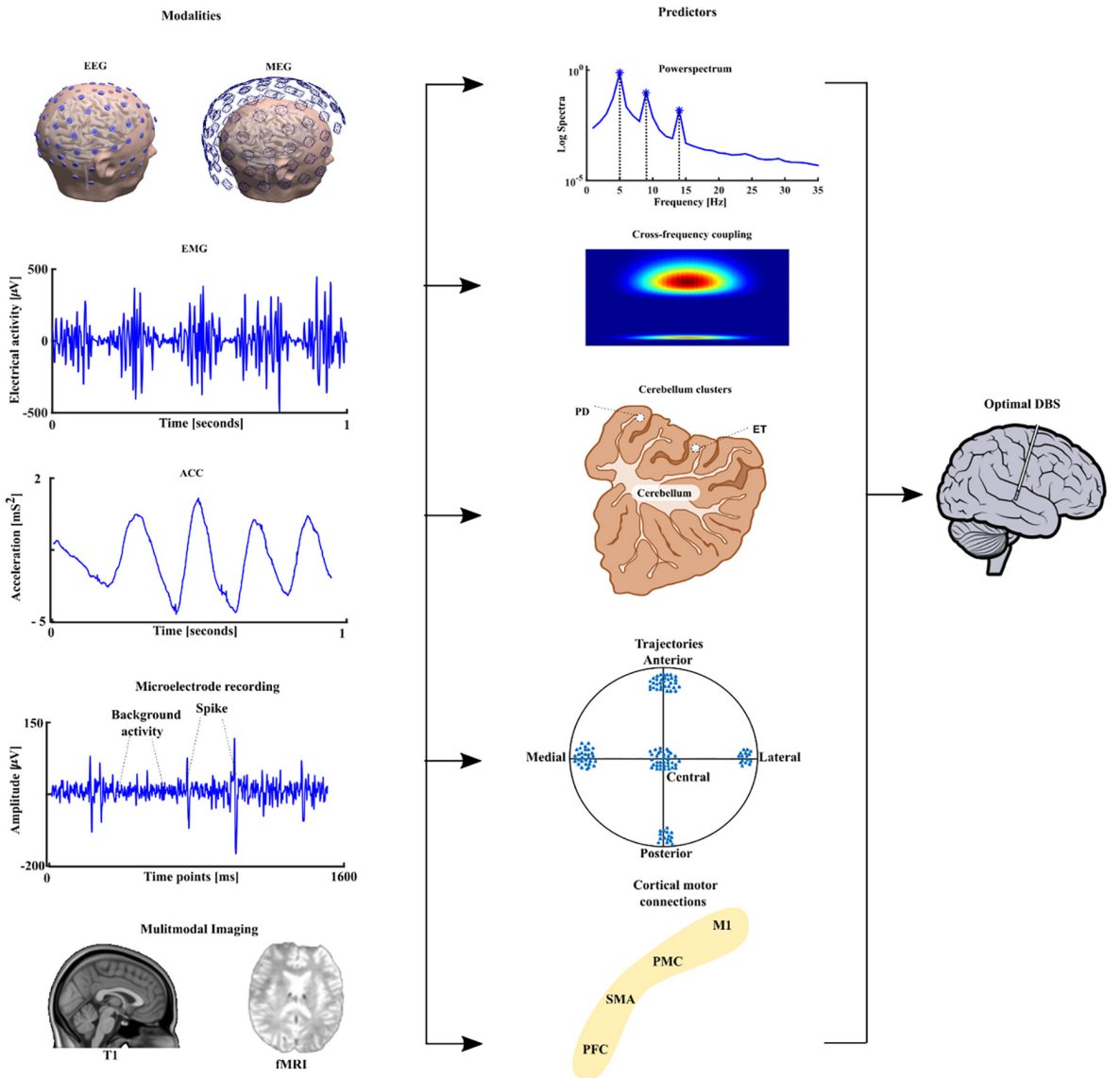

FIGURE 3 | The different modalities are depicted in the first column namely the electroencephalography (EEG), magnetoencephalography (MEG) followed by peripheral signals namely electromyography (EMG), accelerometer (ACC), microelectrode recording (MER), and neuroimaging namely structural T1 magnetic resonance imaging and functional magnetic resonance imaging (fMRI). The extracted predictors are shown in the second column power spectrum, cross-frequency coupling, source analyses-based cerebellum clusters for PD and ET. Trajectory based oscillatory predictors and finally cortical motor connectivity with the four main motor regions, primary motor cortex (M1), premotor cortex (PMC), supplementary motor area (SMA) and prefrontal cortex (PFC) to sub thalamic nucleus (STN). The multimodal integration of all these features can lead to optimal deep brain stimulation in PD patients.

for the long-term outcome prediction and improvement or real-time electrophysiological monitoring will be useful. These models should be easily introduced into clinical practice and should guide our focus of future directions, inclusive of sensor engineering.

Updates on Deep Brain Stimulation for Tourette's Syndrome in Australia

In our Neuroscience Centre (Neurosciences Queensland), DBS of the anteromedial globus pallidus internus (amGPi) has shown sustained significant benefit for Tourette's syndrome (TS), motor tics and non-motor symptoms such as obsessive-compulsive disorder (OCD), depression, and overall quality of life (Cannon et al., 2012; Sachdev et al., 2012, 2014).

Since 2008 we have performed DBS on 24 patients with severe medically refractive TS often with associated behavioral neuropsychiatric issues. Of these, the first two cases had leads implanted in the posteroventral globus pallidus internus (pvGPi) due to the severity of the motor tics and self-harm. In both of these cases, additional leads were placed in the Nucleus Accumbens (NAcc) to control significant obsessive-compulsive

symptoms. The original patient in 2008, prior to DBS, was institutionalized in an adolescent psychiatric facility but required removal of the DBS system in 2016, due to the implanted pulse generator and lead infection. This patient has remained stimulation free now for 5 years. There was significant return of her TS symptoms, but they are living with assistance in the general community.

The third patient had OCD symptoms greater than the motor and phonic tics, and the leads were placed into the NAcc with a good clinical outcome of the OCD, and to a lesser extent motor tics.

The remaining 21 patients had leads placed in the amGPI with significant benefit for TS and OCD symptoms as well as depression and overall quality of life. This benefit has been sustained over the years since these people had their surgery. They have had ongoing follow-up and important to note, minimal to no change in the DBS programming parameters were required beyond a 6–12-month time point post-operatively.

One patient with amGPi leads requested removal of the system as they did not feel any different in themselves, despite the fact they were able to obtain gainful employment and interact face-to-face with the public on a daily basis; they have been lost to follow-up.

Our experience now spanning 13 years, overall has demonstrated significant sustained clinical improvement in the quality of life of TS patients in both the primary TS symptoms as well as in sustained reduction in OCD symptoms, depression and improved quality of life.

We feel it is imperative to help medically refractive TS patients obtain wider access to DBS and we strongly support the aims of The International TS DBS Registry and Database. Large double-blind studies at a Class 1 level would delay this access due to low case rates. This delay would be at the cost of humanitarian benefit for TS patients, careers, and society.

Updates on Telemedicine for Deep Brain Stimulation Care in China

We recently introduced the advances of remote DBS programming in China. Our team made great efforts to design and to develop this remote programming system, which is now widely used in China. Safe remote communication is our priority. The team employed both software protection and hardware protection into the system. The system consists of a physician terminal, server, and patient terminal and offers personalized management and a user-friendly interface, plus real time video consulting and recording. In addition to DBS, the platform also works for vagus nerve stimulation, sacral neuromodulation, and spinal cord stimulation.

Over the past year, we developed an interactive video acquisition and learning system for telemedicine, which will be critical for remote programming. Specifically, the system can automatically record, provide video instructions, and provide real time interactive guidance, and control quality using advanced artificial intelligence (AI) techniques. It offers a default mode for recording with the help of others and a selfie mode for independent recording. Importantly, the system integrates face changing technology for privacy protection. Currently, we can change face identity while preserving facial movements like blinking. We also showed new advances in Bluetooth real time recording DBS: this technique not only stimulates the brain, but also records local field potential (LFP) activity, electrocardiography data, acceleration, and wirelessly transmits to a smart phone simultaneously.

We believe that the remote programming platform and system is highly innovative and will help to democratize DBS therapy. We expect new challenges in adopting this platform, such as the protection of patient privacy or capturing subtle symptoms from remote sensing.

Advances in Deep Brain Stimulation in Japan

Automatic DBS optimization may be a future perspective that may potentially improve DBS therapy. It includes two main directions: an automatic optimization of initial DBS settings and an on-demand adjustment of stimulation intensity. We performed a single-center, randomized, double-blind, crossover study to evaluate the performance of DBS programming by a closed-loop algorithm (CLA) using an external sensor-based motor assessment which was compared to a standard of care programming method (SOC) in terms of clinical outcomes and programming burden (Sasaki et al., 2021). Both motor score and sensor-based score were significantly improved by both SOC and CLA settings compared to the baseline. In addition, the programming steps were significantly reduced in the CLA settings compared to those in the SOC. This novel algorithm prospectively estimated the optimal stimulation settings for objective assessments and required minimum clinician involvement. Thus, this could lead to a reduction in the number of steps required to program a device in contrast to previous studies that required the same steps as the conventional monopolar DBS screening. This study was performed in patients with octopolar leads, but this novel DBS programming method may enable automatic programming even in more complex DBS leads, such as directional leads. Indeed, AI may upgrade algorithms that enable automatic programming even in more complex DBS leads, such as in a directional lead (Wenzel et al., 2021).

On-demand adjustments of stimulation amplitude using closed-loop stimulation or adaptive DBS may improve DBS therapy. In Japan, the Percept PC (Medtronic Inc.) was launched in November 2020. It offers adaptive stimulation functionality, which at this time is only approved for use in Japan. We are conducting a data collection study to observe the real-world practicality and performance of an adaptive DBS algorithm in patients with PD to observe the resulting LFP dynamics under adaptive DBS in 10 patients (Oyama et al., 2021). The preliminary data revealed that adaptive DBS using the dual-thresholds mode worked as expected. In addition, we are currently conducting a multi-center, open-label study to compare two different adaptive DBS modes; the single and dual thresholds mode, and a multi-center, randomized study to compare adaptive DBS (jRCT1042200088; jRCT1032210376).

THE FRONT LINE OF CUTTING-EDGE TECHNOLOGIES

Where Is the Future Going? *It's About Time*

Recent studies have highlighted that patterned stimulation may engage the nervous system in fundamentally different ways than can be achieved with conventional single-frequency stimulation (Tass and Majtanik, 2006; Mastro et al., 2017; Seier et al., 2018; Lo et al., 2020; Spix et al., 2020; Willsey et al., 2020; Ho et al., 2021; Pfeifer et al., 2021). Coordinated reset stimulation may affect synaptic plasticity and result in long-lasting (after stimulation is turned off) effects (Tass and Majtanik, 2006; Ho et al., 2021; Pfeifer et al., 2021). Spatio-temporal paired pulse stimulation can be used to induce spike timing dependent strengthening or weakening of synaptic connections between brain regions and might be used for therapeutic purposes (Lo et al., 2020). Burst stimulation may enable cell-type specific targeting, as recently shown in rodent models of PD and in thalamic stimulation studies in humans (Mastro et al., 2017; Spix et al., 2020; Willsey et al., 2020). Further, adaptive processes of the nervous system would be expected to respond differently to patterned stimulation than to single-frequency stimulation; for example, potentially avoiding the habituation sometimes seen in DBS for ET (Paschen et al., 2019).

The findings suggest the need for a flexible stimulation system that enables further exploration of current and novel patterns in DBS. Chronos is a new research software from Boston Scientific that utilizes the existing flexibility of the commercially available Vercise Genus™ pulse generators, to satisfy this need. Chronos allows the user to choose on a pulse-by-pulse basis, the polarity, amplitude, pulse-width, inter-pulse interval or rate and the spatial location of stimulation (electrodes) while applying historical stimulation safety limits. Importantly, no new firmware is required. Chronos works with the off-the-shelf rechargeable Vercise Genus pulse generators. The ability of Chronos to shape stimulation in time, complements the already existing capability to sculpt stimulation in space and will enable research on the potential of spatio-temporal patterned DBS.

Responsive Stimulation for Epilepsy

The Long-Term Treatment of responsive stimulation Trial in epilepsy showed a 75% median reduction in seizure frequency at 9 years (Nair et al., 2020). The RNS System Real World Outcome Study showed accelerated results with patients achieving 67 and 82% seizure frequency reductions at 1 and $\geq$ 3 years, respectively (Razavi et al., 2020). Interim results from an FDA mandated Post Approval Study reported a median 68% reduction at 1 year (Shin and Morrell, 2020).

The Responsive Stimulation for Adolescents with Epilepsy (RESPONSE) Study will begin enrollment in late 2021. This study will enroll 200 participants aged 12–17. The primary end points are the short-term serious device-related adverse event rate and responder rate at 1 year.

NeuroPace received a 5-year NIH grant for a collaborative effort involving eight U.S. academic centers. Six sites will enroll a total of 20 patients with Lennox-Gastaut Syndrome (LGS) and drug-resistant generalized onset seizures. Two sites will create patient-specific maps of the brain seizure networks, providing insight into how to personalize the treatment for each participant. The IDE based study, once approved by FDA, will evaluate the safety and effectiveness of the RNS System in treating seizures associated with LGS. Experience from the study will inform the design of a future larger clinical study. NeuroPace has received Breakthrough Device Designation status from FDA for the potential use of the RNS® System to treat idiopathic generalized epilepsy (IGE) and plans to pursue a clinical study. NeuroPace introduced several product updates including full body MRI conditional labeling, mobile updating of programming tablets, and the launch of the nSight Platform for streamlined physician review of patient data.

A Role for Local Field Potentials Signals in Supporting the Objective Guidance of Deep Brain Stimulation Therapy Programming and Titration

Next-generation DBS therapy systems have been developed that deliver both standard electrical stimulation therapy and record chronic LFP data through DBS leads implanted in the brain. Medtronic's first and second-generation DBS + sensing systems, the Activa™ PC + S and Summit™ RC + S, have been utilized in dozens of investigational studies of neurological disorders characterizing unique biomarkers of brain state changes associated with activities of daily living and disease symptomatic states, and for exploring the application of LFP controls signals in adaptive therapy algorithms (aDBS). More recently the Medtronic Percept™ PC with BrainSense™ technology was approved commercially worldwide, offering the capability to apply LFP sensing for monitoring brain activity under real-world conditions in potentially thousands of new DBS patients each year (Paff et al., 2020; Goyal et al., 2021; Jimenez-Shahed, 2021). Two initial case studies of the Percept™ PC implanted in Parkinson's disease patients report the key finding that the strength of the LFP signal spectral power in the beta range (e.g., 13–30 Hz) corresponds to akinetic rigidity symptoms and their responses to DBS and medication therapies (Feldmann et al., 2021; Koeglsperger et al., 2021), replicating previous studies using investigational recording configurations (Neumann et al., 2016; Ozturk et al., 2020). Importantly, one multi-center study also demonstrates a high prevalence of detectable LFP beta signals of interest in PD patients undergoing each DBS implant center's standard of care (Thenaisie et al., 2021), which is consistent with a previous multi-center analysis of data collected using the investigational Activa™ PC + S device. Additional Percept™ PC studies confirm the presence of LFP signals of interest in other approved DBS indications, including generalized dystonia, ET and epilepsy (Fasano et al., 2021; Goyal et al., 2021). Further, the emerging implications from these studies and others in progress strongly suggest a role for LFP signals in supporting the objective guidance of DBS therapy programming and titration (Fasano et al., 2021; Sirica et al., 2021). Moreover, several ongoing industry-sponsored trials are evaluating the safety and

effectiveness of LFP-beta controlled aDBS in PD. aDBS is already commercially unlocked in the Medtronic Percept^{TM} PC in Japan, where early published results are promising and continue to build upon the evidence of aDBS patient benefit demonstrated by several previous investigational trials (Little et al., 2013; Arlotti et al., 2018; Velisar et al., 2019; Nakajima et al., 2021). Overall, the recent widespread availability of LFP sensing technology embedded in commercial DBS devices offers unprecedented access to objective real-world data and promises a faster path to personalized care for DBS patients. Nonetheless, this large and growing amount of sensing data now being made available by DBS and potentially other neuromodulation devices highlights a critical need for the development of specialized algorithms, tools and infrastructure in order to provide the most potential benefit for patients (Chen et al., 2021).

NEUROETHICS OF NEUROMODULATION "OVERSEAS AND OUTSIDE THE LINES"

DBS and implantable neurotechnologies are transforming into a more globalized phenomenon. While major advancements in the field are occurring, primarily in developed countries, these advancements have spurred bioeconomic dependencies between developed, developing, and non-developed nations. Such multi-national efforts have brought into focus the culturally based distinctions in ethical norms and practices that would govern (and thus either constrain or advance) research and translational enterprises (Shook and Giordano, 2017; Giordano, 2018). This differential permissibility and capability has given rise to growing enterprises—and markets—in research and medical tourism.

Of note is that differing ethico-legal standards, when coupled to incentives for multi-dimensional (e.g., economic, social, political, military) leverage (if not hegemony) may result in incurring concerns about safety and security (DeFranco et al., 2020). Thus, while efforts in DBS are aimed at achieving definable "goods" (e.g., treating disease and injury), it is important to address which "goods" are being posited, and the idiosyncratic as well as systemic benefits, burdens, and risks in and across multinational scales that could most likely be incurred by such use(s) in practice (Giordano, 2015, 2017; DeFranco and Giordano, 2020).

Toward such ends, we propose a paradigm of "biosecurity-by-design," yoked to a cosmopolitan-communitarian neuroethico-legal approach to accurately assess, depict, and mitigate (if not prevent) probable and possible near- and intermediate term effects of DBS use in various contexts (Lanzilao et al., 2013; Shook and Giordano, 2014; DiEuliis and Giordano, 2021).

The Risks of Differing Ethics to Public Health and National Security

As innovations in neurotechnology such as DBS continue to advance, the use of DBS in military members should be carefully assessed. While primarily used for restoration of health and function (e.g., PTSD or depression), there is a growing trend toward use of neuromodulation for cognitive or behavioral optimization (Lavano et al., 2018; Cinel et al., 2019; Wu et al., 2021). Studies have shown that the most concerning ethical, legal, and social implications of the use of neurotechnology in healthy individuals involves long term safety, invasiveness, reversibility, data security, device security, and social perceptions (Funk et al., 2016; Emanuel et al., 2021). Global economic and military competition will continue to drive much of the policy conversation, as US competitors such as China pursue military advantage through neurotechnologies in combination with artificial intelligence and machine learning advances (Kania, 2019; Center for Security and Emerging Technology et al., 2020). Thus, there exists a compelling need for early risk assessments that involve subject matter expert input, not only to develop risk mitigation strategies, but to enable the discussion of realistic expectations of what neurotechnology such as DBS can potentially deliver. The Think Tank session provided a robust discussion of these issues and offered some novel considerations of device ownership, regulatory approvals, and the potential inevitability of neurotechnology use outside of the amelioration of disease or medical supervision.

A Proposed "Internationally Relevant" Neuroethicolegal Framework for Deep Brain Stimulation

DBS has proven to be interactive with, and transformational upon, the self-conceptions and patient self-identity. Medical ethical demands include non-maleficence, beneficence and autonomy. However, these retrospective criteria, while necessary, are not sufficient for brain interventions such as DBS to be able to affect prospective agency: one's ongoing self-conception and self-determination. DBS can be implicated with transforming identity. Narrative ID is about "Who am I becoming?" and possible self-estrangement whereas relational ID is about "How will I be conducting myself?" and the future potential for social estrangement. To address implications for patient identity and autonomy, we must keep in mind how agency and autonomy are generally not considered neurological or physiological matters. DBS cannot be applied in a "medically neutral" environment. The social surroundings and cultural traditions will impact DBS. Questions must be asked to challenge culture-bound presumptions. How do people experience the application of DBS in the ongoing course of their lives within their own social groups? How do people assess DBS's value for themselves, in terms of their healthcare needs and their mutable self-conceptions and values? How has the application of DBS for members of society been evaluated for responsible innovation, genuine social need and justice? How does a culture generally assess DBS's impacts on people's lives, according to customary values, cherished ideals, and established laws? In general, a brain cannot determine the self, since self-conceptions are tied to social capabilities. Neuroethics should not presume that one nation's culture holds unique standards for mental health, responsible agency and good character.

INTERVENTIONAL PSYCHIATRY: UPDATES FROM THE NIH BRAIN INITIATIVE

Non-linear Recovery in Electroencephalography and Fine-Grained Behavior During Subcallosal Cingulate Deep Brain Stimulation for Depression

Evidence from studies of subcallosal cingulate (SCC) DBS for treatment resistant depression demonstrate that antidepressant effects occur in two stages: a rapid change in negative mood and psychomotor slowness with initial bilateral stimulation at the optimized target within the SCC white matter, and a slower progressive improvement in symptom ratings over weeks to months that if achieved, is generally maintained long-term. Combined behavioral, imaging, and electrophysiological strategies may facilitate a more fine-grained characterization of this chronology. We describe our strategic acquisition of qualitative and quantitative behavioral measures with LFP recordings suitable for both direct hypothesis testing and for unsupervised machine learning approaches. Building on previous experiences using weekly standardized ratings and video analyses of weekly clinical interviews, our studies capitalize on twice daily sampling of SCC LFPs, self-report behavioral ratings, online depression severity scales and video diaries with concurrent SCC LFPs. These results demonstrate that there are meaningful behavioral features that track with acute and chronic brain changes, potentially enabling the future development of clinically tractable biomarkers that can be used to guide therapy.

New Data-Driven Electrophysiology Outcome Measures and Insights Into Subcallosal Cingulate Cortex Deep Brain Stimulation for Depression

The SCC has been an effective target for DBS in treating patients with treatment-resistant depression, but individual patients exhibit high variability in recovery trajectories. Understanding the changes in neural activity underlying sustained recovery will help us to identify a physiological marker to track this variability in recovery trajectories. The marker is also particularly relevant in the context of adaptive neurotechnologies for CL stimulation. The increasing interest in adaptive neuromodulation has led to the collection of large amounts of multi-modal data, as well as to the application of machine learning (ML) techniques to provide insight. In conventional ML approaches, there is typically a tradeoff between complexity and interpretability: simple models can be interpretable but capture only rudimentary structure in the data, while complex "black-box" models can capture more intricate relationships at the expense of interpretability. Recently, the framework of "explainable artificial intelligence (xAI)" has introduced approaches that aim to explain these powerful "black-box" models, making them especially suited for identifying biomarkers. During this Think Tank, we discussed an example of using generative causal explainers (GCE) to analyze an existing machine learning network and its associated output data (O'Shaughnessy et al., 2020). The GCE is a type of neural network that will capture features from an existing ML network and identify a spectral discriminative component (SDC). This SDC represents the relationships between the original training data and output that were not provided by the original machine learning model and can then be used to identify potential biomarkers. We have collected LFPs from six participants undergoing SCC DBS who showed variable recovery trajectories preceding robust therapeutic response at the 24-week endpoint. We used recently developed techniques from xAI to show that meaningful objective markers of disease state can be extracted from LFP data that correspond to independent behavioral and anatomical measures. These results demonstrate the potential for xAI techniques to be used to develop biomarkers in complex neuromodulation therapies.

Combined Cortical and Subcortical Recording and Stimulation as a Circuit-Oriented Treatment for Obsessive-Compulsive Disorder

OCD is associated with hyperconnectivity in a specific cortico-striato-thalamo-cortical (CSTC) circuit including the orbitofrontal cortex (OFC), the head of the caudate and the dorsomedial nucleus of the thalamus. Traditional DBS at the FDA-approved ventral capsule/ventral striatum (VC/VS) target for intractable OCD is believed to exert its beneficial effects by disrupting this hyperconnectivity. Here we present a case report of an attempt to desynchronize this CSTC circuit using multi-site stimulation: the standard VC/VS target plus bilateral cortical leads at the supplementary motor area (SMA). Clinically, the patient's Yale–Brown Obsessive Compulsive Scale (YBOCS) score decreased from the low 30's to 16. There was immediate subjective improvement, with a sense of ability to focus away from obsessions, without the mirthful or anxiolytic qualities of VC/VS stimulation. This took years to be reflected in the YBOCS. Physiologically, there was a hyper-synchronized peak in the high alpha band in both acute intraoperative and long-term Medtronic PC + S recordings. It was stimulation sensitive, but contrary to the initial model, synchrony increased over time, and higher synchrony reflected clinical improvement. These preliminary findings suggest that multi-site stimulation may be effective for treating intractable OCD. Electrophysiological biomarker changes may be associated with this improvement. These changes may reflect a DBS mechanism where hypo-functioning CSTC loops are augmented, rather than a disruption of a hyper-connected loop.

Deep Brain Stimulation for Depression Using "Inverse Solutions" Enabled by Intracranial Recordings

Current biological views suggest that (1) disorders of mental health are network disorders, and (2) that they therefore demand network-minded solutions. With this idea in mind, we embarked on our NIH-funded (UH3 NS103549) trial (NCT03437928) of

DBS for treatment-resistant depression (TRD). Our approach borrows the platform of intracranial recording and stimulation which is common to the field of epilepsy surgery (Allawala et al., 2021). We recruited patients with severe TRD implanted with bilateral DBS leads in both sub-callosal cingulate (SCC) and ventral capsule/ventral striatum (VC/VS) targets. In addition, we implanted stereo-EEG (sEEG) electrodes in regions across the putative frontotemporal network which were relevant to TRD (Vedam-Mai et al., 2021). This strategy facilitated recording from mood-relevant areas during rest, during specific activities and behavioral tasks, and while delivering stimulation across a wide range of parameter space. Following this inpatient phase, the sEEG electrodes were removed, and the patient continued in an outpatient trial consisting of an 8-month open label optimization phase followed by a randomized, double-blinded discontinuation phase.

An important innovation in this trial was the use of intracranial electrophysiology data to calculate "inverse solutions": DBS parameters that are calculated to produce a healthier brain network state (as measured by neural activity on the sEEG electrodes) and therefore to reduce symptoms. Our first attempt at this calculation involved a template-matching process. We determined a desirable network state based on both spontaneous mood changes and mood changes induced by a behavioral task. We also measured network states produced by stimulation across many parameter combinations (**Figure 4**). We then used an iterative general linear model to identify parameter combinations that best matched the desired state. The first subject in this trial achieved remission that was robust to the double-blinded discontinuation, suggesting true rather than sham response to DBS.

ADVANCES IN ADAPTIVE DEEP BRAIN STIMULATION

Optimizing Subthalamic Adaptive Deep Brain Stimulation for Parkinson's Disease

Successful aDBS in neurological diseases requires inputs that are relevant to the behavior targeted for therapy. Although Subthalamic Adaptive Deep Brain Stimulation (STN aDBS) has been shown to be safe, feasible, efficacious and more efficient than open loop or continuous (c)DBS, several variables remain to be optimized (Little et al., 2013, 2016a,b; Rosa et al., 2015; Malekmohammadi et al., 2016; Cagnan et al., 2017; O'Day et al., 2020). The STN alpha and beta LFP power spectrum usually comprises more than one band and one of these may demonstrate more attenuation from STN DBS than the other (**Figure 5D**; Shreve et al., 2017; Afzal et al., 2019). The beta band with the greatest power has been the usual neural input and we have shown that aDBS driven by either the modulated or unmodulated band was efficacious (Afzal et al., 2019). Both dual and single threshold control policy algorithms are feasible (**Figures 5E,F**), and depend on choosing beta thresholds that correspond to the minimum and maximum DBS intensities (Imin, Imax) that provide acceptable therapy, which we determine using individual titrations of DBS intensity during movement (**Figure 5**; Little et al., 2013; Velisar et al., 2019; Kehnemouyi et al., 2021). Other relevant neural inputs include prolonged beta burst durations, which are related to disease severity, bradykinesia, and freezing of gait (FOG) (Tinkhauser et al., 2017; Anidi et al., 2018; Kehnemouyi et al., 2021). aDBS can also be driven by relevant behavioral inputs, such as tremor intensity or gait kinematics (Malekmohammadi et al., 2016; Cagnan et al., 2017; Herron et al., 2017; O'Day et al., 2020; Diep et al., 2021). The goal of therapy will determine the rates, at which DBS intensity is adjusted: slow ramps will adjust DBS intensity based on the time course of the onset and offset of medication doses, whereas faster ramps may respond to beta burst durations, and stochastic events such as tremor or FOG (Arlotti et al., 2018; Petrucci et al., 2020a,b, 2021). These therapy values can be determined on an individual basis.

Adaptive Deep Brain Stimulation in Parkinson's Disease: Technical Considerations and Lessons Learned

Efforts to develop aDBS in PD have focused on two different strategies: (1) Detection and truncation of pathologically prolonged bursts of beta oscillatory activity, on a time scale of seconds ("fast" aDBS). (2) Detection of neurophysiologic signatures of medication "on" and medication "off states, with concomitant decreases and increases in stimulation amplitude on a time scale of minutes to hours ("slow" aDBS). A challenge with fast aDBS is that rapid changes in stimulation have been associated with brief electrical artifacts whose spectral signature is broadband. Thus, rapid down-ramping at the end of a beta burst may produce an artifactual detection of elevated beta activity, triggering an inappropriate increase in stimulation even in the absence of underlying beta bursting. Mitigation strategies include blanking of sensing during an interval after stimulation ramp-down and reducing the difference between stimulation amplitude limits. A challenge of slow aDBS is that many empirical iterations of aDBS parameters may be required for personalized optimization. We have developed a "principled" approach for rapid prototyping of adaptive control policies for slow aDBS. First, we identify upper and lower stimulation limits corresponding to a patient's needs in different medication states, in the clinic setting or at home. We stream time series neural activity at those two stimulation amplitudes for several medication cycles. We then plot the statistical distribution of spectral power at each frequency band up to 90 Hz, and identify bands that best distinguish medication states, and can do so regardless of stimulation amplitude (**Figure 6**). These frequency bands or band combinations are then used in a dual threshold control policy with lower and upper thresholds determined by percentiles of the biomarker distributions.

Using Physiology to Drive Tremor Suppression

ET is defined as a rhythmical, involuntary, oscillatory movement of the limbs and is one of the most common movement disorders DBS has been an effective therapy for the suppression of

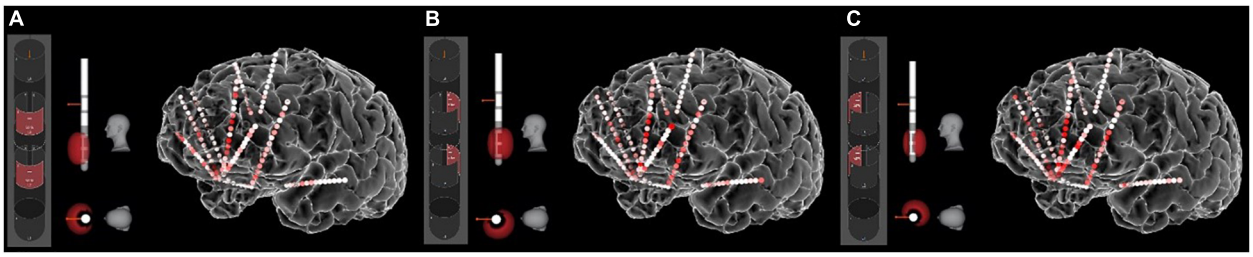

FIGURE 4 | Stimulation-induced network states. The sEEG recordings allow us to measure the "neural state" produced by any particular set of stimulation parameters. Here the heat map shows gamma (40–70 Hz) power in response to stimulation of various contact combinations on the left SCC DBS lead. **(A)** Contact configuration 2–5 (anterior stack of segmented contacts). **(B)** Contact configuration 3–6 (posterior-left stack). **(C)** Contact configuration 4–7 (posterior-right stack). Other parameters were frequency of 130 Hz, pulse width of 180 ms, and amplitude of 5 mA. Other combinations of these parameters produce different neural states, all of which can be quantified with the sEEG recordings.

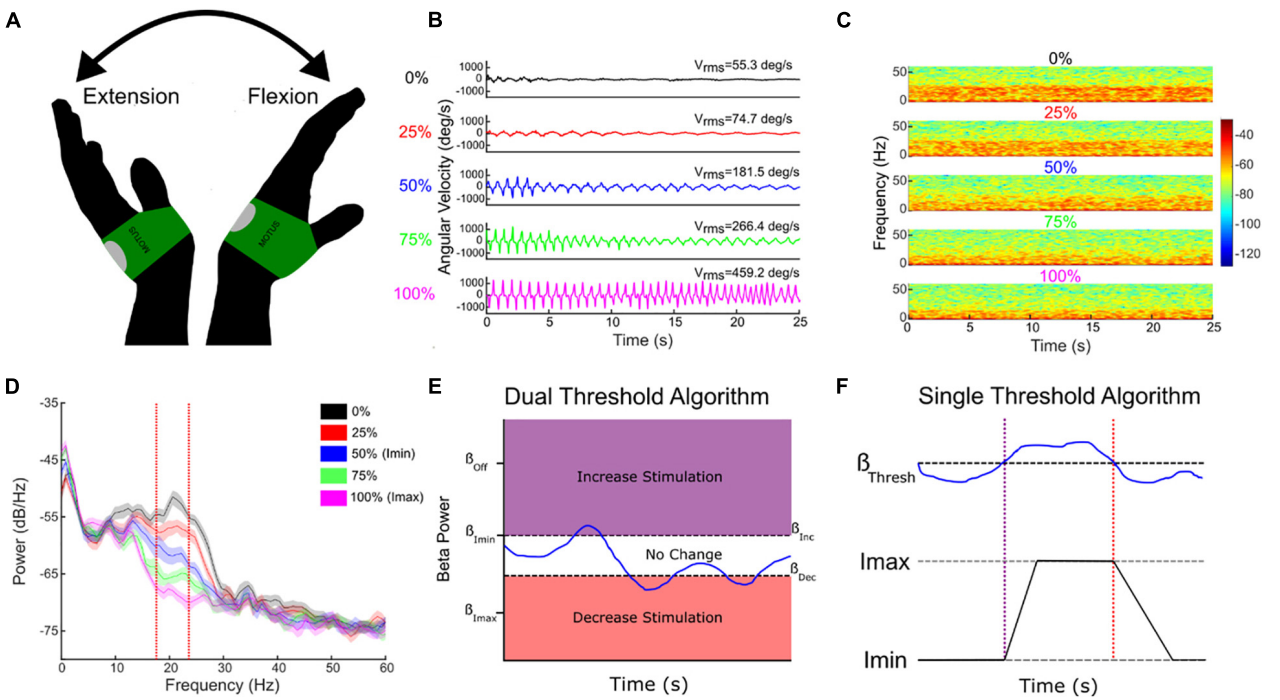

FIGURE 5 | Individual randomized presentations of STN DBS intensity, normalized to the maximum tolerated without side effects (Imax, 100%, pink traces), during a repetitive wrist flexion extension task **(A,B)**, determine the safe and acceptable range (Imin (here 50% Imax) to Imax), through which DBS intensity will fluctuate **(B–E)**. Corresponding beta power measured at Imin and Imax determine the upper and lower beta thresholds for the dual threshold algorithm **(D,E)**, and the beta power for the single threshold algorithm **(F)**. Blue line **(E,F)**—fluctuating beta power.

medically refractory tremor. However, as intention tremor occurs mostly in the upper limbs during the initiation and execution of goal-directed reaching motions, while it is absent at rest, continuous stimulation (cDBS) is in large part unnecessarily delivered, consequently leading to inefficient therapy and unneeded potential DBS-induced side-effects. An aDBS approach facilitates targeting a direct or indirect neuromarker(s) of reference, to deliver stimulation only when the patient truly needs it (e.g., during movement).

We established the feasibility of behavior-based aDBS for ET, fully embedded in a chronic investigational neurostimulator (Activa PC + S), for three patients implanted with a VIM-DBS, enrolled in a longitudinal (6 months) within-subject crossover protocol (DBS OFF, cDBS, and aDBS). As tremor manifests once movement is initiated, we explored the efficacy in modulating the stimulation amplitude based on the cortical motor activity of the patient's upper limbs. The proposed aDBS paradigm resulted in clinical efficacy and tremor suppression comparable with cDBS within a range of common actions (cup reaching, proximal and distal posture, water pouring, and writing), with a considerable reduction of stimulation delivered, showing the potential for integrating DBS therapy with the patient behavior and for potentially addressing pitfalls of cDBS for ET, such as DBS-induced side effects and premature device replacements.

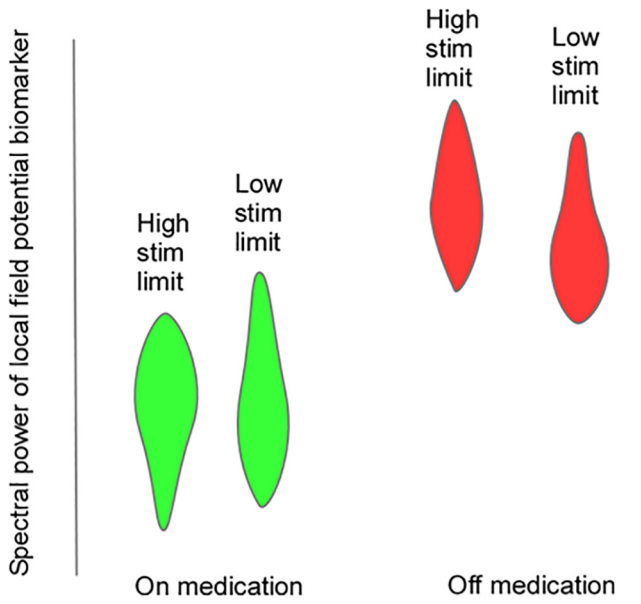

FIGURE 6 | Hypothetical violin plots showing distribution of a putative LFP biomarker that would be useful for "slow" aDBS. The biomarker distributions distinguish on-medication (green) and off-medication (red) states at both upper and lower stimulation amplitude limits.

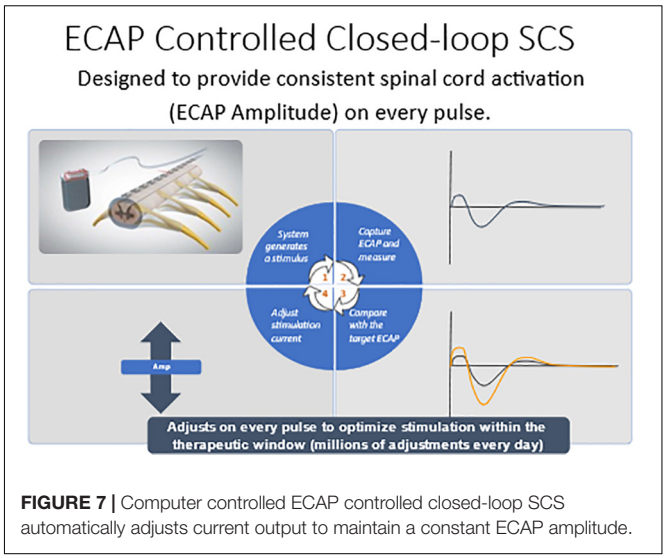

FIGURE 7 | Computer controlled ECAP controlled closed-loop SCS automatically adjusts current output to maintain a constant ECAP amplitude.

NEUROMODULATION FOR PAIN

Real-Time Evoked Compound Action Potential Controlled Closed-Loop Spinal Cord Stimulation

Evoked compound action potential (ECAP) recording provides an objective measure of spinal cord (SC) activation during spinal cord stimulation (SCS) and can assist in programing of the SCS system. The Evoke Study Group conducted a double-blind randomized controlled trial (RCT) to compare the safety and efficacy of real-time ECAP-controlled closed-loop stimulation (investigational group) with open-loop (fixed output) stimulation (OL, control) to treat chronic back and leg pain.

There were 134 subjects enrolled and randomized after test trial leads were implanted. The target ECAP amplitude was recorded on the same lead as the stimulating electrode was set in the clinic and it was maintained either manually by the patient (OL) or by a computer-controlled feedback closed-loop control (CL) mechanism (**Figure 7**). The primary endpoint evaluated as $\geq$ 50% reduction in overall back and leg pain as measured by the Visual Analog Scale (VAS). Opioid usage and other patient-reported outcomes (PROs) including emotional/physical functioning, sleep quality, and quality of life were also collected. Additionally, objective neurophysiological data, including SC activation and time spent in the therapeutic range, were collected.

Herein the Evoke Study Group reports the 24-month outcomes from this ongoing RCT. The proportion of implanted subjects with $\geq$ 50% overall back and leg pain reduction at 24 months was statistically superior in the EVOKE CL vs. OL group (84.0 vs. 65.9% subjects, respectively; $p = 0.040$) (**Figure 3**). Long-term improvements in all other PROs, including Profile of Mood States, Oswestry Disability Index, Pittsburgh Sleep Quality Index, EuroQol quality of life (EQ-5D-5L), and the Short-Form Health Survey (SF-12), were also demonstrated. In addition, the patient/physician identified the target ECAP amplitude during programming that was the same for both groups, however, the OL group was unable to maintain this ECAP target in the outpatient setting (**Figure 8**). The most frequent level of SC activation was three times greater for CL (median ECAP Amplitude: 22.5 μV CL vs. 7.5 μV OL).

SC activation was better maintained within the therapeutic range with EVOKE CL (median: 93.9% CL vs. 46.1% OL). There were no differences in the safety profiles between treatment groups, and the type, nature, and severity of adverse events were similar to other SCS studies.

In this ongoing study, ECAP-controlled closed-loop spinal cord stimulation provided statistically superior pain relief and greater improvement in all other measures compared with the OL group at 3, 6, 12, and 24 months. This significant improvement in clinical outcomes was consistent with the CL group being able to better maintain the targeted spinal cord activation level as measured by the stability in the ECAP amplitudes.

Personalized Circuit Mapping and Deep Brain Stimulation for Pain

Pain is the most fundamental human experience yet understanding of basic brain mechanisms relevant to human disease has been elusive. Following the workflow for refractory epilepsy, we proposed trialing brain stimulation and recording through temporary placement of invasive electrodes to identify therapeutic neural targets for each patient. After such a trial, we have been able to achieve enduring pain relief for research subjects by targeting these brain regions with a permanent DBS system. Although this process was labor intensive and economically more challenging, this approach could provide flexibility needed to address the wide heterogeneity observed in

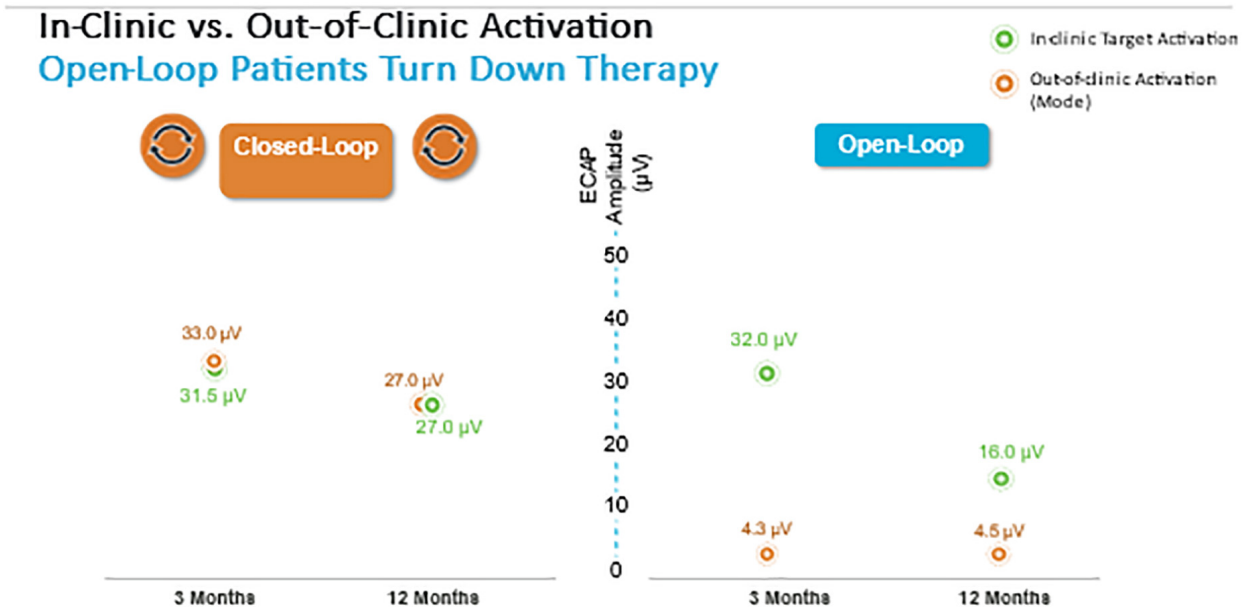

FIGURE 8 | Closed-loop but not Open-loop group was able to maintain the target ECAP level in the clinic and well as in the out of clinic environment.

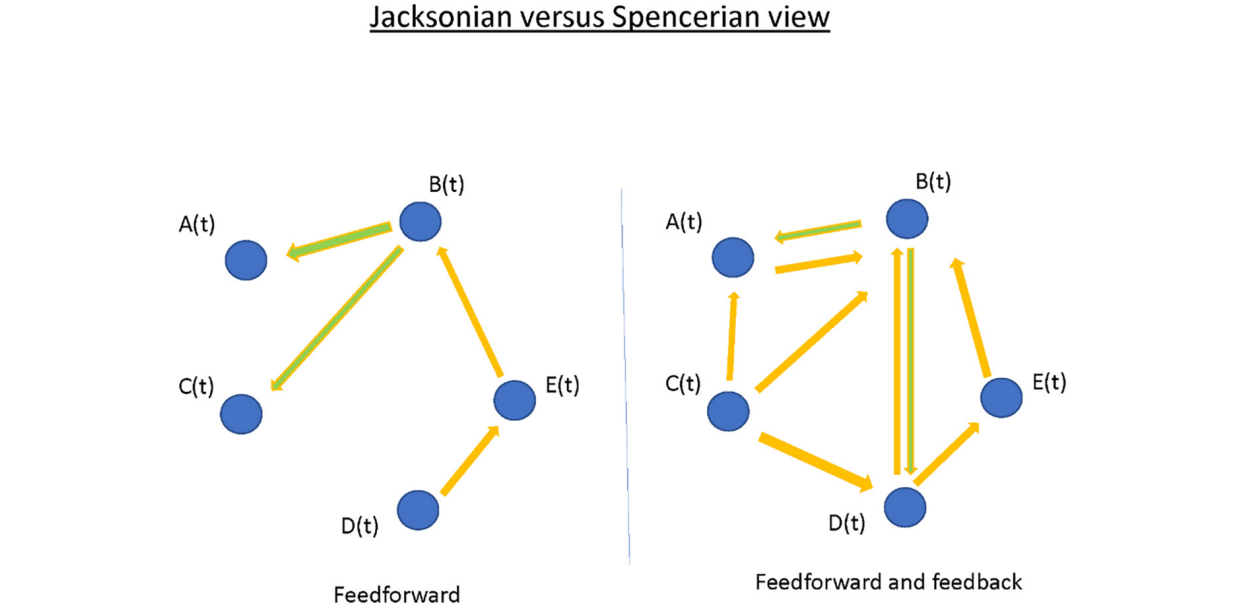

FIGURE 9 | Network propagation models of partial epilepsy syndromes.

individual brain function during pain. Fundamental questions regarding optimizing brain stimulation for chronic pain remain. Is experimentally induced pain supported by similar brain circuits as a legitimate chronic pain syndrome(s)? If a brain region harbors signals important for decoding an individual's pain state, can stimulating this same region modify pain perception? While working toward answers to such questions, some early clues have emerged. The research community should be more sensitive to quantitative measures of pain that have a wide dynamic range within subjects. Brain-based neurophysiology methods such as intracranial recording and electroencephalography (EEG) may help to better characterize clinical pain phenotypes. Finally, to avoid the long-term loss of therapy that has plagued many prior DBS efforts for pain, it may help to limit the cumulative electrical dosage by using adaptive stimulation paradigms. Solving these critical issues will aid in the development of new options to treat refractory chronic pain.

NETWORK MODULATION FOR DRUG RESISTANT EPILEPSY

Drug Resistant Epilepsy: Generalized and Focal Epilepsy Networks

Positing focal epilepsy as a "disorder of brain networks" has several interpretations. In one sense, the comorbidities associated with chronic partial epilepsy—memory dysfunction, or anxiety and depression—imply compromise of functional networks involved in integrated cortical action. In another and more immediate sense, the phenomenon of the seizure itself is proposed as a collective property of multiple, non-contiguous, brain areas. The latter view, often traced back to Spencer, seemingly countermands the traditional ("Jacksonian") view of a partial seizure having a delimited "focus" that recruits other brain areas by propagation (**Figure 9**; Spencer, 2002). I argue that the Jacksonian and Spencerian views are not mutually exclusive. I describe three cases of focal epilepsy, all investigated by invasive EEG (stereo-electroencephalography; SEEG), where seizures were observed to behave at either extreme and/or at an intermediate level. More abstractly, I propose the Jacksonian view as modeled by a network with feed-forward connections only, such that information (i.e., seizure) flows along a definite causal path. In contrast, the Spencerian view is modeled by both feedforward and feedback connections, where coupling between nodal network elements makes the question of an "initiating" focus and the direction of its propagation irrelevant. I speculate all focal epilepsies fall within the spectrum defined by these extremes. Finally, I outline the analytical challenges in understanding multivariable interacting dynamical elements such as in the proposed conceptualization. However, rational choices for surgical therapies and neuromodulatory targets for the most difficult patients may depend on scientific progress.

Reassessing the Purpose of Stereoelectroencephalography

During surgical treatment and assessment for epilepsy, patients are considered in multidisciplinary epilepsy conference (MDEC) by a team of neurologists, neuroradiologists, psychiatrists, neuropsychologists, and neurosurgeons. The patients' symptoms surrounding seizure (semiology), brain imaging (abnormality = "lesional"), and scalp electroencephalography are compared for agreement (concordance) by the team. In the case of concordance indicating seizure initiation from a non-eloquent brain site, we proceed to resection to cure the epilepsy. In cases of indeterminate concordance surgical implantation of monitoring intracranial electrodes, including brain-penetrating, Stereoelectroencephalography (sEEG) electrodes may further localize the seizure onset. The current paradigm is to place each sEEG lead in a candidate brain region to identify (or to rule out) a resectable seizure onset zone. However, the likelihood of ultimate resection with excellent outcome (Engel 1) for a patient considered in MDEC can be as low as 10–20%, with the likelihood increasing to ∼30–40% for those who undergo intracranial monitoring (about ∼50% of the ∼60% who proceed from intracranial monitoring to resection) (Téllez-Zenteno et al., 2005; Noe, 2013; Jehi, 2015). For patients who do not undergo resection, or those with persistent seizures refractory to resection, implanted brain stimulators are an important palliative option for potential reduction of seizure frequency and intensity.

Brain stimulation for epilepsy currently falls into two general paradigms: The first of these is stimulation of the electrophysiologically-identified seizure onset zone(s) (SOZ)—the node(s) idiosyncratic to each patient's epilepsy. This stimulation with a "customized construct" may be responsive to detected electro-graphic activity, or it may be OL with pre-set stimulation parameters (Morrell, 2006). A second paradigm is to stimulate additional network nodes in the seizure circuit that are not at the SOZ but is a common site of confluence. These sites will be the same across different patients, with a "general construct," and typically target a thalamic nucleus. To date, the anterior nucleus of the thalamus (ANT) is the only location to be assessed through an FDA premarket approval clinical trial (Fisher, 2010; Salanova, 2021). However, one size does not fit all when it comes to thalamic nuclei, and the ANT, a component of limbic circuitry, is not a universal node in all seizure networks. Epilepsies come from discernible networks, so the nucleus of thalamic stimulation should be determined by the putative network involved. The centromedian nucleus is suggested for basal-ganglial, motoric, and generalized epilepsies; the pulvinar has been suggested as a common target for occipital-onset seizures, and those with eye movement semiologies; the central lateral (intralaminar) nucleus is being trialed for non-lesional, extratemporal epilepsies of impaired awareness; further such targets will be identified based upon the evolving neuroscientific understanding of how the hemispheres interact with the thalamus (Gummadavelli, 2015; Warren, 2020; Burdette, 2021). We propose that each patient's epilepsy should be characterized for distinct thalamic and hemispheric nodes for potential stimulation, depending on semiology, electrophysiology (ictal and inter-ictal), and stimulation during sEEG monitoring (test stimulation and stimulation evoked potentials). As we move to more optimized stimulation constructs, we will move beyond a "node-based" philosophy, toward a "network-based" philosophy, using patient-specific diagnostics to stimulate multiple nodes within and across networks (**Figure 10**).

Because most patients will not progress to an excellent outcome by way of resection, we propose that the role of sEEG should be elevated to emphasize optimization of subsequent stimulator implant in addition to the traditional role of identifying resection regions. After the period of diagnostic passive monitoring for seizure localization, test stimulation through the sEEG leads may be performed, monitoring the patient for reduction in seizures or a reduction in interictal epileptic spiking rate (Lundstrom, 2019). A trial of CL sense-and-stim during this period is also possible (Kossoff, 2004). Single-pulse electrical stimulation is an emerging tool to study interactions between network nodes, with new insight(s) enabling simplifying interpretation circuit electrophysiology (Miller et al., 2021). Informed placement of thalamic electrodes may be performed to understand stimulation targets and seizure propagation, though these sites are not a potential resection

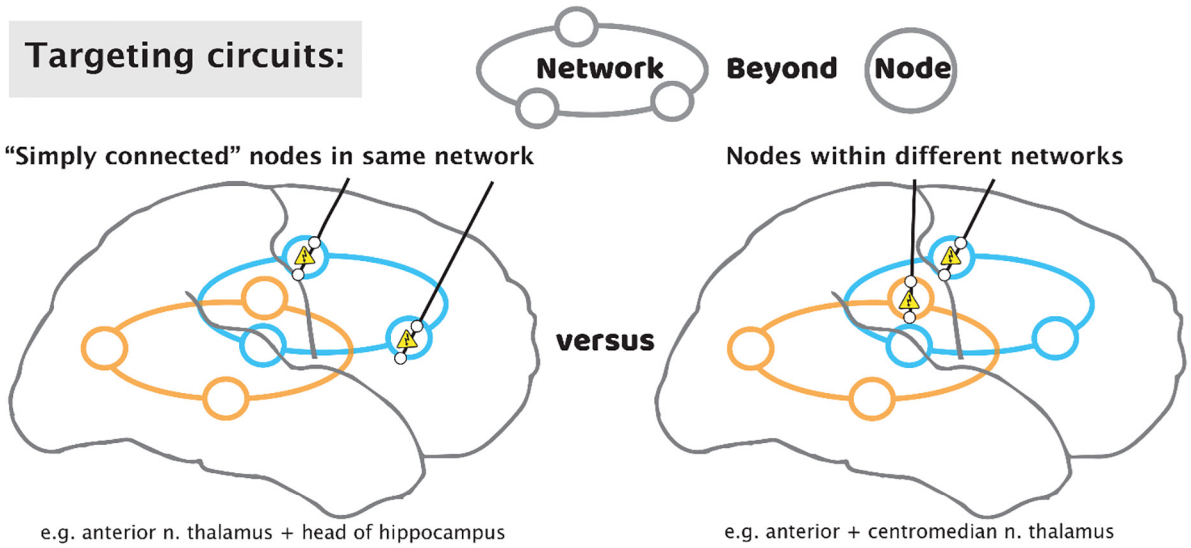

FIGURE 10 | Targeting circuits with stimulating leads for epilepsy. As we move beyond a paradigm that focuses solely on the seizure focus, approaches may include targeting of multiple "simply connected" nodes in the same network **(left)**, or tandem nodes within different networks **(right)**.

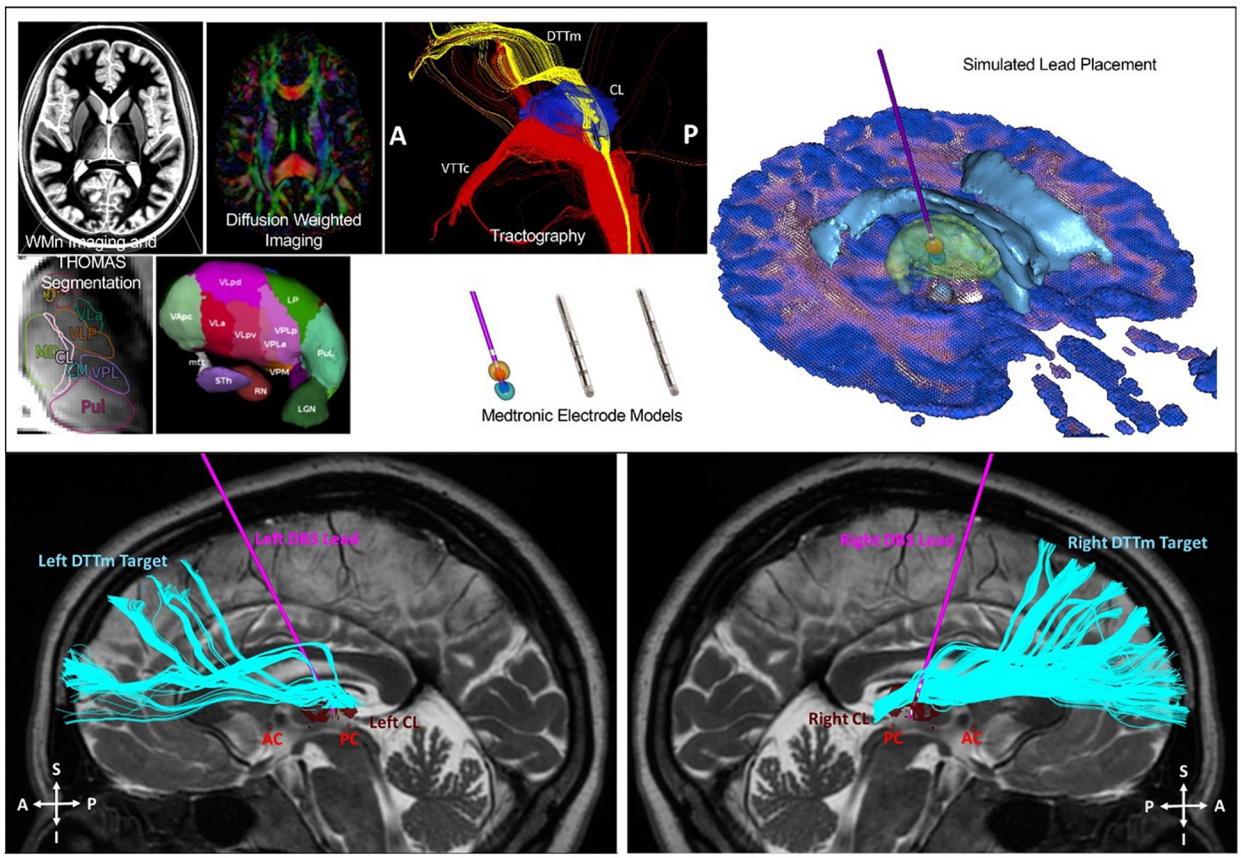

FIGURE 11 | Top image: Identification of the CL and DTTm. Automated patient-specific thalamic segmentation was performed to obtain detailed representations of the central lateral (CL) nucleus for use as a spatial filter to identify the DTTm projecting from the brainstem to the frontal cortex. Bottom image: Two Medtronic 3389 4 contact DBS leads were implanted into the CL nucleus under monitored anesthesia care with microelectrode mapping. The leads were attached to a right infraclavicular Activa PC + S pulse generator under general anesthesia in the same surgical session.

target. Informed by these thalamic recordings, we may leverage sEEG studies to place tandem leads aiming for nodes that are "simply connected" within the same circuit (Gregg, 2021), or nodes in distinct circuits for a broader effect in seizure suppression (**Figure 10**).

NEUROMODULATION FOR TRAUMATIC BRAIN INJURY

Traumatic Brain Injury (TBI) is a leading cause of long-term disability, due in large part to a lack of effective treatment options. Successful treatment of impaired mental processing speed and executive function could improve patient quality of life. Converging evidence from prior work in rodents, non-human primates and humans has provided evidence to support improving arousal and cognition through stimulation of central thalamus. We initiated a 6-participant feasibility study (CENTURY-S, NCT02881151, funded by NIH BRAIN Initiative grant UH3 NS095554) of central thalamic DBS (CT-DBS) in patients with moderate to severe TBI (msTBI). The trial was based on the hypothesis that activation of down-regulated frontostriatal systems would improve cognitive dysfunction, increase information processing speed and decrease fatiguability. We have reported our preliminary findings on CT-DBS in five participants to date with longstanding functional disability related to persistent cognitive dysfunction after severe TBI (age 23–60, 3–18 years after injury).

Six patients underwent implantation of bilateral electrodes into the central lateral (CL) nuclei, specifically targeting the medial dorsal tegmental tract (DTTm) guided by diffusion tensor imaging tractography and a participant-specific map of the thalamus generated by the THOMAS thalamic segmentation pipeline (**Figure 11**). CL and other thalamic nuclei were identified using the THOMAS atlas template in combination with a white matter nulled image sequence (Tourdias et al., 2014; Su et al., 2019). The DTTm was identified using tractography seeded from CL and the pedunculopontine nucleus. Avoidance fiber tracts were identified by seeding the centromedian (CM) and mediodorsal (MD) thalamic nuclei. The virtual DBS platform was used pre-operatively to explore and to select the DBS lead trajectory in each hemisphere (Janson and Butson, 2018). This plan was imported into the surgical planning system. The 30-day post-operative computed tomography imaging was used to determine actual lead location after being registered to the pre-operative T2 MRI, which was used as the base image for surgical planning and patient-specific modeling. This updated model was used to guide post-operative selection of DBS parameters. We have successfully used this approach to implant DBS leads bilaterally in six study participants to date. One participant was explanted due to infection and was not reimplanted; five subjected therefore received stimulation during the open-label period with four having completed the full treatment phase. Two subjects were randomized to a blinded withdrawal at treatment end and two refused randomization due to a perceived therapeutic effect that was lost with brief stimulator deactivation (one intentional, one accidental) during the open-label period.

The study design included a 2-week stimulation titration phase (TP) and a 3-month open label treatment phase. All participants completing the treatment phase to date met the pre-selected primary outcome benchmark of a greater than 10% improvement in completion time on the Trail-Making Test part B (TMT-B) from pre-surgical baseline to the end of the TP (median = 24.84%; IQR: 21.8–32.2). On the TBIQoL-Fatigue measure, one participant of the four met the improvement benchmark, two remained stable and one met the benchmark for decline (although this single measurement was obtained during an intercurrent viral illness). The improvement in processing speed observed on the TMT (A and B) was concordant with the self-reported improvement noted on the TBIQoL-Attention measure. Despite the short 3-month open label phase, two of the four subjects who completed the trial showed a 1-point increase in the GOS-E rating from the presurgical baseline to the end of the TP. These findings preliminarily demonstrated the safety of implantation, evidence for improved mental control under speeded conditions and resistance to fatigue.

Our primary rationale was to match the underlying pathophysiological substrate of chronic cognitive impairment in patients with severe to moderate TBI to the use of CT-DBS as an intervention. The severity of initial overall cerebral deafferentation as indexed by clinical variables was linked to neuropsychological measures of working memory, learning, attention, and information processing speed deficits after msTBI (Dikmen et al., 2003). The central thalamus is anatomically specialized to provide strong synaptic drive across the frontal (particularly medial frontal) and prefrontal cortices and rostral striatum in response to cognitive demands that support these "executive functions" (Liu et al., 2015; Baker et al., 2016). CT-DBS was proposed to activate these systems sufficiently to provide effective functional improvements. Our group previously carried out a first-in-human study of CT-DBS in subjects with very severe traumatic brain injuries. In one subject studied, we established that the recovery of spoken language, deglutition, and executive functions (including but not limited to attentive behavioral responsiveness, motor executive control and access of episodic memory) 6 years following injury was causally linked to CT-DBS (Schiff et al., 2007).

Electrical stimulation of the primary CL lateral wing cell bodies/DTTm fibers was not associated with abnormal sensations or movements. Regions more ventral to CL/DTTm elicited transient side effects in patients including speech slurring, jaw sensations and perseveration; these effects may relate to activation of the centromedian-parafasicularis (Cm-Pf) and more medial components of the median dorsalis (MD) nucleus, respectively. There was marked improvement in performance on the primary outcome measure from the pre-surgical baseline to the end of the 90-day treatment phase for all four subjects completing the study (to date).

This is the first study of DBS electrode implantation in moderate to severe traumatic brain injury with subsequent recovery (outcome range of GOSE 5–7) to remediate impaired cognitive function. The generalizability of these findings will require testing in a larger sample.

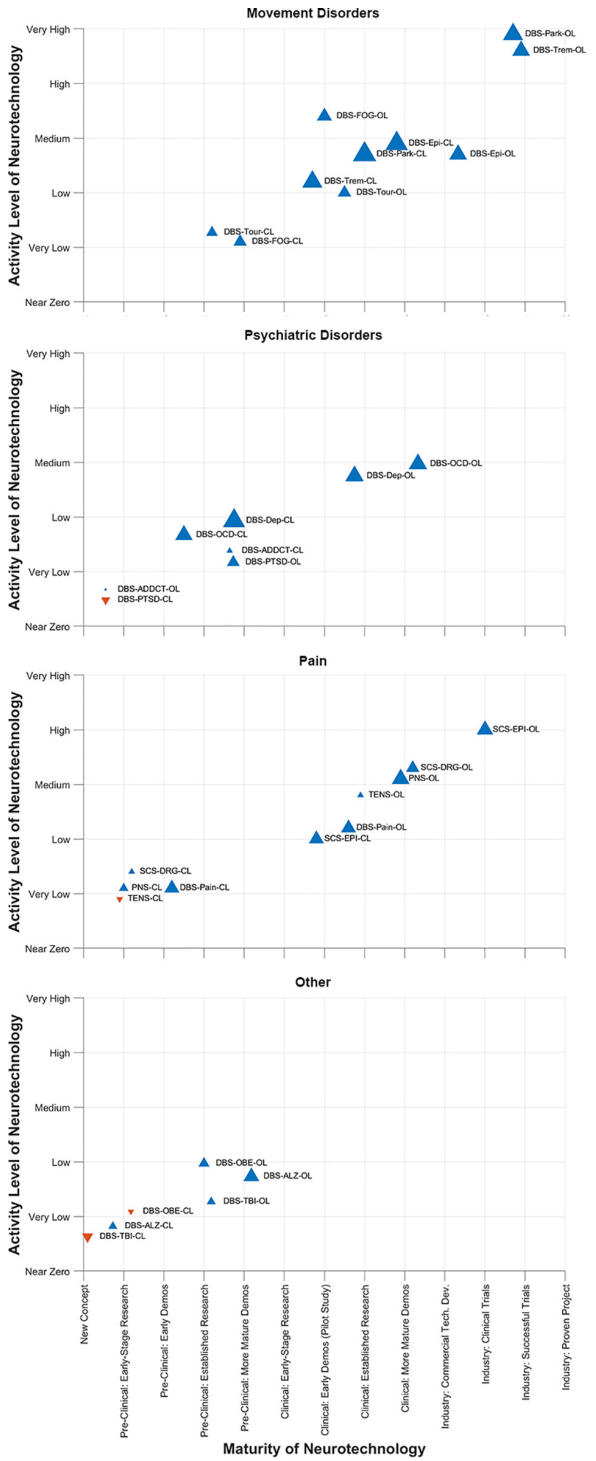

FIGURE 12 | DBS-Think-Tank Neurotechnology Activity-Maturity Graphs. This figure presents four graphs that illustrate the perceptions of DBS-Think-Tank attendees about the maturity, activity, and change in activity of a variety of neurotechnologies. The neurotechnologies are organized into the following four groups and graphed separately: movement disorders, psychiatric disorders, pain disorders, and other syndromes. The upward pointing blue triangles represent increasing activity and downwards pointing orange triangles represent decreasing activity. The magnitude of the change is proportional to the size of the triangles. The definitions of the abbreviations used to identify each triangle are as follows: DBS, deep brain stimulation; OL, open loo; CL, closed loop; Park, Parkinson's disease; FOG, freezing of gait; Epi, epilepsy; Trem, tremor; Tour, Tourette's syndrome; OCD, obsessive-compulsive disorde; Dep, depression; PTSD, posttraumatic stress disorder; ADDCT, addiction; PNS, peripheral nerve stimulation; TENS, transcutaneous electrical nerve stimulation; Pain, chronic pain; DRG, dorsal root ganglia stimulation; SCS, spinal cord stimulation; ALZ, Alzheimer's disease; OBE, obesity; TBI, traumatic brain injury. The data presented were derived from survey respondents with clinical, scientific, engineering, and commercial expertise and had academic, industrial, government, and non-profit professional backgrounds.

SUMMARY AND CONCLUSION

This year, the DBS Think Tank IX advances focused on cutting-edge technologies and the use of novel methodologies for tracking and suppression of symptoms. The neuroethics of neuromodulation session focused on international issues, device security and a path forward. The DBS Think Tank group agreed that a brain cannot determine the self, since self-conceptions are tied to social capabilities. Neuroethics should not presume that one nation's culture holds unique standards for mental health, responsible agency and good character. This year we saw exciting growth in DBS for depression, pain, epilepsy and TBI. Advances in the application of physiology and imaging have driven novel indications and the hope is that these technologies will also drive improved outcomes. Investigation of neurophysiological signals in neurological disorders continue to explore new biomarkers and involved networks potentially amenable to neuromodulation. The CL physiology approaches to DBS will likely present important barriers to implementation and the programming strategies will likely be highly individual. It was not clear to the DBS Think Tank group that CL DBS would be effective for all disease indications. Interactive video acquisition and facial recognition was considered as possible biomarkers for depression and other diseases and also was considered for use in telemedicine adjustments for DBS. The neurotechnology "hype curve" for these topics are shown in **Figure 12**.

This year the DBS Think Tank IX also discussed self-actualization. Many people have heard of Maslow's hierarchy of needs, but most of what people know about his famous "pyramid" is wrong (Maslow, 1943). Briefly, the hierarchy of needs describes five levels of human needs. From bottom to top, the levels are physiological needs, safety needs, love and belonging needs, esteem needs, and the topmost layer of self-actualization. The underlying model posits that one cannot attend to needs of a higher level until the needs of a lower level have been satisfied. This concept is often depicted as a pyramid with self-actualization positioned at the top. However, Maslow did not draw a pyramid. He was suggesting a journey toward self-actualization, but did not limit his concept to a simple pyramidal structure. We discussed both the person with an implanted device and the clinician-scientist-engineer-researcher's journey toward self-actualization and eventually transcendence. We discussed Dr. Kaufman's research placing the hierarchy of needs on a more stable scientific foundation and we examined the list of the

characteristics of self-actualizing people. This work has provided a revision of the hierarchy of needs. This revision draws on the science of creativity, on love and on transcendence. Using this revision, we can apply self-actualization and transcendence to the community of people involved in brain implant technology development and deployment, as well as to the journey of the patient and caregiver. The integration of these concepts has the potential to be important for people in the implantable device arena as well as other areas of medicine. It can help others reach higher states of consciousness while maintaining agency despite an implantable device being present in the body.

DATA AVAILABILITY STATEMENT

The original contributions presented in the study are included in the article/supplementary material, further inquiries can be directed to the corresponding author/s.

ETHICS STATEMENT

The studies involving human participants were reviewed and approved by the individual academic institutions. The patients/participants provided their written informed consent to participate in this study.

AUTHOR CONTRIBUTIONS

All authors listed have made a substantial, direct, and intellectual contribution to the work, and approved it for publication.

FUNDING

JW's research was supported by NIH R25NS108939. SAS was a consultant for Boston Scientific, Abbott, Zimmer Biomet, and Neuropace. SAS was also funded by NIH UH3 NS103549, the McNair Foundation, and the Dana Foundation. HB-S served on the Clinical Advisory Board for Medtronic. PAS received research support and fellowship training support from Medtronic. NS was a member of the scientific advisory board for EnspireDBS, Inc. and QuantalX, Inc. NS also received current grant funding from the BRAIN Initiative, National Institute of Neurological Disorders and Stroke, and the James S. McDonnell Foundation. CB holds intellectual property related to some of the results presented. CB has served as a consultant for NeuroPace, Advanced Bionics, Boston Scientific, IntelectMedical, Abbott (St. Jude Medical), Functional Neuromodulation, NeuraModix. JH served on the advisory board for Enspire DBS, a consultant for Neuralink and received research support from Boston Scientific. JH also received hardware support from Medtronic for the study described in this article. JJ has received research grants from the Michael J. Fox Foundation. DDD received research support and honoraria from Medtronic. HM received grant support from NIH UH3NS103550, 2R01MH102238, and the Hope for Depression Research Foundation, and consulting and licensing fees from Abbott Labs. PSh received research support from Medtronic but not financial support. MSO served as a consultant for the Parkinson's Foundation, and has received research grants from NIH, Parkinson's Foundation, the Michael J. Fox Foundation, the Parkinson Alliance, Smallwood Foundation, the Bachmann-Strauss Foundation, the Tourette Syndrome Association, and the UF Foundation. MSO's DBS research was supported by: NIH R01 NR014852 and R01NS096008. MSO was PI of the NIH R25NS108939 Training Grant.

REFERENCES

Afzal, M. F., Velisar, A., Anidi, C., Neuville, R., Prabhakar, V., and Bronte-Stewart, H. (2019). Proceedings #61: subthalamic neural closed-loop deep brain stimulation for bradykinesia in Parkinson's disease. *Brain Stimulat.* 12, e152–e154.

Allawala, A., Bijanki, K. R., Goodman, W., Cohn, J. F., Viswanathan, A., Yoshor, D., et al. (2021). A novel framework for network-targeted neuropsychiatric deep brain stimulation. *Neurosurgery* 89, E116–E121. doi: 10.1093/neuros/nyab112

Anidi, C., O'Day, J. J., Anderson, R. W., Afzal, M. F., Syrkin-Nikolau, J., Velisar, A., et al. (2018). Neuromodulation targets pathological not physiological beta bursts during gait in Parkinson's disease. *Neurobiol. Dis.* 120, 107–117. doi: 10.1016/j.nbd.2018.09.004

Arlotti, M., Marceglia, S., Foffani, G., Volkmann, J., Lozano, A. M., Moro, E., et al. (2018). Eight-hours adaptive deep brain stimulation in patients with Parkinson disease. *Neurology* 90, e971–e976. doi: 10.1212/WNL.0000000000005121

Baker, J. L., Ryou, J.-W., Wei, X. F., Butson, C. R., Schiff, N. D., and Purpura, K. P. (2016). Robust modulation of arousal regulation, performance and frontostriatal activity through central thalamic deep brain stimulation in healthy non-human primates. *J. Neurophysiol.* 116, 2383–2404. doi: 10.1152/jn.01129.2015

Burdette, D. (2021). Brain-responsive corticothalamic stimulation in the pulvinar nucleus for the treatment of regional neocortical epilepsy: a case series. *Epilepsia Open* 6, 611–617. doi: 10.1002/epi4.12524

Cagnan, H., Pedrosa, D., Little, S., Pogosyan, A., Cheeran, B., Aziz, T., et al. (2017). Stimulating at the right time: phase-specific deep brain stimulation. *Brain* 140, 132–145. doi: 10.1093/brain/aww286

Cannon, E., Silburn, P., Coyne, T., O'Maley, K., Crawford, J. D., and Sachdev, P. S. (2012). Deep brain stimulation of anteromedial globus pallidus interna for severe Tourette's syndrome. *Am. J. Psychiatry* 169, 860–866. doi: 10.1176/appi.ajp.2012.11101583

Center for Security and Emerging Technology, Hannas, W., Chang, H.-M., Aiken, C., Chou, D., and Wang, J. (2020). *China AI-Brain Research: Brain-Inspired AI, Connectomics, Brain-Computer Interfaces*. Washington, DC: Center for Security and Emerging Technology.

Charles, P. D., Van Blercom, N., Krack, P., Lee, S. L., Xie, J., Besson, G., et al. (2002). Predictors of effective bilateral subthalamic nucleus stimulation for PD. *Neurology* 59, 932–934. doi: 10.1212/wnl.59.6.932

Chen, W., Kirkby, L., Kotzev, M., Song, P., Gilron, R., and Pepin, B. (2021). The role of large-scale data infrastructure in developing next-generation deep brain stimulation therapies. *Front. Hum. Neurosci.* 15:717401. doi: 10.3389/fnhum.2021.717401

Cinel, C., Valeriani, D., and Poli, R. (2019). Neurotechnologies for human cognitive augmentation: current state of the art and future prospects. *Front. Hum. Neurosci.* 13:13. doi: 10.3389/fnhum.2019.00013

DeFranco, J., and Giordano, J. (2020). Mapping the past, present, and future of brain research to navigate directions, dangers, and discourses of dual-use. *EC Neurol.* 12, 1–6.

DeFranco, J., Rhemann, M., and Giordano, J. (2020). The emerging neurobioeconomy: implications for national security. *Health Secur.* 18, 267–277. doi: 10.1089/hs.2020.0009

di Biase, L., Brittain, J.-S., Shah, S. A., Pedrosa, D. J., Cagnan, H., Mathy, A., et al. (2017). Tremor stability index: a new tool for differential diagnosis in tremor syndromes. *Brain* 140, 1977–1986. doi: 10.1093/brain/awx104

Diep, C., O'Day, J., Kehnemouyi, Y., Burnett, G., and Bronte-Stewart, H. (2021). Gait parameters measured from wearable sensors reliably detect freezing of gait in a stepping in place task. *Sensors* 21:2661. doi: 10.3390/s21082661

DiEuliis, D., and Giordano, J. J. (2021). *"Designer Biology" and the Need for Biosecurity-by-Design. NCT Magazine*. Available online at: http://nct-magazine.com/nct-magazine-july/designer-biology-and-the-need-for-biosecurity-by-design/ (accessed October 20, 2021).

Dikmen, S. S., Machamer, J. E., Powell, J. M., and Temkin, N. R. (2003). Outcome 3 to 5 years after moderate to severe traumatic brain injury. *Arch. Phys. Med. Rehabil.* 84, 1449–1457. doi: 10.1016/S0003-9993(03)00287-9

Emanuel, P., Walper, S., DiEuliis, D., Klein, N., Petro, J., and Giordano, J. J. (2021). *CCDC CBC-TR-1599, Cyborg Soldier 2050: Human/Machine Fusion and the Implications for the Future of the DOD. APAN Community*. Available online at: https://community.apan.org/wg/tradoc-g2/mad-scientist/m/articles-of-interest/300458 (accessed October 20, 2021).

Fasano, A., Gorodetsky, C., Paul, D., Germann, J., Loh, A., Yan, H., et al. (2021). Local field potential-based programming: a proof-of-concept pilot study. *Neuromodulation* doi: 10.1111/ner.13520 [Epub ahead of print].

Feldmann, L. K., Neumann, W.-J., Krause, P., Lofredi, R., Schneider, G.-H., and Kühn, A. A. (2021). Subthalamic beta band suppression reflects effective neuromodulation in chronic recordings. *Eur. J. Neurol.* 28, 2372–2377. doi: 10.1111/ene.14801

Fisher, R. (2010). Electrical stimulation of the anterior nucleus of thalamus for treatment of refractory epilepsy. *Epilepsia* 51, 899–908. doi: 10.1111/j.1528-1167.2010.02536.x

Funk, C., Kennedy, B., and Sciupac, E. (2016). *U.S. Public Wary About Use of Biomedical Technology for Human Enhancement. Pew Research Center Science & Society*. Available online at: https://www.pewresearch.org/science/2016/07/26/u-s-public-wary-of-biomedical-technologies-to-enhance-human-abilities/ (accessed October 20, 2021).

Gavriliuc, O., Paschen, S., Andrusca, A., Schlenstedt, C., and Deuschl, G. (2021). Prediction of the effect of deep brain stimulation on gait freezing of Parkinson's disease. *Parkinsonism Related Disord.* 87, 82–86. doi: 10.1016/j.parkreldis.2021.04.006

Giordano, J. (2015). A preparatory neuroethical approach to assessing developments in neurotechnology. *Virtual Mentor* 17, 56–61. doi: 10.1001/virtualmentor.2015.17.01.msoc1-1501

Giordano, J. (2017). Toward an operational neuroethical risk analysis and mitigation paradigm for emerging neuroscience and technology (neuroS/T). *Exp. Neurol.* 287, 492–495. doi: 10.1016/j.expneurol.2016.07.016

Giordano, J. (2018). Looking ahead: the importance of views, values, and voices in neuroethics-now. *Camb. Q. Healthc. Ethics* 27, 728–731. doi: 10.1017/S096318011800021X

Gonzalez-Escamilla, G., Muthuraman, M., Ciolac, D., Coenen, V. A., Schnitzler, A., and Groppa, S. (2020). Neuroimaging and electrophysiology meet invasive neurostimulation for causal interrogations and modulations of brain states. *NeuroImage* 220:117144. doi: 10.1016/j.neuroimage.2020.117144

Goyal, A., Goetz, S., Stanslaski, S., Oh, Y., Rusheen, A. E., Klassen, B., et al. (2021). The development of an implantable deep brain stimulation device with simultaneous chronic electrophysiological recording and stimulation in humans. *Biosens Bioelectron* 176:112888. doi: 10.1016/j.bios.2020.112888

Gregg, N. M. (2021). Anterior nucleus of the thalamus seizure detection in ambulatory humans. *Epilepsia* 62, e158–e164. doi: 10.1111/epi.17047

Guang, J., Baker, H., Ben-Yishay Nizri, O., Firman, S., Werner-Reiss, U., Kapuller, V., et al. (2021). Toward asleep DBS: cortico-basal ganglia spectral and coherence activity during interleaved propofol/ketamine sedation mimics NREM/REM sleep activity. *NPJ Parkinsons Dis.* 7, 1–12. doi: 10.1038/s41531-021-00211-9

Gummadavelli, A. (2015). Thalamic stimulation to improve level of consciousness after seizures: evaluation of electrophysiology and behavior. *Epilepsia* 56, 114–124. doi: 10.1111/epi.12872

Habets, J. G. V., Janssen, M. L. F., Duits, A. A., Sijben, L. C. J., Mulders, A. E. P., De Greef, B., et al. (2020). Machine learning prediction of motor response after deep brain stimulation in Parkinson's disease-proof of principle in a retrospective cohort. *PeerJ* 8:e10317. doi: 10.7717/peerj.10317

Herron, J. A., Thompson, M. C., Brown, T., Chizeck, H. J., Ojemann, J. G., and Ko, A. L. (2017). Chronic electrocorticography for sensing movement intention and closed-loop deep brain stimulation with wearable sensors in an essential tremor patient. *J. Neurosurg.* 127, 580–587. doi: 10.3171/2016.8.JNS16536

Ho, A. L., Feng, A. Y., Barbosa, D. A. N., Wu, H., Smith, M. L., Malenka, R. C., et al. (2021). Accumbens coordinated reset stimulation in mice exhibits ameliorating aftereffects on binge alcohol drinking. *Brain Stimul.* 14, 330–334. doi: 10.1016/j.brs.2021.01.015

Janson, A. P., and Butson, C. R. (2018). Targeting neuronal fiber tracts for deep brain stimulation therapy using interactive, patient-specific models. *J. Visualized Exp.* 138, 57292. doi: 10.3791/57292

Jehi, L. (2015). Development and validation of nomograms to provide individualised predictions of seizure outcomes after epilepsy surgery: a retrospective analysis. *Lancet Neurol.* 14, 283–290. doi: 10.1016/S1474-4422(14)70325-4

Jimenez-Shahed, J. (2021). Device profile of the percept PC deep brain stimulation system for the treatment of Parkinson's disease and related disorders. *Exp. Rev. Med. Devices* 18, 319–332. doi: 10.1080/17434440.2021.1909471

Jost, S. T., Visser-Vandewalle, V., Rizos, A., Loehrer, P. A., Silverdale, M., Evans, J., et al. (2021). Non-motor predictors of 36-month quality of life after subthalamic stimulation in Parkinson disease. *NPJ Parkinsons Dis.* 7, 1–7. doi: 10.1038/s41531-021-00174-x

Kania, E. B. (). Minds at war: China's pursuit of military advantage through cognitive science and biotechnology. *Prism* 8, 82–101.

Kehnemouyi, Y. M., Wilkins, K. B., Anidi, C. M., Anderson, R. W., Afzal, M. F., and Bronte-Stewart, H. M. (2021). Modulation of beta bursts in subthalamic sensorimotor circuits predicts improvement in bradykinesia. *Brain* 144, 473–486. doi: 10.1093/brain/awaa394

Koeglsperger, T., Mehrkens, J. H., and Bötzel, K. (2021). Bilateral double beta peaks in a PD patient with STN electrodes. *Acta Neurochir* 163, 205–209. doi: 10.1007/s00701-020-04493-5

Koirala, N., Serrano, L., Paschen, S., Falk, D., Anwar, A. R., Kuravi, P., et al. (2020). Mapping of subthalamic nucleus using microelectrode recordings during deep brain stimulation. *Sci. Rep.* 10:19241. doi: 10.1038/s41598-020-74196-5

Kossoff, E. H. (2004). Effect of an external responsive neurostimulator on seizures and electrographic discharges during subdural electrode monitoring. *Epilepsia* 45, 1560–1567. doi: 10.1111/j.0013-9580.2004.26104.x

Lanzilao, E., Shook, J. R., Newman, R., and Giordano, J. (2013). Advancing neuroscience on the 21st− century world stage: the need for and a proposed structure of an internationally relevant neuroethics. *Ethics Biol. Eng. Med.: Int. J.* 4, 211–229. doi: 10.1615/EthicsBiologyEngMed.2014010710

Lavano, A., Guzzi, G., Della Torre, A., Lavano, S. M., Tiriolo, R., and Volpentesta, G. (2018). DBS in treatment of post-traumatic stress disorder. *Brain Sci.* 8:18. doi: 10.3390/brainsci8010018

Little, S., Beudel, M., Zrinzo, L., Foltynie, T., Limousin, P., Hariz, M., et al. (2016a). Bilateral adaptive deep brain stimulation is effective in Parkinson's disease. *J. Neurol. Neurosurg. Psychiatry* 87, 717–721. doi: 10.1136/jnnp-2015-310972

Little, S., Tripoliti, E., Beudel, M., Pogosyan, A., Cagnan, H., Herz, D., et al. (2016b). Adaptive deep brain stimulation for Parkinson's disease demonstrates reduced speech side effects compared to conventional stimulation in the acute setting. *J. Neurol. Neurosurg. Psychiatry* 87, 1388–1389. doi: 10.1136/jnnp-2016-313518

Little, S., Pogosyan, A., Neal, S., Zavala, B., Zrinzo, L., Hariz, M., et al. (2013). Adaptive deep brain stimulation in advanced Parkinson disease. *Ann. Neurol.* 74, 449–457. doi: 10.1002/ana.23951

Litvak, V., Florin, E., Tamás, G., Groppa, S., and Muthuraman, M. (2021). EEG and MEG primers for tracking DBS network effects. *NeuroImage* 224:117447. doi: 10.1016/j.neuroimage.2020.117447

Liu, J., Lee, H. J., Weitz, A. J., Fang, Z., Lin, P., Choy, M., et al. (2015). Frequency-selective control of cortical and subcortical networks by central thalamus. *eLife* 4, 1–27. doi: 10.7554/elife.09215

Lo, M.-C., Younk, R., and Widge, A. S. (2020). Paired electrical pulse trains for controlling connectivity in emotion-related brain circuitry. *IEEE Trans. Neural. Syst. Rehabil. Eng.* 28, 2721–2730. doi: 10.1109/TNSRE.2020.3030714

Lundstrom, B. N. (2019). Chronic subthreshold cortical stimulation and stimulation-related EEG biomarkers for focal epilepsy. *Brain Commun.* 1:010. doi: 10.1093/braincomms/fcz010

Malekmohammadi, M., Herron, J., Velisar, A., Blumenfeld, Z., Trager, M. H., Chizeck, H. J., et al. (2016). Kinematic adaptive deep brain stimulation for resting tremor in Parkinson's disease. *Mov. Disord.* 31, 426–428. doi: 10.1002/mds.26482

Maslow, A. H. (1943). A theory of human motivation. *Psychol. Rev.* 50, 370–396. doi: 10.1037/h0054346

Mastro, K. J., Zitelli, K. T., Willard, A. M., Leblanc, K. H., Kravitz, A. V., and Gittis, A. H. (2017). Cell-specific pallidal intervention induces long-lasting motor recovery in dopamine-depleted mice. *Nat. Neurosci.* 20, 815–823. doi: 10.1038/nn.4559

Miller, K. J., Mueller, K.-R., and Hermes, D. (2021). Basis profile curve identification to understand electrical stimulation effects in human brain networks. *PLoS Computat. Biol.* 17:e1008710. doi: 10.1371/journal.pcbi.1008710

Morrell, M. (2006). Brain stimulation for epilepsy: can scheduled or responsive neurostimulation stop seizures? *Curr. Opin. Neurol.* 19, 164–168. doi: 10.1097/01.wco.0000218233.60217.84

Muthuraman, M., Bange, M., Koirala, N., Ciolac, D., Pintea, B., Glaser, M., et al. (2020). Cross-frequency coupling between gamma oscillations and deep brain stimulation frequency in Parkinson's disease. *Brain* 143, 3393–3407. doi: 10.1093/brain/awaa297

Muthuraman, M., Hossen, A., Heute, U., Deuschl, G., and Raethjen, J. (2011). A new diagnostic test to distinguish tremulous Parkinson's disease from advanced essential tremor. *Mov. Disord.* 26, 1548–1552. doi: 10.1002/mds.23672

Muthuraman, M., Raethjen, J., Koirala, N., Anwar, A. R., Mideksa, K. G., Elble, R., et al. (2018). Cerebello-cortical network fingerprints differ between essential, Parkinson's and mimicked tremors. *Brain* 141, 1770–1781. doi: 10.1093/brain/awy098

Nair, D. R., Laxer, K. D., Weber, P. B., Murro, A. M., Park, Y. D., Barkley, G. L., et al. (2020). Nine-year prospective efficacy and safety of brain-responsive neurostimulation for focal epilepsy. *Neurology* 95, e1244–e1256. doi: 10.1212/WNL.0000000000010154

Nakajima, A., Shimo, Y., Fuse, A., Tokugawa, J., Hishii, M., Iwamuro, H., et al. (2021). Case report: chronic adaptive deep brain stimulation personalizing therapy based on Parkinsonian State. *Front. Hum. Neurosci.* 15:702961. doi: 10.3389/fnhum.2021.702961

Neumann, W.-J., Degen, K., Schneider, G.-H., Brücke, C., Huebl, J., Brown, P., et al. (2016). Subthalamic synchronized oscillatory activity correlates with motor impairment in patients with Parkinson's disease. *Mov. Disord.* 31, 1748–1751. doi: 10.1002/mds.26759

Noe, K. (2013). Long-term outcomes after nonlesional extratemporal lobe epilepsy surgery. *JAMA Neurol.* 70, 1003–1008. doi: 10.1001/jamaneurol.2013.209

O'Day, J. J., Kehnemouyi, Y. M., Petrucci, M. N., Anderson, R. W., Herron, J. A., and Bronte-Stewart, H. M. (2020). "Demonstration of kinematic-based closed-loop deep brain stimulation for mitigating freezing of gait in people with Parkinson's disease," in *Proceedings of the 2020 42nd Annual International Conference of the IEEE Engineering in Medicine & Biology Society (EMBC) [Internet]*, (Montreal, QC: IEEE), 3612–3616. doi: 10.1109/EMBC44109.2020.9176638

O'Shaughnessy, M., Canal, G., Connor, M., Davenport, M., and Rozell, C. (2020). "Generative causal explanations of black-box classifiers," in *Proceedings of the Advances in Neural Information Processing Systems*, (Vancouver). doi: 10.1093/bib/bbaa049

Oyama, G., Bovet, A., Kamo, H., Iwamuro, H., James, E., Giona, S., et al. (2021). Adaptive deep brain stimulation in real world: first observational data from the Japanese early adapter studies on adaptive deep brain stimulation (aDBS). *Brain Stimul.* 14, 1600–1601.

Ozturk, M., Abosch, A., Francis, D., Wu, J., Jimenez-Shahed, J., and Ince, N. F. (2020). Distinct subthalamic coupling in the ON state describes motor performance in Parkinson's disease. *Mov. Disord.* 35, 91–100. doi: 10.1002/mds.27800

Paff, M., Loh, A., Sarica, C., Lozano, A. M., and Fasano, A. (2020). Update on current technologies for deep brain stimulation in Parkinson's disease. *J. Mov. Disord.* 13, 185–198. doi: 10.14802/jmd.20052

Paschen, S., Forstenpointner, J., Becktepe, J., Heinzel, S., Hellriegel, H., Witt, K., et al. (2019). Long-term efficacy of deep brain stimulation for essential tremor: an observer-blinded study. *Neurology* 92, e1378–e1386. doi: 10.1212/WNL.0000000000007134

Petrucci, M. N., Anderson, R. W., O'Day, J. J., Kehnemouyi, Y. M., Herron, J. A., and Bronte-Stewart, H. M. (2020a). "A closed-loop deep brain stimulation approach for mitigating burst durations in people with Parkinson's disease," in *Proceedings of the 2020 42nd Annual International Conference of the IEEE Engineering in Medicine & Biology Society (EMBC) [Internet]*, (Montreal: IEEE), 3617–3620. doi: 10.1109/EMBC44109.2020.9176196

Petrucci, M. N., Neuville, R. S., Afzal, M. F., Velisar, A., Anidi, C. M., Anderson, R. W., et al. (2020b). Neural closed-loop deep brain stimulation for freezing of gait. *Brain Stimul.* 13, 1320–1322. doi: 10.1016/j.brs.2020.06.018

Petrucci, M. N., Wilkins, K. B., Orthlieb, G. C., Kehnemouyi, Y. M., O'Day, J. J., Herron, J. A., et al. (2021). *10th International IEEE/EMBS Conference on Neural Engineering (NER) [Internet (Italy: IEEE)*. 959–962. Available online at: https://ieeexplore.ieee.org/document/9441336/ (accessed August 27, 2021).

Pfeifer, K. J., Kromer, J. A., Cook, A. J., Hornbeck, T., Lim, E. A., Mortimer, B. J. P., et al. (2021). Coordinated reset vibrotactile stimulation induces sustained cumulative benefits in Parkinson's disease. *Front. Physiol.* 12:624317. doi: 10.3389/fphys.2021.624317

Razavi, B., Rao, V. R., Lin, C., Bujarski, K. A., Patra, S. E., Burdette, D. E., et al. (2020). Real-world experience with direct brain-responsive neurostimulation for focal onset seizures. *Epilepsia* 61, 1749–1757. doi: 10.1111/epi.16593

Rosa, M., Arlotti, M., Ardolino, G., Cogiamanian, F., Marceglia, S., Di Fonzo, A., et al. (2015). Adaptive deep brain stimulation in a freely moving Parkinsonian patient. *Mov. Disord.* 30, 1003–1005. doi: 10.1002/mds.26241

Sachdev, P. S., Cannon, E., Coyne, T. J., and Silburn, P. (2012). Bilateral deep brain stimulation of the nucleus accumbens for comorbid obsessive compulsive disorder and Tourette's syndrome. *BMJ Case Rep.* 2012:bcr2012006579. doi: 10.1136/bcr-2012-006579

Sachdev, P. S., Mohan, A., Cannon, E., Crawford, J. D., Silberstein, P., Cook, R., et al. (2014). Deep brain stimulation of the antero-medial globus pallidus interna for tourette syndrome. *PLoS One* 9:e104926. doi: 10.1371/journal.pone.0104926

Salanova, V. (2021). The SANTÉ study at 10 years of follow-up: effectiveness, safety, and sudden unexpected death in epilepsy. *Epilepsia* 62, 1306–1317. doi: 10.1111/epi.16895

Santillán-Guzmán, A., Heute, U., Muthuraman, M., Stephani, U., and Galka, A. (2013). DBS artifact suppression using a time-frequency domain filter. *Annu. Int. Conf. IEEE Eng. Med. Biol. Soc.* 2013, 4815–4818. doi: 10.1109/EMBC.2013.6610625

Sasaki, F., Oyama, G., Sekimoto, S., Nuermaimaiti, M., Iwamuro, H., Shimo, Y., et al. (2021). Closed-loop programming using external responses for deep brain stimulation in Parkinson's disease. *Parkinsonism Relat. Disord.* 84, 47–51. doi: 10.1016/j.parkreldis.2021.01.023

Schiff, N. D., Giacino, J. T., Kalmar, K., Victor, J. D., Baker, K., Gerber, M., et al. (2007). Behavioural improvements with thalamic stimulation after severe traumatic brain injury. *Nature* 448, 600–603. doi: 10.1038/nature06041

Seier, M., Hiller, A., Quinn, J., Murchison, C., Brodsky, M., and Anderson, S. (2018). Alternating thalamic deep brain stimulation for essential tremor: a trial to reduce habituation. *Mov. Disord. Clin. Pract.* 5, 620–626. doi: 10.1002/mdc3.12685

Shin, H., and Morrell, M. (2020). *Interim Safety and Effectiveness Outcomes from a Prospective Post-Approval Trial of the RNS® System (4322). Neurology*, Vol. 94. Available online at: https://n.neurology.org/content/94/15_Supplement/4322 (accessed October 13, 2021).

Shook, J. R., and Giordano, J. (2014). A principled and cosmopolitan neuroethics: considerations for international relevance. *Philos. Ethics Humanit. Med.* 9:1. doi: 10.1186/1747-5341-9-1

Shook, J. R., and Giordano, J. (2017). Ethics transplants? Addressing the risks and benefits of guiding international biomedicine. *AJOB Neurosci.* 8, 230–232. doi: 10.1080/21507740.2017.1392377

Shreve, L. A., Velisar, A., Malekmohammadi, M., Koop, M. M., Trager, M., Quinn, E. J., et al. (2017). Subthalamic oscillations and phase amplitude coupling

are greater in the more affected hemisphere in Parkinson's disease. *Clin. Neurophysiol.* 128, 128–137. doi: 10.1016/j.clinph.2016.10.095

Sirica, D., Hewitt, A. L., Tarolli, C. G., Weber, M. T., Zimmerman, C., Santiago, A., et al. (2021). Neurophysiological biomarkers to optimize deep brain stimulation in movement disorders. *Neurodegener. Dis. Manag.* 11, 315–328. doi: 10.2217/nmt-2021-0002

Spencer, S. S. (2002). Neural networks in human epilepsy: evidence of and implications for treatment. *Epilepsia* 43, 219–227. doi: 10.1046/j.1528-1157.2002.26901.x

Spix, T., Toong, N., Isett, B. R., Kaplow, I. M., Goksen, Y., Pfenning, A. R., et al. (2020). *Electrically-Driven Cell-Type Specific Neuromodulation in the External Globus Pallidus*. Rochester, NY: Social Science Research Network.

Su, J. H., Thomas, F. T., Kasoff, W. S., Tourdias, T., Choi, E. Y., Rutt, B. K., et al. (2019). Thalamus Optimized Multi Atlas Segmentation (THOMAS): fast, fully automated segmentation of thalamic nuclei from structural MRI. *NeuroImage* 194, 272–282. doi: 10.1016/j.neuroimage.2019.03.021

Tamás, G., Chirumamilla, V. C., Anwar, A. R., Raethjen, J., Deuschl, G., Groppa, S., et al. (2018). Primary sensorimotor cortex drives the common cortical network for gamma synchronization in voluntary hand movements. *Front. Hum. Neurosci.* 12:130. doi: 10.3389/fnhum.2018.00130

Tass, P. A., and Majtanik, M. (2006). Long-term anti-kindling effects of desynchronizing brain stimulation: a theoretical study. *Biol. Cybern* 94, 58–66. doi: 10.1007/s00422-005-0028-6

Téllez-Zenteno, J. F., Dhar, R., and Wiebe, S. (2005). Long-term seizure outcomes following epilepsy surgery: a systematic review and meta-analysis. *Brain* 128, 1188–1198. doi: 10.1093/brain/awh449

Thenaisie, Y., Palmisano, C., Canessa, A., Keulen, B. J., Capetian, P., Jiménez, M. C., et al. (2021). Towards adaptive deep brain stimulation: clinical and technical notes on a novel commercial device for chronic brain sensing. *J. Neural. Eng.* 18, 1–20. doi: 10.1088/1741-2552/ac1d5b

Tinkhauser, G., Pogosyan, A., Little, S., Beudel, M., Herz, D. M., Tan, H., et al. (2017). The modulatory effect of adaptive deep brain stimulation on beta bursts in Parkinson's disease. *Brain* 140, 1053–1067. doi: 10.1093/brain/awx010

Tourdias, T., Saranathan, M., Levesque, I. R., Su, J., and Rutt, B. K. (2014). Visualization of intra-thalamic nuclei with optimized white-matter-nulled MPRAGE at 7T. *NeuroImage* 84, 534–545. doi: 10.1016/j.neuroimage.2013.08.069

Vedam-Mai, V., Deisseroth, K., Giordano, J., Lazaro-Munoz, G., Chiong, W., Suthana, N., et al. (2021). Proceedings of the eighth annual deep brain stimulation think tank: advances in optogenetics, ethical issues affecting dbs research, neuromodulatory approaches for depression, adaptive neurostimulation, and emerging DBS technologies. *Front. Hum. Neurosci.* 15:644593. doi: 10.3389/fnhum.2021.644593

Velisar, A., Syrkin-Nikolau, J., Blumenfeld, Z., Trager, M. H., Afzal, M. F., Prabhakar, V., et al. (2019). Dual threshold neural closed loop deep brain stimulation in Parkinson disease patients. *Brain Stimul.* 12, 868–876. doi: 10.1016/j.brs.2019.02.020

Warren, A. E. (2020). Targeting the centromedian thalamic nucleus for deep brain stimulation. *J. Neurol. Neurosurg. Psychiatry* 91, 339–349. doi: 10.1136/jnnp-2019-322030

Wenzel, G. R., Roediger, J., Brücke, C., Marcelino, A. L., de, A., Gülke, E., et al. (2021). CLOVER-DBS: algorithm-guided deep brain stimulation-programming based on external sensor feedback evaluated in a prospective, randomized, crossover, double-blind, two-center study. *J. Parkinsons Dis*. 11, 1887–1899. doi: 10.3233/JPD-202480

Willsey, M. S., Lu, C. W., Nason, S. R., Malaga, K. A., Lempka, S. F., Chestek, C. A., et al. (2020). Distinct perceptive pathways selected with tonic and bursting patterns of thalamic stimulation. *Brain Stimul.* 13, 1436–1445. doi: 10.1016/j.brs.2020.07.007

Wu, Y., Mo, J., Sui, L., Zhang, J., Hu, W., Zhang, C., et al. (2021). Deep brain stimulation in treatment-resistant depression: a systematic review and meta-analysis on efficacy and safety. *Front. Neurosci.* 15:655412. doi: 10.3389/fnins.2021.655412

Yin, Z., Bai, Y., Zou, L., Zhang, X., Wang, H., Gao, D., et al. (2021). Balance response to levodopa predicts balance improvement after bilateral subthalamic nucleus deep brain stimulation in Parkinson's disease. *NPJ Parkinsons Dis.* 7, 1–9. doi: 10.1038/s41531-021-00192-9

Conflict of Interest: RR was employed by Medtronic, Inc. HBo was employed by Boston Scientific Neuromodulation Corporation. DG was employed by the NeuroPace, Inc.

The remaining authors declare that the research was conducted in the absence of any commercial or financial relationships that could be construed as a potential conflict of interest.

Publisher's Note: All claims expressed in this article are solely those of the authors and do not necessarily represent those of their affiliated organizations, or those of the publisher, the editors and the reviewers. Any product that may be evaluated in this article, or claim that may be made by its manufacturer, is not guaranteed or endorsed by the publisher.

frontiers | Frontiers in Human Neuroscience

ORIGINAL RESEARCH
published: 11 May 2022
doi: 10.3389/fnhum.2022.888701

Unilateral GPi-DBS Improves Ipsilateral and Axial Motor Symptoms in Parkinson's Disease as Evidenced by a Brain Perfusion Single Photon Emission Computed Tomography Study

Yuka Hayashi[1], Takayasu Mishima[1], Shinsuke Fujioka[1], Takashi Morishita[2], Tooru Inoue[2], Shigeki Nagamachi[3] and Yoshio Tsuboi[1]**

[1] Department of Neurology, Faculty of Medicine, Fukuoka University, Fukuoka, Japan, [2] Department of Neurosurgery, Faculty of Medicine, Fukuoka University, Fukuoka, Japan, [3] Department of Radiology, Faculty of Medicine, Fukuoka University, Fukuoka, Japan

OPEN ACCESS

Edited by:
Adolfo Ramirez-Zamora, University of Florida, United States

Reviewed by:
Jun Yu, University of Florida, United States
Karlo Lizárraga, University of Rochester, United States

***Correspondence:**
Takayasu Mishima
mishima1006@fukuoka-u.ac.jp
Yoshio Tsuboi
tsuboi@cis.fukuoka-u.ac.jp

Specialty section:
This article was submitted to Brain Imaging and Stimulation, a section of the journal Frontiers in Human Neuroscience

Received: *03 March 2022*
Accepted: *07 April 2022*
Published: *11 May 2022*

Citation:
Hayashi Y, Mishima T, Fujioka S, Morishita T, Inoue T, Nagamachi S and Tsuboi Y (2022) Unilateral GPi-DBS Improves Ipsilateral and Axial Motor Symptoms in Parkinson's Disease as Evidenced by a Brain Perfusion Single Photon Emission Computed Tomography Study. Front. Hum. Neurosci. 16:888701. doi: 10.3389/fnhum.2022.888701

Introduction: Deep brain stimulation (DBS) is an effective treatment for advanced Parkinson's disease (PD) with the targeting bilateral subthalamic nucleus or globus pallidus internus (STN or GPi-DBS). So far, detailed studies on the efficacy of unilateral STN-DBS for motor symptoms have been reported, but few studies have been conducted on unilateral GPi-DBS.

Materials and Methods: Seventeen patients with Parkinson's disease (PwPD) who underwent unilateral GPi-DBS were selected. We conducted comparison analyses between scores obtained 6–42 months pre- and postoperatively using the following measurement tools: the Movement Disorder Society Unified Parkinson's Disease Rating Scale (MDS-UPDRS) part III, the Hoehn and Yahr stage, the presence/absence of dyskinesia, Mini-Mental State Examination (MMSE), Frontal Assessment Battery (FAB), Geriatric Depression Scale (GDS), levodopa equivalent dose (LED), and cerebral blood flow by single photon emission computed tomography (SPECT). Patient backgrounds were compared between four cohorts with favorable (good responders, $\geq$50% improvement) and unfavorable (poor responders, <50% improvement) postoperative outcome.

Results: Significant improvement was observed postoperatively in the following: total MDS-UPDRS Part III scores during the off period, contralateral scores, ipsilateral scores, and axial scores. Similarly, the Hoehn and Yahr stages during the off period, and GDS also showed significant decrease. In contrast, LED, MMSE, and FAB remained unchanged while the number of patients who scored positive for dyskinesia decreased by 40%. Abnormal cerebral blood flow preoperatively seen in the cerebral cortex had normalized in the total score-based good responder cohort. In the ipsilateral score-based good responder cohort, cerebral blood flow increased in the contralateral frontal

lobe including in the premotor cortex, contralateral to the DBS. Compared to the poor responders, postoperative good responders demonstrated significantly higher preoperative MMSE scores.

Discussion: Unilateral GPi-DBS therapy was effective in improving contralateral, ipsilateral, and axial motor symptoms of patients with advanced PD; in particular, it was found to be especially beneficial in PwPD whose cognitive function was unimpaired; the treatment efficacy rivaled that of bilateral counterparts up till at least 6 months postoperatively. Finally, normalization of preoperative abnormalities in cerebral blood flow and increased cerebral blood flow in the contralateral frontal lobe indicated the beneficial potential of this therapy on ipsilateral motor symptoms.

Keywords: Parkinson's disease (PD), unilateral, deep brain stimuation, globus pallidum internus (Gpi), subthalamic nucleus (STN), ipsilateral, axial, single photon emission computed tomography (SPECT)

INTRODUCTION

Parkinson's disease (PD) is a progressive neurodegenerative disorder characterized by both motor and non-motor symptoms such as tremor, muscle rigidity, bradykinesia, and inability to retain a suitable posture, in addition to dysosmia, dysautonomia, cognitive impairment, psychosis, and sleep disturbance. The effectiveness of dopamine replacement therapy (DRT) at the early stage of PD has been well-documented; DRT in combination with a routine exercise regimen enables long-term preservation of activity of daily living (ADL). Nevertheless, levodopa-induced motor complications, such as wearing off or dyskinesia, eventually emerge as the disease progresses and necessitate a dosage increase. Inevitably, ADL and quality of life (QOL) deteriorate as it becomes increasingly harder for patients to move freely (Berganzo et al., 2016; Gökçal et al., 2017). Upon reaching this stage, maintaining regular motor functions while controlling motor complications becomes an insurmountable challenge for patients with Parkinson's disease (PwPD) even with the appropriate prescription of drug therapy and a routine exercise regimen. Fortunately, device-assisted therapies such as deep brain stimulation (DBS) and levodopa-carbidopa intestinal gel (LCIG) are available and have been shown to be highly effective for a carefully selected group of PwPD who reached such a plateau at advanced stages (Deep-Brain Stimulation for Parkinson's Disease Study Group et al., 2001; Antonini et al., 2017).

By frequently stimulating two electrode targets implanted in the subthalamic nucleus (STN) and the internal segment of the globus pallidus (GPi), advanced PD symptoms improve under DBS therapy. Although differences in treatment effects do exist between STN and GPi, both therapies are equally useful in reducing both core motor symptoms and motor complications (Deep-Brain Stimulation for Parkinson's Disease Study Group et al., 2001). While bilateral STN and GPi-DBS therapies have recently been established as standard treatment, there are also promising reports on the effectiveness of unilateral DBS therapies (Merello et al., 1999; Loher et al., 2002; Linazasoro et al., 2003; Germano et al., 2004; Chung et al., 2006; Kim et al., 2009; Okun et al., 2009, 2014; Walker et al., 2009; Zahodne et al., 2009). A steadily accumulating body of evidence (Kumar et al., 1999; Merello et al., 1999; Loher et al., 2002; Linazasoro et al., 2003; Germano et al., 2004; Chung et al., 2006; Nakamura et al., 2007; Kim et al., 2009; Okun et al., 2009, 2014; Walker et al., 2009; Zahodne et al., 2009) suggests that unilateral STN-DBS therapy improves motor symptoms even in research that evaluated motor symptoms separately from the contralateral, ipsilateral, and axial aspects (Kumar et al., 1999; Chung et al., 2006; Nakamura et al., 2007; Agostino et al., 2008; Tabbal et al., 2008; Walker et al., 2009; Hasegawa et al., 2020). Moreover, unilateral STN-DBS therapy is capable of improving ipsilateral symptoms in other movement disorders such as essential tremor (Peng-Chen et al., 2013). Other noteworthy benefits of unilateral STN-DBS therapy for PwPD include reducing dyskinesia, depression, and the levodopa equivalent dose (LED) (Linazasoro et al., 2003; Chung et al., 2006; Kim et al., 2009; Walker et al., 2009) as well as improving ADL and QOL (Kumar et al., 1999; Linazasoro et al., 2003; Chung et al., 2006; Walker et al., 2009; Zahodne et al., 2009; Okun et al., 2014). While there is plenty of evidence in the literature that supports the overall effectiveness of unilateral GPi-DBS on PD (Merello et al., 1999; Vingerhoets et al., 1999; Loher et al., 2002; Nakamura et al., 2007; Rodrigues et al., 2007; Okun et al., 2009, 2014; Zahodne et al., 2009), studies that examined the effect of unilateral GPi-DBS on motor symptoms of PD in the contralateral, ipsilateral, and axial sides are scarce (Merello et al., 1999; Loher et al., 2002). Thus, in order to clarify the effectiveness of unilateral GPi-DBS from a different angle and identify suitable patient candidates, this study conducted a detailed comparative analyses of the pre- and postoperative changes in motor and

Abbreviations: ADL, activity of daily living; BW, Butterworth filter; DBS, deep brain stimulation; DRT, dopamine replacement therapy; Fine SRT, fine stereotaxic region of interest template; FAB, Frontal Assessment Battery; GDS, Geriatric Depression Scale; GPi, globus pallidus internus; LDCT, levodopa challenge test; LED, levodopa equivalent dose; LCIG, levodopa-carbidopa intestinal gel; MMSE, Mini-Mental State Examination; MDS-UPDRS, Movement Disorder Society Unified Parkinson's Disease Rating Scale; NIRS, near-infrared spectroscopy; PD, Parkinson's disease; PwPD, patients with Parkinson's disease; PPN, pedunculopontine tegmental nucleus; QOL, quality of life; RI, radioisotope; ROI, region of interest; SPECT, single photon emission computed tomography; STN, subthalamic nucleus; STN-DBS, subthalamic nucleus deep brain stimulation; UKBBC, United Kingdom Parkinson's Disease Society Brain Bank Clinical Diagnostic Criteria.

non-motor symptoms of PwPD who underwent unilateral GPi-DBS.

MATERIALS AND METHODS

This is a retrospective observational study conducted at a single institution, the Fukuoka University Hospital. Of the database of 343 PwPD who visited our hospital during the period of 1 December 2014 to 30 September 2019, 17 patients, who received unilateral GPi-DBS stimulation to either right or left side and who were available for a 6 month postoperative assessment, were selected (**Figure 1**). All procedures were performed by a fellowship-trained functional neurosurgeon (T.M.), and the same DBS system was used in all study subjects (model 3387 DBS lead and Activa SC pulse generator, Medtronic, Minneapolis, MN, United States). Although our hospital is primarily focused on the staged GPi-DBS approach (Samii et al., 2007), we selected patients who requested either a unilateral or a staged DBS therapy when presented with the choice of bilateral, unilateral, or staged DBS therapy. These 17 patients all met the United Kingdom Parkinson's Disease Society Brain Bank Clinical Diagnostic Criteria (UKBBC) and had been diagnosed with sporadic PD by a specialized neurologist (Hughes et al., 1992). Furthermore, all patients were preoperatively suffering from motor complications that: were difficult to control with a combined drug and exercise regimen; had shown >33% improvement in a total score obtained in the Movement Disorder Society Unified Parkinson's Disease Rating Scale Part III (MDS-UPDRS Part III) in response to the levodopa challenge test (LDCT) that compared assessment during the off-stage and after taking levodopa; and were without prominent cognitive impairment [Mini-Mental State Examination (MMSE) score < 24] (Mishima et al., 2021). Concerning the programming, we follow the basic programming concept (Volkmann et al., 2002). Following testing the threshold levels of stimulation-induced side effects and therapeutic windows of monopolar stimulation at each contact, we usually select contact 1 or 2 as the active contact as the initial setting. Patients were instructed to regularly visit the programming clinic once a month for the stimulation adjustment performed by neurologists specializing movement disorders (Y.H., T.M., S.F., and Y.T.). The stimulation intensity and pulse width were gradually increased or decreased, and bipolar setting was selected when the intensity of monopolar stimulation reached the threshold level of side effects.

Measurements used for the assessment of motor and non-motor function respectively were as follows: MDS-UPDRS Part III, Hoehn and Yahr stages, presence/absence of dyskinesia; MMSE, Frontal Assessment Battery (FAB), and Geriatric Depression Scale (GDS). In addition, oral treatment was assessed with the levodopa equivalent dose (LED) (Tomlinson et al., 2010). A comparison analysis between pre- and approximately 6-month postoperative scores (mean, 6.6 ± 0.7 months; range, 6–7 months) was performed for each item. Both pre- and postoperative assessment with MDS-UPDRS Part III was undertaken during the off state. The assessment was conducted not only with total MDS-UPDRS Part III score, but also considered the ipsilateral and contralateral (total unilateral MDS-UPDRS Part III score from the sub-item 20–26) and axial scores (Kotagal et al., 2014) (total MDS-UPDRS Part III score from the sub-item 1, 9, 10, 12, 13) independently. In addition, two cohorts (**Table 1**) were created for comparison consisting of PwPD with favorable (good responder, total MDS-UPDRS Part III score ≥ 50%) and unfavorable (poor responder, total

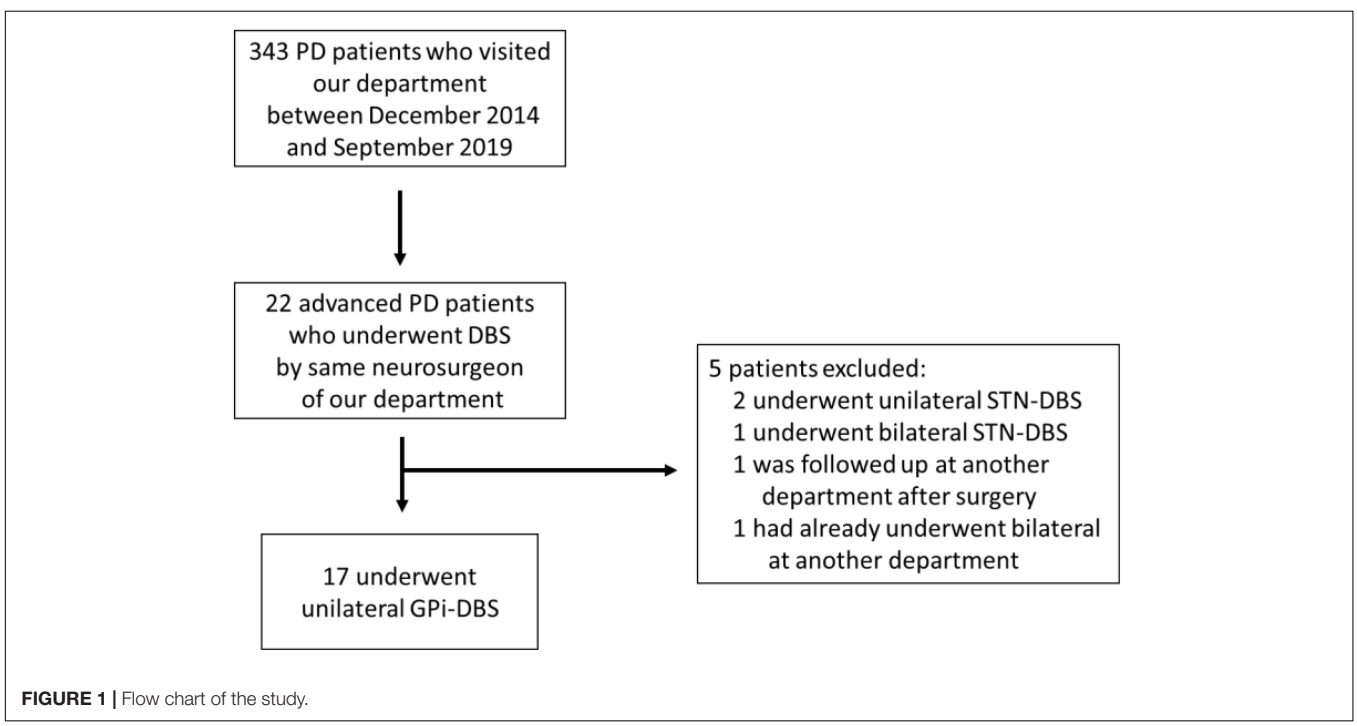

FIGURE 1 | Flow chart of the study.

TABLE 1 | Comparison of each item at baseline between good responders (changes of Movement Disorder Society-Unified Parkinson's Disease Rating Scale (MDS-UPDRS) part III total score after surgery ≧50%) and poor responders (<50%).

		Good responders (*n* = 9)	Poor responders (*n* = 8)	*P*
Age (years)		60.3 ± 5.5	64.4 ± 5.5	0.17
Sex (M:F)		4:5	3:5	0.77
Duration of PD (years)		9.9 ± 3.9	12.6 ± 6.1	0.61
LED (mg)		1,072.0 ± 363.8	990.6 ± 300.5	0.54
Hoehn and Yahr stage	Off	4 ± 0	4.1 ± 0.3	0.67
	On	2.7 ± 0.5	2.6 ± 0.5	0.89
MMSE		28.2 ± 0.8	26.9 ± 1.5	0.03
FAB		15.2 ± 1.2	15.8 ± 1.5	0.48
GDS		4.2 ± 2.8	4.8 ± 2.3	0.67
MDS-UPDRS part III total score		54.0 ± 12.4	48.6 ± 11.6	0.37
Dyskinesia (+: −)		7:2	8:0	0.77

MDS-UPDRS Part III score < 50%) postoperative outcome. Comparisons were made in the following item categories obtained preoperatively: age, sex, disease duration, total MDS-UPDRS Part III score, Hoehn and Yahr stage (each on/off period), MMSE, FAB, GDS, LED, and presence/absence of dyskinesia.

Changes in pre- and approximately 11-month postoperative distribution of cerebral blood flow (mean, 11.1 ± 9.7 months; range, 6 months–3.5 years) were examined with ^{99m}Tc-ECD single photon emission computed tomography (SPECT). SPECT data was missing from 3 patients (Case No. 4, 11, 17); therefore, the SPECT examination was based on available data from 14 patients. A SPECT examination was performed with patients' eyes closed at resting state using a Technetium-99m ethyl cysteinate dimer (^{99m}Tc-ECD) 600–900 MBq. A triple-detector gamma camera system (GCA-9300R; Cannon Medical Systems, Tokyo, Japan) was used for imaging. Data were collected during the period 5–16 min after a radioisotope (RI) was administered under the following conditions: 120°, 30 locations × 3, 120 s, a main energy window (20% of 141 KeV), a sub window (<7%). A high-resolution fan beam collimator was selected. SPECT images were corrected with 3D-OSEM reconstruction using absorptive correction (+), scatter−correction (+), μ value 0.15, and the Butterworth filter (BW); it was performed at order 4 (cut-off frequency, 0.13 cy/pixel), repetition time 10, and adding frequency of 10 times. The image analysis software eZIS (Fujifilm RI Pharma., Tokyo, Japan) was used to conduct image statistical analysis; this could be performed on a personal computer and was concordant with the patient SPECT image. Specifically, anatomically standardized SPECT images were compared with the images stored in the database of a standard brain of the corresponding age, for each patient's data. Z-score for a region of interest (ROI) for each of 52 regions was determined with a fine stereotaxic region of interest template (Fine SRT) (Fuji Film, Tokyo, Japan) (**Figure 2**; Takeuchi, 2005). A total of four cohorts (**Tables 2A,B**) were created based on: (a) the total MDS-UPDRS Part III score, with favorable (good responder, ≥50%) and unfavorable (poor responder, <50%) postoperative outcome; (b) ipsilateral score, with favorable (good responder, improvement rate ≥ 50%) and unfavorable (poor responder, improvement rate < 50%) postoperative outcome (Antonini et al., 2003a). A comparison was made between pre- and postoperative Z-scores for each item category. For all item categories, paired *t*-tests were used for pre- and postoperative comparison and the Mann-Whitney test and the chi−square test were applied in the comparative analysis of good vs. poor postoperative responders. The threshold of statistical significance was established at $p < 0.05$ with a two-sided testing procedure. This study was approved by the Ethics Committee of the Fukuoka University Hospital (number, U20-04-001).

RESULTS

Table 3 gives the background data of the 17 patients who participated in our study: male to female sex ratio, 7:10; average age, 62.2 ± 5.8 years old; average disease duration, 11.2 ± 5.2 years, mean preoperative LED 1,033.7 ± 284.6 mg/day; average pre- and postoperative differences in Hoehn and Yahr stages during off period, 4.1 ± 0.2/2.8 ± 0.8. Only two patients met the EARLYSTIM criteria (Schuepbach et al., 2013). No adverse events such as intra- and postoperative bleeding or infection occurred during our study. All patients underwent CT postoperative day 9 to evaluate the electrode position in the GPi, and a board-certified neurosurgeon (T.M.) confirmed that there was no lead misplacement. **Figures 3A,B** show MDS-UPDRS Part III score, Hoehn and Yahr stage, MMSE, FAB, GDS, and LED. Compared to preoperative data, significant postoperative improvement was identified in the following item categories: total MDS-UPDRS Part III score, 50.2 ± 12.3 vs. 25.5 ± 12.2, improvement rate 50.7%, $p < 0.0001$; contralateral score, 15.0 ± 4.8 vs. 7.4 ± 4.1, improvement rate 48.1%, $p < 0.0001$; ipsilateral score, 14.4 ± 5.5 vs. 7.1 ± 4.9, improvement rate 50.6%, $p < 0.0001$; and axial score 10.5 ± 3.1 vs. 4.9 ± 3.4, improvement rate 53.6%, $p < 0.0001$. In all cases, postoperative total MDS-UPDRS part III score during the off period improved compared to preoperative (**Supplementary Table 1**). The Hoehn and Yahr stage for both on period ($p < 0.0001$) and off period ($p < 0.04$) were significantly decreased postoperatively. Although not significant, the number of patients with dyskinesia decreased from 15 (88.2%) to 9 (52.9%) after GPi-DBS therapy, while no

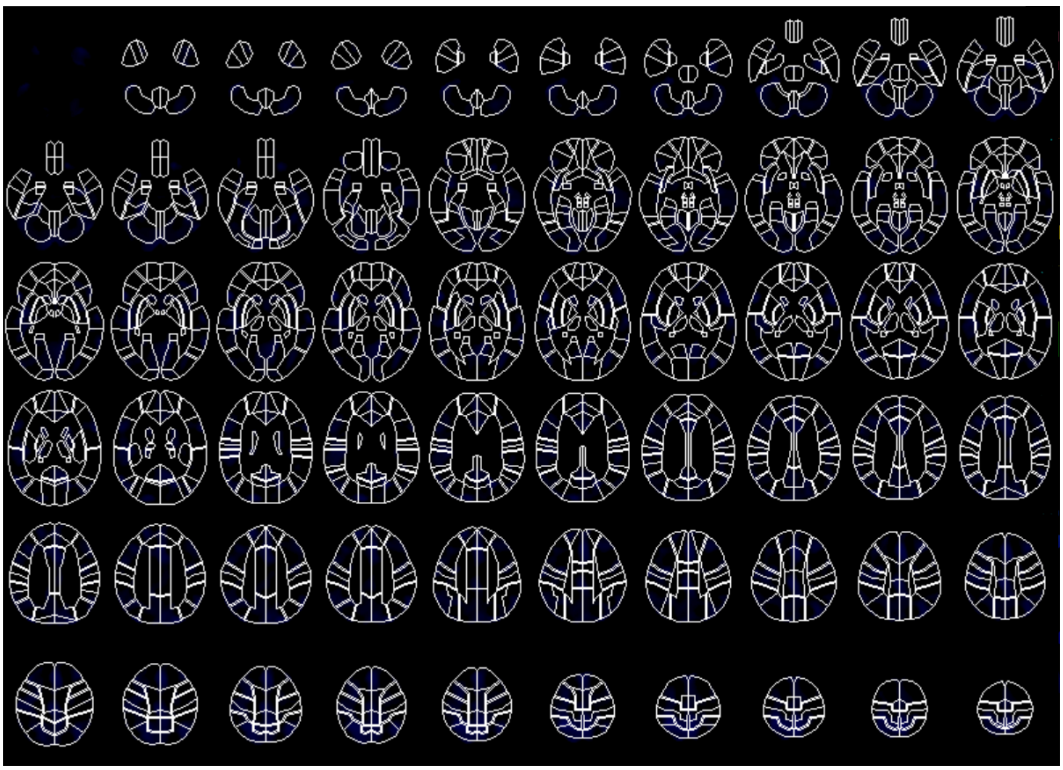

FIGURE 2 | Fine stereotactic region of interest (ROI) template (SRT) image composed of 52 areas of ROI in Single Photon Emission Computed Tomography (SPECT) study.

TABLE 2A | Comparison of *Z*-score between baseline and after unilateral deep brain stimulation of the globus pallidus internus (GPi-DBS) by brain perfusion Single Photon Emission Computed Tomography (SPECT).

Location*	Change in pre- and post-op CBF	*Z*-score		*p*	Normalization in post-op CBF
		Pre-op	Post-op		
<Good responders>					
Ipsilateral transverse temporal	↓	−0.304	0.154	0.03	Yes
Contralateral premotor	↑	0.344	0.026	0.03	Yes
Ipsilateral cingulate	↓	0.229	0.475	0.04	Not
Contralateral primary auditory**	↑	0.130	−0.049	0.04	Yes
Contralateral inferior parietal	↑	0.641	0.373	0.045	Yes
<Poor responders>					
Ipsilateral subcallosal	↑	−0.271	−0.842	0.01	Not
Ipsilateral inferior temporal	↓	−0.069	0.305	0.01	Not
Contralateral fusiform	↑	0.023	0.123	0.01	Not
Contralateral orbital	↑	−0.106	0.497	0.02	Not
Ipsilateral globus pallidus	↓	−0.212	0.426	0.02	Not
Ipsilateral substantia nigra	↓	−0.228	0.476	0.03	Not
Ipsilateral anterior cingulate	↓	−0.194	−0.456	0.03	Not
Contralateral paracentral lobule	↑	0.117	−0.166	0.03	Not
Ipsilateral orbital	↑	−0.251	−0.608	0.03	Not
Ipsilateral nucleus ruber	↓	0.021	0.575	0.03	Not

*Patients were divided into good and poor responders in changes of Movement Disorder Society-Unified Parkinson's Disease Rating Scale (MDS-UPDRS) part III total scores after surgery. *Only locations with significant changes in post-op CBF were extracted. **Primary auditory overlaps anatomically with frontal lobes. ↑: increased CBF, ↓: decreased CBF.*

TABLE 2B | Comparison of *Z*-score between baseline and after unilateral deep brain stimulation of the globus pallidus internus (GPi-DBS) by brain perfusion single photon emission computed tomography (SPECT).

Location*	Change in pre- and post-op CBF	*Z*-score		*p*	Normalization in post-op CBF
		Pre-op	Post-op		
<Good responders>					
Ipsilateral transverse temporal	↓	−0.271	0.185	0.02	Yes
Contralateral premotor	↑	0.303	−0.001	0.02	Yes
Contralateral medial frontal	↑	−0.258	−0.482	0.02	Not
Contralateral inferior frontal	↑	−0.236	−0.569	0.03	Not
Contralateral Broca*	↑	−0.100	−0.443	0.03	Not
Contralateral Wernicke*	↑	0.676	0.301	0.03	Yes
Contralateral orbital	↑	−0.597	−0.908	0.04	Not
Contralateral middle frontal	↑	−0.091	−0.400	0.04	Not
Ipsilateral globus pallidus	↓	−0.476	0.318	0.04	Yes
Ipsilateral cingulate	↓	0.279	0.499	0.04	Not
Contralateral primary auditory**	↑	0.138	−0.021	0.04	Yes
Contralateral middle temporal	↑	0.104	−0.249	0.045	Not
<Poor responders>					
Ipsilateral parahippocampal	↓	−0.370	0.747	0.002	Not
Contralateral caudate head	↓	0.677	0.887	0.002	Not
Ipsilateral nucleus ruber	↓	−0.151	0.532	0.01	Not
Ipsilateral inferior temporal	↑	−0.079	−0.342	0.02	Not
Ipsilateral globus pallidus	↓	−0.243	0.261	0.02	Not
Contralateral fusiform	↓	−0.016	0.164	0.04	Not
Ipsilateral anterior cingulate	↓	−0.128	0.331	0.047	Not

*Patients were divided into good and poor responders based on changes in Movement Disorder Society-Unified Parkinson's Disease Rating Scale (MDS-UPDRS) part III ipsilateral sub scores after surgery. *These locations overlap anatomically with frontal and temporal lobes. **Primary auditory overlaps anatomically with frontal lobes. ↑: increased CBF, ↓: decreased CBF.*

changes were detected in LED. Similarly, MMSE and FAB were unchanged whereas GDS (4.5 ± 2.6 vs. 3.2 ± 2.1, $p = 0.04$) showed improvement. The postoperative good responder cohort ($n = 9$, including two patients who met the EARLYSTIM criteria) demonstrated significantly higher MMSE scores (28.2 ± 0.8 vs. 26.9 ± 1.5, $p < 0.05$) compared to postoperative poor responder counterparts even before undergoing GPi-DBS therapy (**Table 1**). No patient has displayed serious adverse events at the 6-month postoperative period, to date. Pre- and postoperative Z-scores for 14 patients who experienced ^{99m}-Tc-ECD SPECT are presented in **Table 2A** (Comparisons were made between good and poor responders based on total MDS-UPDRS Part III score) and **Table 2B** (Comparisons were made between good and poor responders based on ipsilateral score). Two noteworthy changes were detected postoperatively. First, abnormalities in cerebral blood flow observed in the bilateral cerebral cortex before GPi-DBS had normalized postoperatively in the total MDS-UPDRS Part III score good responder cohort ($n = 8$, mean age 62.0 ± 3.2 years old, postoperative improvement rate 69.2 ± 14.5%). In contrast, the poor responder cohort ($n = 6$, 62.7 ± 4.3 years old 27.3 ± 8.3%) showed scores that further deviated from the normal value in the bilateral cerebral cortex postoperatively (**Table 2A**). The second noticeable change was the significant postoperative increase in blood flow in the contralateral frontal lobe of the ipsilateral good responder cohort ($n = 9$, 61.8 ± 3.2 years old, 74.0 ± 13.9%). However, scores for the bilateral cerebral cortex showed greater deviation from the normal value or baseline in the poor responder counterparts ($n = 5$, 63.0 ± 4.6 years old, 5.9 ± 36.0%) after GPi-DBS therapy (**Table 2B**).

DISCUSSION

At postoperative 6 months, motor symptoms of PwPD significantly improved in the axis and sides contralateral or ipsilateral to the target area treated with DBS. Given the 50.7% improvement rates of the total UPDRS part III scores obtained in this study, and the 24–67% (postoperative 6 months) (Kumar et al., 1999; Houeto et al., 2000; Molinuevo et al., 2000; Deep-Brain Stimulation for Parkinson's Disease Study Group et al., 2001; Volkmann et al., 2001, 2009; Simuni et al., 2002; Thobois et al., 2002; Schupbach et al., 2005; Tanei et al., 2009a; Mei et al., 2020) or 38–56% (postoperative 3–7 months) (Vingerhoets et al., 1999; Deep-Brain Stimulation for Parkinson's Disease Study Group et al., 2001; Volkmann et al., 2001; Loher et al., 2002; Tanei et al., 2009a) improvement rates from the bilateral STN or GPi-DBS in previous studies, it is reasonable to conclude that unilateral GPi-DBS therapy is equally as effective as bilateral DBS therapy. Improvement rates in our study (50.7%) were similar to the rates obtained in other unilateral GPi-DBS studies: 16.0–48.5% (Merello et al., 1999; Vingerhoets et al., 1999;

TABLE 3 | Baseline characteristics of 17 patients with advanced Parkinson's disease received unilateral deep brain stimulation of the globus pallidus internus (GPi-DBS).

Case no.	Age (years), sex	Duration of PD preop (years)	LED (mg)	Dyskinesia	Hoehn and Yahr stage Off/on	MDS-UPDRS part III				MMSE	FAB	GDS
						Total	Contralateral	Ipsilateral	Axial			
1	58, M	5	1,035	–	4/2	62	14	23	11	28	16	0
2	60, M	15	1,483.7	+	4/2	56	13	17	12	28	17	0
3	67, F	10	1,348	+	4/2	35	16	7	6	30	13	6
4	74, M	25	719.7	+	4/3	48	16	14	11	28	15	2
5	65, F	8	700	+	4/3	65	17	20	15	28	15	7
6	67, F	7	875	+	4/3	74	22	21	18	26	17	6
7	62, M	6	1,098	+	4/2	64	21	17	14	29	15	4
8	66, F	19	1,404.7	+	4/2	50	16	14	10	25	16	1
9	61, F	5	537.05	+	4/3	41	11	11	11	27	15	6
10	68, F	14	1,098	+	4/3	62	14	23	11	30	15	5
11	65, M	12	1,300	+	5/2	42	11	9	11	27	15	6
12	59, M	9	1,100	–	4/3	37	14	9	8	28	15	3
13	54, M	11	925	+	4/3	41	15	13	5	26	17	3
14	65, F	5	1,024.1	+	4/3	46	14	11	9	27	14	4
15	58, F	14	660	+	4/3	64	18	21	10	28	13	6
16	61, F	12	815	+	4/3	58	16	22	10	26	18	8
17	48, F	13	1,449.95	+	4/3	30	8	5	8	28	17	9
Average ± SD	51.1 ± 6.5 (M:F) 7:10	11.2 ± 5.2	1,033.7 ± 284.6	(+: –)15:2	4.1 ± 0.2/ 2.65 ± 0.5	50.2 ± 12.3	15.4 ± 4.8	14.4 ± 5.5	10.5 ± 3.1	27.6 ± 1.3	15.5 ± 1.4	4.5 ± 2.6

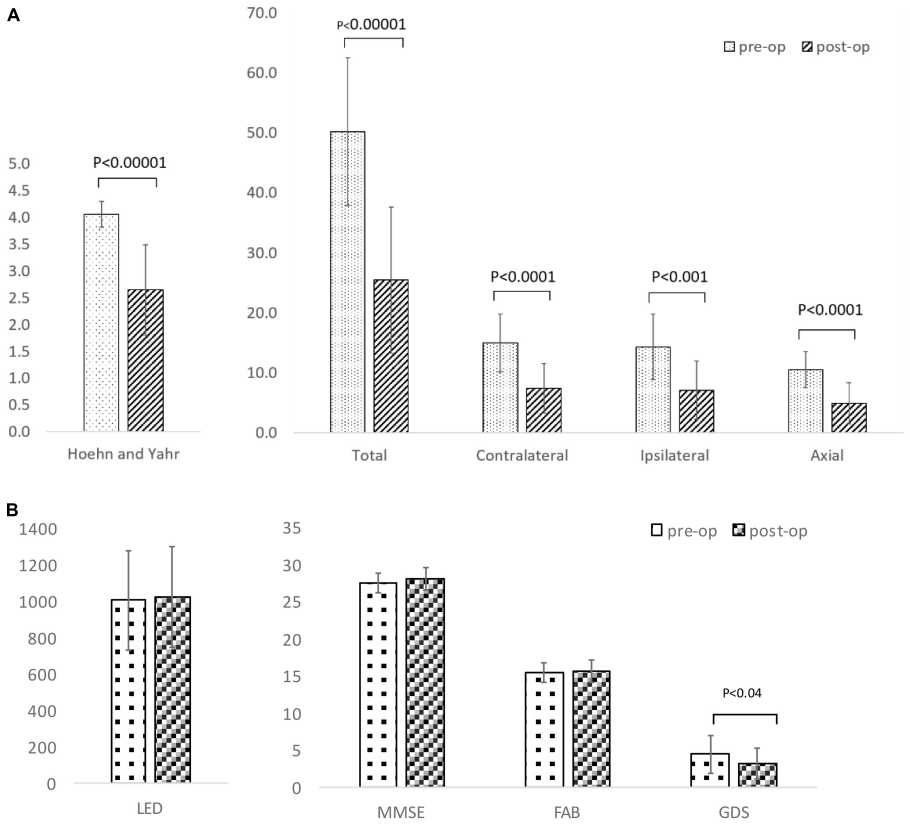

FIGURE 3 | (A) Comparison of Movement Disorder Society-Unified Parkinson's Disease Rating Scale (MDS-UPDRS) motor scores and Hoehn and Yahr stage between baseline and after unilateral deep brain stimulation of the globus pallidus internus (GPi-DBS). **(B)** Comparison of levodopa equivalent dose (LED), Mini-Mental State Examination (MMSE), Frontal Assessment Battery (FAB), Geriatric depression scale (GDS) between baseline and after unilateral deep brain stimulation of globus pallidus internus (GPi-DBS).

Loher et al., 2002; Rodrigues et al., 2007; Okun et al., 2009, 2014; Zahodne et al., 2009). Contralateral scores also improved in similar rates to other studies (28.8–50.0%) (Merello et al., 1999; Loher et al., 2002) in the current study (48.1%). On the other hand, while improvement rates (23–24%) for the ipsilateral scores did not reach significance in other studies (Loher et al., 2002), our improvement rate was significant at 50.6%. There is only one study that previously showed a significant improvement in ipsilateral scores in unilateral GPi-DBS therapy; it evaluated the improvement solely on fingertip mobility (Nakamura et al., 2007). It is not clear what contributed to the remarkable improvement rates of the ipsilateral scores in this study; however, one might be the difference in measurement methods as MDS-UPDRS part III has not been used to assess motor symptoms of the ipsilateral side before this study. Interestingly, an equally remarkable improvement to ipsilateral scores was observed in the contralateral scores. Furthermore, improvement rate for axial score was notably high (56.7%) and rivaled improvements in contralateral and ipsilateral scores. This warrants further study since results concerning improvement rates for axial score after unilateral GPi-DBS therapy have been inconsistent: while Loher et al. (2002) reports a significant rate of improvement (41%), no improvement was identified in two other studies (Merello et al., 1999; Rodrigues et al., 2007). The current study assessed the significant differences between gait and postural stability scales of the MDS-UPDRS Part III; and freezing, walking, and balance scales in the Part II section of the same scale. The fact that we removed a total sum of item 1, 9, 10, 12, 13 (Takeuchi, 2005) in the MDS-UPDRS Part III of the motor examination section and defined them as an "axial score" may have contributed to the incomparably remarkable improvement in our study.

Studies (Merello et al., 1999; Loher et al., 2002; Volkmann et al., 2009) that assessed severity of dyskinesia after bilateral or unilateral GPi-DBS therapy, with the Rush Dyskinesia Rating Scale and the UPDRS part IV, have demonstrated a significant postoperative improvement. Although results were not significant, the number of patients who scored positive for dyskinesia (or who reported the presence of dyskinesia) during the on period decreased by 40%: from 15/17 preoperatively to 9/15 postoperatively. Caution must be exercised when interpreting this result; rather than the severity of dyskinesia, this analysis only focused on the presence or absence of dyskinesia.

After the unilateral GPi-DBS therapy, PwPD showed reduced depression; however, no change was detected in their cognitive function during the evaluation of non-motor symptoms. Consistent with other unilateral GPi-DBS studies

(Loher et al., 2002; Simuni et al., 2002; Rothlind et al., 2007; Zahodne et al., 2009), this positive effect on depression found in the present study further increased confidence in GPi-DBS's ability to ease depression in PwPD. Compared to the poor responder counterparts, the good responder cohort, who showed favorable outcomes in motor symptoms after unilateral GPi-DBS therapy, scored significantly higher in MMSE, indicating a better cognitive function. Thus, it is speculated that unilateral GPi-DBS is most effective for PwPD with preserved cognitive functions. Furthermore, the fact that the two cases that met the EARLYSTIM criteria in this study belonged to the good responder cohort, also suggests that the use of the unilateral GPi-DBS in the early stages of PD can be especially beneficial. Nevertheless, the small sample size warrants caution and further replication.

This study examined ^{99m}ECD-SPECT pre- and postoperatively and noted that abnormal cerebral blood flow, preoperatively observed in the bilateral cortex, normalized after unilateral GPi-DBS in PwPD who showed improvement in motor symptoms. In addition, cerebral blood flow increased in the frontal lobe including in the premotor cortex contralateral to the side stimulated with DBS. The majority of studies that investigated correlations to improvement in motor symptoms with cerebral blood flow tomography or SPECT, concerned patients who underwent STN-DBS therapy. A potential link between the increase in cerebral blood flow in the motor-related areas of the frontal lobe (e.g., premotor cortex, pre-SMA, SMA, and anterior cingulate) and reduced motor symptoms after unilateral STN-DBS therapy has been suggested in ^{99m}Tc-ECD SPECT studies (Sestini et al., 2002, 2005; Antonini et al., 2003a; Paschali et al., 2013). In addition, potential links between the postoperative normalization of abnormal blood flow (Cilia et al., 2009) in the bilateral cerebral cortex, nucleus basalis, or hypothalamic loop, and improvement in motor symptoms have been documented in the literature (Antonini et al., 2003b). Only a single assessment study (Tanei et al., 2009b) exists regarding the postoperative effect of unilateral STN-DBS; a significant vascular flow increase within the bilateral cingulate gyrus and cerebellum was identified, whereas vascular flow significantly decreased in both the bilateral medial frontal and superior temporal lobes. A significant correlation has also been found in the literature (van Laere et al., 2000) concerning GPi-DBS and ^{99m}ECD-SPECT between decreased vascular flow in the ipsilateral thalamus and corpus striatum in relation to improvement in motor symptoms. However, comparison of the latter study to the current study is not relevant since the lesion effect of inserting electrodes serves as a confounding factor. Revitalized cortical activity was detected postoperatively in the motor-related areas of the frontal lobe, including in the ipsilateral side, in a unilateral GPi-DBS study using near-infrared spectroscopy (NIRS) (Morishita et al., 2016).

Insights are offered in the unilateral STN-DBS study, regarding the potential improvement mechanism in the ipsilateral symptoms. Motor symptoms of the ipsilateral side may be positively affected by the stimulation received by the ipsilateral pedunculopontine tegmental nucleus (PPN) (Nakano, 2000) transmitted through the contralateral side of the brain; this takes place via input from the ipsilateral supplementary motor area including the neuronal network of the cortex-basal ganglia-thalamus loop to the bilateral basal ganglia (Parent and Hazrati, 1995a,b; Chung et al., 2006; Tabbal et al., 2008) and input from the bilateral GPi and substantia nigra compacta into the bilateral thalamus and brain stem (Parent and Hazrati, 1995a,b; Levy et al., 1997; Chung et al., 2006; Tabbal et al., 2008; Peng-Chen et al., 2013). Based on our findings that showed a significant increase in cerebral blood flow in the contralateral frontal lobe, including in the premotor cortex, it is speculated that ipsilateral symptoms might be improved by using unilateral GPi-DBS therapy that stimulates the area contralateral to the side being stimulated in the cortex-basal ganglia-thalamus loop. The unilateral pyramidal tracts are involved in about 20% of control in motor functions of the body axis on the ipsilateral side (Germano et al., 2004). Thus, axial symptoms may be mitigated by improvement in blood flow of the unilateral premotor cortex areas. Previous study indicates that a deterioration in blood flow is noticeable in the frontal cingulate gyrus of PwPD who had dominant axial symptoms (Mito et al., 2006). Therefore, a significant increase in blood flow in areas that affect motor symptoms after unilateral GPi-DBS therapy, such as the frontal cingulate gyrus and frontal lobe areas including the premotor cortex, might contribute to the improvement in axial symptoms.

LIMITATIONS OF THE STUDY

Despite being one of the few detailed studies on the effectiveness of unilateral GPi-DBS therapy, this study has several limitations. Firstly, readers should be reminded that this was a retrospective observational study based on data from a single institution and the period of observation only lasted for 6 months with a small sample size of 17 patients. Secondly, this study attempted to offer insights by comparing the analyses of patients who underwent unilateral GPi-DBS in the current study to similar previous studies. Because it is impossible to fully control the conditions of studies that have already been conducted, our interpretations may be confounded. Thirdly, the period when ^{99m}Tc-ECD SPECT was performed postoperatively ranged widely; therefore, our assessment of cerebral blood flow may have been affected by other factors, such as the rate of progression in PD. Finally, this study examined the cerebral hemisphere ipsilateral or contralateral to the side where the DBS lead was inserted, without any clear knowledge of which side should be prioritized for which symptoms. In addition, this study did not evaluate the relationships between stimulation fields and the clinical responses/SPECT findings. Further studies are warranted to address these limitations.

CONCLUSION

Regardless of these limitations, this 6-month postoperative assessment was valuable in that it underscored the potential of unilateral GPi-DBS therapy, in improving both motor- and non-motor symptoms including depression and in maintaining speech and cognitive function of PwPD, that does not pale in comparison to bilateral GPi-DBS therapy. The unilateral

GPS-DBS therapy performed on PwPD, whose cognitive function remains unimpaired at relatively early stages of the disease, demonstrated therapeutic benefit equivalent to that of the bilateral counterparts, at over 6 months postoperatively. However, the results of this study constitute only a snapshot of information regarding the effect of unilateral GPi-DBS therapy and warrant a further investigation into long-term effects of the therapy and mechanisms responsible for mitigating various PD symptoms. Given the fact that unilateral GPi-DBS is less invasive and requires less battery energy than bilateral counterparts, the former could prove economically advantageous if it could systematically be shown that its effects on debilitating PD symptoms are long-lasting.

DATA AVAILABILITY STATEMENT

The raw data supporting the conclusions of this article will be made available by the authors, without undue reservation.

ETHICS STATEMENT

The studies involving human participants were reviewed and approved by the University of Fukuoka Institutional Review Board. Written informed consent for participation was not required for this study in accordance with the national legislation and the institutional requirements.

AUTHOR CONTRIBUTIONS

YT, TMi, and YH: conception and design. YT, TMi, SN, and YH: analysis and interpretation of data. YH: drafting the manuscript. YT, TMi, SF, TI, TMo, and SN: revising manuscript critically for important intellectual content. YT: final approval of the version to be submitted. All authors contributed substantially to this study.

FUNDING

This study was partly supported by a Japan Society for the Promotion of Science grant-in-aid for scientific research (C) (Grant No. 18K08956).

ACKNOWLEDGMENTS

We would like to thank the staff at Fukuoka University Hospital for their kind support and for the management of patients.

SUPPLEMENTARY MATERIAL

The Supplementary Material for this article can be found online at: https://www.frontiersin.org/articles/10.3389/fnhum.2022.888701/full#supplementary-material

REFERENCES

Agostino, R., Dinapoli, L., Modugno, N., Iezzi, E., Gregori, B., Esposito, V., et al. (2008). Ipsilateral sequential arm movements after unilateral subthalamic deep-brain stimulation in patients with Parkinson's disease. *Mov. Disord.* 23, 1718–1724. doi: 10.1002/mds.22203

Antonini, A., Landi, A., Benti, R., Mariani, C., De Notaris, R., Marotta, G., et al. (2003a). Functional neuroimaging (PET and SPECT) in the selection and assessment of patients with Parkinson's disease undergoing deep brain stimulation. *J. Neurosurg. Sci.* 47, 40–46.

Antonini, A., Marotta, G., Benti, R., Landi, A., De Notaris, R., Mariani, C., et al. (2003b). Brain flow changes before and after deep brain stimulation of the subthalamic nucleus in Parkinson's disease. *Neurol. Sci.* 24, 151–152. doi: 10.1007/s10072-003-0104-4

Antonini, A., Poewe, W., Chaudhuri, K. R., Jech, R., Pickut, B., Pirtošek, Z., et al. (2017). Levodopa-carbidopa intestinal gel in advanced Parkinson's: final results of the GLORIA registry. *Parkinsonism Relat. Disord.* 45, 13–20. doi: 10.1016/j.parkreldis.2017.09.018

Berganzo, K., Tijero, B., González-Eizaguirre, A., Somme, J., Lezcano, E., Gabilondo, I., et al. (2016). Motor and non-motor symptoms of Parkinson's disease and their impact on quality of life and on different clinical subgroups. *Neurologia* 31, 585–591. doi: 10.1016/j.nrl.2014.10.010

Chung, S. J., Jeon, S. R., Kim, S. R., Sung, Y. H., and Lee, M. C. (2006). Bilateral effects of unilateral subthalamic nucleus deep brain stimulation in advanced Parkinson's disease. *Eur. Neurol.* 56, 127–132. doi: 10.1159/000095704

Cilia, R., Marotta, G., Landi, A., Isaias, I. U., Mariani, C. B., Vergani, F., et al. (2009). Clinical and cerebral activity changes induced by subthalamic nucleus stimulation in advanced Parkinson's disease: a prospective case-control study. *Clin. Neurol. Neurosurg.* 111, 140–146. doi: 10.1016/j.clineuro.2008.09.018

Deep-Brain Stimulation for Parkinson's Disease Study Group, Obeso, J. A., Olanow, C. W., Rodriguez-Oroz, M. C., Krack, P., Kumar, R., et al. (2001). Deep-brain stimulation of the subthalamic nucleus or the pars interna of the globus pallidus in Parkinson's disease. *N. Engl. J. Med.* 345, 956–963. doi: 10.1056/NEJMoa000827

Germano, I. M., Gracies, J. M., Weisz, D. J., Tse, W., Koller, W. C., and Olanow, C. W. (2004). Unilateral stimulation of the subthalamic nucleus in Parkinson disease: a double-blind 12-month evaluation study. *J. Neurosurg.* 101, 36–42. doi: 10.3171/jns.2004.101.1.0036

Gökçal, E., Gür, V. E., Selvitop, R., Babacan Yildiz, G., and Asil, T. (2017). Motor and non-motor symptoms in Parkinson's disease: effects on quality of life. *Noro Psikiyatr. Ars.* 54, 143–148. doi: 10.5152/npa.2016.12758

Hasegawa, H., Fischer, P., Tan, H., Pogosyan, A., Samuel, M., Brown, P., et al. (2020). The effect of unilateral subthalamic nucleus deep brain stimulation on contralateral subthalamic nucleus local field potentials. *Neuromodulation* 23, 509–514. doi: 10.1111/ner.13155

Houeto, J. L., Damier, P., Bejjani, P. B., Staedler, C., Bonnet, A. M., Arnulf, I., et al. (2000). Subthalamic stimulation in Parkinson disease: a multidisciplinary approach. *Arch. Neurol.* 57, 461–465. doi: 10.1001/archneur.57.4.461

Hughes, A. J., Daniel, S. E., Kilford, L., and Lees, A. J. (1992). Accuracy of clinical diagnosis of idiopathic Parkinson's disease: a clinico-pathological study of 100 cases. *J. Neurol. Neurosurg. Psychiatry* 55, 181–184. doi: 10.1136/jnnp.55.3.181

Kim, H. J., Paek, S. H., Kim, J. Y., Lee, J. Y., Lim, Y. H., Kim, D. G., et al. (2009). Two-year follow-up on the effect of unilateral subthalamic deep brain stimulation in highly asymmetric Parkinson's disease. *Mov. Disord.* 24, 329–335. doi: 10.1002/mds.22211

Kotagal, V., Albin, R. L., Müller, M. L., Koeppe, R. A., Frey, K. A., and Bohnen, N. I. (2014). Modifiable cardiovascular risk factors and axial motor impairments in Parkinson disease. *Neurology* 82, 1514–1520. doi: 10.1212/WNL.0000000000000356

Kumar, R., Lozano, A. M., Sime, E., Halket, E., and Lang, A. E. (1999). Comparative effects of unilateral and bilateral subthalamic nucleus deep brain stimulation. *Neurology* 53, 561–566. doi: 10.1212/wnl.53.3.561

Levy, R., Hazrati, L. N., Herrero, M. T., Vila, M., Hassani, O. K., Mouroux, M., et al. (1997). Re-evaluation of the functional anatomy of the basal ganglia in

normal and Parkinsonian states. *Neuroscience* 75, 335–343. doi: 10.1016/s0306-4522(96)00409-5

Linazasoro, G., Van Blercom, N., and Lasa, A. (2003). Unilateral subthalamic deep brain stimulation in advanced Parkinson's disease. *Mov. Disord.* 18, 713–716. doi: 10.1002/mds.10407

Loher, T. J., Burgunder, J. M., Pohle, T., Weber, S., Sommerhalder, R., and Krauss, J. K. (2002). Long-term pallidal deep brain stimulation in patients with advanced Parkinson disease: 1-year follow-up study. *J. Neurosurg.* 96, 844–853. doi: 10.3171/jns.2002.96.5.0844

Mei, S., Eisinger, R. S., Hu, W., Tsuboi, T., Foote, K. D., Hass, C. J., et al. (2020). Three-year gait and axial outcomes of bilateral STN and GPi Parkinson's disease deep brain stimulation. *Front. Hum. Neurosci.* 14:1. doi: 10.3389/fnhum.2020.00001

Merello, M., Nouzeilles, M. I., Kuzis, G., Cammarota, A., Sabe, L., Betti, O., et al. (1999). Unilateral radiofrequency lesion versus electrostimulation of posteroventral pallidum: a prospective randomized comparison. *Mov. Disord.* 14, 50–56. doi: 10.1002/1531-8257(199901)14:1<50:aid-mds1010<3.0.co;2-6

Mishima, T., Fujioka, S., Morishita, T., Inoue, T., and Tsuboi, Y. (2021). Personalized medicine in Parkinson's Disease: new options for advanced trearments. *J. Pers. Med.* 11:650. doi: 10.3390/jpm11070650

Mito, Y., Yoshida, K., Yabe, I., Makino, K., Tashiro, K., Kikuchi, S., et al. (2006). Brain SPECT analysis by 3D-SSP and phenotype of Parkinson's disease. *J. Neurol. Sci.* 241, 67–72. doi: 10.1016/j.jns.2005.10.017

Molinuevo, J. L., Valldeoriola Tolosa, E., Tolosa, E., Rumia, J., Valls-Sole, J., Roldan, H., et al. (2000). Levodopa withdrawal after bilateral subthalamic nucleus stimulation in advanced Parkinson disease. *Arch. Neurol.* 57, 983–988. doi: 10.1001/archneur.57.7.983

Morishita, T., Higuchi, M. A., Saita, K., Tsuboi, Y., Abe, H., and Inoue, T. (2016). Changes in motor-related cortical activity following deep brain stimulation for parkinson's disease detected by functional near infrared spectroscopy: a pilot study. *Front. Hum. Neurosci.* 10:629. doi: 10.3389/fnhum.2016.00629

Nakamura, K., Christine, C. W., Starr, P. A., and Marks, W. J. Jr. (2007). Effects of unilateral subthalamic and pallidal deep brain stimulation on fine motor functions in Parkinson's disease. *Mov. Disord.* 22, 619–626. doi: 10.1002/mds.21300

Nakano, K. (2000). Neural circuits and topographic organization of the basal ganglia and related regions. *Brain Dev.* 22, S5–S16. doi: 10.1016/s0387-7604(00)00139-x

Okun, M. S., Fernandez, H. H., Wu, S. S., Kirsch-Darrow, L., Bowers, D., Bova, F., et al. (2009). Cognition and mood in Parkinson disease in STN versus GPi DBS: the COMPARE Trial. *Ann. Neurol.* 65, 586–595. doi: 10.1002/ana.21596

Okun, M. S., Wu, S. S., Fayad, S., Ward, H., Bowers, D., Rosado, C., et al. (2014). Acute and chronic mood and apathy outcomes from a randomized study of unilateral STN and GPi DBS. *PLoS One* 9:e1141404. doi: 10.1371/journal.pone.0114140

Parent, A., and Hazrati, L. N. (1995a). Functional anatomy of the basal ganglia. I. The cortico-basal ganglia-thalamo-cortical loop. *Brain Res. Brain Res. Rev.* 20, 91–127. doi: 10.1016/0165-0173(94)00007-c

Parent, A., and Hazrati, L. N. (1995b). Functional anatomy of the basal ganglia. II. The place of subthalamic nucleus and external pallidum in basal ganglia circuitry. *Brain Res. Brain Res. Rev.* 20, 128–154. doi: 10.1016/0165-0173(94)00008-d

Paschali, A., Constantoyannis, C., Angelatou, F., and Vassilakos, P. (2013). Perfusion brain SPECT in assessing motor improvement after deep brain stimulation in Parkinson's disease. *Acta Neurochir.* 155, 497–505. doi: 10.1007/s00701-012-1610-z

Peng-Chen, Z., Morishita, T., Vaillancourt, D., Favilla, C., Foote, K. D., Okun, M. S., et al. (2013). Unilateral thalamic deep brain stimulation in essential tremor demonstrates long-term ipsilateral effects. *Parkinsonism Relat. Disord.* 19, 1113–1117. doi: 10.1016/j.parkreldis.2013.08.001

Rodrigues, J. P., Walters, S. E., Watson, P., Stell, R., and Mastaglia, F. L. (2007). Globus pallidus stimulation in advanced Parkinson's disease. *J. Clin. Neurosci.* 14, 208–215. doi: 10.1016/j.jocn.2005.11.023

Rothlind, J. C., Cockshott, R. W., Starr, P. A., and Marks, W. J. (2007). Neuropsychological performance following staged bilateral pallidal or subthalamic nucleus deep brain stimulation for Parkinson's disease. *J. Int. Neuropsychol. Soc.* 13, 68–79. doi: 10.1017/S1355617707070105

Samii, A., Kelly, V. E., Slimp, J. C., Shumway-Cook, A., and Goodkin, R. (2007). Staged unilateral versus bilateral subthalamic nucleus stimulator implantation in Parkinson disease. *Mov. Disord.* 22, 1476–1481. doi: 10.1002/mds.21554

Schuepbach, W. M., Rau, J., Knudsen, K., Volkmann, J., Krack, P., Timmermann, L., et al. (2013). Neurostimulation for Parkinson's disease with early motor complications. *N. Engl. J. Med.* 368, 610–622. doi: 10.1056/NEJMoa1205158

Schupbach, W. M., Chastan, N., Welter, M. L., Houeto, J. L., Mesnage, V., Bonnet, A. M., et al. (2005). Stimulation of the subthalamic nucleus in Parkinson's disease: a 5 year follow up. *J. Neurol. Neurosurg. Psychiatry* 76, 1640–1644. doi: 10.1136/jnnp.2005.063206

Sestini, S., Ramat, S., Formiconi, A. R., Ammannati, F., Sorbi, S., and Pupi, A. (2005). Brain networks underlying the clinical effects of long-term subthalamic stimulation for Parkinson's disease: a 4-year follow-up study with rCBF SPECT. *J. Nucl. Med.* 46, 1444–1454.

Sestini, S., Scotto, di Luzio, A., Ammannati, F., De Cristofaro, M. T., Passeri, A., et al. (2002). Changes in regional cerebral blood flow caused by deep-brain stimulation of the subthalamic nucleus in Parkinson's disease. *J. Nucl. Med.* 43, 725–732.

Simuni, T., Jaggi, J. L., Mulholland, H., Hurtig, H. I., Colcher, A., Siderowf, A. D., et al. (2002). Bilateral stimulation of the subthalamic nucleus in patients with Parkinson disease: a study of efficacy and safety. *J. Neurosurg.* 96, 666–672. doi: 10.3171/jns.2002.96.4.0666

Tabbal, S. D., Ushe, M., Mink, J. W., Revilla, F. J., Wernle, A. R., Hong, M., et al. (2008). Unilateral subthalamic nucleus stimulation has a measurable ipsilateral effect on rigidity and bradykinesia in Parkinson disease. *Exp. Neurol.* 211, 234–242. doi: 10.1016/j.expneurol.2008.01.024

Takeuchi, R. (2005). *Atlas of the Constant Regions of Interest on the Brain Anatomically Standardized by SPM*. La Mesa, CA: Kyouritsu.

Tanei, T., Kajita, Y., Kaneoke, Y., Takebayashi, S., Nakatsubo, D., and Wakabayashi, T. (2009a). Staged bilateral deep brain stimulation of the subthalamic nucleus for the treatment of Parkinson's disease. *Acta Neurochir.* 151, 589–594. doi: 10.1007/s00701-009-0293-6

Tanei, T., Kajita, Y., Nihashi, T., Kaneoke, Y., Takebayashi, S., Nakatsubo, D., et al. (2009b). Changes in regional blood flow induced by unilateral subthalamic nucleus stimulation in patients with Parkinson's disease. *Neurol. Med. Chir.* 49, 507–513. doi: 10.2176/nmc.49.507

Thobois, S., Metens, P., Guenot, M., Hermier, M., Mollion, H., Bouvard, M., et al. (2002). Subthalamic nucleus stimulation in Parkinson's disease: clinical evaluation of 18 patients. *J. Neurol.* 249, 529–534. doi: 10.1007/s004150200059

Tomlinson, C. L., Stowe, R., Patel, S., Rick, C., Gray, R., and Clarke, C. E. (2010). Systematic review of levodopa dose equivalency reporting in Parkinson's disease. *Mov. Disord.* 25, 2649–2653.

van Laere, K., van der Linden, C., Santens, P., Vandewalle, V., Caemaert, J., Ir, P. L., et al. (2000). 99Tc(m)-ECD SPET perfusion changes by internal pallidum stimulation in Parkinson's disease. *Nucl. Med. Commun.* 21, 1103–1112. doi: 10.1097/00006231-200012000-00003

Vingerhoets, G., van der Linden, C., Lannoo, E., Vandewalle, V., Caemaert, J., Wolters, M., et al. (1999). Cognitive outcome after unilateral pallidal stimulation in Parkinson's disease. *J. Neurol. Neurosurg. Psychiatry* 66, 297–304. doi: 10.1136/jnnp.66.3.297

Volkmann, J., Albanese, A., Kulisevsky, J., Tornqvist, A. L., Houeto, J. L., Pidoux, B., et al. (2009). Long-term effects of pallidal or subthalamic deep brain stimulation on quality of life in Parkinson's disease. *Mov. Disord.* 24, 1154–1161. doi: 10.1002/mds.22496

Volkmann, J., Allert, N., Voges, J., Weiss, P. H., Freund, H. J., and Sturm, V. (2001). Safety and efficacy of pallidal or subthalamic nucleus stimulation in advanced PD. *Neurology* 56, 548–551. doi: 10.1212/wnl.56.4.548

Volkmann, J., Herzog, J., Kopper, F., and Deuschl, G. (2002). Introduction to the programming of deep brain stimulators. *Mov. Disord.* 17, S181–S187. doi: 10.1002/mds.10162

Walker, H. C., Watts, R. L., Guthrie, S., Wang, D., and Guthrie, B. L. (2009). Bilateral effects of unilateral subthalamic deep brain stimulation on Parkinson's disease at 1 year. *Neurosurgery* 65, 302–309. doi: 10.1227/01.NEU.0000349764.34211.74

Zahodne, L. B., Okun, M. S., Foote, K. D., Fernandez, H. H., Rodriguez, R. L., Wu, S. S., et al. (2009). Greater improvement in quality of life following unilateral deep brain stimulation surgery in the globus pallidus as compared to the subthalamic nucleus. *J. Neurol.* 256, 1321–1329. doi: 10.1007/s00415-009-5121-7

Conflict of Interest: The authors declare that the research was conducted in the absence of any commercial or financial relationships that could be construed as a potential conflict of interest.

Publisher's Note: All claims expressed in this article are solely those of the authors and do not necessarily represent those of their affiliated organizations, or those of the publisher, the editors and the reviewers. Any product that may be evaluated in this article, or claim that may be made by its manufacturer, is not guaranteed or endorsed by the publisher.

frontiers | Frontiers in Human Neuroscience

BRIEF RESEARCH REPORT
published: 02 June 2022
doi: 10.3389/fnhum.2022.896435

Current Steering Using Multiple Independent Current Control Deep Brain Stimulation Technology Results in Distinct Neurophysiological Responses in Parkinson's Disease Patients

Jana Peeters[1], Alexandra Boogers[1,2], Tine Van Bogaert[1], Robin Gransier[1], Jan Wouters[1], Bart Nuttin[3,4] and Myles Mc Laughlin[1]*

[1] Experimental Oto-rhino-laryngology, Department of Neurosciences, Leuven Brain Institute, KU Leuven, Leuven, Belgium, [2] Department of Neurology, UZ Leuven, Leuven, Belgium, [3] Experimental Neurosurgery and Neuroanatomy, Department of Neurosciences, Leuven Brain Institute, KU Leuven, Leuven, Belgium, [4] Department of Neurosurgery, UZ Leuven, Leuven, Belgium

OPEN ACCESS

Edited by:
Joshua K. Wong,
University of Florida, United States

Reviewed by:
Jackson N. Cagle,
University of Florida, United States
Bassam Al-Fatly,
Charité Universitätsmedizin Berlin, Germany

***Correspondence:**
Jana Peeters
jana.peeters@kuleuven.be

Specialty section:
This article was submitted to Brain Imaging and Stimulation, a section of the journal Frontiers in Human Neuroscience

Received: 15 March 2022
Accepted: 16 May 2022
Published: 02 June 2022

Citation:
Peeters J, Boogers A, Van Bogaert T, Gransier R, Wouters J, Nuttin B and Mc Laughlin M (2022) Current Steering Using Multiple Independent Current Control Deep Brain Stimulation Technology Results in Distinct Neurophysiological Responses in Parkinson's Disease Patients. Front. Hum. Neurosci. 16:896435. doi: 10.3389/fnhum.2022.896435

Background: Deep brain stimulation (DBS) is an effective neuromodulation therapy to treat people with medication-refractory Parkinson's disease (PD). However, the neural networks affected by DBS are not yet fully understood. Recent studies show that stimulating on different DBS-contacts using a single current source results in distinct EEG-based evoked potentials (EPs), with a peak at 3 ms (P3) associated with dorsolateral subthalamic nucleus stimulation and a peak at 10 ms associated with substantia nigra stimulation. Multiple independent current control (MICC) technology allows the center of the electric field to be moved in between two adjacent DBS-contacts, offering a potential advantage in spatial precision.

Objective: Determine if MICC precision targeting results in distinct neurophysiological responses recorded *via* EEG.

Materials and Methods: We recorded cortical EPs in five hemispheres (four PD patients) using EEG whilst employing MICC to move the electric field from the most dorsal DBS-contact to the most ventral in 15 incremental steps.

Results: The center of the electric field location had a significant effect on both the P3 and P10 amplitude in all hemispheres where a peak was detected (P3, detected in 4 of 5 hemispheres, $p < 0.0001$; P10, detected in 5 of 5 hemispheres, $p < 0.0001$). *Post hoc* analysis indicated furthermore that MICC technology can significantly refine the resolution of steering.

Conclusion: Using MICC to incrementally move the center of the electric field to locations between adjacent DBS-contacts resulted in significantly different neurophysiological responses that may allow further precision of the programming of individual patients.

Keywords: movement disorders, Parkinson's disease, deep brain stimulation, multiple independent current control, electroencephalography, evoked potentials

INTRODUCTION

Deep brain stimulation (DBS) is an effective therapy for medication-refractory movement disorders such as Parkinson's disease (PD) (Limousin et al., 1998; Lyons, 2011; Kalia et al., 2013; Fasano et al., 2014). This treatment involves electrical stimulation through an electrode array (i.e., the DBS lead) implanted in a deep brain structure. For PD patients, the lead is most often implanted in the dorsolateral subthalamic nucleus (STN). Careful selection of optimal stimulation parameters is critical in ensuring an effective clinical outcome. The parameter space is large and includes stimulation intensity, stimulation rate, pulse width, configuration, and polarity (Wagle Shukla et al., 2017; Santaniello et al., 2018; Koeglsperger et al., 2019). The advent of directional leads and multiple independent current controlled (MICC) DBS now allow for even more precise targeting of the electric field toward the target region and away from side effect-causing regions (Steigerwald et al., 2019). These advances have been shown to improve clinical outcomes (Pollo et al., 2014; Steigerwald et al., 2016; Dembek et al., 2017; Krack et al., 2019; Vitek et al., 2020), but due to variance in lead placement, parameter space and patient heterogeneity, programming individual patients to determine the optimal electric field location has become increasingly time-consuming and labor-intensive (Sasaki et al., 2021). To improve this, better understanding of the different neural circuits activated with the different DBS parameters could help elucidate how DBS affects specific neural networks, and thereby it could guide DBS programming. DBS activation has been investigated in PD patients through evoked potential (EP) recordings using electroencephalography (EEG) (Walker et al., 2012) and electrocorticography (Miocinovic et al., 2018). These studies suggest that an EP recorded around 3 ms post stimulus (P3) may be important for predicting clinical outcomes.

Furthermore, in a recent study performed by our research group (Peeters et al., 2021), we recorded, in addition to a P3 peak, a peak around 10 ms post stimulus (P10) using EEG in eight patients implanted with directional leads. In that study, we showed that changing the stimulation contact using a single current source approach significantly affected the amplitude of both P3 and P10. Furthermore, combining the EEG with fused pre-operative MR and postoperative CT images showed that P3 was largest when stimulating on the dorsal DBS-contacts closest to dorsolateral STN and P10 the largest when stimulating on the ventral DBS-contacts closest to the substantia nigra pars reticulata (SNr). This suggests that P3 could serve as a biomarker for contacts closest to the dorsolateral STN, while P10 may be useful for predicting which contacts will give SNr-related side effects. Thus, EEG-based EPs could provide useful information to objectively guide programming in patients implanted with directional leads.

Multiple independent current control (MICC) technology now provides the ability to divide the total current delivered independently over two or more DBS-contacts. In the present study, we investigated if using MICC to move the electric field vertically in small incremental steps would result in distinct changes in the EEG recorded P3 and P10 amplitudes. If successful, P3 and P10 amplitudes could serve as a biomarker to evaluate the precise targeting of electric field locations for optimal clinical outcome. Here, we measured EEG-based EPs during low frequency (10 Hz) DBS and used MICC DBS to stimulate at sixteen different depths along tightly spaced (distance of 0.5 mm between two depths) directional leads in PD patients.

MATERIALS AND METHODS

Participants

The study was approved by the Ethics committee Research UZ/KU Leuven (S62373) and registered on Clinicaltrials.gov (NCT04658641). All participants received oral and written information and provided oral and written consent. The study was conducted in conformity with the Declaration of Helsinki, the Belgian law of May 7th 2004 on experiments on the human person and in agreement with Good Clinical Practice guidelines.

Participants that met the "UK PD Society Brain Bank Clinical Diagnostic Criteria" for the diagnosis of idiopathic PD, were included in the study (Postuma et al., 2015). Directional leads (Vercise Cartesia®, Boston Scientific; BSC, Valencia, CA, United States) were bilaterally implanted in the STN and subcutaneously connected to the implantable pulse generator (IPG; Vercise DBS Systems, BSC, Valencia, CA, United States) that has MICC technology designed to allow for refined division of the total current over multiple DBS-contacts (Boston Scientific Corporation, 2018). The DBS-leads consist of eight DBS-contacts with a length of 1.5 mm, separated from one another by interspaces of 0.5 mm and arranged in a tip-3-3-1 configuration (Paff et al., 2020) (distal-to-proximal axis of the electrode contact numbering of left lead: C1-C8; and the right lead: C9-C16, where "C" stands for "Contact"). The surgical procedure was performed as standard-of-care at our center using the microrecording technique (Gross et al., 2006).

Patients that already participated in the previous study (Peeters et al., 2021) were now enrolled in a follow-up study, where we tested the MICC technology (see further). Four patients participated, one of which participated twice, yielding data from both hemispheres in this patient. In total, five hemispheres were tested. All participants were asked to refrain from taking their medication 12 h prior to the study visit. Demographic data and stimulation parameters used during the experiment are summarized in **Supplementary Table 1**.

Deep Brain Stimulation

First, stimulation was turned off in both hemispheres. One hemisphere was tested at a time, with the other hemisphere remaining off. Thereafter, the stimulation intensity was defined on the clinical contact (monopolar cathodic pulse with return on the case; 60 μs and 130 Hz) as the highest stimulation intensity without non-transient stimulation-induced side effects. For the experimental setup, stimulation was then decreased to 10 Hz. An *in vitro* phantom head experiment was performed as a negative control where no EPs were expected. The set-up used a head-sized watermelon, where a directional lead (Vercise Cartesia®, BSC, Valencia, CA, United States) was positioned

approximately 6.0 cm from the surface. EEG channels were then positioned on the surface and an anterior-posterior direction was appointed depending on the location of the EEG channels. All processing steps and analyses performed on real patient datasets were repeated for the phantom head dataset.

At the start of the experiment, the electric field (which had an approximately constant volume throughout the experiment as the same stimulation intensity was applied throughout the experiment) was set at the center of the most dorsal DBS-contact (i.e., 100% on C8 for the left hemisphere and C16 for the right hemisphere) for 50 s, yielding a total of 500 epochs of 100-ms duration. Then, the electric field was moved in a ventral direction in fifteen equal steps until the most ventral DBS-contact was tested. Thus, we tested sixteen incremental positions in total. The two most distant electric field locations had a distance of 6.0 mm in total, thus equating each proportional shift in the electric field was about 0.4 mm (6.0 mm/15 steps) per step. The segmented contacts were only tested in ring mode to avoid confounding the results with horizontal steering as a variable.

Electroencephalography and Artifact-Reduction Method

EEG recordings were performed with a 64-channel ActiveTwo BioSemi system with a sample rate of 16,384 Hz and a built-in low-pass filter with a cut-off frequency of 3,200 Hz. This EEG system uses active recording channels positioned according to the internationally standardized 10–20 system (Jasper, 1958) and referenced to the vertex EEG channel (Cz). One additional EEG channel (EXG1) was positioned on the skin on top of the implanted IPG to record the stimulation pulse, which served as a trigger channel to align EPs. Two additional EEG channels were positioned on the left (EXG2) and right (EXG3) mastoid to record the stimulation pulse at a cranial location with negligible neural responses. We stimulated each of the 16 depths for 50 s at 10 Hz, yielding a total of 500 epochs with a duration of 100 ms for each depth. Each epoch was baseline corrected by subtracting the average of a 1-ms period prior to stimulus onset. Then the epochs were averaged to get the averaged EP. We applied a combination of linear interpolation and template-subtraction to reduce the total stimulation-induced artifact. Template subtraction was based on the artifact recorded with EEG electrodes EXG2 and EXG3. Two bandpass 2nd-order Butterworth filters were applied to these EPs. One was designed for evaluation of short-latency responses with a high-pass cutoff frequency of 150 Hz and low-pass cutoff frequency of 1,000 Hz. The other was designed for evaluation of long-latency responses with a high-pass cutoff frequency of 1 Hz and low-pass cutoff frequency of 150 Hz. A more detailed description of the EEG protocol and artifact-reduction method can be found in Peeters et al. (2021).

Software and Statistical Analysis

All data processing and statistical analyses were done in MATLAB 2021a (Mathworks, Natick, MA, United States). A significance level of 5% was used in all tests. Based on the previous study (Peeters et al., 2021), we recorded a short-latency peak at 3 ms (P3) *via* the motor cortex EEG channel ipsilateral to stimulation (i.e., F3 for left hemisphere, F4 for right hemisphere) as in this EEG channel the strongest P3 was recorded. For the same reason, we recorded a long-latency peak at 10 ms (P10) *via* the prefrontal cortex EEG channel ipsilateral to stimulation (i.e., AF7 for left hemisphere, AF8 for right hemisphere). By central limit theorem, the individual EPs recorded conform to Gaussian assumptions so parametric statistics were used (Central Limit Theorem, 2008). Thus, we used one-way ANOVA to evaluate if the MICC depth of stimulation affected the P3 and P10 peak amplitude as measured in each individual hemisphere. Each EP consisted of more than 400 epochs, thus enough data were available to perform robust statistics at the individual hemispheric level. In the previous study, a one-way ANOVA was used to investigate if increasing stimulation intensity significantly affected P3 and P10 amplitude. If no significant effect of intensity was found on the peak amplitude, no further analysis was performed in this hemisphere (see **Supplementary Table 1**). For the remaining hemispheres, we used one-way ANOVA to evaluate if MICC technology significantly affected EP peak amplitude. Next, to test the separability of MICC on the P3 and P10 peak amplitude between different electric field pairs (varying from one step between two immediately adjacent electric field pairs to fifteen steps between two electric field pairs). For this, a *post hoc* analysis with a Bonferroni correction for multiple comparisons was applied (MATLAB, multcompare).

To investigate the relationship between the distance from each electric field center to relevant anatomical regions, we grouped all tested hemispheres (analysis on the individual hemisphere level can be found in **Supplementary Figure 5**). The open-source Lead-DBS image processing pipeline (version 2.5.3, Berlin, Germany) (Horn and Kühn, 2015; Horn et al., 2019) was used for postoperative lead reconstruction analyses, allowing the determination of the specific lead position and orientation on an individual hemispheric level. We then calculated the distance between the center of each electric field and the closest voxel of certain brain regions using the Distal atlas (Ewert et al., 2018).

RESULTS

Short-and Long-Latency Responses Using Multiple Independent Current Control Technology

Figure 1 shows the short- and long-latency EPs in response to DBS when using the MICC technology to vertically migrate the center of the electric field from the most dorsal DBS-contacts in 16 steps to the most ventral contact for a representative subject. Each of the 16 EPs are shown in a different color, as indicated in the legend. **Figures 1A,B** illustrate the short- and long-latency EPs recorded in participant 1 (left hemisphere), respectively, while **Figures 1C,D** the short- and long-latency EPs show recorded in a phantom head. All stimulation settings were well tolerated. In general, the EP morphology was similar to previously reported data recorded in a similar patient population (Walker et al., 2012; Miocinovic et al., 2018; Peeters et al., 2021). As expected, the P3 peak appeared strongest in the most dorsal

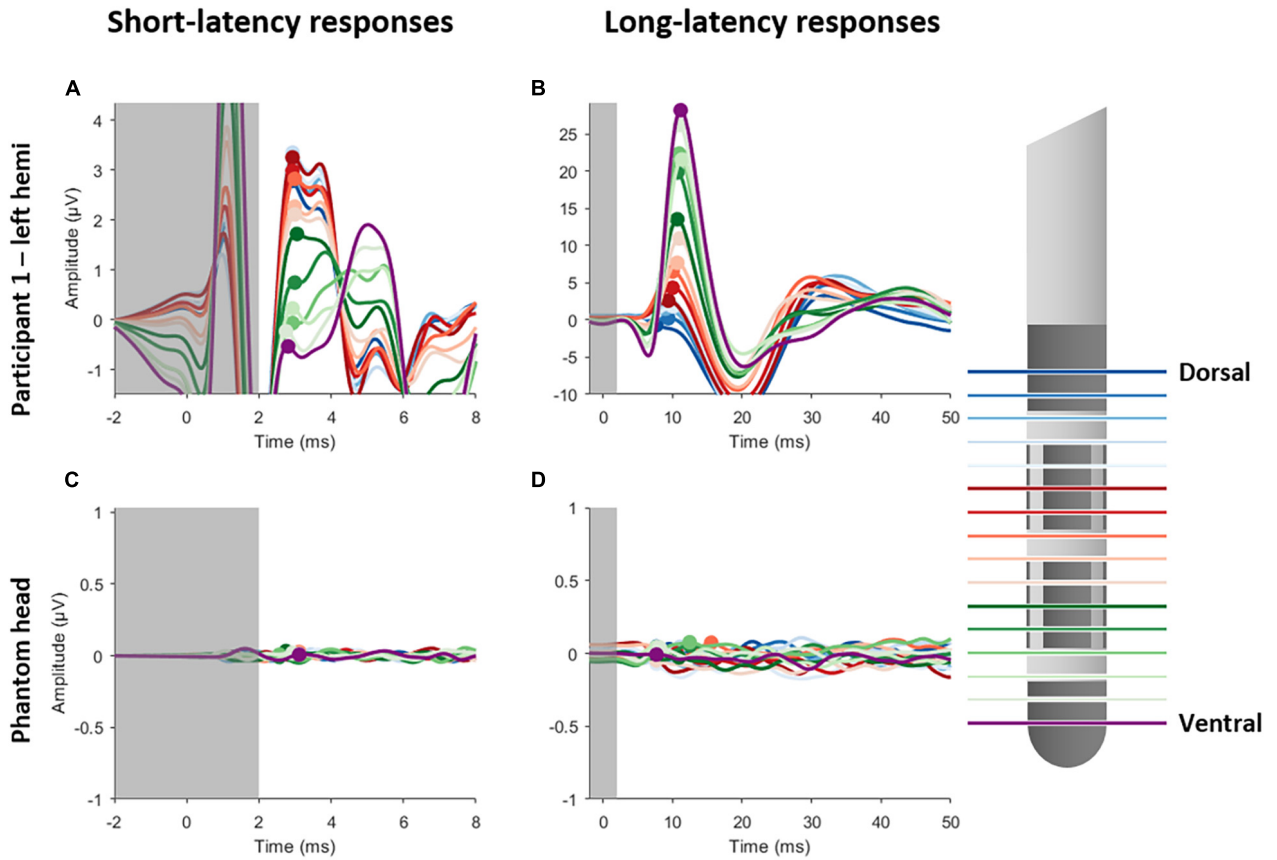

FIGURE 1 | Short- and long-latency EPs recorded whilst employing MICC technology in steps of 20%, yielding a total of 16 EPs. Left panels show the short-latency EPs for participant 1 **(A)** and the phantom head **(C)**. Right panels show the long-latency EPs for participant 1 **(B)** and the phantom head **(D)**. Each EP is colored differently, as is indicated on the legend on the right side. The gray transparent box indicates the time window (–1 to 2 ms) where residual artifact might still be present. The peak amplitudes are indicated with a circle for P3 (left panels) and P10 (right panels).

DBS-contacts, while the P10 peak appeared strongest in the most ventral DBS-contacts (Peeters et al., 2021). Based on the analysis of the previous study (Peeters et al., 2021) we found a significant P3 peak in four out of five hemispheres and a significant P10 peak in all five hemispheres (see **Supplementary Figures 1, 2**). Therefore, further analysis on P3 was only performed in the four hemispheres where a significant P3 peak was detected. A summary of this analysis is provided in **Supplementary Table 2**.

Distinct Evoked Potential Amplitudes Were Observed When Multiple Independent Current Control Was Used to Move the Center of the Electric Field to Location Between Two Vertically Adjacent Deep Brain Stimulation Contacts

Figure 2 illustrates the change in EP amplitude for P3 peak (left panels) and P10 peak (right panels) for participant 1 (upper panels) and the phantom head (lower panels). Each of the 16 EPs are shown in a different color (see legend). A one-way ANOVA showed that there was a significant effect of the MICC-controlled electric field depth on P3 amplitude [$F_{(15,\ 6399)} = 36.21$; $p < 0.0001$] for participant 1. Additionally, a significant effect of MICC-controlled electric field depth on P10 amplitude [$F_{(15,\ 6399)} = 395.57$; $p < 0.0001$] was also found in this participant. Importantly, control stimulation in the phantom head showed no effect of MICC-controlled electric field depth on P3 nor P10 amplitude [P3: $F_{(15,\ 6399)} = 0.30$; $p = 0.956$; P10: $F_{(15,\ 6399)} = 1.13$; $p = 0.3259$] In total, we found that the MICC-controlled electric field depth had a significant effect on P3 amplitude in all four tested hemispheres and a significant effect on P10 amplitude in all five tested hemispheres (see **Table 1** and **Supplementary Figures 3, 4**).

Post hoc analysis was performed to investigate the separability of MICC-controlled electric field depth on P3 and P10 amplitudes. **Figure 3** shows the electric field pair separation in incremental steps, varying from one step to fifteen steps on the x-axis, and the percentage of electric field pairs showing a significantly different P3 (A) or P10 (B) peak amplitude (mean ± CI) on the y-axis for all tested hemispheres after Bonferroni correction was applied. The P10 peak was

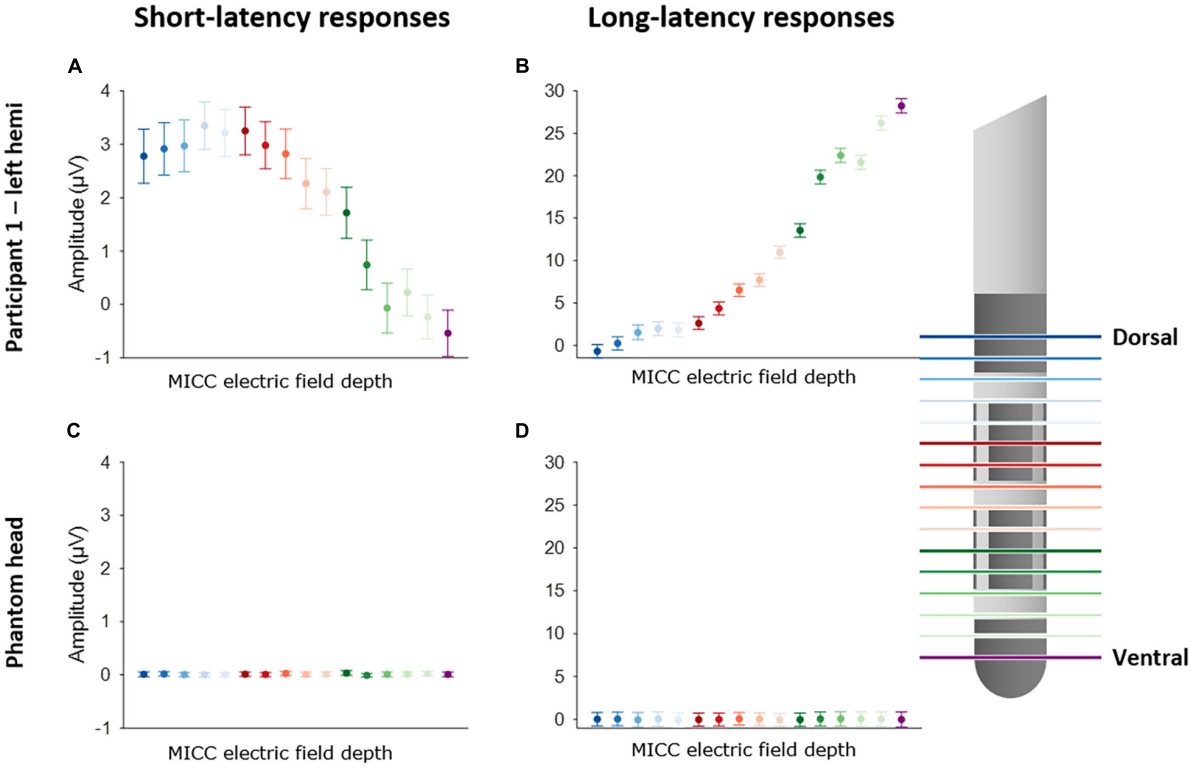

FIGURE 2 | Effect of using MICC to change the center of the electric field on P3 and P10 amplitude. Left panels show the effect of MICC technology on P3 amplitude for participant 1 **(A)** and the phantom head **(C)**. Right panels show the effect on P10 amplitude for participant 1 **(B)** and the phantom head **(D)**. Each EP is colored differently, as is indicated on the legend on the right side. The dots show the mean peak amplitude (P3 or P10) calculated across all epochs (n = 400), the error bars show the 95% confidence interval (CI).

significantly different on around 30% of immediately adjacent electric field pairs (1 step separation) increasing to 100% of electric field pairs when the separation was increased to 15 steps (**Figure 3B**). The P3 peak was only significantly different on around 5% of electric field pairs when the separation was increased to 2 steps. This percentage of significantly different electric field pairs increased steadily to around 80% of pairs as the separation was increased to 15 steps.

TABLE 1 | Effect of MICC on P3 and P10 amplitude.

Participant no.	P3 (one-way ANOVA)		P10 (one-way ANOVA)	
	P-value	F-statistics	*P*-value	F-statistics
1L	<0.0001	36.21	<0.0001	395.57
1R	<0.0001	94.94	<0.0001	489.59
2L	<0.0001	3.71	<0.0001	18.31
3L	<0.0001	7.51	<0.0001	6.73
4L	–	–	<0.0001	229.87
Phantom head	NS	0.52	NS	0.33
Total (%)	4/4 (100%)		5/5 (100%)	

L, left hemisphere tested; R, right hemisphere tested; NS, not significant; Total (%), total number of participants tested. One-way ANOVA was applied to evaluate if MICC technology significantly affected the P3 and P10 peak amplitudes as measured in each individual hemisphere.

Correlation Between Evoked Potential Amplitudes and Image-Derived Lead and Contact Position

The above results strengthen the idea published in a previous article (Peeters et al., 2021), stating that stimulation on the different depths preferentially modulates different nuclei, thereby causing the different EP peaks. We therefore plotted the average P3 and P10 amplitudes from all tested hemispheres as a function of the distance of each of the 16 electric field depths to dorsolateral STN and to SNr, respectively (**Figure 4**). This indicates indeed that the closer the MICC-controlled depth is to motor STN, the stronger the P3 peak amplitude appears and P10 peak amplitude appears strongest when stimulating from an MICC-controlled depth closest to SN.

DISCUSSION

We used MICC stimulation to vertically move the center of the electric field in fifteen incremental steps from the most dorsal DBS-contact to the most ventral DBS-contact while recording multichannel EEG EPs in PD patients. Thus, sixteen electric field

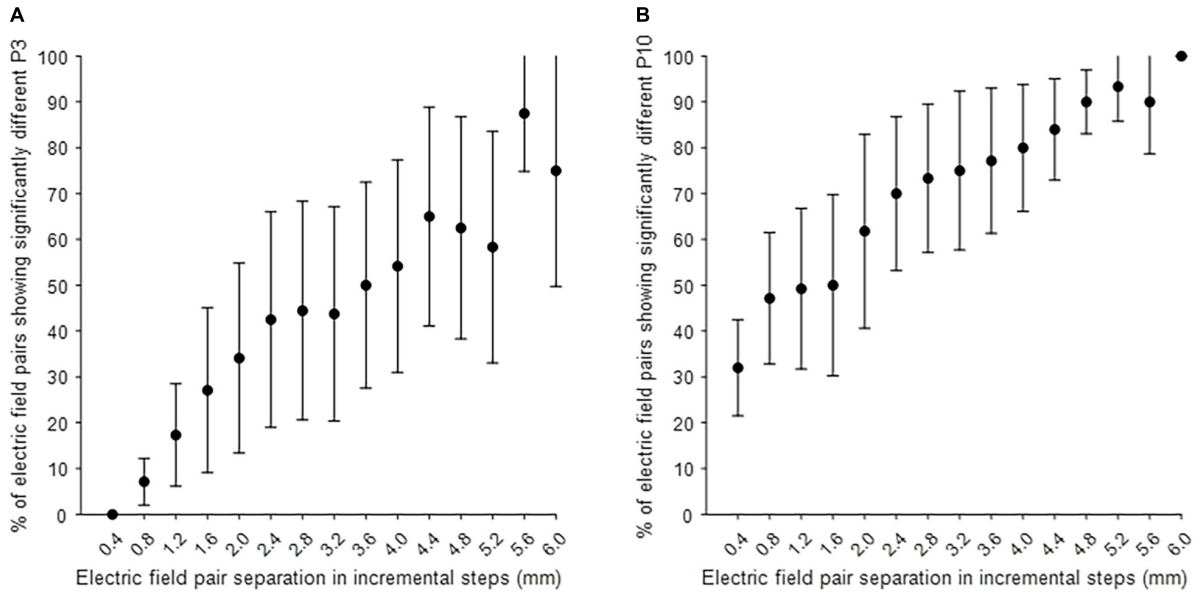

FIGURE 3 | *Post hoc* analysis on the separability of electric field pairs on P3 and P10 amplitude. **(A)** The separability of MICC-controlled electric field depth on P3 amplitude in all tested hemispheres (n = 4). **(B)** The separability of MICC-controlled electric field depth on P10 amplitude in all tested hemispheres (n = 5). The x-axis shows the separation of electric field pairs in incremental steps (mm), varying from one step to fifteen steps with a proportional distance of 0.4 mm and the y-axis shows the percentage of electric field pairs showing a significantly different P3 or P10 peak amplitude (mean ± CI) in all tested hemispheres after Bonferroni correction was applied.

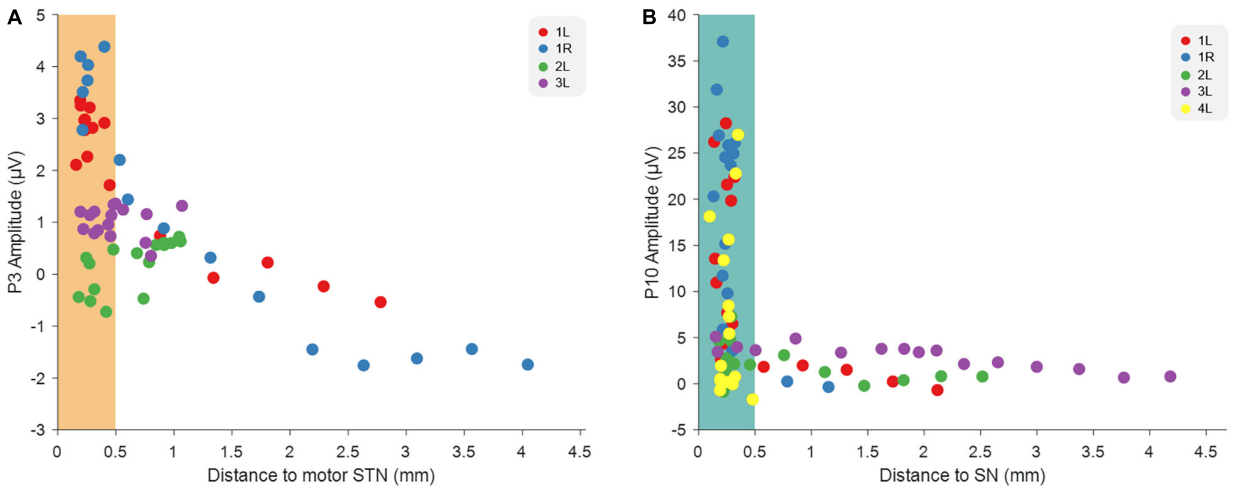

FIGURE 4 | Relationship between EP amplitudes and the distance to image-derived anatomical structures. **(A)** The relationship between the distance of each MICC-controlled electric field depth to STN and the P3 amplitude recorded on that MICC-controlled depth in four hemispheres (n = 64). **(B)** The relationship between the distance of each MICC-controlled electric field depth to SN and the P10 amplitude recorded on that MICC-controlled depth in five hemispheres (n = 80). The colors indicate the sixteen MICC-controlled depths of the same hemisphere. When the distance was smaller than 0.5 mm, the electric field center was determined as "within" either dorsolateral STN (orange rectangle) or SN (blue rectangle).

locations were tested in total with a shift of approximately 0.4 mm per step calculated proportionally. In the four hemispheres were a P3 peak could be detected, incrementally changing the center of the electric field had a significant effect on the P3 amplitude. Furthermore, a P10 peak was detected in all five hemispheres and incrementally moving the electric field also had a significant effect on P10 amplitude. Importantly, in a control experiment using a phantom head, no P3 or P10 peaks were detected, nor was a significant effect of MICC on P3 or P10 peak amplitude detected when the stimulation location was moved. These results indicate that the small changes in vertical current steering can be achieved with MICC stimulation adjustments, and cause distinct neurophysiological responses. The center of the electric field in reference to the P3 and P10 peak amplitudes do not follow a

straight line, which indicate that EP responses show a rather heterogeneous sensitivity to steering along the lead, an effect that is probably dependent on the lead positioning in the brain.

Previously, we have reported that P3 and P10 peak amplitudes were significantly different when stimulating on different directional contacts (vertical and horizontal current steering). Furthermore, we showed that stimulating on DBS-contacts closest to dorsolateral STN resulted in the largest P3 peak, while stimulating on DBS-contacts closest to SNr caused the largest P10 peak. Those results indicated that P3 may be a good predictor for the best DBS-contact to initiate programming in a new patient, while P10 might help predict which contacts will results in SNr-related side effects (Peeters et al., 2021). In the current study, we went one step further by investigating the more precise changes in programming possibilities that can be achieved with MICC stimulation, i.e., moving the center of the electric field to targets located between two adjacent DBS-contacts. Overall, our present results show that small incremental shifts in electric field location using MICC technology result in significant differences in P3 and P10 peak amplitudes. These distinct neurophysiological responses suggest that MICC technology can deliver measurably more precise stimulation in DBS patients. Group analysis furthermore indicated that the closer the center of the electric field is positioned to dorsolateral STN, the stronger P3 amplitude appears to be, while the closer the electric field center is positioned to SN, the stronger P10 amplitude appears.

Post hoc analyses showed that MICC technology can result in significantly distinct P3 peak amplitudes when comparing electric field pairs with just two steps (i.e., with a distance of only 0.8 mm) in between, and distinct P10 peak amplitudes when comparing two adjacent electric field pairs (i.e., with a distance of only 0.4 mm). Thus, results reported here indicate that MICC technology can significantly increase the resolution of vertical steering by at least 60% (0.4 mm compared to 1 mm dual-monopolar). A multicenter, randomized, controlled study has investigated MICC devices in a large population, where they found improvements in motor function and quality of life, while maintaining the safety profile in Parkinson's disease patients. However, these clinicians were not able to assess the full spectrum of MICC on clinical outcomes (Vitek et al., 2020). Despite these promising results, it is therefore still not completely clear whether the more precise spatial targeting offered by MICC technology also results in improved therapeutic outcomes.

Similar to the previous study (Peeters et al., 2021), we found that P3 had the largest amplitude when stimulating from a MICC-controlled depth closest to dorsolateral STN, which suggest that P3 is associated with STN modulation. Furthermore, P10 had the largest amplitude when stimulating from a depth closest to SN, suggesting that P10 is associated with SN modulation (**Figure 4**). This strengthens the previous conclusion that different neural circuits are activated and that EPs thus might serve as a neurophysiological marker of STN-and SNr-DBS. On a clinical level, EPs could be used complementary to imaging approaches to guide DBS programming in individual patients.

One potential drawback of the increased parameter space offered by MICC technology is that is can be time consuming for the programmer to find the optimal center of the electric field. Imaging approaches can already offer a partial solution to this problem by suggesting hotspots where a programmer can begin. Our data now show that the P3 amplitude could offer a potential complimentary EEG-based approach. Furthermore, the study described here works further on previously reported study correlating P3 to dorsolateral STN (Peeters et al., 2021), provides more refined electrophysiological indication as to why we should direct the stimulation field toward dorsolateral STN.

There are some limitations to be noted for this study. We report here on data from just four patients (five hemispheres). However, even in this small group we found consistent results. All statistics on the effect of MICC on EP peak amplitude were also performed on an individual (hemisphere) level and it is important to note that DBS programming happens on a patient-specific level. Furthermore, the vertical steering was not performed in a randomized order due to time constraints. We believe that this method did not largely affect the results as low frequency DBS-EPs are similar regardless of time of capture in our dataset.

In conclusion, changing the electric field during electrical stimulation in STN in parkinsonian patients using MICC technology resulted in distinct EEG-based EP responses. More specifically, results indicate that MICC electric field pairs can produce statistically separable responses down to distances of approximately 0.8 mm or 0.4 mm. The results reported here enable future investigations to test whether these differences in electric field locations are also clinically distinct. Lastly, these results, together with those previously reported (Peeters et al., 2021), strengthen the idea that EPs may provide clinically relevant information to help guide programming in individual DBS patients.

DATA AVAILABILITY STATEMENT

The raw data supporting the conclusions of this article will be made available by the authors, without undue reservation.

ETHICS STATEMENT

The studies involving human participants were reviewed and approved by KU Leuven/UZ Leuven Ethics committee. The patients/participants provided their written informed consent to participate in this study.

AUTHOR CONTRIBUTIONS

All authors listed have made a substantial, direct, and intellectual contribution to the work, and approved it for publication.

SUPPLEMENTARY MATERIAL

The Supplementary Material for this article can be found online at: https://www.frontiersin.org/articles/10.3389/fnhum.2022.896435/full#supplementary-material

REFERENCES

Boston Scientific Corporation (2018). *Vercise DBS Leads*. Marlborough: Boston Scientific Corporation.

Central Limit Theorem (2008). *The Concise Encyclopedia of Statistics*. New York, NY: Springer, doi: 10.1007/978-0-387-32833-1_50

Dembek, T. A., Reker, P., Visser-Vandewalle, V., Wirths, J., Treuer, H., Klehr, M., et al. (2017). Directional DBS increases side-effect thresholds—A prospective, double-blind trial. *Mov. Disord.* 32, 1380–1388. doi: 10.1002/mds.27093

Ewert, S., Plettig, P., Li, N., Chakravarty, M. M., Collins, D. L., Herrington, T. M., et al. (2018). Toward defining deep brain stimulation targets in MNI space: a subcortical atlas based on multimodal MRI, histology and structural connectivity. *Neuroimage* 170, 271–282. doi: 10.1016/J.NEUROIMAGE.2017.05.015

Fasano, A., Bove, F., and Lang, A. E. (2014). The treatment of dystonic tremor: a systematic review. *J. Neurol. Neurosurg. Psychiatry* 85, 759–769. doi: 10.1136/jnnp-2013-305532

Gross, R. E., Krack, P., Rodriguez-Oroz, M. C., Rezai, A. R., and Benabid, A. L. (2006). Electrophysiological mapping for the implantation of deep brain stimulators for Parkinson's disease and tremor. *Mov. Disord.* 21, S259–S283. doi: 10.1002/MDS.20960

Horn, A., and Kühn, A. A. (2015). Lead-DBS: a toolbox for deep brain stimulation electrode localizations and visualizations. *Neuroimage* 107, 127–135. doi: 10.1016/j.neuroimage.2014.12.002

Horn, A., Li, N., Dembek, T. A., Kappel, A., Boulay, C., Ewert, S., et al. (2019). Lead-DBS v2: towards a comprehensive pipeline for deep brain stimulation imaging Region of Interest. *Neuroimage* 184, 293–316. doi: 10.1016/j.neuroimage.2018.08.068

Jasper, H. (1958). The ten twenty electrode system of the international federation. *Electroencephalogr. Clin. Neurophysiol.* 52, 3–6.

Kalia, S. K., Sankar, T., and Lozano, A. M. (2013). Deep brain stimulation for Parkinson,s disease and other movement disorders. *Curr. Opin. Neurol.* 26, 374–380. doi: 10.1097/WCO.0b013e3283632d08

Koeglsperger, T., Palleis, C., Hell, F., Mehrkens, J. H., and Bötzel, K. (2019). Deep brain stimulation programming for movement disorders: current concepts and evidence-based strategies. *Front. Neurol.* 10:410. doi: 10.3389/fneur.2019.00410

Krack, P., Volkmann, J., Tinkhauser, G., and Deuschl, G. (2019). Deep Brain Stimulation in Movement Disorders: from Experimental Surgery to Evidence-Based Therapy. *Mov. Disord.* 34, 1795–1810. doi: 10.1002/mds.27860

Limousin, P., Krack, P., Pollak, P., Benazzouz, A., Ardouin, C., Hoffmann, D., et al. (1998). Electrical Stimulation of the Subthalamic Nucleus in Advanced Parkinson's Disease. *N. Engl. J. Med.* 339, 1105–1111. doi: 10.1056/nejm199810153391603

Lyons, M. K. (2011). Deep brain stimulation: current and future clinical applications. *Mayo Clin. Proc.* 86, 662–672. doi: 10.4065/mcp.2011.0045

Miocinovic, S., de Hemptinne, C., Chen, W., Isbaine, F., Willie, J. T., Ostrem, J. L., et al. (2018). Cortical potentials evoked by subthalamic stimulation demonstrate a short latency hyperdirect pathway in humans. *J. Neurosci.* 38, 9129–9141. doi: 10.1523/JNEUROSCI.1327-18.2018

Paff, M., Loh, A., Sarica, C., Lozano, A. M., and Fasano, A. (2020). Update on Current Technologies for Deep Brain Stimulation in Parkinson's Disease. *J. Mov. Disord.* 13:185. doi: 10.14802/JMD.20052

Peeters, J., Boogers, A., Van Bogaert, T., Davidoff, H., Gransier, R., Wouters, J., et al. (2021). Electrophysiological evidence that directional deep brain stimulation activates distinct neural networks in patients with Parkinson's disease. *Neuromodulation Technol. Neural Interface* doi: 10.1016/j.neurom.2021.11.002 [Epub ahead of print].

Pollo, C., Kaelin-Lang, A., Oertel, M. F., Stieglitz, L., Taub, E., Fuhr, P., et al. (2014). Directional deep brain stimulation: an intraoperative double-blind pilot study. *Brain* 137, 2015–2026. doi: 10.1093/brain/awu102

Postuma, R. B., Berg, D., Stern, M., Poewe, W., Olanow, C. W., Oertel, W., et al. (2015). MDS clinical diagnostic criteria for Parkinson's disease. *Mov. Disord.* 30, 1591–1601. doi: 10.1002/mds.26424

Santaniello, S., Gale, J. T., and Sarma, S. V. (2018). Systems approaches to optimizing deep brain stimulation therapies in Parkinson's disease. *Wiley Interdiscip Rev. Syst. Biol. Med.* doi: 10.1002/wsbm.1421 [Epub ahead of print].

Sasaki, F., Oyama, G., Sekimoto, S., Nuermaimaiti, M., Iwamuro, H., Shimo, Y., et al. (2021). Closed-loop programming using external responses for deep brain stimulation in Parkinson's disease. *Park. Relat. Disord.* 84, 47–51. doi: 10.1016/j.parkreldis.2021.01.023

Steigerwald, F., Matthies, C., and Volkmann, J. (2019). Directional Deep Brain Stimulation. *Neurotherapeutics* 16, 100–104. doi: 10.1007/s13311-018-0667-7

Steigerwald, F., Müller, L., Johannes, S., Matthies, C., and Volkmann, J. (2016). Directional deep brain stimulation of the subthalamic nucleus: a pilot study using a novel neurostimulation device. *Mov. Disord.* 31, 1240–1243. doi: 10.1002/mds.26669

Vitek, J. L., Jain, R., Chen, L., Tröster, A. I., Schrock, L. E., House, P. A., et al. (2020). Subthalamic nucleus deep brain stimulation with a multiple independent constant current-controlled device in Parkinson's disease (INTREPID): a multicentre, double-blind, randomised, sham-controlled study. *Lancet Neurol.* 19, 491–501. doi: 10.1016/S1474-4422(20)30108-3

Wagle Shukla, A., Zeilman, P., Fernandez, H., Bajwa, J. A., and Mehanna, R. D. B. S. (2017). Programming: an Evolving Approach for Patients with Parkinson's Disease. *Parkinsons Dis.* 2017:8492619. doi: 10.1155/2017/8492619

Walker, H. C., Huang, H., Gonzalez, C. L., Bryant, J. E., Killen, J., Cutter, G. R., et al. (2012). Short latency activation of cortex during clinically effective subthalamic deep brain stimulation for Parkinson's disease. *Mov. Disord.* 27, 864–873. doi: 10.1002/mds.25025

Conflict of Interest: JP, AB, and TB were funded by Boston Scientific, VLAIO and EIT Health. BN received grants from Medtronic and Boston Scientific.

The remaining authors declare that the research was conducted in the absence of any commercial or financial relationships that could be construed as a potential conflict of interest.

frontiers | Frontiers in Human Neuroscience

METHODS
published: 09 June 2022
doi: 10.3389/fnhum.2022.916627

Long Term Performance of a Bi-Directional Neural Interface for Deep Brain Stimulation and Recording

Scott R. Stanslaski, Michelle A. Case, Jonathon E. Giftakis, Robert S. Raike and Paul H. Stypulkowski*

Medtronic, Minneapolis, MN, United States

Background: In prior reports, we described the design and initial performance of a fully implantable, bi-directional neural interface system for use in deep brain and other neurostimulation applications. Here we provide an update on the chronic, long-term neural sensing performance of the system using traditional 4-contact leads and extend those results to include directional 8-contact leads.

Methods: Seven ovine subjects were implanted with deep brain stimulation (DBS) leads at different nodes within the Circuit of Papez: four with unilateral leads in the anterior nucleus of the thalamus and hippocampus; two with bilateral fornix leads, and one with bilateral hippocampal leads. The leads were connected to either an Activa PC+S® (Medtronic) or Percept PC®(Medtronic) deep brain stimulation and recording device. Spontaneous local field potentials (LFPs), evoked potentials (EPs), LFP response to stimulation, and electrode impedances were monitored chronically for periods of up to five years in these subjects.

Results: The morphology, amplitude, and latencies of chronic hippocampal EPs evoked by thalamic stimulation remained stable over the duration of the study. Similarly, LFPs showed consistent spectral peaks with expected variation in absolute magnitude dependent upon behavioral state and other factors, but no systematic degradation of signal quality over time. Electrode impedances remained within expected ranges with little variation following an initial stabilization period. Coupled neural activity between the two nodes within the Papez circuit could be observed in synchronized recordings up to 5 years post-implant. The magnitude of passive LFP power recorded from directional electrode segments was indicative of the contacts that produced the greatest stimulation-induced changes in LFP power within the Papez network.

Conclusion: The implanted device performed as designed, providing the ability to chronically stimulate and record neural activity within this network for up to 5 years of follow-up.

Keywords: deep brain stimulation, local field potentials, evoked potentials, deep brain sensing, long term brain signal stability

OPEN ACCESS

Edited by:
Adolfo Ramirez-Zamora, University of Florida, United States

Reviewed by:
Xu Liu, Beijing University of Technology, China
Salman Ehtesham Qasim, Columbia University, United States
Jackson N. Cagle, University of Florida, United States

****Correspondence:***
Scott R. Stanslaski
scott.stanslaski@medtronic.com

Specialty section:
This article was submitted to Brain Imaging and Stimulation, a section of the journal Frontiers in Human Neuroscience

Received: *09 April 2022*
Accepted: *16 May 2022*
Published: *09 June 2022*

Citation:
Stanslaski SR, Case MA, Giftakis JE, Raike RS and Stypulkowski PH (2022) Long Term Performance of a Bi-Directional Neural Interface for Deep Brain Stimulation and Recording. Front. Hum. Neurosci. 16:916627. doi: 10.3389/fnhum.2022.916627

INTRODUCTION

Deep brain stimulation (DBS) continues to evolve toward the standard of care for medically refractory movement disorders including Parkinson's disease, essential tremor, and dystonia (Miocinovic et al., 2013) and is in the early stages of adoption in the treatment of pharmaco-resistant epilepsy (Laxpati et al., 2014). Clinical investigations of DBS to treat other neurologic and psychiatric disorders also continue, despite recent setbacks in larger, industry-sponsored clinical trials (Dougherty et al., 2015; Holtzheimer et al., 2017). Although initially approved in the late 1990s, the delivery of DBS for movement disorders today remains virtually unchanged from the early reports of Benabid and colleagues (Benabid et al., 2009). Technology improvements have included more robust hardware, rechargeable batteries, and recent innovations in electrode design (Steigerwald et al., 2016), however, the fundamental therapy remains a tonic, continuous delivery of a high-frequency pulse train, of fixed amplitude, to the targeted neural network. And unlike implantable devices used for cardiac therapies, which can measure and report the physiologic effects of stimulation on the target organ, commercial DBS systems for movement disorders remain "open-loop," relying solely on patient and clinician feedback for parameter adjustment.

The concept of closed-loop or adaptive DBS (aDBS), using local field potentials (LFPs) from basal ganglia nuclei as a control signal, was described over a decade ago (Rossi et al., 2007; Marceglia et al., 2007). Subsequently, aDBS has been investigated in pilot acute, or semi-chronic studies in Parkinson's patients (Little et al., 2013, 2016; Priori et al., 2013) using percutaneous access to implanted DBS leads. However, the broad translational potential of aDBS is still debated, particularly with respect to the chronic accessibility of sufficient LFP control signals. We previously reported on the design (Stanslaski et al., 2009, 2012), and initial chronic performance in animals (Stypulkowski et al., 2013) of a fully implantable stimulation and recording system (Activa PC+S®) that permits sampling of brain electrical activity, and also demonstrated its capability to deliver closed-loop DBS using this LFP based approach (Afshar et al., 2013; Stypulkowski et al., 2014). Here we provide an update on the chronic long-term (up to 5 years) performance of this system in the initial ovine subject cohort, and report on a second cohort implanted with directional DBS leads and Percept PC®.

MATERIALS AND METHODS

This study was conducted at the Physiological Research Laboratory (Medtronic, Inc; Minneapolis, MN) under a protocol approved by the institutional Animal Care and Use Committee. Detailed implant and stimulation/recording methods have been previously reported (Stypulkowski et al., 2011) and are briefly summarized here.

The initial cohort of three adult Polypay mixed breed sheep was implanted with unilateral DBS leads in the anterior nucleus of the thalamus (AN; Model 3389) and hippocampus (HC; Model 3387) using MRI-based and frameless stereotactic methods similar to those used in human surgery (Holloway et al., 2005). Subsequently, four additional animals were implanted with investigational directional DBS leads (1-3-3-1 configuration): two with bilateral fornix (FX) leads; one with bilateral HC leads; and one with unilateral AN and HC leads. The leads were connected to DBS extensions (**Figure 1**) which were tunneled to a post-scapular pocket and connected to either the investigational Activa PC+S® (Medtronic) neurostimulator/recording device (initial cohort) or Percept PC® (Medtronic) device (second cohort). Post-operative images were collected to confirm the stereotactic location of the DBS leads. The electrode configuration for the 4-contact 3389 and 3387 leads are labeled E0, E1, E2, and E3 and are shown in **Figure 1C**. While the directional 1-3-3-1 DBS leads are labeled E0, E1abc, E2abc, E3 and are shown in **Figure 1C**.

Stimulation and Recording

The implanted system allowed for stimulation and recording from both leads, with specific contact configurations selected *via* programmable telemetry interfaces. The implanted system always records differentially between two electrodes for example E0-E3. Recording parameters (sampling rate, filter cutoffs, center frequency, bandwidth, etc.) for time domain signals were set *via* a custom-designed programming interface tablet. Stimulation parameters were controlled using a standard DBS Physician Programmer (Model 8840; first cohort) and a custom-designed programming interface for the directional leads in the second group.

In-person recording sessions with stimulation in the initial cohort were conducted for approximately 2-h periods with the animals awake and resting in a sling. Hippocampal evoked potentials (EPs) were elicited by trains of stimuli delivered to the thalamic lead (5 Hz, 30 s duration, 1–7 V, 120 μs pulse width). The device also permitted simultaneous LFP recordings from the two leads to be triggered at pre-set times, when the subjects were in their free-roaming, home environment. All time domain signals were recorded by the implanted device (200–800 Hz sampling rate; 0.5 Hz HP, 100 Hz LP filters), downloaded, and analyzed offline. At the time of this report, chronic implant durations for all three subjects ranged from 6 to 7 years.

Similar LFP recordings were obtained in person in a sling (with stimulation) and remote free-roaming conditions in the second group. Remote recording capability was a new capability added to enable remote data collection from home. The 8-contact directional leads in these animals allowed recording from a selected montage of 15 bipolar pairs. To assess the effects of directional stimulation on LFP activity, monopolar DBS (1 mA, 300 μs, 100 Hz, 10 s duration) was applied to each segmented contact in a randomized order. Bipolar sensing was configured either around the stimulation electrode or with angular contact pairs (e.g., E1a-E1b, etc.). Baseline LFP data were recorded for 20 s before stimulation and up to 10 min after stimulation.

Data Analyses

Electrophysiologic data was analyzed using Acqknowledge 4.1 software (BioPac Systems). EPs were averaged offline using the stimulus artifact as the trigger, as no external

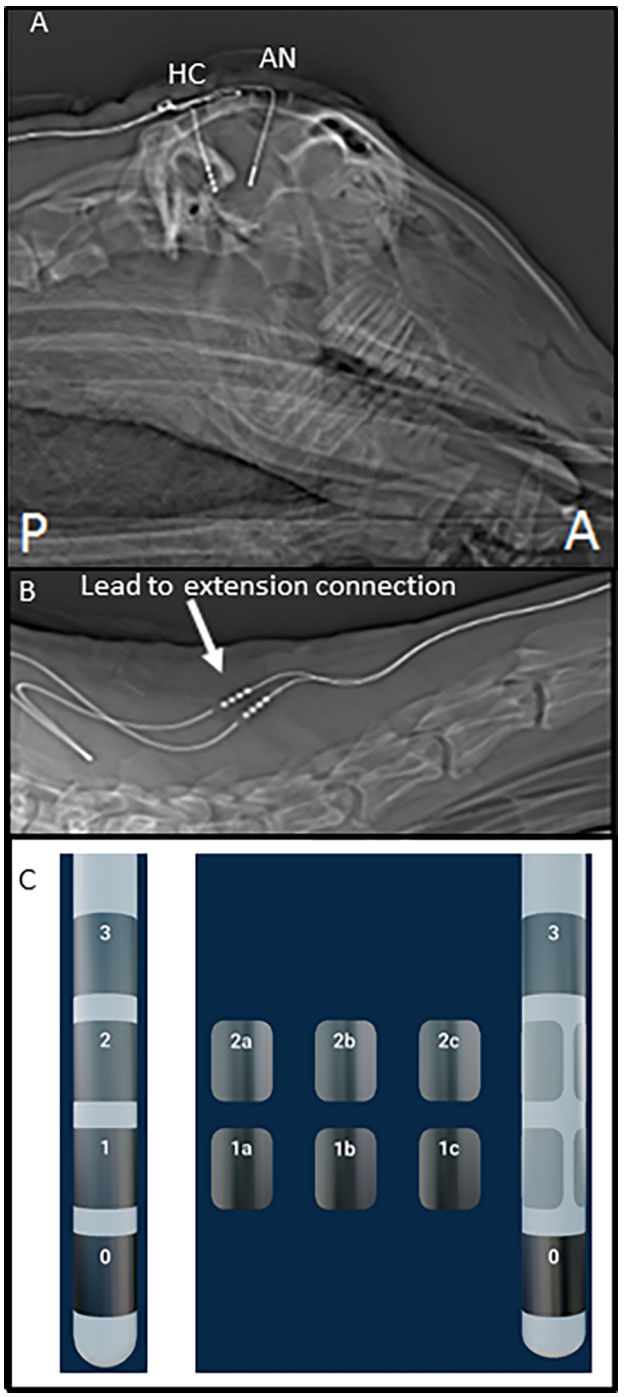

FIGURE 1 | Post-operative images of deep brain stimulation (DBS) implant. **(A)** Top panel shows the sagittal X-ray image of the head of one subject with DBS leads in place. **(B)** This panel illustrates the position of lead-extension connector (arrow) at the base of the neck, near the junction of cervical, and the thoracic spine. **(C)** This panel illustrates the two lead types used in this testing and electrode numbering.

time sync signal was available. In some cases, within-subject records were aligned approximately to the main peak in the EP due to variability over time in the stimulus artifact used as the averaging trigger. LFP spectrograms (intensity of instantaneous frequency vs. time; Hann window) were generated with Sigview software (v3.1.1) and are displayed using a logarithmic Z-axis with color representing relative intensity. The spectral density of the LFP signals was calculated with MATLAB R2017a (intensity of instantaneous amplitude vs. frequency; Hann window) and is displayed with a logarithmic Y-axis in units of $\mu V/\sqrt{Hz}$ vs. frequency. The LFP power was measured from each contact segment on the directional leads, ranked according to magnitude, and plotted over time. Additionally, the response to stimulation was examined by comparing median LFP power (avg/s.d.) at baseline (pre-stimulus) and each minute after stimulation for each segmented electrode.

RESULTS

Stimulation Evoked Responses

Hippocampal EPs in response to thalamic stimulation were recorded for up to 5 years in two of the initial subjects and 3 years in the other, due to lead breakage. **Figure 2** shows representative EPs from each animal at different time points over the duration of the study. As described in earlier reports, there were subtle differences in the morphology and main peak latency (35–40 ms) of the EPs between subjects. These across-subject variations were expected, due to slight differences in hippocampal lead location and recording contact configuration relative to the source dipole of the EP. In addition, the required use of stimulus artifact as the averaging trigger also resulted in several milliseconds of difference in the absolute latencies measured. Within-subject recordings, however, were consistent throughout the duration of the study period with respect to morphology, amplitude, and latency. In some cases, changes in stimulation or recording contact configurations were necessary due to lead breakage (subjects C1—year 3; C2—years 1 and 3) or presumed lead shift (subject C3) over time (details in the figure legend). In addition, the morphology of the evoked response changed in subject C1 at 3 months. This is thought to be due to minor threshold shifts over time and not due to a lead breakage. Despite these minor modifications, in all cases, it was possible to record a consistent, reliable hippocampal EP with AN stimulation, for an extended period of years in these subjects using the implanted device.

In addition to thalamic stimulation, the response to direct hippocampal DBS was also evaluated in these subjects over the course of the study. Hippocampal LFPs recorded from one subject at two different time points separated by approximately 3.5 years are shown in **Figure 3**. Each trace shows a series of increasing amplitude stimulus bursts delivered to the hippocampus and the resultant effects on LFP activity. At the lowest amplitude (0.4 V) there was little to no apparent effect; as the stimulation amplitudes were increased (0.6 and 0.8 V), the inhibitory threshold was reached and suppression of ongoing activity following each stimulus burst was observed. As the amplitude was further increased, the after discharge threshold (1 V) was exceeded and a large excitatory burst of activity

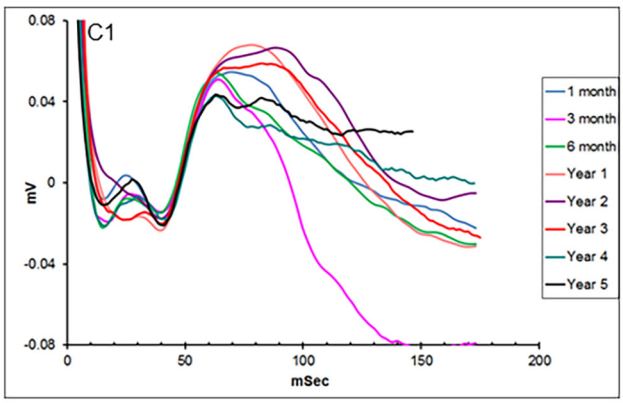

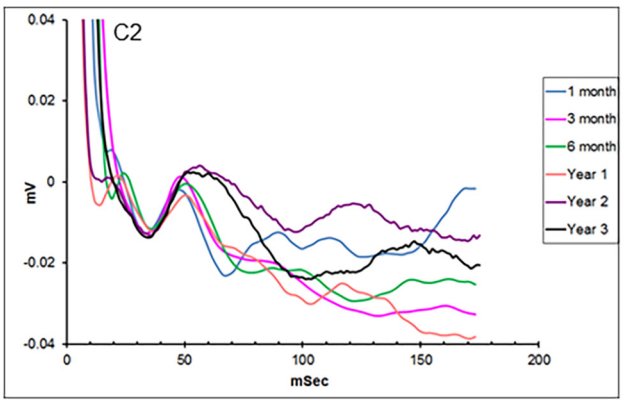

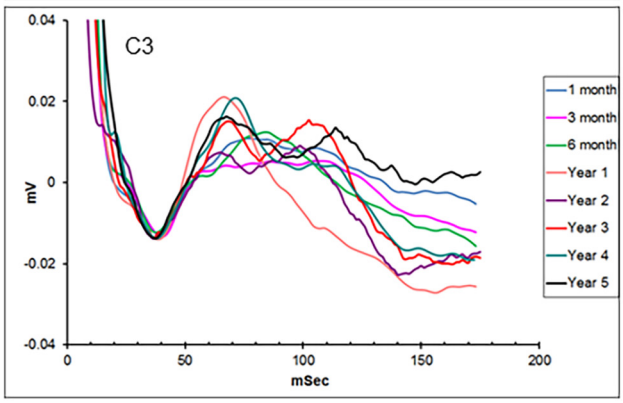

	1 mo	3 mo	6 mo	1 Y	2Y	3Y	4Y	5Y
C1 Stim	E2-E1+	E2-E1+	E2-E1+	E2-E1+	E2-E1+	E2-E1+	E2-EC+	E2-EC+
C1 Rec	E0-E3	E0-E3	E0-E3	E0-E3	E0-E3	E0-E3	E0-E3	E0-E3
C2 Stim	E1-E2+	E1-E2+	E1-E2+	E0-E1+	E0-E1+	E0-E1+	-	-
C2 Rec	E1-E3	E1-E3	E1-E3	E1-E3	E0-E3	E0-E3	-	-
C3 Stim	E2-E1+	E2-E1+	E2-E1+	E2-E1+	E2-E3+	E2-E3+	E2-E3+	E2-E3+
C3 Rec	E0-E1	E0-E1	E0-E1	E0-E1	E0-E3	E0-E3	E0-E3	E0-E3

FIGURE 2 | Chronic hippocampal evoked responses. Evoked potentials (EPs) recorded at multiple time points from the three subjects in response to anterior nucleus (AN) stimulation. Slight changes in electrode contact pairs were made in some cases due to lead breakage or possible electrode shift over time. Subject C1: recording (HC E0-E3), stimulation (AN E2-E1+, 5 V; AN E2-C+, 1.5 V); subject C2: recording (HC E1-E3/E0-E3), stimulation (AN E1-E2+; E0-E1+, 5 V); subject C3: recording (HC E0-E1/E0-E3), stimulation (AN E2-E1+, E2-E3+, 5 V). HC, hippocampus.

occurred. The thresholds for these inhibitory and excitatory effects produced by direct hippocampal DBS were remarkably stable in this subject over this extended period of time.

Spontaneous Local Field Potentials

Simultaneous recordings of spontaneous local field potentials from the thalamus and hippocampus were also collected at regular intervals in the initial subjects. These timed recordings (typically 5 min duration) were set to trigger throughout the day when the subjects were in their home environment, and, therefore, included a variety of behavioral states, ranging from sleep to fully active. **Figure 4** illustrates the hippocampal power spectra for example recordings from the three subjects at various time points in the study. Each recording represents an averaged power spectral density plot for 30 s of data. The records selected represented the most common type of neural activity pattern observed for each subject in these sampled recordings, which could vary considerably based on behavioral state, time of day, etc. Two of the subjects (C1, C3) exhibited predominant hippocampal theta activity, with a strong spectral peak at 4–5 Hz. Initially, the recordings from subject C2 (contacts HC E1-E3) contained primarily hippocampal sharp wave activity, with a dominant lower frequency peak in the power spectrum. A lead breakage (contact HC E1) occurred in this subject at approximately 14 months, which required a shift to recording pair HC E0-E3. With this recording configuration, the spectral power shifted to a much more theta dominant profile, similar to that observed in the other two subjects. Just after year 3 in this subject, the remaining contacts on the hippocampal lead became non-functional, and further recordings were not possible.

Spontaneous LFP activity was recorded periodically from the FX, HC, and AN in the subjects implanted with directional leads, during both sling and free-roaming sessions. The recordings took place over a 2-min period, where the 15 bipolar pairs were split into three groups and each group was recorded for a 40 s duration. The corresponding segment pairs (E1a-E2a, E1b-E2b, E1c-E2c) are plotted to show the LFP activity in each radial direction (**Figure 5**). Each neural target in the network showed predominant theta activity with a strong spectral peak at 4–5 Hz, similar to what was observed in the subjects in the first cohort. The dominant direction of strongest LFP power tended to be consistent for similar conditions (sling vs. remote) throughout the monitoring period, up to 1 year. Two subjects with directional

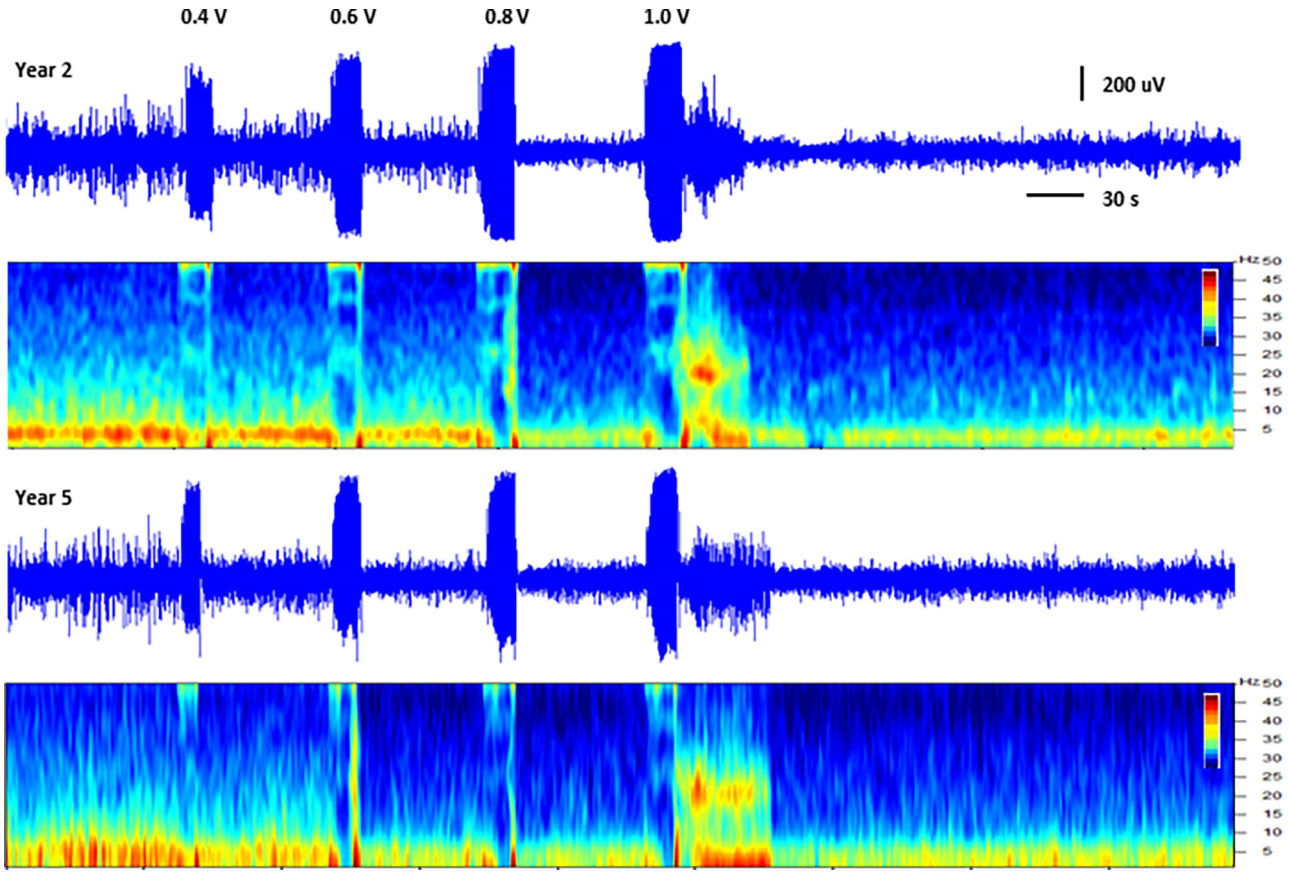

FIGURE 3 | Direct hippocampal stimulation. Hippocampal local field potentials (LFPs) and spectrograms (40 dB scale) recorded at approximately 15 months (year 2, top panels) and 57 months (year 5, bottom panels) post-implant from subject C1 illustrating the response to stimulation of the hippocampus. Stimulation was delivered to contacts HC E1-C+ at the amplitudes shown (50 Hz, 10 s ramped burst, 300 μs PW) while recording from contacts HC E0-E2. The large signal below the amplitude labels represents the recorded stimulus artifact.

leads experienced a lead breakage: one in the bilateral FX subject and one in the AN-HC subject.

Directional Stimulation

The LFP power-based rank over time for each contact segment in the bilateral HC subject was calculated and compared to the stimulation results (**Figure 6**). The top-ranked electrode for the majority of the monitoring period (E2b) in the left hemisphere corresponded with the electrode that had the greatest LFP suppression in response to stimulation. A similar pattern was observed on the right side, with higher-ranked contacts (e.g., E10a, E10c) producing greater levels of local LFP suppression. Impedance data were also collected and presented over time and shown to be in normal ranges. More on impedance measurements will be presented in the "Discussion" Section. The goal of this work was to demonstrate signal stability over time. However, to motivate future work, the coefficient of determination was calculated between the ranking of LFP power at the 4-month time point and the ranking of LFP suppression for each hemisphere, where the left was $R^2 = 0.1$ and the right was $R^2 = 0.4$. **Figure 7** shows the same type of analysis conducted for the AN-HC subject, with stimulation applied remotely to the AN target and the LFP suppression assessed in the HC. Here again, contact segments that were ranked higher based upon spontaneous LFP power (e.g., E1a, E1c) tended to produce the greatest LFP suppression, as measured both within the Papez network (HC) and locally (AN). The coefficient of determination was $R^2 = 0.8$ for the AN and $R^2 = 0.4$ for the HC using the 10-month data. The results from these two subjects suggest that both the local and network response to stimulation tended to align with the rankings derived from the passive LFP sensing data.

Network Activity

The simultaneous LFP recordings from the thalamus and hippocampus often showed coupled patterns of activity within this network, as described previously (Stypulkowski et al., 2013). Typically, during periods of high theta activity in the hippocampus, generally considered to be an "input" state, there was little coincident activity in the thalamus. In contrast, during periods of hippocampal sharp wave activity, an "output" state where information is passed to cortical and sub-cortical regions,

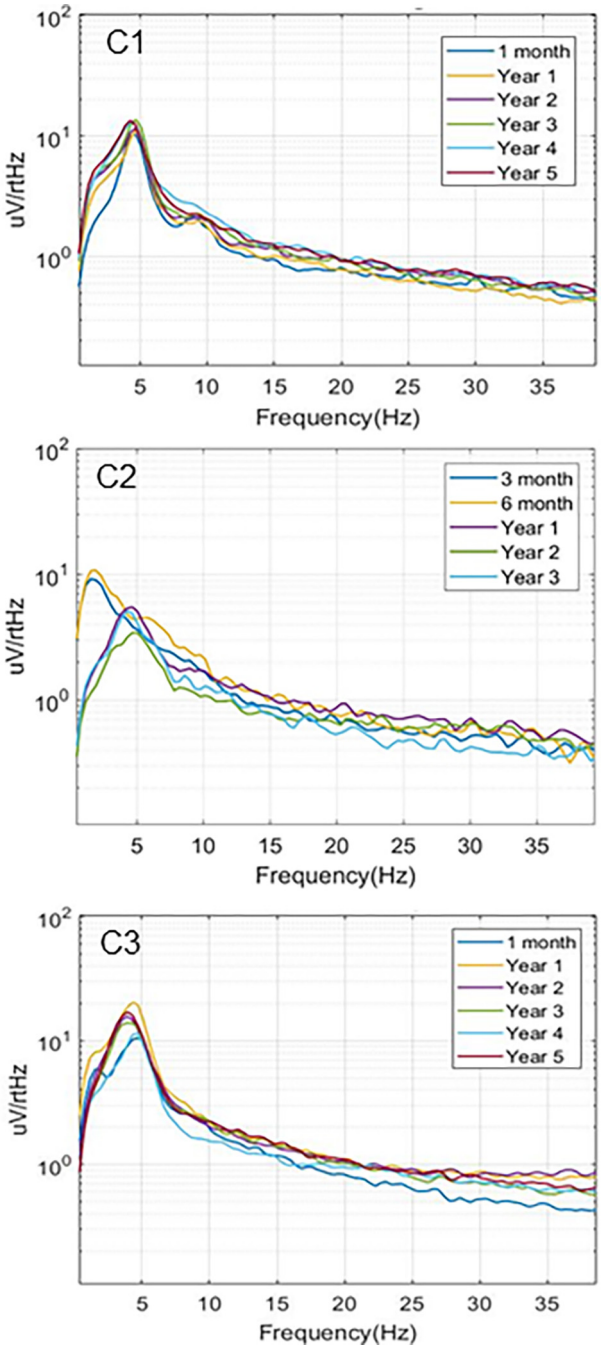

FIGURE 4 | Local field potentials. Representative examples of hippocampal LPF power spectra recorded over the study period for the three subjects. C1 (HC E0-E3) and C3 (HC E0-E3) recordings exhibited predominant theta activity. Initial recordings from C2 (HC E1-E3) contained mainly sharp wave activity while later recordings from a different electrode pair (HC E0-E3), due to lead breakage, were more theta dominant.

it was common to observe parallel changes in thalamic firing. An interesting recording from subject C3 captured approximately 4.5 years post-implant is shown in **Figure 8**. This record was obtained at roughly 1 a.m. (lights out) and presumably reflects a sleep state. Large amplitude spikes can be seen in the hippocampus with co-incident spikes observed in the thalamic recording. At an increased resolution (right inset) it is apparent that the spikes in the hippocampus lead the activity in the AN by approximately 30–40 ms, suggesting that these events originate in the hippocampus and propagate *via* the fornix outflow to the thalamus. In contrast, early in this recording, there was a large amplitude event in the AN record (left inset) with only a small co-incident spike in the hippocampus. This thalamic event is consistent with the appearance of a K-complex, which is generated in cortical regions during specific sleep stages and propagates to the thalamus (Wennberg, 2010). The inset shows the timing of this spike event to be essentially simultaneous at the two recording sites, which, along with the small amplitude, suggests that it was likely a far-field recording of this event at the hippocampal electrode.

DISCUSSION

Closed loop stimulation is a promising approach for advancing DBS therapies, with the ultimate goal of improving efficacy and reducing side effects. The ability to deliver a successful aDBS therapy clinically will depend critically upon two factors: (1) identification of a dependable control signal that provides an indication of the patients' symptomatic state; and (2) the ability of the implanted hardware to reliably and durably monitor this signal to inform the therapy control algorithm.

With respect to Parkinson's disease, the magnitude of specific frequency bands of cortical and subcortical LFP signals appears to correlate reasonably well with the clinical state (Brown, 2006). Both therapeutic levels of medication (Silberstein et al., 2003) and DBS (Kühn et al., 2008) suppress excessive low-frequency LFP signals in parallel with improvement of bradykinesia and rigidity (Ray et al., 2008). In contrast, high-frequency LFP components associated with dyskinesias are increased by peak medication doses or over-stimulation (Swann et al., 2018a). Although most of these studies have been conducted over relatively short time periods, raising questions of long-term applicability, subcortical LFP signals have been demonstrated to be stable over many years when recorded at different intervals from externalized DBS leads (Abosch et al., 2012).

Our current results suggest that it should also be possible to record similarly stable LFP signals from sub-cortical or cortical sites, over long periods of time, with this fully implanted system. This sets up the key question on how this will translate to closed loop feature development. The first step in closed loop feature development lies in having a stable therapy and measurement system which this work supports. The next step in that process is understanding the stability of the biological signals clinically. Questions like, how do those biological signals change with disease progression for example. Initial reports of clinical experience with these implantable devices have provided encouraging near-term performance results (Quinn et al., 2015; Trager et al., 2016; Neumann et al., 2017). Long-term results with a responsive device to treat epilepsy using cortical signals also support the ability of fully implantable systems to record neural activity over multiple years (Geller et al., 2017). Although the multi-electrode single unit recording arrays used for brain-

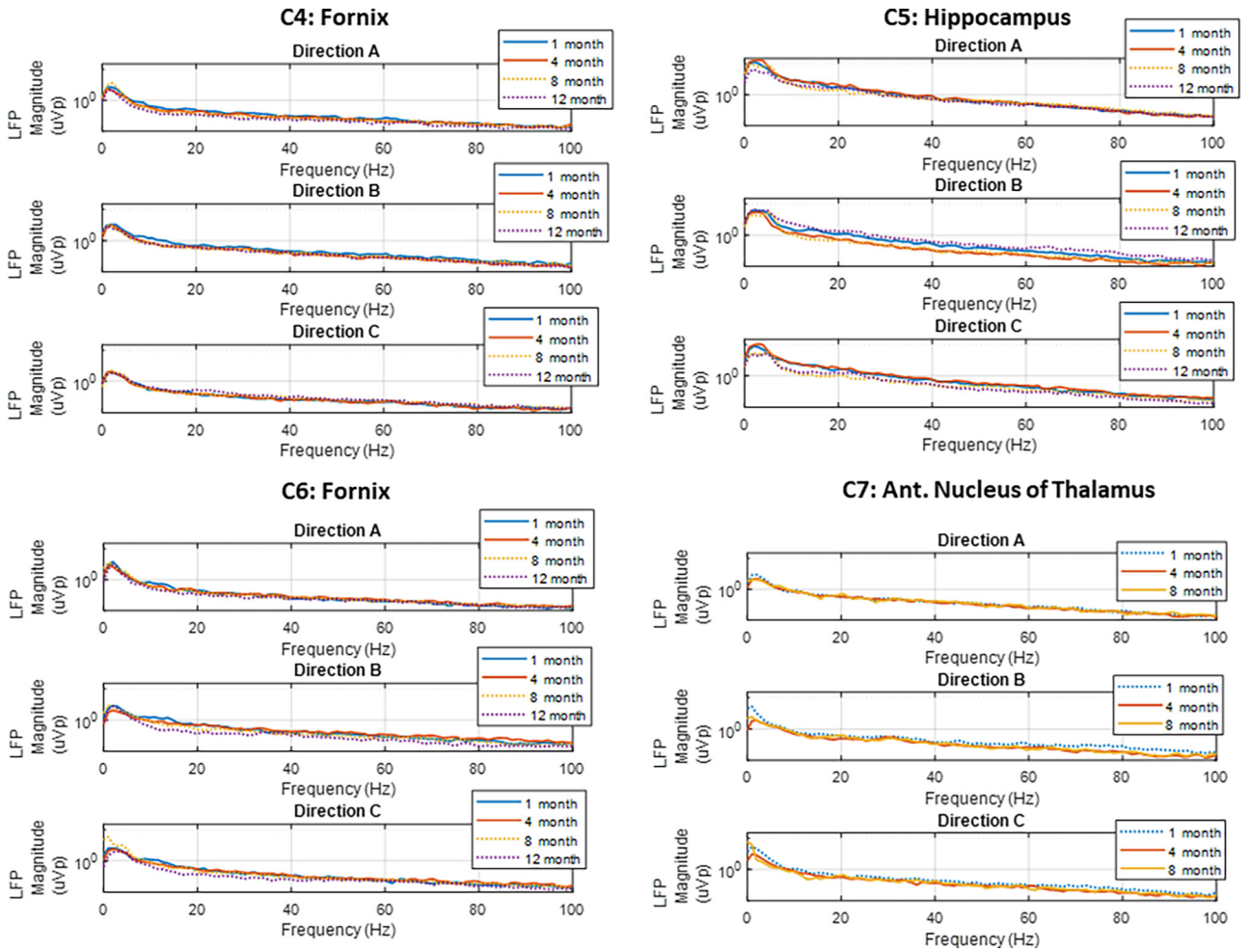

FIGURE 5 | Local field potentials. Representative examples of LFP power spectra from directional pairs (E1a-E2a, E1b-E2b, E1c-E2c) recorded over the study period for the four subjects implanted with directional leads. Recordings showed predominant theta activity in all nodes monitored. The dotted line denotes the free-roaming condition, and the solid line denotes the sling condition. Each line represents one 30 s sense recording for the representative study period.

machine interfaces can provide extremely rich information content, their long-term stability has been a recurring issue in experimental and clinical applications (Barrese et al., 2013). Instead, DBS or surface macroelectrodes may provide more reliable long-term access to the appropriate neural control signals for mainstream clinical applications.

Lead and extension integrity is a key component to the long-term stability of neural recordings. In this work, four of the seven subjects exhibited multiple lead conductor breakages over the course of the investigation, which would be unexpected in a human clinical setting. Upon analysis of post-operative images, it was determined that the veterinary surgeon who implanted these systems had placed the connectors of the DBS extensions in the neck region of the animals due to limited space at the skull surgical site which contained the two burr hole caps (**Figure 1**). In human surgeries, the extension connector is always placed on the side of the head so that the extension, and not the lead body, is exposed to flexion due to head and neck motion. This is based on the early clinical experience just after DBS was first approved, where multiple lead fractures were observed when connectors were placed in the neck (Schwalb et al., 2001; Hariz, 2002). Moreover, a recent study in this same ovine animal model also reported a high incidence of DBS lead fractures found to be related to connector location (Lentz et al., 2015).

The materials and construction of the DBS extensions are by design, intended to be resistant to fatigue from repeated flexion cycles. The DBS leads, however, use different materials and construction and the lead conductors are more susceptible to mechanical fatigue. The placement of the lead-extension connection in the muscular neck region of these animals appeared to be the cause of the lead breakages that were experienced. Despite these failures, it was possible in most cases through programming changes to stimulation or recording configurations, to re-capture evoked responses or LFPs similar to those obtained with the original contact configurations.

We previously described the concept of local and remote modulation within this Papez circuit, as it related to the treatment of epilepsy, by using either direct hippocampal stimulation or

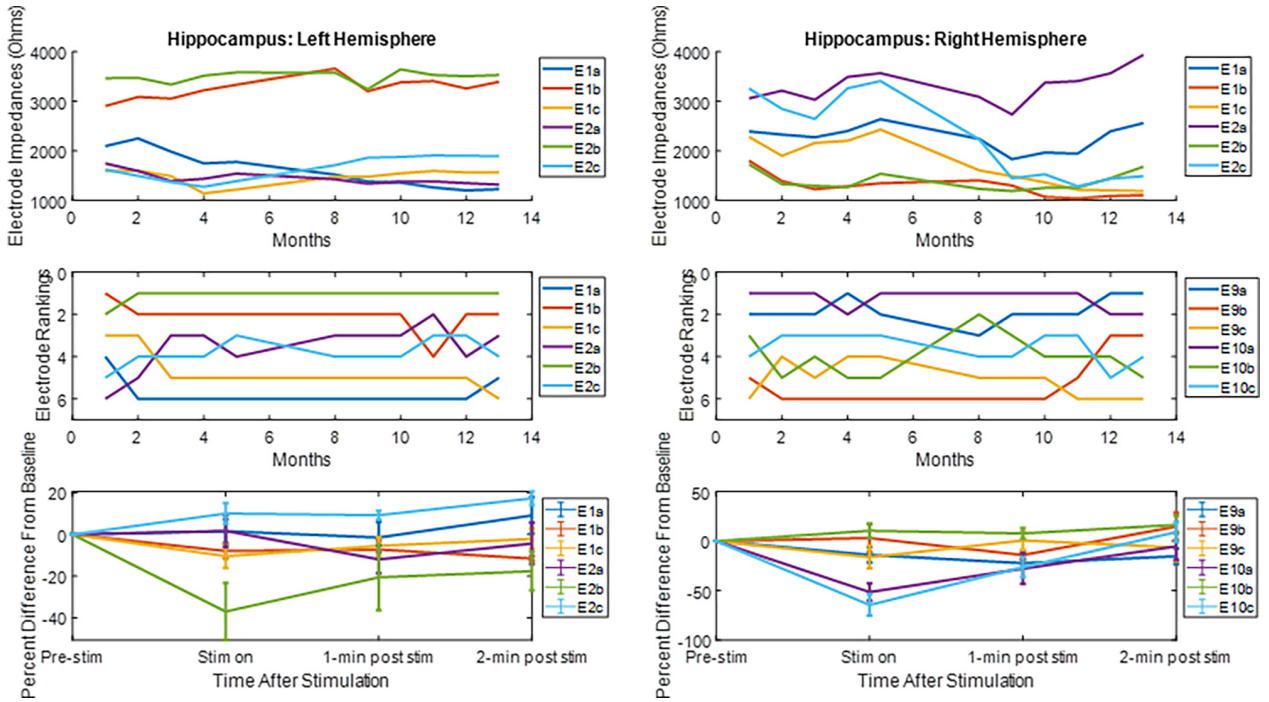

FIGURE 6 | Electrode impedance and rankings and local LFP response to hippocampal stimulation. For the electrode rankings, in-person monitors took place between months 1 and 4 and remote monitors took place between months 5 and 13. For the LFP response to stimulation, the LFP response compared to baseline is plotted for the duration of the recordings. The average response and standard error are displayed. For both hemispheres, the top-ranked electrode corresponded with an electrode that had an observable decrease in LFP activity after stimulation.

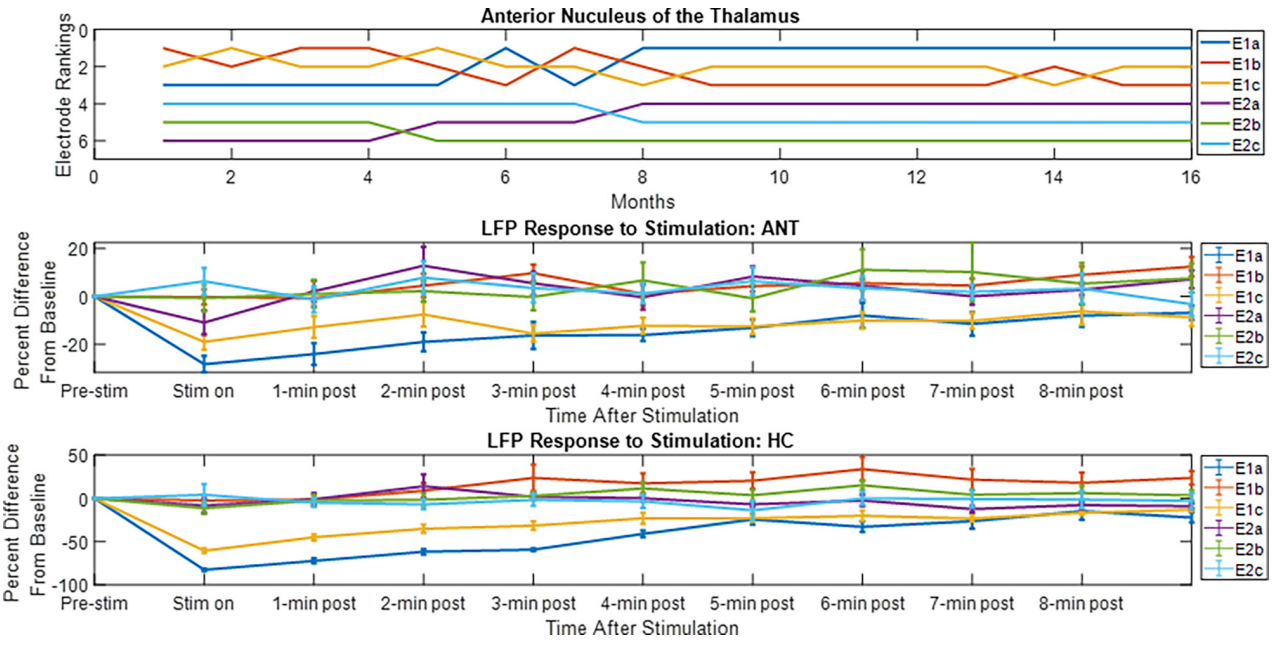

FIGURE 7 | Electrode rankings and the LFP response to thalamic stimulation. For the electrode rankings, in-person monitors took place between weeks 9 and 16 and remote monitors took place between weeks 1 and 9. For the LFP response to stimulation, the LFP response compared to baseline is plotted for the duration of the recordings. The average response and standard error are displayed. For the local response in the AN and for the network response in the HC, the top-ranked electrodes corresponded with the electrodes that had an observable decrease in LFP activity after stimulation.

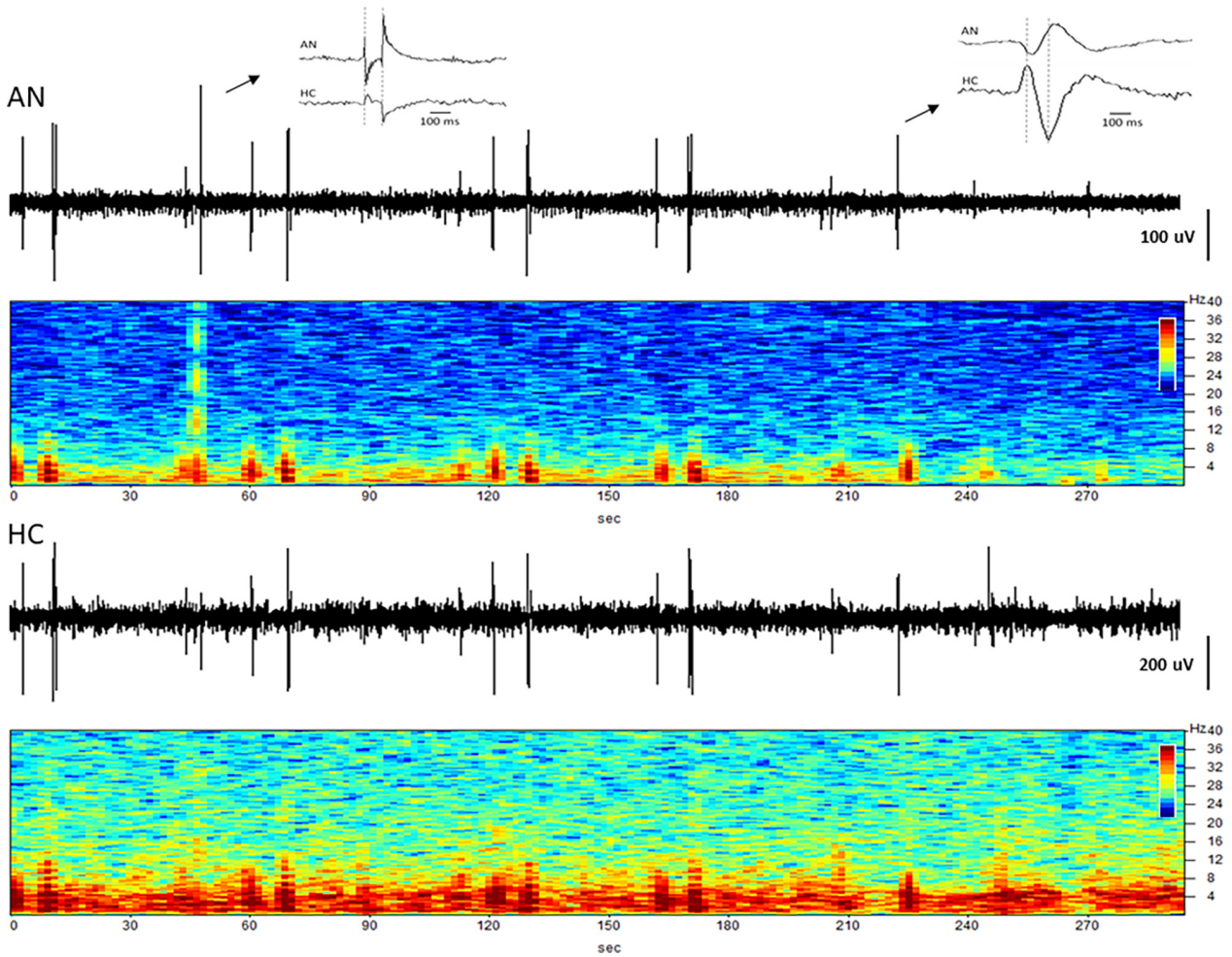

FIGURE 8 | Coupling between the hippocampus and anterior nucleus. Time domain and spectrograms from simultaneously recorded signals from the AN (top) and HC (bottom) in subject C3 (Year 4). Spike activity originating in the HC is recorded 30–40 ms later in the AN (right inset), consistent with evoked potential (EP) latency measures. The left inset shows a K-complex recorded as a large signal in the AN, but a small signal with no latency difference in HC, suggesting a far-field recording at that site.

anterior thalamic DBS, to influence hippocampal excitability (Stypulkowski et al., 2014) and recently extended those findings to a second cohort of subjects with leads in the hippocampus and fornix (Stypulkowski et al., 2017). In both cases, recording of LFP activity from the hippocampus provided insight into the effects of DBS at different network nodes on this target structure. Moreover, it was possible to demonstrate the use of these hippocampal LFPs as a control signal for closed-loop stimulation, delivered from either the local or remote stimulation sites. The results shown in **Figure 3** provide encouraging data regarding the long-term stability of these types of recordings as well as the apparent stability of the DBS thresholds to induce both inhibitory and excitatory effects within this network. This demonstration of both recording and stimulation threshold stability over a period of several years supports the viability of these methods for clinical use. The approach of employing a remote recording electrode within the targeted therapy network, to monitor the effects induced by DBS at a second site, has recently been clinically investigated for both epilepsy (Van Gompel et al., 2015) and movement disorders (Shute et al., 2016; Swann et al., 2018a) using the implantable device described here.

New lead geometries with segmented electrodes are now available for some approved DBS therapies. These new directional lead designs allow for more detailed information to be collected using LFP sensing. An intraoperative study in Parkinson's disease patients that measured monopolar LFP data from traditional cylindrical contacts in the Subthalamic Nucleus (STN) showed that LFP beta power correlated with the top-ranked electrodes for clinical efficacy (Aman et al., 2020). More recently, another study using externalized directional leads demonstrated that individual Parkinson's patients had unique frequency spectrum patterns that varied across the lead, and that the contacts with the highest LFP amplitude matched the electrodes selected for therapy (Tinkhauser et al., 2017). These studies show the potential value of LFP sensing from DBS leads and the possibility of using it as a clinical tool. Our current study

showed that LFP sensing on directional leads can be obtained from a fully internalized DBS system and that these signals can be obtained chronically. Encouragingly, the preliminary results from the directional stimulation experiments suggest that passive LFP sensing may be useful in the Papez network to identify electrodes that produce the greatest response to stimulation, consistent with the results reported in STN DBS.

The current study has clear limitations including the small sample size. However, the ability to record chronically for very long periods of time with repeated measures in the same subjects is a unique opportunity not afforded with acute or semi-chronic (percutaneous) experimental approaches. With the exception of the unanticipated, but explained lead breakages, the implanted hardware performed as expected over the course of the study. Electrode impedance measurements were taken over time using the implanted device. The implanted device delivers a constant current stimulus output and measures the resulting voltage output for that waveform using an analog to digital converter (ADC). Stimulation is delivered at 100 Hz and 80 μs. By knowing the delivered constant current and measured voltage, the implanted device calculates $|Z|=|V/I|$. A representative trend is shown in **Figure 6**. Electrode impedances followed typical patterns as reported by others (Sillay et al., 2010; Cheung et al., 2013) with generally stable impedances after a period of initial stabilization. Contacts that were used for stimulation typically exhibited lower, and more stable impedance than those used purely for passive recordings (e.g., by a factor of 2–3 over the long-term; Satzer et al., 2014). In addition, the input impedance of the recording amplifier is set by the high pass filter and in the Megaohm range (Stanslaski et al., 2012). Given this high input impedance, normal impedance variations do not attenuate the measures signals. Local field potential recordings were consistent over the course of the study, with no apparent systematic degradation of signal quality. Evoked responses and simultaneous recordings from the two target sites demonstrate the ability to measure and monitor the strength of network connectivity with this implanted system for periods of up to 5 years. As DBS therapies continue to evolve and expand into new indications, this potential to monitor the targeted neural network for acute and chronic effects of stimulation may become more important (Freestone et al., 2013). With respect to closed-loop DBS for current movement disorder therapies, the system appears to be a viable platform for long-term delivery of such a therapy. Initial studies using this system to test closed-loop DBS in human subjects have recently been reported (Swann et al., 2018b) and the first clinical investigations employing chronic closed-loop DBS are anticipated.

DATA AVAILABILITY STATEMENT

The raw data supporting the conclusions of this article will be made available by the authors upon request, without undue reservation.

ETHICS STATEMENT

The animal study was reviewed and approved by Medtronic PLC ethics committee.

AUTHOR CONTRIBUTIONS

SS, MC, and PS: manuscript preparation, data collection and analysis. JG: data collection and analysis. RR: manuscript review and edit. All authors contributed to the article and approved the submitted version.

FUNDING

All funding provided by Medtronic PLC.

ACKNOWLEDGMENTS

We would like to thank the veterinary and animal care staff at Medtronic Physiological Research Laboratory for the excellent long-term care of these chronic experimental subjects.

REFERENCES

Abosch, A., Lanctin, D., Onaran, I., Eberly, L., Spaniol, M., Ince, N. F., et al. (2012). Long-term recordings of local field potentials from implanted deep brain stimulation electrodes. *Neurosurgery* 71, 804–814. doi: 10.1227/NEU.0b013e3182676b91

Afshar, P., Khambhati, A., Stanslaski, S., Carlson, D., Jensen, R., Linde, D., et al. (2013). A translational platform for prototyping closed-loop neuromodulation systems. *Front. Neural Circuits* 6:117. doi: 10.3389/fncir.2012.00117

Aman, J., Johnson, L., Sanabria, D., Wang, J., and Patriat, R. (2020). Directional deep brain stimulation leads reveal spatially distinct oscillatory activity in the globus pallidus internus of Parkinson's disease patients. *Neurobiol. Dis.* 139:104819. doi: 10.1016/j.nbd.2020.104819

Barrese, J. C., Rao, N., Paroo, K., Triebwasser, C., Vargas-Irwin, C., Franquemont, L., et al. (2013). Failure mode analysis of silicon-based intracortical microelectrode arrays in non-human primates. *J. Neural Eng.* 10:066014. doi: 10.1088/1741-2560/10/6/066014

Benabid, A. L., Chabardes, S., Torres, N., Piallat, B., Krack, P., Fraix, V., et al. (2009). Functional neurosurgery for movement disorders: a historical perspective. *Prog. Brain Res.* 175, 379–391. doi: 10.1016/S0079-6123(09)17525-8

Brown, P. (2006). Bad oscillations in Parkinson's disease. *J. Neural Transm. Suppl.* 70, 27–30. doi: 10.1007/978-3-211-45295-0_6

Cheung, T., Nuño, M., Hoffman, M., Katz, M., Kilbane, C., Alterman, R., et al. (2013). Longitudinal impedance variability in patients with chronically implanted DBS devices. *Brain Stimul.* 6, 746–751. doi: 10.1016/j.brs.2013.03.010

Dougherty, D. D., Rezai, A. R., Carpenter, L. L., Howland, R. H., Bhati, M. T., O'Reardon, J. P., et al. (2015). A randomized sham-controlled trial of deep brain stimulation of the ventral capsule/ventral striatum for chronic treatment-resistant depression. *Biol. Psychiatry* 78, 240–248. doi: 10.1016/j.biopsych.2014.11.023

Freestone, D. R., Long, S. N., Frey, S., Stypulkowski, P. H., Giftakis, J. E., Cook, M. J., et al. (2013). A method for actively tracking excitability of brain networks using a fully implantable monitoring system. *Conf. Proc. IEEE Eng. Med. Biol. Soc.* 2013, 6151–6154. doi: 10.1109/EMBC.2013.6610957

Geller, E. B., Skarpaas, T. L., Gross, R. E., Goodman, R. R., Barkley, G. L., Bazil, C. W., et al. (2017). Brain-responsive neurostimulation in patients with medically intractable mesial temporal lobe epilepsy. *Epilepsia* 58, 994–1004. doi: 10.1111/epi.13740

Hariz, M. I. (2002). Complications of deep brain stimulation surgery. *Mov. Disord.* 17, S162–S166. doi: 10.1002/mds.10159

Holloway, K. L., Gaede, S. E., Starr, P. A., Rosenow, J. M., Ramakrishnan, V., Henderson, J. M., et al. (2005). Frameless stereotaxy using bone fiducial markers for deep brain stimulation. *Neurosurgery* 103, 404–413. doi: 10.3171/jns.2005.103.3.0404

Holtzheimer, P. E., Husain, M. M., Lisanby, S. H., Taylor, S. F., Whitworth, L. A., McClintock, S., et al. (2017). Subcallosal cingulate deep brain stimulation for treatment-resistant depression: a multisite, randomised, sham-controlled trial. *Lancet Psychiatry* 4, 839–849. doi: 10.1016/S2215-0366(17)30371-1

Kühn, A. A., Kempf, F., Brücke, C., Gaynor Doyle, L., Martinez-Torres, I., Pogosyan, A., et al. (2008). High-frequency stimulation of the subthalamic nucleus suppresses oscillatory beta activity in patients with Parkinson's disease in parallel with improvement in motor performance. *J. Neurosci.* 28, 6165–6173. doi: 10.1523/JNEUROSCI.0282-08.2008

Laxpati, N. G., Kasoff, W. S., and Gross, R. E. (2014). Deep brain stimulation for the treatment of epilepsy: circuits, targets and trials. *Neurotherapeutics* 11, 508–526. doi: 10.1007/s13311-014-0279-9

Lentz, L., Zhao, Y., Kelly, M. T., Schindeldecker, W., Goetz, S., Nelson, D. E., et al. (2015). Motor behaviors in the sheep evoked by electrical stimulation of the subthalamic nucleus. *Exp. Neurol.* 273, 69–82. doi: 10.1016/j.expneurol.2015.07.022

Little, S., Beudel, M., Zrinzo, L., Foltynie, T., Limousin, P., Hariz, M., et al. (2016). Bilateral adaptive deep brain stimulation is effective in Parkinson's disease. *J. Neurol. Neurosurg. Psychiatry* 87, 717–721. doi: 10.1136/jnnp-2015-310972

Little, S., Pogosyan, A., Neal, S., Zavala, B., Zrinzo, L., Hariz, M., et al. (2013). Adaptive deep brain stimulation in advanced Parkinson disease. *Ann. Neurol.* 74, 449–457. doi: 10.1002/ana.23951

Marceglia, S., Rossi, L., Foffani, G., Bianchi, A., Cerutti, S., Priori, A., et al. (2007). Basal ganglia local field potentials: applications in the development of new deep brain stimulation devices for movement disorders. *Expert Rev. Med. Devices* 4, 605–614. doi: 10.1586/17434440.4.5.605

Miocinovic, S., Somayajula, S., Chitnis, S., and Vitek, J. L. (2013). History, applications and mechanisms of deep brain stimulation. *JAMA Neurol.* 70, 163–171. doi: 10.1001/2013.jamaneurol.45

Neumann, W. J., Staub-Bartelt, F., Horn, A., Schanda, J., Schneider, G. H., Brown, P., et al. (2017). Long term correlation of subthalamic beta band activity with motor impairment in patients with Parkinson's disease. *Clin. Neurophysiol.* 128, 2286–2291. doi: 10.1016/j.clinph.2017.08.028

Priori, A., Foffani, G., Rossi, L., and Marceglia, S. (2013). Adaptive deep brain stimulation (aDBS) controlled by local field potential oscillations. *Exp. Neurol.* 245, 77–86. doi: 10.1016/j.expneurol.2012.09.013

Quinn, E. J., Blumenfeld, Z., Velisar, A., Koop, M. M., Shreve, L. A., Trager, M. H., et al. (2015). Beta oscillations in freely moving Parkinson's subjects are attenuated during deep brain stimulation. *Mov. Disord.* 30, 1750–1758. doi: 10.1002/mds.26376

Ray, N. J., Jenkinson, N., Wang, S., Holland, P., Brittain, J. S., Joint, C., et al. (2008). Local field potential beta activity in the subthalamic nucleus of patients with Parkinson's disease is associated with improvements in bradykinesia after dopamine and deep brain stimulation. *Exp. Neurol.* 213, 108–113. doi: 10.1016/j.expneurol.2008.05.008

Rossi, L., Foffani, G., Marceglia, S., Bracchi, F., Barbieri, S., Priori, A., et al. (2007). An electronic device for artefact suppression in human local field potential recordings during deep brain stimulation. *J. Neural Eng.* 4, 96–106. doi: 10.1088/1741-2560/4/2/010

Satzer, D., Lanctin, D., Eberly, L. E., and Abosch, A. (2014). Variation in deep brain stimulation electrode impedance over years following electrode implantation. *Stereotact. Funct. Neurosurg.* 92, 94–102. doi: 10.1159/000358014

Schwalb, J. M., Riina, H. A., Skolnick, B., Jaggi, J. L., Simuni, T., Baltuch, G. H., et al. (2001). Revision of deep brain stimulator for tremor. Technical note. *J. Neurosurg.* 94, 1010–1012. doi: 10.3171/jns.2001.94.6.1010

Shute, J. B., Okun, M. S., Opri, E., Molina, R., Rossi, P. J., Martinez-Ramirez, D., et al. (2016). Thalamocortical network activity enables chronic tic detection in humans with tourette syndrome. *Neuroimage Clin.* 12, 165–172. doi: 10.1016/j.nicl.2016.06.015

Silberstein, P., Kühn, A. A., Kupsch, A., Trottenberg, T., Krauss, J. K., Wöhrle, J. C., et al. (2003). Patterning of globus pallidus local field potentials differs between Parkinson's disease and dystonia. *Brain* 126, 2597–2608. doi: 10.1093/brain/awg267

Sillay, K. A., Chen, J. C., and Montgomery, E. B. (2010). Long-term measurement of therapeutic electrode impedance in deep brain stimulation. *Neuromodulation* 13, 195–200. doi: 10.1111/j.1525-1403.2010.00275.x

Stanslaski, S., Afshar, P., Cong, P., Giftakis, J., Stypulkowski, P., Carlson, D., et al. (2012). Design and validation of a fully implantable, chronic, closed-loop neuromodulation device with concurrent sensing and stimulation. *IEEE Trans. Neural Syst. Rehabil. Eng.* 20, 410–421. doi: 10.1109/TNSRE.2012.2183617

Stanslaski, S., Cong, P., Carlson, D., Santa, W., Jensen, R., Molnar, G., et al. (2009). An implantable bi-directional brain-machine interface system for chronic neuroprosthesis research. *Annu. Int. Conf. Proc. IEEE Eng. Med. Biol. Soc.* 2009, 5494–5497. doi: 10.1109/IEMBS.2009.5334562

Steigerwald, F., Müller, L., Johannes, S., Matthies, C., and Volkmann, J. (2016). Directional deep brain stimulation of the subthalamic nucleus: a pilot study using a novel neurostimulation device. *Mov. Disord.* 31, 1240–1243. doi: 10.1002/mds.26669

Stypulkowski, P. H., Giftakis, J. E., and Billstrom, T. M. (2011). Development of a large animal model for investigation of deep brain stimulation for epilepsy. *Stereotact. Funct. Neurosurg.* 89, 111–122. doi: 10.1159/000323343

Stypulkowski, P. H., Stanslaski, S. R., Denison, T. J., and Giftakis, J. E. (2013). Chronic evaluation of a clinical system for deep brain stimulation and recording of neural network activity. *Stereotact. Funct. Neurosurg.* 91, 220–232. doi: 10.1159/000345493

Stypulkowski, P. H., Stanslaski, S. R., and Giftakis, J. E. (2017). Modulation of hippocampal activity with fornix Deep Brain Stimulation. *Brain Stimul.* 10, 1125–1132. doi: 10.1016/j.brs.2017.09.002

Stypulkowski, P. H., Stanslaski, S. R., Jensen, R. M., Denison, T. J., and Giftakis, J. E. (2014). Brain stimulation for epilepsy--local and remote modulation of network excitability. *Brain Stimul.* 7, 350–358. doi: 10.1016/j.brs.2014.02.002

Swann, N. C., de Hemptinne, C., Miocinovic, S., Qasim, S., Ostrem, J. L., Galifianakis, N. B., et al. (2018a). Chronic multisite brain recordings from a totally implantable bidirectional neural interface: experience in 5 patients with Parkinson's disease. *J. Neurosurg.* 128, 605–616. doi: 10.3171/2016.11.JNS161162

Swann, N. C., de Hemptinne, C., Thompson, M. C., Miocinovic, S., Miller, A. M., Gilron, R., et al. (2018b). Adaptive deep brain stimulation for Parkinson's disease using motor cortex sensing. *J. Neural Eng.* 15:046006. doi: 10.1088/1741-2552/aabc9b

Tinkhauser, G., Pogosyan, A., Debove, I., Nowacki, A., Shah, S. A., Seidel, K., et al. (2017). Directional local field potentials: A tool to optimize deep brain stimulation. *Mov. Disord.* 33, 1–6. doi: 10.1002/mds.27215

Trager, M. H., Koop, M. M., Velisar, A., Blumenfeld, Z., Nikolau, J. S., Quinn, E. J., et al. (2016). Subthalamic beta oscillations are attenuated after withdrawal of chronic high frequency neurostimulation in Parkinson's disease. *Neurobiol. Dis.* 96, 22–30. doi: 10.1016/j.nbd.2016.08.003

Van Gompel, J. J., Klassen, B. T., Worrell, G. A., Lee, K. H., Shin, C., Zhao, C. Z., et al. (2015). Anterior nuclear deep brain stimulation guided by concordant hippocampal recording. *Neurosurg. Focus* 38:E9. doi: 10.3171/2015.3.FOCUS1541

Wennberg, R. (2010). Intracranial cortical localization of the human K-complex. *Clin. Neurophysiol.* 121, 1176–1186. doi: 10.1016/j.clinph.2009.12.039

Conflict of Interest: All of the authors are employees of Medtronic PLC.

Publisher's Note: All claims expressed in this article are solely those of the authors and do not necessarily represent those of their affiliated organizations, or those of the publisher, the editors and the reviewers. Any product that may be evaluated in this article, or claim that may be made by its manufacturer, is not guaranteed or endorsed by the publisher.

frontiers | Frontiers in Human Neuroscience

BRIEF RESEARCH REPORT
published: 21 June 2022
doi: 10.3389/fnhum.2022.931858

Does Motor Symptoms Asymmetry Predict Motor Outcome of Subthalamic Deep Brain Stimulation in Parkinson's Disease Patients?

Francesco Bove[1], Francesco Cavallieri[2], Anna Castrioto[3], Sara Meoni[3], Emmanuelle Schmitt[3], Amélie Bichon[3], Eugénie Lhommée[3], Pierre Pélissier[3], Andrea Kistner[3], Eric Chevrier[3], Eric Seigneuret[4], Stephan Chabardès[4], Franco Valzania[2], Valerie Fraix[3] and Elena Moro[3]*

[1] Neurology Unit, Fondazione Policlinico Universitario A. Gemelli IRCCS, Rome, Italy, [2] Neurology Unit, Department of Neuromotor and Rehabilitation, Azienda USL-IRCCS di Reggio Emilia, Reggio Emilia, Italy, [3] Division of Neurology, Grenoble Institute of Neurosciences, Inserm U1216, CHU of Grenoble, Grenoble Alpes University, Grenoble, France, [4] Division of Neurosurgery, CHU of Grenoble, Grenoble Alpes University, Grenoble, France

OPEN ACCESS

Edited by:
Michael S. Okun,
University of Florida, United States

Reviewed by:
Sergiu Groppa,
Johannes Gutenberg University Mainz, Germany
Harrison Carroll Walker,
University of Alabama at Birmingham, United States

***Correspondence:**
Francesco Cavallieri
Francesco.Cavallieri@ausl.re.it

Specialty section:
This article was submitted to Brain Imaging and Stimulation, a section of the journal Frontiers in Human Neuroscience

Received: 29 April 2022
Accepted: 23 May 2022
Published: 21 June 2022

Citation:
Bove F, Cavallieri F, Castrioto A, Meoni S, Schmitt E, Bichon A, Lhommée E, Pélissier P, Kistner A, Chevrier E, Seigneuret E, Chabardès S, Valzania F, Fraix V and Moro E (2022) Does Motor Symptoms Asymmetry Predict Motor Outcome of Subthalamic Deep Brain Stimulation in Parkinson's Disease Patients? Front. Hum. Neurosci. 16:931858. doi: 10.3389/fnhum.2022.931858

Background: In Parkinson's disease (PD), the side of motor symptoms onset may influence disease progression, with a faster motor symptom progression in patients with left side lateralization. Moreover, worse neuropsychological outcomes after subthalamic nucleus deep brain stimulation (STN-DBS) have been described in patients with predominantly left-sided motor symptoms. The objective of this study was to evaluate if the body side of motor symptoms onset may predict motor outcome of bilateral STN-DBS.

Methods: This retrospective study included all consecutive PD patients treated with bilateral STN-DBS at Grenoble University Hospital from 1993 to 2015. Demographic, clinical and neuroimaging data were collected before (baseline condition) and 1 year after surgery (follow-up condition). The predictive factors of motor outcome at one-year follow-up, measured by the percentage change in the MDS-UPDRS-III score, were evaluated through univariate and multivariate linear regression analysis.

Results: A total of 233 patients were included with one-year follow-up after surgery [143 males (61.40%); 121 (51.90 %) right body onset; 112 (48.10%) left body onset; mean age at surgery, 55.31 ± 8.44 years; mean disease duration, 11.61 ± 3.87]. Multivariate linear regression analysis showed that the left side of motor symptoms onset did not predict motor outcome ($\beta = 0.093$, 95% CI = −1.967 to 11.497, $p = 0.164$).

Conclusions: In this retrospective study, the body side of motor symptoms onset did not significantly influence the one-year motor outcome in a large cohort of PD patients treated with bilateral STN-DBS.

Keywords: deep brain stimulation, motor asymmetry, motor outcome, Parkinson's disease, predictors, subthalamic nucleus

INTRODUCTION

Bilateral deep brain stimulation of the subthalamic nucleus (STN-DBS) is an effective treatment in patients with Parkinson's Disease (PD), allowing a significant improvement in cardinal motor symptoms of disease, motor complications (dyskinesias and fluctuations) and quality of life in the long-term follow-up (Bove et al., 2021). Several works have characterized the predictive factors of postoperative DBS outcomes to improve the selection phase and provide reliable prognostic information to patients (Cavallieri et al., 2021).

In the general PD population, the side of motor symptoms onset has been recently investigated as a potential predictor of disease severity or progression. In particular, left side lateralization has been related to greater motor and non-motor impairment (Cubo et al., 2020; Zhu et al., 2021) and faster motor symptom progression (Elkurd et al., 2021). Further, in PD patients with STN-DBS, worse neuropsychological outcomes have been described in patients with predominantly left-sided motor symptoms (Voruz et al., 2022). To date, it is unknown if left side lateralization might also be a predictor of worse motor outcome after STN-DBS.

In this study, we retrospectively assessed a cohort of PD patients who underwent STN-DBS to investigate if the side of motor symptoms onset represents a predictive factor of motor outcome.

MATERIALS AND METHODS

Participants

This single-center retrospective study included all consecutive PD patients who underwent bilateral STN-DBS at Grenoble University Hospital (France) from 1993 to 2015. PD patients need to fulfill the following inclusion criteria to be included: age at surgery younger than 75 years; presence of disabling motor complications not well optimized with antiparkinsonian medications. Meanwhile, the presence of systemic comorbidities interfering with surgery, severe psychiatric disorders, dementia, severe brain atrophy or diffuse cerebral ischemic lesions on brain magnetic resonance imaging (MRI) were exclusion criteria. The surgical procedure has been previously described in detail (Limousin et al., 1995, 1998).

Clinical Assessment

All patients were assessed before (baseline condition) and 1 year after bilateral STN-DBS surgery (follow-up condition). Demographic variables, PD characteristics, cognitive and neuroimaging data have been collected by reviewing medical records. The clinical evaluation was performed in accordance with the Core Assessment Program for Intracerebral Transplantations (CAPIT) (from 1993 to 1999) (Langston et al., 1992) and the Core Assessment Program for Surgical Interventional Therapies in Parkinson's Disease (CAPSIT-PD) protocol (from 2000 to 2015) (Defer et al., 1999). PD motor severity was quantified with the Hoehn and Yahr scale (H&Y) (Hoehn and Yahr, 1967) and the UPDRS part III score (from 1993 to 2010) (Fahn et al., 1987) or the Movement Disorder Society–sponsored revision of the UPDRS (MDS-UDPRS; from 2011) part III score (Goetz et al., 2008), as previously reported (Bove et al., 2020; Cavallieri et al., 2021). Preoperatively, each patient underwent an acute levodopa challenge to evaluate levodopa responsiveness. All patients were evaluated in the defined "OFF" condition (obtained after a 12-h antiparkinsonian medication withdrawal) and in the defined "ON" condition (obtained after 60 min and the administration of a 50% higher dose of the usual levodopa morning intake). One year after surgery, patients were reevaluated in the on-stimulation/off-medication condition. Moreover, an extensive neuropsychological assessment was performed before surgery including the Mattis Dementia Rating Scale (MDRS) (Marson et al., 1997), the frontal score (Pillon et al., 1995) and the Beck Depression Inventory-II (BDI-II) (Beck et al., 1996). The total amount of chronic antiparkinsonian medications was calculated as levodopa equivalent daily dose (LEDD) milligrams (mg) according to previously reported conversion factors (Tomlinson et al., 2010).

Statistical Analysis

Continuous variables were expressed as mean (±SD) and median (range), while frequencies and percentage were calculated for categorical variables. The aim of the study was to evaluate if the side of motor symptoms onset represents a predictive factor of motor outcome 1 year after surgery. We selected as primary outcome measure the motor percentage change between the MDS-UPDRS part III score in the on-stimulation/off-medication condition 1 year after surgery and the preoperative score in the defined off condition.

To test if the variation of the outcome measure was statistically significant, we applied paired *t*-test or Wilcoxon signed rank test depending on the distribution of the continuous variables.

We selected different independent preoperative variables for regression modeling including: age at surgery; age of PD onset; sex; side of motor symptoms onset; PD duration at surgery; presence or absence of chronic vascular lesions on preoperative brain MRI; BDI-II score; Frontal Score; MATTIS score; MDS-UDPRS part III score and Hoehn and Yahr stage in the defined-off and defined-on condition; levodopa responsiveness; LEDD and motor phenotype (postural instability/gait disorders [PIGD]; tremor dominant, indeterminate) (Stebbins et al., 2013). We performed univariate and multivariate standard linear regression analyses to define if the side of motor symptoms onset could predict motor outcome at 1 year after surgery. We included in the standard multivariate model only significant variables from the univariate models. To rule out collinearity or absence of independence, pairwise correlations were checked among key covariates. Moreover, the two subgroups (right side vs. left side of motor symptoms onset) were compared to find significant differences in demographic and clinical variables. As regards to continuous and ordinal variables, the Kolmogorov–Smirnov test was used to verify the normal distribution. Considering that most of them was not normally distributed, the Mann-Whitney test was used. For categorical variables the chi-square independence test was applied. A $p < 0.05$ was considered significant and results were reported as standardized β coefficient followed by 95% confidence interval (CI) of β coefficient. Statistical analysis was performed using the IBM SPSS Statistics for Windows software version 20.0 (IBM, Armonk, NY, USA).

TABLE 1 | Demographic and clinical characteristics of the PD patients included in the analysis ($n = 233$).

Variable	No. (%); mean [SD]; median {range}	Patients with right side of motor symptoms onset	Patients with left side of motor symptoms onset	*p* value
Sex	143 (61.40%)/90 (38.60 %)	78 (64.50%)/43 (35.50 %)	65 (58.00%)/47 (42.00%)	0.383
Men/women				
Side of motor symptoms onset	121 (51.90%)/112 (48.10%)			
Right/Left				
Presence of chronic vascular lesions on preoperative brain MRI	173 (74.20%)/26 (11.20%)/34 (14.60%)	88 (72.70%)/16 (13.20 %)/ 17 (14.00 %)	85 (75.90%)/10 (8.90%)/17 (15.20%)	0.421
No/Yes/Missing data				
PD motor subtype	126 (54.10%)/33 (14.10%)/74 (31.80%)	67 (55.40%)/15 (12.40 %)/ 39 (32.20 %)	59 (52.70%)/18 (16.00%)/35 (31.30%)	0.811
PIGD/Indeterminate/TD				
Disease duration (years)	11.61 [± 3.87]; 12.00 {3.00–27.00}	11.40 [± 3.94]; 11.00 {3.00–27.00}	11.83 [± 3.79]; 12.00 {4.0–22.0}	0.276
Age at surgery (years)	55.31 [± 8.44]; 56.00 {29.00–74.00}	54.23 [± 8.84]; 55.00 {29.00–71.00}	56.48 [± 7.86]; 57.00 {31.00–74.00}	0.072
Age at PD onset (years)	43.89 [± 7.90]; 44.00 {19.00–62.00}	43.09 [± 8.01]; 44.00 {19.00–62.00}	44.76 [± 7.73]; 45.00 {24.00–62.00}	0.127
MDS-UPDRS part III defined-off condition	55.17 [± 17.04]; 53.70 {20.30–106.50}	54.62 [± 16.67]; 53.70 {20.30–105.40}	55.76 [± 17.50]; 52.60 {23.90–106.50}	0.724
MDS-UPDRS part III defined-on condition	17.95 [± 9.00]; 16.10 {3.50–62.30}	18.25 [± 8.57]; 15.50 {3.50–45.50}	17.63 [± 9.46]; 16.35 {3.50–62.30}	0.414
L-dopa responsiveness (% of improvement)	70.04 [± 14.43]; 71.87 {7.14–97.43}	68.64 [± 15.73]; 70.00 {7.14–97.43.}	71.54 [± 12.77]; 72.09 {30.00–97.22}	0.211
BDI-II	11.31 [± 7.33]; 9.00 {0.00–42.00}	11.93 [± 7.34]; 10.00 {0.00–42.00}	10.67 [± 7.30]; 9.00 {0.00–37.00}	0.145
MDRS	136.98 [± 6.01]; 139.00 {111.00–144.00}	136.93 [± 5.92]; 139.00 {116.00–144.00}	137.01 [± 6.14]; 138.00 {111.00–144.00}	0.905
Frontal score	39.01 [± 7.82]; 40.50 {17.60–50.00}	38.03 [± 8.38]; 39.30 {17.60–50.00}	40.18 [± 6.98]; 41.25 {23.40–50.00}	0.101
LEDD (mg)	1,356.85 [± 560.37]; 1,325.00 {265.00–4,200.00}	1,303.00 [± 540.08]; 1,265.00 {265.00–3,600.00}	1,414.17 [± 578.51]; 1,400.00 {320.00–4,200.00}	0.122

BDI-II, Beck Depression Inventory-II; LEDD, L-dopa equivalent daily dose; MDRS, Mattis Dementia Rating Scale; MDS-UPDRS, Movement Disorder Society–sponsored revision of the UPDRS; MRI, magnetic resonance imaging; PD, Parkinson's disease; PIGD, dominant postural instability and gait disorder; SD, standard deviation; TD, tremor dominant.

TABLE 2 | Changes in the MDS-UPDRS part III score 1 year after STN-DBS surgery ($n = 233$).

Variable	Baseline		1-year follow-up
	Defined off condition	Defined on condition	On-stimulation/off-medication condition
MDS-UPDRS part-III			
mean [± SD];	55.17 [± 17.04];	17.95 [± 9.00];	16.69 [± 10.34];
median {range}	53.70 {20.30–106.50}	16.10 {3.50–62.30}	14.30 {2.30–61.40}

MDS-UPDRS, Movement Disorder Society–sponsored revision of the UPDRS.

RESULTS

From a total of 546 consecutive PD patients treated with bilateral STN-DBS from 1993 to 2015 at the Movement Disorders Center of Grenoble University Hospital (France), we excluded from the analyses 313 patients because: incomplete medical records ($n = 264$); surgical complications responsible for persistent neurological sequelae ($n = 18$); other brain surgical procedures ($n = 17$); electrode misplacement ($n = 14$). Demographic and clinical characteristics of the remaining 233 patients included in the analysis are shown in **Table 1**. By comparing the two subgroups (right vs. left side of motor symptoms onset) no significant statistical differences in demographic and clinical variables were found, meaning that the two subgroups were homogenous, as reported in **Table 1**.

One year after surgery, the MDS-UPDRS part III scores in the on-stimulation/off-medication condition significantly decreased

TABLE 3 | Preoperative predictive factors of motor outcome after STN-DBS ($n = 233$).

Baseline variable	Univariate Analysis			Multivariate Analysis		
	Standardized β coefficient	95% CI	*p* value	Standardized β coefficient	95% CI	*p* value
Left side of motor symptoms onset	0.150	1.10 to 14.24	0.022	0.093	−1.967 to 11.497	0.164
Age at surgery	−0.268	−1.195 to −0.436	<0.001	0.053	−0.664 to 0.986	0.701
Age at PD onset	−0.296	−1.362 to −0.558	<0.001	−0.148	−1.347 to 0.389	0.277
Presence of chronic vascular lesions on preoperative brain MRI	−0.301	−33.055 to −12.693	<0.001	−0.158	−22.330 to −1.618	0.024
MDRS	0.256	0.538 to 1.650	<0.001	0.087	−0.281 to 1.020	0.264
Frontal Score	0.361	0.751 to 1.615	<0.001	0.222	0.202 to 1.253	0.007
MDS-UPDRS part-III off-medication	0.298	0.263 to 0.635	<0.001	0.262	0.193 to 0.597	<0.001
L-dopa responsiveness	0.302	0.317 to 0.757	<0.001	0.133	−0.003 to 0.476	0.053
TD phenotype	0.173	1.268 to 8.545	0.008	0.103	−0.765 to 6.611	0.119

MDRS, Mattis Dementia Rating Scale; MDS-UPDRS, Movement Disorder Society–sponsored revision of the UPDRS; MRI, magnetic resonance imaging; PD, Parkinson's disease; TD, tremor dominant.

if compared with the preoperative medication-off condition ($p < 0.001$) (**Table 2**).

The side of motor symptoms onset emerged as a possible predictor of motor outcome on univariate analysis together with age at surgery, age at PD onset, presence of chronic vascular lesions, MDRS, Frontal Score, the MDS-UPDRS part-III score in the defined-off condition, L-dopa responsiveness and tremor dominant phenotype. However, on the multivariate regression analysis, the side of motor symptoms onset was not confirmed as a predictor of STN-DBS motor outcome.

On the contrary, multivariate regression analysis confirmed that higher Frontal Score ($\beta = 0.222$, 95% CI = 0.202 to 1.253, $p = 0.007$) and higher MDS-UPDRS-III score in preoperative off-medication condition ($\beta = 0.262$, 95% CI = 0.193 to 0.597, $p < 0.001$) were significant predictors of a better motor outcome, while the presence of chronic vascular lesions on preoperative brain MRI ($\beta = -0.158$, 95% CI = −22.330 to −1.618, $p = 0.024$) was predictor of a worse outcome at 1 year after surgery. The results of the univariate and multivariate regression analyses are reported in **Table 3**.

DISCUSSION

In this large cohort of PD patients, the side of motor symptoms onset did not predict the motor outcome of STN-DBS at 1 year after surgery. Although in the general PD population left side lateralization has been related to worse motor outcomes (Cubo et al., 2020; Elkurd et al., 2021; Fiorenzato et al., 2021), DBS was equally effective in restoring motor symptoms regardless of motor side lateralization. Further, the good motor response to STN-DBS of both the groups of left- and right-dominant side patients was not in contrast with previous findings of different neuropsychological outcomes according to the motor side lateralization (Voruz et al., 2022). As a matter of the facts, motor and non-motor outcomes of STN-DBS are not strictly related, as they likely rely on different factors and different neurobiological basis (Kurtis et al., 2017).

In this well-selected population (with a good preoperative responsiveness to levodopa), the main predictors of DBS motor outcome were the Frontal Score, the MDS-UPDRS-III score in the preoperative off-medication condition, and the presence of chronic vascular lesions on preoperative brain MRI, as recently reported by our group (Cavallieri et al., 2021). The side of motor symptoms onset did not interact with these factors and did not add a risk of poor motor response. It is interesting to note that the two subgroups were homogenous for both clinical and demographic variables, thus allowing to exclude the possible bias related to inter-group differences.

The main limitation of the study is the unavailability of information about the dominant hemisphere of the patients. In fact, it has been previously postulated that dominant hemisphere would have more efficient motor networks with greater neural reserve, and this may influence motor phenotype and disease progression (Ham et al., 2015). Another limitation to be considered is the retrospective nature of the study.

CONCLUSIONS

The side of motor symptoms onset does not influence the motor outcome of PD patients with one-year STN-DBS. Other predictive factors should be considered before surgery. Our findings are relevant to the clinicians in the preoperative selection phase and to properly inform the patients.

DATA AVAILABILITY STATEMENT

The raw data supporting the conclusions of this article will be made available by the authors, without undue reservation.

ETHICS STATEMENT

The studies involving human participants were reviewed and approved by Grenoble CHU Research Center Authority. Written informed consent for participation was not required for this

study in accordance with the national legislation and the institutional requirements.

AUTHOR CONTRIBUTIONS

FB and FC conceived the study and were responsible for data analysis and writing the first draft of the manuscript. AC, SM, ESc, AB, EL, AK, PP, EC, ESe, SC, and VF performed the clinical evaluations of the patients and collected the data. FV was responsible for data analysis and writing the first draft of the manuscript. EM conceived the study and revised the manuscript for intellectual content. All authors read and approved the final manuscript.

REFERENCES

Beck, A. T., Steer, R. A., and Brown, G. K. (1996). *Manual for the Beck Depression Inventory-II*. San Antonio, TX: Psychological Corporation. doi: 10.1037/t00742-000

Bove, F., Fraix, V., Cavallieri, F., Schmitt, E., Lhommee, E., Bichon, A., et al. (2020). Dementia and subthalamic deep brain stimulation in Parkinson disease: a long-term overview. *Neurology.* 95, e384–e392. doi: 10.1212/WNL.0000000000009822

Bove, F., Mulas, D., Cavallieri, F., Castrioto, A., Chabardes, S., Meoni, S., et al. (2021). Long-term outcomes (15 Years) after subthalamic nucleus deep brain stimulation in patients with Parkinson disease. *Neurology.* 97, e254–e262. doi: 10.1212/WNL.0000000000012246

Cavallieri, F., Fraix, V., Bove, F., Mulas, D., Tondelli, M., Castrioto, A., et al. (2021). Predictors of long-term outcome of subthalamic stimulation in parkinson disease. *Ann Neurol.* 89, 587–597. doi: 10.1002/ana.25994

Cubo, E., Martinez-Martin, P., Gonzalez-Bernal, J., Casas, E., Arnaiz, S., Miranda, J., et al. (2020). Effects of motor symptom laterality on clinical manifestations and quality of life in Parkinson's disease. *J. Parkinsons Dis.* 10, 1611–1620. doi: 10.3233/JPD-202067

Defer, G. L., Widner, H., Marie, R. M., Remy, P., and Levivier, M. (1999). Core assessment program for surgical interventional therapies in Parkinson's disease (CAPSIT-PD). *Mov Disord.* 14, 572–584. doi: 10.1002/1531-8257(199907)14:4<572::AID-MDS1005>3.0.CO;2-C

Elkurd, M., Wang, J., and Dewey, R. B. Jr. (2021). Lateralization of Motor Signs Affects Symptom Progression in Parkinson Disease. *Front. Neurol* 12, 711045. doi: 10.3389/fneur.2021.711045

Fahn, S., Elton, R., and Members of the Updrs Development Committee. (1987). "The Unified Parkinson's Disease Rating Scale," in *Recent Developments in Parkinson's Disease.* Florham Park, NJ: Macmillan Healthcare Information. p. 153–163.

Fiorenzato, E., Antonini, A., Bisiacchi, P., Weis, L., and Biundo, R. (2021). Asymmetric dopamine transporter loss affects cognitive and motor progression in Parkinson's disease. *Mov. Disord.* 36, 2303–2313. doi: 10.1002/mds.28682

Goetz, C. G., Tilley, B. C., Shaftman, S. R., Stebbins, G. T., Fahn, S., Martinez-Martin, P., et al. (2008). Movement disorder society-sponsored revision of the unified Parkinson's disease rating scale (MDS-UPDRS): scale presentation and clinimetric testing results. *Mov Disord.* 23, 2129–2170. doi: 10.1002/mds.22340

Ham, J. H., Lee, J. J., Kim, J. S., Lee, P. H., and Sohn, Y. H. (2015). Is dominant-side onset associated with a better motor compensation in Parkinson's disease? *Mov. Disord.* 30, 1921–1925. doi: 10.1002/mds.26418

Hoehn, M. M., and Yahr, M. D. (1967). Parkinsonism: onset, progression and mortality. *Neurology.* 17, 427–442. doi: 10.1212/WNL.17.5.427

Kurtis, M. M., Rajah, T., Delgado, L. F., and Dafsari, H. S. (2017). The effect of deep brain stimulation on the non-motor symptoms of Parkinson's disease: a critical review of the current evidence. *NPJ Parkinsons Dis.* 3, 16024. doi: 10.1038/npjparkd.2016.24

Langston, J. W., Widner, H., Goetz, C. G., Brooks, D., Fahn, S., Freeman, T., et al. (1992). Core assessment program for intracerebral transplantations (CAPIT). *Mov. Disord.* 7, 2–13. doi: 10.1002/mds.870070103

Limousin, P., Krack, P., Pollak, P., Benazzouz, A., Ardouin, C., Hoffmann, D., et al. (1998). Electrical stimulation of the subthalamic nucleus in advanced Parkinson's disease. *N. Engl. J. Med.* 339, 1105–1111. doi: 10.1056/NEJM199810153391603

Limousin, P., Pollak, P., Benazzouz, A., Hoffmann, D., Le Bas, J. F., Broussolle, E., et al. (1995). Effect of parkinsonian signs and symptoms of bilateral subthalamic nucleus stimulation. *Lancet.* 345, 91–95. doi: 10.1016/S0140-6736(95)90062-4

Marson, D. C., Dymek, M. P., Duke, L. W., and Harrell, L. E. (1997). Subscale validity of the mattis dementia rating scale. *Arch. Clin. Neuropsychol.* 12, 269–275. doi: 10.1093/arclin/12.3.269

Pillon, B., Gouider-Khouja, N., Deweer, B., Vidailhet, M., Malapani, C., Dubois, B., et al. (1995). Neuropsychological pattern of striatonigral degeneration: comparison with Parkinson's disease and progressive supranuclear palsy. *J. Neurol. Neurosurg. Psychiatry.* 58, 174–179. doi: 10.1136/jnnp.58.2.174

Stebbins, G. T., Goetz, C. G., Burn, D. J., Jankovic, J., Khoo, T. K., and Tilley, B. C. (2013). How to identify tremor dominant and postural instability/gait difficulty groups with the movement disorder society unified Parkinson's disease rating scale: comparison with the unified Parkinson's disease rating scale. *Mov. Disord.* 28, 668–670. doi: 10.1002/mds.25383

Tomlinson, C. L., Stowe, R., Patel, S., Rick, C., Gray, R., and Clarke, C. E. (2010). Systematic review of levodopa dose equivalency reporting in Parkinson's disease. *Mov. Disord.* 25, 2649–2653. doi: 10.1002/mds.23429

Voruz, P., Pierce, J., Ahrweiller, K., Haegelen, C., Sauleau, P., Drapier, S., et al. (2022). Motor symptom asymmetry predicts non-motor outcome and quality of life following STN DBS in Parkinson's disease. *Sci. Rep.* 12, 3007. doi: 10.1038/s41598-022-07026-5

Zhu, S., Zhong, M., Bai, Y., Wu, Z., Gu, R., Jiang, X., et al. (2021). The Association Between Clinical Characteristics and Motor Symptom Laterality in Patients With Parkinson's Disease. *Front. Neurol.* 12, 663232. doi: 10.3389/fneur.2021.663232

Conflict of Interest: FC received personal fees from Zambon outside the submitted work. AC received research grants from France Parkinson Association and Medtronic. SM has received grant support from Medtronic. SC received grants and personal fees from Medtronic and Boston Scientific. VF received honoraria from AbbVie and Medtronic for consulting services and lecturing. EM has received honoraria from Abbott, Medtronic, Kyowa and Newronika for consulting and lecturing and received an educational grant from Boston Scientific.

The remaining authors declare that the research was conducted in the absence of any commercial or financial relationships that could be construed as a potential conflict of interest.

frontiers | Frontiers in Human Neuroscience

METHODS
published: 07 July 2022
doi: 10.3389/fnhum.2022.934063

PELP: Accounting for Missing Data in Neural Time Series by Periodic Estimation of Lost Packets

*Evan M. Dastin-van Rijn[1], Nicole R. Provenza[2], Gregory S. Vogt[3], Michelle Avendano-Ortega[4], Sameer A. Sheth[2], Wayne K. Goodman[4], Matthew T. Harrison[5] and David A. Borton[6,7,8]**

[1]Department of Biomedical Engineering, University of Minnesota, Minneapolis, MN, United States, [2]Department of Neurosurgery, Baylor College of Medicine, Houston, TX, United States, [3]Department of Psychological and Brain Sciences, Texas A&M University, College Station, TX, United States, [4]Menninger Department of Psychiatry and Behavioral Sciences, Baylor College of Medicine, Houston, TX, United States, [5]Division of Applied Mathematics, Brown University, Providence, RI, United States, [6]School of Engineering, Brown University, Providence, RI, United States, [7]Carney Institute for Brain Science, Brown University, Providence, RI, United States, [8]Center for Neurorestoration and Neurotechnology, Rehabilitation R&D Service, United States Department of Veterans Affairs, Providence, RI, United States

Recent advances in wireless data transmission technology have the potential to revolutionize clinical neuroscience. Today sensing-capable electrical stimulators, known as "bidirectional devices", are used to acquire chronic brain activity from humans in natural environments. However, with wireless transmission come potential failures in data transmission, and not all available devices correctly account for missing data or provide precise timing for when data losses occur. Our inability to precisely reconstruct time-domain neural signals makes it difficult to apply subsequent neural signal processing techniques and analyses. Here, our goal was to accurately reconstruct time-domain neural signals impacted by data loss during wireless transmission. Towards this end, we developed a method termed Periodic Estimation of Lost Packets (PELP). PELP leverages the highly periodic nature of stimulation artifacts to precisely determine when data losses occur. Using simulated stimulation waveforms added to human EEG data, we show that PELP is robust to a range of stimulation waveforms and noise characteristics. Then, we applied PELP to local field potential (LFP) recordings collected using an implantable, bidirectional DBS platform operating at various telemetry bandwidths. By effectively accounting for the timing of missing data, PELP enables the analysis of neural time series data collected *via* wireless transmission—a prerequisite for better understanding the brain-behavior relationships underlying neurological and psychiatric disorders.

Keywords: PELP, DBS (deep brain stimulation), packet loss, LFP (local field potential), EEG

OPEN ACCESS

Edited by:
Joshua K. Wong, University of Florida, United States

Reviewed by:
Jun Yu, University of Florida, United States
Jonas Zimmermann, Wyss Center for Bio and Neuroengineering, Switzerland

****Correspondence:***
David A. Borton
david_borton@brown.edu

Specialty section:
This article was submitted to Brain Imaging and Stimulation, a section of the journal Frontiers in Human Neuroscience

Received: *02 May 2022*
Accepted: *06 June 2022*
Published: *07 July 2022*

Citation:
Dastin-van Rijn EM, Provenza NR, Vogt GS, Avendano-Ortega M, Sheth SA, Goodman WK, Harrison MT and Borton DA (2022) PELP: Accounting for Missing Data in Neural Time Series by Periodic Estimation of Lost Packets. Front. Hum. Neurosci. 16:934063. doi: 10.3389/fnhum.2022.934063

INTRODUCTION

Targeted electrical stimulation of the brain and spinal cord has proven to be highly effective for treatment of movement disorders, mental illness, and pain (Lozano et al., 2019). However, the neural correlates of these disorders remain poorly understood. To better investigate the electrophysiological basis of these disorders and the impact of stimulation, several device manufacturers have designed "bidirectional" implants capable of concurrently stimulating and

sensing from the nervous system (Stanslaski et al., 2012, 2018; Sun and Morrell, 2014; Skarpaas et al., 2019; Goyal et al., 2021). One decision point in the design of these devices is when and how to offload data. Some devices, including the Medtronic PC+S (Stanslaski et al., 2012) and NeuroPace RNS (Sun and Morrell, 2014) store data onboard the implanted hardware that can be transferred to an external computer after data collection. Other devices, including the Medtronic Summit RC+S (Stanslaski et al., 2018), the Medtronic Percept PC (Goyal et al., 2021), and the CereplexW (Yin et al., 2014; Simeral et al., 2021) enable real-time streaming of neural data to external devices meters away. These devices can be used to collect chronic neural recordings in natural environments, enabling the identification and development of personalized biomarkers and therapies (Wozny et al., 2017; Kremen et al., 2018; Gilron et al., 2021; Provenza et al., 2021).

During wireless transmission, neural data samples are grouped into formatted units called "packets" (Bazaka and Jacob, 2012). Packets typically contain a series of subsequent samples of a particular length as well as timing information and other relevant metadata. When transmitted, it is possible for packets to fail to reach the receiver, resulting in lost packets. The timing information contained in each packet should hypothetically enable time-domain signal reconstruction. However, the metadata contained in each packet may be inexact due to hardware, network, and software delays and inaccuracies (Levesque and Tipper, 2016), resulting in uncertainty in the number and timing of missing data samples (**Figure 1**).

Herein we will use the Medtronic Summit RC+S as an example. In this case, a combination of inexact packet sizes and inaccurate timing variables make it difficult to exactly account for the number of lost samples (Sellers et al., 2021). Particularly in less controlled environments where the patient, telemeter, or receiver may frequently move, recordings are especially prone to packet loss (Mazzenga et al., 2002; Tsimbalo et al., 2015; Gilron et al., 2021). Lower sampling rates, and thus lower bandwidth needs, generally reduce the number of dropped packets and increase transmission ranges, however, it is still typical for as much as 5% of the data to be lost even with such adjustments. Significant work from Sellers et al. (2021) has been devoted to ensuring neural timeseries data can be accurately analyzed and aligned in the presence of packet losses. This work was designed to ensure packet timing for long-term neural recordings (>1 h) on the order of 50 ms. For short timescale effects such as individual trials in behavioral tasks, alignment errors on the order of 50 ms lead to the introduction of timing inaccuracies, artifacts during filtering, and reduced ability to identify meaningful neural signals, driving the need for more precise data reconstruction (Dastin-van Rijn et al., 2021b; **Figure 1**).

Here, we develop Periodic Estimation of Lost Packets (PELP) to exactly estimate packet losses in neural data collected from bidirectional, implanted devices during neurostimulation. PELP is a data-driven procedure that leverages the highly periodic and predictable nature of stimulation to accurately account for the number of samples missing due to each dropped packet. We show that PELP is robust across a range of amplitude ratios between stimulation and signal, pulse to pulse variations in stimulation amplitude, drift in stimulation frequency, and uncertainties in loss size estimates. Lastly, we successfully apply PELP to data recorded using the Summit RC+S from a human participant performing a behavioral task both in the clinic and at home to exactly estimate every occurrence of packet loss. PELP enables accurate reconstruction of the timing of missing data and facilitates analyses of neural time series data collected using bidirectional, implanted devices.

MATERIALS AND METHODS

Periodic Estimation of Lost Packets (PELP)

Periodic Estimation of Lost Packets (PELP) is a method for estimating the exact number of samples missing due to a packet loss for recordings where stimulation is present. Before PELP can be applied to a recording, the locations of packet losses and their estimated sizes must first be determined. As an exemplar device, we focus our methodological development on the wireless data transmission from the Medtronic Summit RC+S; however, the methodology is generally applicable. For recordings using the Medtronic Summit RC+S, each packet has three integer timing variables of note for this purpose: "dataTypeSequence" indicating the packet number that rolls over every 256 packets, "systemTick" time of the last sample in a packet with 0.1 ms resolution that rolls over every 6.5536 s, and "timestamp" with 1 s resolution and no rollover (Sellers et al., 2021). The "dataTypeSequence" is necessary for identifying packets, "systemTick" is used for highly accurate timing over short timescales and sub-second resolution, and "timestamp" is used for highly accurate timing over long timescales and second resolution. While these specific variables are unique to the Medtronic Summit RC+S, their specific functionalities are common to wireless transmission protocols. A packet loss has occurred when the dataTypeSequence between subsequent packets skips an index or the timestamps are inconsistent with the systemTick data. For sampling rate F_s and m rollovers, the number of samples lost N can be estimated according to the following equation:

$$N = (((S_2 - S_1) \bmod 65536) + 65536 \times m) \times 10^{-4} - n$$

where S_1 and S_2 are the system ticks of the packets preceding and following the loss respectively and is the number of samples in the packet after the loss. For loss segments greater than 6 s, the resolution of a systemTick is no longer acceptably accurate due to timing drift between the systemTick and timestamp. In these cases, the timing will need to be reset using a coarser metric such as the Unix (PacketGenTime) timestamp (±50 ms vs. ±3 ms) corresponding to the time when the packet was received or generated. These estimates are not sufficiently accurate to ensure the exact reconstruction of the timing between received packets down to sample resolution. PELP leverages the presence of regular stimulation in both the received and missing data to ensure exact estimates of data losses. An illustration of the differences between timing methods is shown in **Figure 2A**.

Before applying PELP, we divide the time series into a set of consecutive "runs", where each run is composed of contiguous

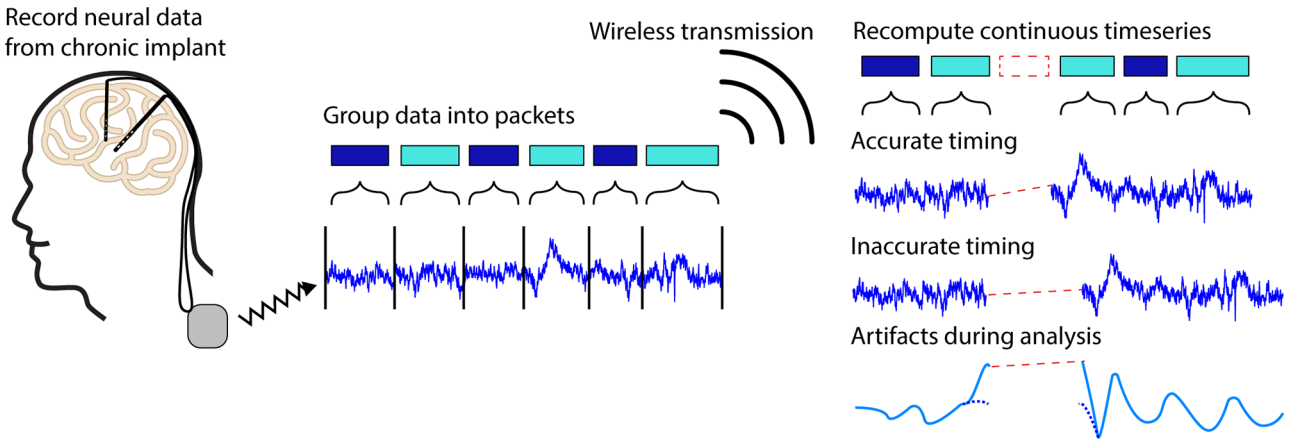

FIGURE 1 | Illustration of packet loss. Neural timeseries data recorded from a chronic implant can be chronically streamed to an external receiver by grouping continuous data into discrete chunks called packets. During transmission, it is possible for packets to fail to reach the receiver leading to regions of missing data known as packet losses. In some systems, it is possible for the timing information contained in each packet to be inaccurate leading to timing offsets in neural signals of interests, artifacts during analyses, and difficulties extracting biologically relevant signals.

packets, and consecutive runs are separated by packet losses. The recording in run r is a sequence of n_r (time, value) pairs $((t_{k,r},y_{k,r}):k = 1,...,n_r)$ where $t_{k,r}$ is the time relative to the start of run r and $y_{k,r}$ is the recorded LFP amplitude at that time. Let δ be the period of stimulation, which we assume is constant across the entire recording. For regular stimulation, the stimulation artifact can be modeled as the δ-periodic function:

$$f_\beta(t) = \beta_1 + \sum_{j=1}^{m} \beta_{2j} \sin\left(\frac{2\pi jt}{\delta}\right) + \sum_{j=1}^{m} \beta_{2j+1} \cos\left(\frac{2\pi jt}{\delta}\right)$$

for appropriate choice of the number of harmonics (m) and the parameter vector $(\beta_j: j = 1,...,2m + 1)$ (Dastin-van Rijn et al., 2021a). Within a single run, β can be estimated *via* least-squares using the harmonic regression model $y_{k,r} = f_\beta(t_{k,r}) + \varepsilon_{k,r}$ with homoscedastic noise $\varepsilon_{k,r}$. Across multiple runs, however, the regression model will only be a good fit for appropriate choice of the packet loss sizes, a fact that we can leverage to estimate these loss sizes from data. Let Δ_r denote the duration of the packet loss between runs r and $r + 1$. We estimate Δ_r by choosing the one that gives the best least-squares fit to the harmonic regression model using the combined data from runs r and $r + 1$, i.e.,

$$\hat{\Delta}_r = \underset{\Delta \in \Omega_r}{\arg\min} \; \min_{\beta} \left[\sum_{k=1}^{n_r} \left(y_{k,r} - f_\beta(t_{k,r})\right)^2 + \sum_{k=1}^{n_{r+1}} \left(y_{k,r+1} - f_\beta\left(t_{n_r,r} + \Delta + t_{k,r+1}\right)\right)^2 \right]$$

where Ω_r is a (small) finite set of candidate loss sizes, in our case, the set of loss sizes corresponding to a positive integer number of samples, centered around the initial loss size estimate, and spanning the uncertainty in the estimate (the range of samples we expect the true loss size to fall in). The minimization over β can be done exactly for each $\Delta \in \Omega_r$ using least-squares, and then the optimal Δ can be selected. It is important that Ω_r is based on an accurate initial estimate without too much uncertainty because candidate loss sizes that differ by an integer multiple of the period δ cannot be distinguished. The method is illustrated in **Figure 2B**.

PELP requires knowledge of the stimulation period (δ) and an appropriate choice of the number of harmonics (m) used by the harmonic regression model. Although δ is known in principle, slight inaccuracies in device system clocks make it important in practice to use data-driven methods to estimate δ. Before using PELP, we estimate δ from combined data across all runs using the multiple-channel period estimation method described in detail in Dastin-van Rijn et al. (2021a) and Provenza et al. (2021) where we treat each run as a separate channel, where we use at most the first 10^4 samples from each run, and where we use only the first two stages of the stagewise search for δ before the final optimization. We similarly choose in a preprocessing step using Akaike Information Criterion (AIC; Akaike, 1974) for the harmonic regression model (with Gaussian errors) applied to the single longest run.

Participant

The research was approved by the Food and Drug Administration and conducted in accordance with the principles embodied in the Declaration of Helsinki and in accordance with local statutory requirements. The participant gave informed consent and the data presented were collected in accordance with recommendations of the federal human subjects' regulations and under protocol H-44941/H-49125 approved by the Baylor College of Medicine Institutional Review Board. EEG data were recorded both with and without stimulation when the participant visited the clinic for DBS programming. LFP data were recorded both in the clinic and when the patient was at home. Electrodes were implanted bilaterally in the VC/VS according to standard stereotactic procedures using computed tomography for target determination. The location of electrode placement was made entirely on clinical grounds.

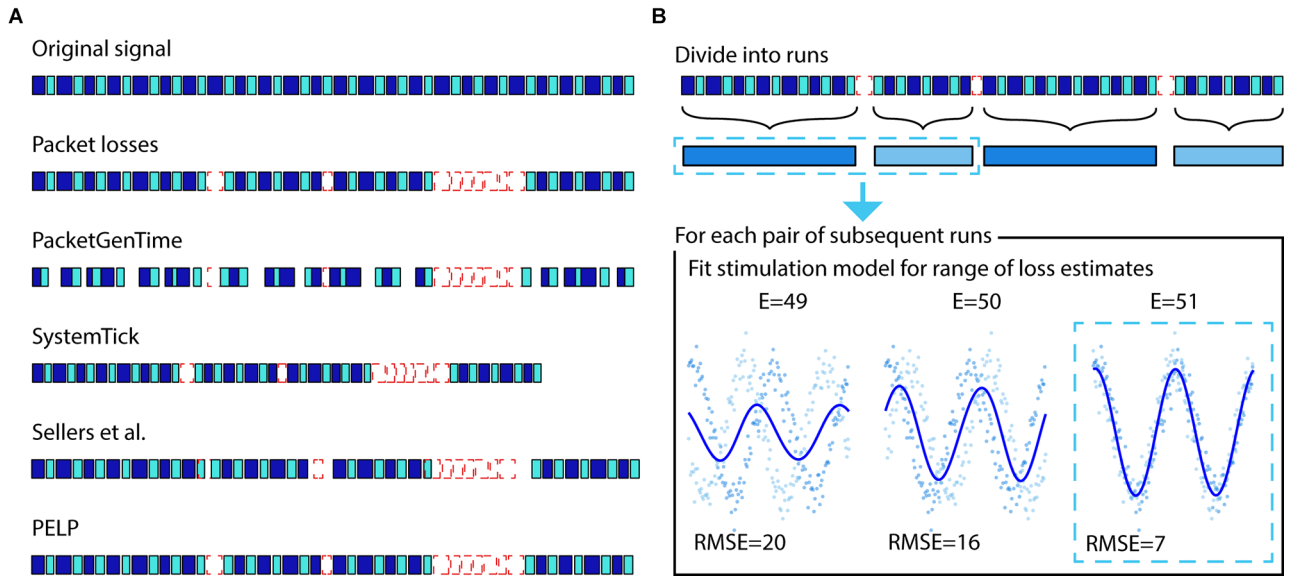

FIGURE 2 | Illustration of packet loss correction and PELP. **(A)** The relative timing of the samples contained in received packets can be uncertain. Adjusting timing solely with PacketGenTime leads to many inaccurate overlaps, systemTicks will accumulate error over long recordings, the approach from Sellers et al. (2021) ensures consistency within runs but offsets at losses, while PELP can ensure exact reconstruction. **(B)** PELP begins by grouping contiguous packets (blue, first row) into continuous runs (blue, second row) where each run is separated from adjacent runs by losses (dashed-red). Loss sizes are estimated but uncertain. The stimulation period is analytically determined using all the data. For each pair of subsequent runs, the root mean squared error (RMSE) between a stimulation model and the samples in the two runs is computed for a range of loss sizes centered around the estimate (indicated by E = for each size). A new stimulation model is fit for each loss estimate. The loss size that minimizes the RMSE is selected as the true loss size.

Bilateral 150.6 Hz stimulation with a pulse width of 90 μs and amplitudes of 4 mA for the left side and 4.5 mA for the right side was used for all recordings where stimulation was turned on.

EEG and LFP Recording Procedures

Continuous electroencephalography (EEG) was recorded using a 64-channel ActiCap BrainVision system (Brain Vision, Morrisville, NC, USA). A common mode sense electrode was located at FCz. The EEG was band-pass filtered online between 0.1 and 1,000 Hz and digitized at 5 kHz. The EEG was downsampled offline to 1,000 Hz with an anti-aliasing filter prior to analysis. The continuous LFP was recorded using the Medtronic Summit RC+S (Medtronic, Minneapolis, MN, USA) *via* wireless data streaming from implanted electrodes to the device running the task. Each DBS probe (Model 3387, one per hemisphere) contains four electrode contacts two of which were used per side to conduct bipolar recordings. LFP recordings were sampled at 1 kHz in the clinic and 250 Hz at home to minimize data losses. Signal processing and analysis were performed in MATLAB (Mathworks, Natick, MA, USA) using in-house code.

Stimulation Simulation Procedure

To simulate stimulation in our recordings, we modeled DBS artifacts as a sum of sinusoidal harmonics of the stimulation frequency (Sun et al., 2014). The effect of stimulation was simulated by adding the artifact component regressed from recordings on a different day where stimulation was turned on to data without stimulation. A high-pass filter at 1 Hz with a gaussian window was first applied to achieve approximately 40 dB attenuation in the stopband before the period of stimulation (δ) was identified using the period estimation component of PARRM (Dastin-van Rijn et al., 2021a). A sum of sinusoids $f_\beta(t)$ with m harmonics of the period and coefficients β was then fit to the data using linear regression. The stimulation amplitude for each cycle was sampled from a normal distribution with mean A_1 and standard deviation V. The mean stimulation amplitude was set relative to the root mean squared amplitude of the stimulation off data (A) according to a ratio (R) and the original root mean squared amplitude of the fit (A_0). To model potential inaccuracies in period estimation, the period of the stimulation model was slightly offset by a drift factor (d) measured in percent drift per 1,000 cycles from the period used during PELP. The effects of these three parameters are illustrated in **Figure 3**.

Computational Experiments

We conducted three sets of experiments to simulate the accuracy of loss estimation while varying different parameters in the stimulation model. For each set, Monte Carlo analyses were used to simulate many experiments by randomly sampling subsets of 50 sample "packets" to remove from a 66 s recording. These simulations were applied while varying one of the following—amplitude ratio, amplitude variability, or drift as a function of the loss uncertainty. For each simulation, the uncertainty (for computing loss size with PELP) ranged from 0 to 50 samples in one sample increments while the

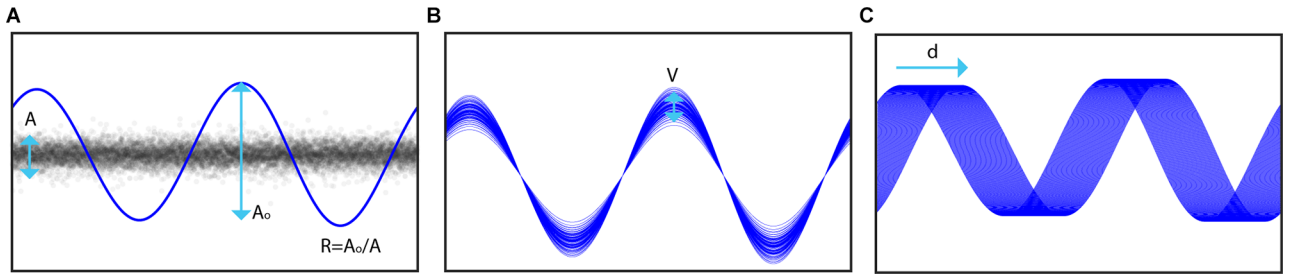

FIGURE 3 | Illustration of simulation components. **(A)** The root mean squared amplitude (A_o) of the stimulation model is set relative to that of the neural signal of interest (A) according to a target ratio R. **(B)** The amplitude of each stimulation pulse is varied on a cycle-wise basis where the amplitude of each pulse is sampled from a normal distribution with mean A_o and standard deviation V. **(C)** Inaccuracies in period estimation, drifting sampling rate, and frequency variability are modeled by adding a drift factor d to the stimulation period in the model.

dependent parameters ranged from 0 to 4 in increments of 0.1 for the amplitude ratio, 0%–10% in increments of 1% for the amplitude variability, and 0%–0.6% in increments of 0.015% per 1,000 cycles for the drift. PELP was applied to each simulation to determine the proportion of losses it was able to estimate correctly depending on the stimulation parameters. This approach is like that of Boudewyn et al. and is informative because it uses a combination of real EEG data analogous to LFP (so that the noise properties are realistic) and artificially induced losses (so the actual truth is known) across a range of modeled stimulation waveforms (Boudewyn et al., 2018).

RESULTS

Stimulation Model Fit

We first sought to estimate the frequency of stimulation to construct a model for time series data alignment. **Figure 4A** shows the stimulation model compared to the raw EEG samples overlapped by computing the modulus of each timepoint with the model's period of stimulation. The period of stimulation was found to be 6.64000 samples. Four sinusoidal harmonics were used for the fit based on model selection *via* AIC. Raw samples are well consolidated about the artifact waveform with a residual standard deviation of 5.90 μV similar to the standard deviation of the stimulation off data (4.55 μV).

Loss Simulations

After building the model of stimulation times, we then ran a set of simulations to provide bounds on the expected recovery and overall loss after using the PELP method for data alignment. The histograms in **Figure 4** illustrate features of the Monte Carlo simulation of 100 loss experiments. The average length of a missing data gap was 63 samples with a median of 50 samples (one loss; **Figure 4B**). Runs of continuous samples between losses ranged from 50 to 2,200 samples with an average length of 251 samples (**Figure 4C**). The max run length in each simulation ranged from 950 to 2,200 samples with an average length of 1,342 samples corresponding to roughly 202 cycles of the 150.6 Hz simulated stimulation frequency (**Figure 4D**).

Loss Estimation Experiments

We then explored the impact of model parameters on the loss of sensing data using PELP. **Figure 5** shows the Monte Carlo simulated loss experiments measuring the accuracy of PELP estimates as a function of the stimulation amplitude ratio, amplitude variability, and estimate uncertainty. Both heat maps show discrete transitions in accuracy at uncertainties of 3, 6, 11, and 21 samples. This occurs because estimate differences at these multiples are more closely overlapping than others for the specific stimulation period of 6.64 samples. The magnitude of estimation errors also increased at these transitions with most errors corresponding to 1, 3, 6, 11, or 21 samples of offset depending on the uncertainty. For constant uncertainty, accuracy increased smoothly for increasing amplitude ratio and decreasing amplitude variability. Changes in drift, in the range tested, had no effect on accuracy. Keeping amplitude ratio or amplitude variability constant while varying uncertainty had little effect on accuracy with exception of the effects at multiples of three samples. Changes in uncertainty for constant drift had no effect on accuracy. Accuracy was near 100% for amplitude ratios above 0.2 for uncertainties less than three samples, amplitude ratios above 0.5 for uncertainties less than nine samples, and amplitude ratios above three for uncertainties greater than nine samples. Accuracy was near 100% for amplitude variabilities below 2% for uncertainties less than nine samples. For uncertainties larger than nine, amplitude variability had to be near zero to maintain 100% estimate accuracy. Across all values for the drift experiment, accuracy was near 100%.

PELP With Medtronic Summit RC+S Recordings

We then applied the PELP methodology of offline data realignment to brain recordings collected from participants of an ongoing clinical study to demonstrate real world performance. **Figure 6** shows LFP data from a behavioral task containing packet losses recorded using the Medtronic Summit RC+S in the clinic and at home after the estimation of losses using PELP. Data recorded in the clinic sampled at 1,000 Hz contained 15 losses with a median size of 200 samples (**Figures 6A,B**). Data recorded at home sampled at 250 Hz contained 121 losses with a median size of 17 samples (**Figures 6C,D**). When

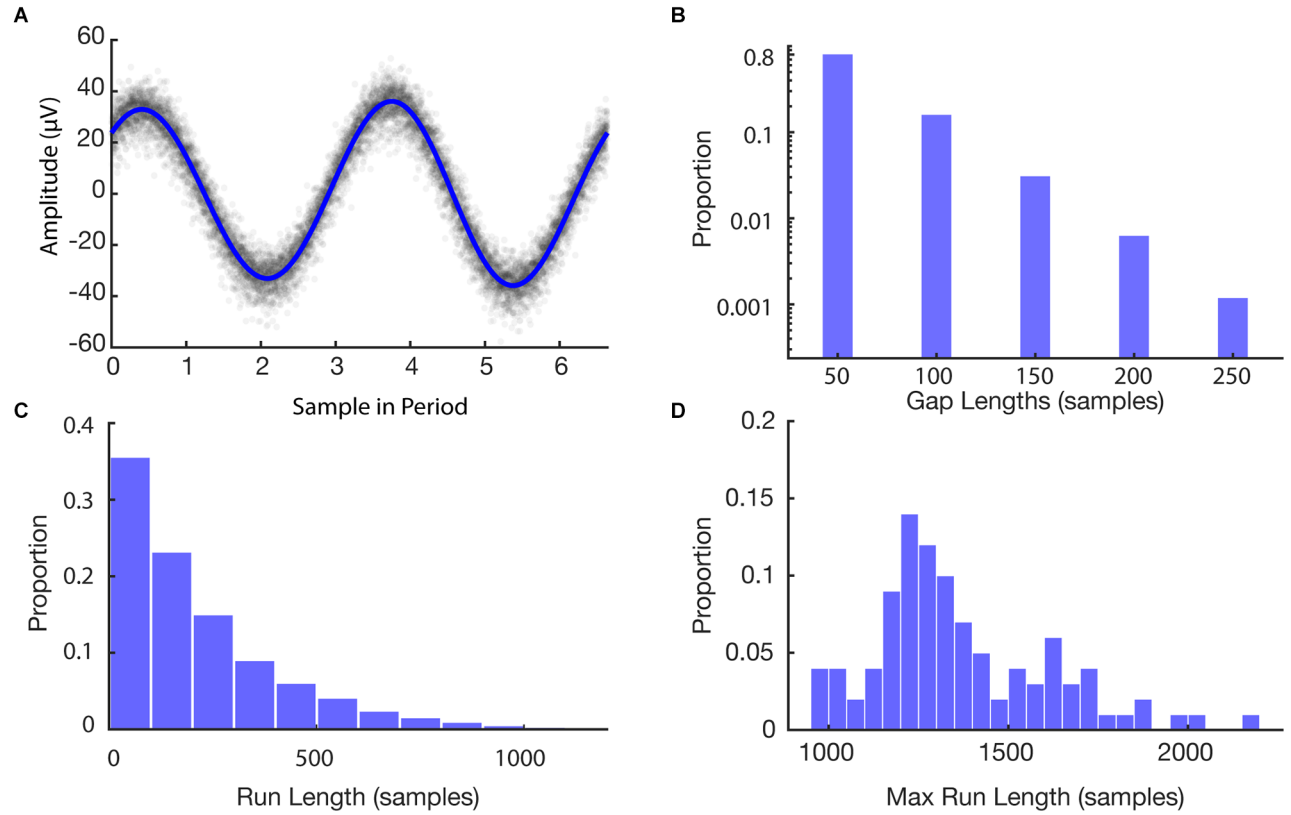

FIGURE 4 | Features of simulation. **(A)** Stimulation model fit to EEG data. Raw data are shown in gray and the model is shown in blue. **(B)** Histogram of missing data gap lengths for all experiments. **(C)** Histogram of continuous run lengths for all experiments. **(D)** Histogram of longest continuous runs in each experiment.

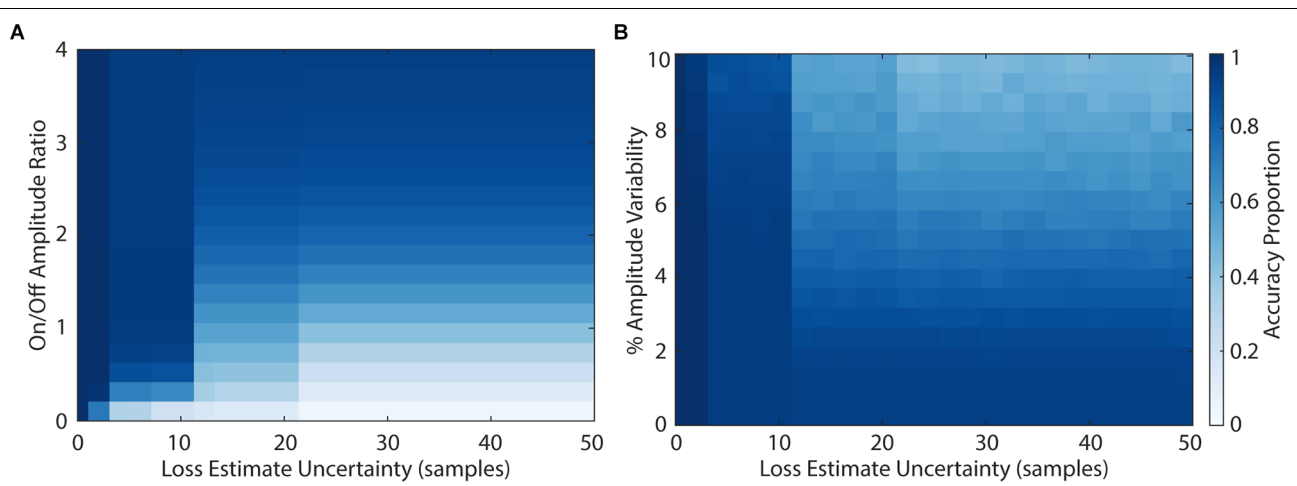

FIGURE 5 | Accuracy of loss estimation as a function of amplitude ratio, amplitude variability, and uncertainty. The accuracy of loss estimation was computed for 100 simulated trials with 20% of the packets removed. More accurate parameter combinations are indicated by darker values in the colormap. Amplitude ratios **(A)** ranged from 0 to 4, amplitude variability **(B)** ranged from 0% to 10%, and uncertainty ranged from 0 to 50 samples.

overlapped on the timescale of the period of stimulation, all samples from both conditions were well consolidated about the stimulation waveform with no observable evidence of significant period drift indicating that losses were accurately accounted for. In contrast to PELP, if the original loss size estimates (**Supplementary Figure 1A**) or the method from Sellers et al. (2021; **Supplementary Figure 1B**) are used for loss size estimation, the samples are not consolidated about the stimulation waveform indicating that losses are not accurately accounted for.

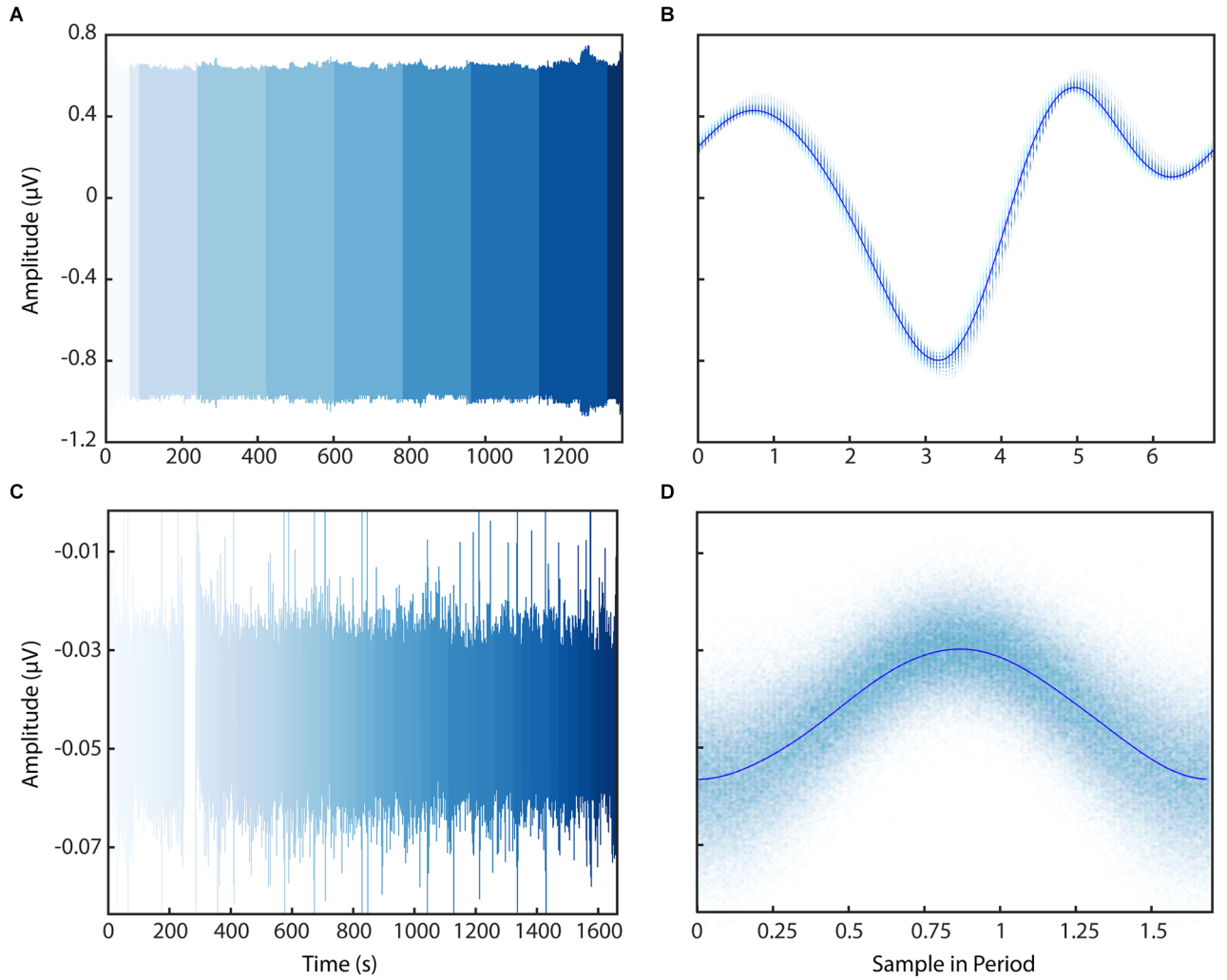

FIGURE 6 | Application of PELP to data from the Medtronic Summit RC+S. PELP was applied to RC+S data containing losses sampled at 1,000 Hz **(A,B)** and 250 Hz **(C,D)**. Each continuous run is indicated by a distinct shade in the colormap **(A–C)**. For both conditions, samples from all runs were overlapped on the timescale of the period of stimulation **(B–D)**. Samples were well consolidated in the stimulation model for both conditions indicating accurate estimation of loss sizes.

DISCUSSION

Streaming of intracranial electrophysiology data in ecologically valid environments is essential for biomarker discovery in a variety of neurological disorders. Bidirectional implanted devices have enabled the acquisition of such datasets, however, data losses during wireless streaming hinder accurate analyses of neural signals. To address these challenges, we have developed PELP to exactly estimate and account for data losses from implanted recordings where stimulation is on. We show using simulations of data losses that PELP can accurately estimate missing samples over a variety of stimulation conditions. Lastly, we successfully applied PELP to reconstruct the timing of data recorded using the Medtronic Summit RC+S using various telemetry settings amenable for both stationary and ambulatory streaming in the laboratory and in natural environments.

PELP is applicable for precise packet alignment for the Summit RC+S and may be applicable to other stimulating devices capable of wireless data streaming with similar acquisition protocols. Our stimulation model accurately accounts for the range of amplitude and variability parameters that could be expected for other implanted devices. In recordings where sensing and stimulation occur on nearby contacts, stimulation amplitude can exceed the underlying neural signal by a factor of 10 (Allen et al., 2010). For recordings where sensing and stimulation occur far apart or the stimulation harmonics fall within the transition band of an online low-pass filter, the amplitude ratio will be closer to 1. Our recordings using the Summit RC+S had amplitude ratios of 27 and 1.2 and estimate accuracy was consistent with predictions from the simulation (as determined from visual inspection of the consolidated stimulation artifact). Pulse to pulse amplitude variability for the Summit RC+S is well within the range of values where

PELP was most accurate. Fluctuations in the battery or the surrounding medium could influence amplitude on longer timescales. While only the run nearest to the loss was used for estimation, drift within the run itself would not be well accounted for. Exceptionally long runs or runs where the drift was identified could be divided to improve estimation accuracy. Similar considerations would also be effective if stimulation frequency drift or errors in period estimation occur.

In the case of clinical devices, it is necessary to work within the confines of the hardware available with little ability to inject external sources of information. In research contexts, where experimental design and data acquisition are more flexible, data losses are handled by utilizing timing systems with greater accuracy and minimal rollover or the injection of reference signals into the recording system that ensure timing is unambiguous. Neither of these solutions is feasible for a fully implanted, closed-source, clinical system necessitating a solution like PELP.

Since PELP requires stimulation artifacts to be present to model the signal during data losses, the method is not applicable for recordings where stimulation is off or significantly attenuated by online filters. In such circumstances, less accurate methods utilizing packet timing metadata must be used for loss estimation. In theory, stimulation could be applied below therapeutic amplitudes and still be used for reconstruction using PELP. However, such modifications would only be reasonable if the inevitable stimulation artifacts did not obscure neural signals of interest. Additionally, the version of PELP described in this manuscript would not be applicable for data streamed during time-varying stimulation (closed-loop DBS). PELP could still be applied if the exact stimulation period and parameters are known for the data neighboring each loss allowing for accurate loss estimation despite changing parameters.

While PELP is highly effective for correcting inaccuracies in loss sizes, the best practice for future devices would certainly be to avoid collecting ambiguous datasets *via* synchronization approaches with consistently accurate clocks and constant packet sizes. We intend PELP to be used as a *post hoc* remediation step for existing datasets where such proactive measures cannot be made. With the Summit RC+S alone, there are several published studies where PELP could be useful for *post hoc* data cleaning (Kremen et al., 2018; O'Day et al., 2020; Petrucci et al., 2020; Gilron et al., 2021; Gregg et al., 2021; Johnson et al., 2021; Provenza et al., 2021). PELP improves over existing solutions (Sellers et al., 2021) for analyses requiring highly accurate timing for small loss sizes, thereby reducing timing offsets, delocalization, and attenuation (Dastin-van Rijn et al., 2021b). In these circumstances, PELP enables near perfect timing and could enable biomarker exploration and task-locked analyses for these studies.

DATA AVAILABILITY STATEMENT

A sample dataset and a MATLAB implementation of PELP are available at: https://github.com/neuromotion/PELP, further inquiries can be directed to the corresponding author.

ETHICS STATEMENT

The studies involving human participants were reviewed and approved by Baylor College of Medicine Institutional Review Board. The patients/participants provided their written informed consent to participate in this study.

AUTHOR CONTRIBUTIONS

ED, NP, MH, and DB contributed to the conception and design of the method. ED completed all analyses and figures with input from NP, MH, and DB. NP, WG, SS, GV, and MA-O conducted LFP recordings with the participant. ED wrote the first draft of the manuscript. NP, MH, and DB wrote sections of the manuscript. WG and SS performed the clinical care aspects of the study. SS performed the study surgical procedures. All authors contributed to the article and approved the submitted version.

FUNDING

DB, MH, WG, SS, NP, and ED were supported by NIH National Institute of Neurological Disorders and Stroke (NINDS) BRAIN Initiative *via* the cooperative agreement UH3NS100549. This work was in part sponsored by the Defense Advanced Research Projects Agency (DARPA) BTO under the auspices of Dr. Alfred Emondi through the (Space and Naval Warfare Systems Center, Pacific OR DARPA Contracts Management Office) grant/contract no. D15AP00112 to DB. ED was supported by the National Science Foundation Graduate Research Fellowship under Grant No. CON-75851.

ACKNOWLEDGMENTS

We would like to thank the participant and their family for their involvement in the research study. Summit RC+S devices were donated by Medtronic as part of the BRAIN Initiative Public-Private Partnership Program. We thank the Open Mind Consortium for their support.

SUPPLEMENTARY MATERIAL

The Supplementary Material for this article can be found online at: https://www.frontiersin.org/articles/10.3389/fnhum.2022.934063/full#supplementary-material.

REFERENCES

Akaike, H. (1974). A new look at the statistical model identification. *IEEE Trans. Automatic Control* 19, 716–723. doi: 10.1109/TAC.1974.1100705

Allen, D. P., Stegemöller, E. L., Zadikoff, C., Rosenow, J. M., and Mackinnon, C. D. (2010). Suppression of deep brain stimulation artifacts from the electroencephalogram by frequency-domain Hampel filtering. *Clin. Neurophysiol.* 121, 1227–1232. doi: 10.1016/j.clinph.2010.02.156

Bazaka, K., and Jacob, M. (2012). Implantable devices: issues and challenges. *Electronics (Basel)* 2, 1–34. doi: 10.3390/electronics2010001

Boudewyn, M. A., Luck, S. J., Farrens, J. L., and Kappenman, E. S. (2018). How many trials does it take to get a significant ERP

effect? It depends. *Psychophysiology* 55:e13049. doi: 10.1111/psyp.13049

Dastin-van Rijn, E. M., Provenza, N. R., Calvert, J. S., Gilron, R., Allawala, A. B., Darie, R., et al. (2021a). Uncovering biomarkers during therapeutic neuromodulation with PARRM: period-based artifact reconstruction and removal method. *Cell Rep. Methods* 1:100010. doi: 10.1016/j.crmeth.2021.100010

Dastin-van Rijn, E. M., Provenza, N. R., Harrison, M. T., and Borton, D. A. (2021b). How do packet losses affect measures of averaged neural signals*f Annu. Int. Conf. IEEE Eng. Med. Biol. Soc.* 2021, 941–944. doi: 10.1109/EMBC46164.2021.9629666

Gilron, R., Little, S., Perrone, R., Wilt, R., de Hemptinne, C., Yaroshinsky, M. S., et al. (2021). Long-term wireless streaming of neural recordings for circuit discovery and adaptive stimulation in individuals with Parkinson's disease. *Nat. Biotechnol.* 39, 1078–1085. doi: 10.1038/s41587-021-00897-5

Goyal, A., Goetz, S., Stanslaski, S., Oh, Y., Rusheen, A. E., Klassen, B., et al. (2021). The development of an implantable deep brain stimulation device with simultaneous chronic electrophysiological recording and stimulation in humans. *Biosens. Bioelectron.* 176:112888. doi: 10.1016/j.bios.2020.11288

Gregg, N. M., Marks, V. S., Sladky, V., Lundstrom, B. N., Klassen, B., Messina, S. A., et al. (2021). Anterior nucleus of the thalamus seizure detection in ambulatory humans. *Epilepsia* 62, e158–e164. doi: 10.1111/epi.17047

Johnson, V., Wilt, R., Gilron, R., Anso, J., Perrone, R., Beudel, M., et al. (2021). Embedded adaptive deep brain stimulation for cervical dystonia controlled by motor cortex theta oscillations. *Exp. Neurol.* 345:113825. doi: 10.1016/j.expneurol.2021.113825

Kremen, V., Brinkmann, B. H., Kim, I., Guragain, H., Nasseri, M., Magee, A. L., et al. (2018). Integrating brain implants with local and distributed computing devices: a next generation epilepsy management system. *IEEE J. Transl. Eng. Health Med.* 6:2500112. doi: 10.1109/JTEHM.2018.2869398

Levesque, M., and Tipper, D. (2016). A survey of clock synchronization over packet-switched networks. *IEEE Commun. Surv. Tutorials* 18, 2926–2947. doi: 10.1109/COMST.2016.2590438

Lozano, A. M., Lipsman, N., Bergman, H., Brown, P., Chabardes, S., Chang, J. W., et al. (2019). Deep brain stimulation: current challenges and future directions. *Nat. Rev. Neurol.* 15, 148–160. doi: 10.1038/s41582-018-0128-2

Mazzenga, F., Cassioli, D., Loreti, P., and Vatalaro, F. (2002). "Evaluation of packet loss probability in Bluetooth networks," in *2002 IEEE International Conference on Communications. Conference Proceedings. ICC 2002 (Cat. No.02CH37333)* (New York, NY), 313–317. doi: 10.1109/ICC.2002.996867

O'Day, J. J., Kehnemouyi, Y. M., Petrucci, M. N., Anderson, R. W., Herron, J. A., and Bronte-Stewart, H. M. (2020). Demonstration of kinematic-based closed-loop deep brain stimulation for mitigating freezing of gait in people with Parkinson's disease. *Annu. Int. Conf. IEEE Eng. Med. Biol. Soc.* (Montreal, QC), 3612–3616. doi: 10.1109/EMBC44109.2020.9176638

Petrucci, M. N., Neuville, R. S., Afzal, M. F., Velisar, A., Anidi, C. M., Anderson, R. W., et al. (2020). Neural closed-loop deep brain stimulation for freezing of gait. *Brain Stimul.* 13, 1320–1322. doi: 10.1016/j.brs.2020.06.018

Provenza, N. R., Sheth, S. A., Dastin-van Rijn, E. M., Mathura, R. K., Ding, Y., Vogt, G. S., et al. (2021). Long-term ecological assessment of intracranial electrophysiology synchronized to behavioral markers in obsessive-compulsive disorder. *Nat. Med.* 27, 2154–2164. doi: 10.1038/s41591-021-01550-z

Sellers, K. K., Gilron, R., Anso, J., Louie, K. H., Shirvalkar, P. R., Chang, E. F., et al. (2021). Analysis-rcs-data: open-source toolbox for the ingestion, time-alignment and visualization of sense and stimulation data from the medtronic summit RC+S system. *Front. Hum. Neurosci.* 15:714256. doi: 10.3389/fnhum.2021.714256

Simeral, J. D., Hosman, T., Saab, J., Flesher, S. N., Vilela, M., Franco, B., et al. (2021). Home use of a percutaneous wireless intracorticalvadjust brain-computer interface by individuals with tetraplegia. *IEEE Trans. Biomed. Eng.* 68, 2313–2325. doi: 10.1109/TBME.2021.3069119

Skarpaas, T. L., Jarosiewicz, B., and Morrell, M. J. (2019). Brain-responsive neurostimulation for epilepsy (RNS® system). *Epilepsy Res.* 153, 68–70. doi: 10.1016/j.eplepsyres.2019.02.003

Stanslaski, S., Afshar, P., Cong, P., Giftakis, J., Stypulkowski, P., Carlson, D., et al. (2012). Design and validation of a fully implantable, chronic, closed-loop neuromodulation device with concurrent sensing and stimulation. *IEEE Trans. Neural Syst. Rehabil. Eng.* 20, 410–421. doi: 10.1109/TNSRE.2012.2183617

Stanslaski, S., Herron, J., Chouinard, T., Bourget, D., Isaacson, B., Kremen, V., et al. (2018). A chronically implantable neural coprocessor for investigating the treatment of neurological disorders. *IEEE Trans. Biomed. Circuits Syst.* 12, 1230–1245. doi: 10.1109/TBCAS.2018.2880148

Sun, F. T., and Morrell, M. J. (2014). The RNS System: responsive cortical stimulation for the treatment of refractory partial epilepsy. *Expert Rev. Med. Devices* 11, 563–572. doi: 10.1586/17434440.2014.947274

Sun, Y., Farzan, F., Garcia Dominguez, L., Barr, M. S., Giacobbe, P., Lozano, A. M., et al. (2014). A novel method for removal of deep brain stimulation artifact from electroencephalography. *J. Neurosci. Methods* 237, 33–40. doi: 10.1016/j.jneumeth.2014.09.002

Tsimbalo, E., Fafoutis, X., Mellios, E., Haghighi, M., Tan, B., Hilton, G., et al. (2015). "Mitigating packet loss in connectionless bluetooth low energy," in *2015 IEEE 2nd World Forum on Internet of Things (WF-IoT)* (Milan, Italy), 291–296. doi: 10.1109/wf-iot.2015.7389068

Wozny, T. A., Lipski, W. J., Alhourani, A., Kondylis, E. D., Antony, A., and Richardson, R. M. (2017). Effects of hippocampal low-frequency stimulation in idiopathic non-human primate epilepsy assessed via a remote-sensing-enabled neurostimulator. *Exp. Neurol.* 294, 68–77. doi: 10.1016/j.expneurol.2017.05.003

Yin, M., Borton, D. A., Komar, J., Agha, N., Lu, Y., Li, H., et al. (2014). Wireless neurosensor for full-spectrum electrophysiology recordings during free behavior. *Neuron* 84, 1170–1182. doi: 10.1016/j.neuron.2014.11.010

Conflict of Interest: Medtronic Summit RC+S devices were provided for this study to DB and WG without charge by Medtronic as part of the NIH BRAIN public-private partnership. A provisional patent application has been filed by Brown University on behalf of ED, NP, MH, and DB on PELP. SS is a consultant for Boston Scientific, Zimmer Biomet, and Neuropace.

The remaining authors declare that the research was conducted in the absence of any commercial or financial relationships that could be construed as a potential conflict of interest.

The handling editor JW declared a past co-authorship with the author SS.

Publisher's Note: All claims expressed in this article are solely those of the authors and do not necessarily represent those of their affiliated organizations, or those of the publisher, the editors and the reviewers. Any product that may be evaluated in this article, or claim that may be made by its manufacturer, is not guaranteed or endorsed by the publisher.

frontiers | Frontiers in Human Neuroscience

ORIGINAL RESEARCH
published: 25 July 2022
doi: 10.3389/fnhum.2022.933401

Patterned Hippocampal Stimulation Facilitates Memory in Patients With a History of Head Impact and/or Brain Injury

Brent M. Roeder[1‡], Mitchell R. Riley[1‡], Xiwei She[2], Alexander S. Dakos[1†], Brian S. Robinson[2†], Bryan J. Moore[2], Daniel E. Couture[3], Adrian W. Laxton[3], Gautam Popli[4], Heidi M. Munger Clary[4], Maria Sam[4], Christi Heck[5], George Nune[5], Brian Lee[6], Charles Liu[6], Susan Shaw[7], Hui Gong[7], Vasilis Z. Marmarelis[2], Theodore W. Berger[2], Sam A. Deadwyler[1], Dong Song[2§] and Robert E. Hampson[1,4§]*

[1] Department of Physiology and Pharmacology, Wake Forest School of Medicine, Winston-Salem, NC, United States, [2] Department Biomedical Engineering, Viterbi School of Engineering, University of Southern California, Los Angeles, CA, United States, [3] Department of Neurosurgery, Wake Forest School of Medicine/Atrium Health Wake Forest Baptist, Winston-Salem, NC, United States, [4] Department of Neurology, Wake Forest School of Medicine/Atrium Health Wake Forest Baptist, Winston-Salem, NC, United States, [5] Department of Neurology, W. M. Keck School of Medicine, University of Southern California, Los Angeles, CA, United States, [6] Department of Neurosurgery, W. M. Keck School of Medicine, University of Southern California, Los Angeles, CA, United States, [7] Department of Neurology, Rancho Los Amigos National Rehabilitation Hospital, Los Angeles, CA, United States

Rationale: Deep brain stimulation (DBS) of the hippocampus is proposed for enhancement of memory impaired by injury or disease. Many pre-clinical DBS paradigms can be addressed in epilepsy patients undergoing intracranial monitoring for seizure localization, since they already have electrodes implanted in brain areas of interest. Even though epilepsy is usually not a memory disorder targeted by DBS, the studies can nevertheless model other memory-impacting disorders, such as Traumatic Brain Injury (TBI). Methods: Human patients undergoing Phase II invasive monitoring for intractable epilepsy were implanted with depth electrodes capable of recording neurophysiological signals. Subjects performed a delayed-match-to-sample (DMS) memory task while hippocampal ensembles from CA1 and CA3 cell layers were recorded to estimate a multi-input, multi-output (MIMO) model of CA3-to-CA1 neural encoding and a memory decoding model (MDM) to decode memory information from CA3 and CA1 neuronal signals. After model estimation, subjects again performed the DMS task while either MIMO-based or MDM-based patterned stimulation was delivered to CA1 electrode sites during the encoding phase of the DMS trials. Each subject was sorted (*post hoc*) by prior experience of repeated and/or mild-to-moderate brain injury (RMBI), TBI, or no history (control) and scored for percentage successful delayed recognition (DR) recall on stimulated vs. non-stimulated DMS trials. The subject's medical history was unknown to the experimenters until after individual subject memory retention results were scored. Results: When examined compared to control subjects, both TBI and RMBI subjects showed increased memory retention in response to both

OPEN ACCESS

Edited by:
Michael S. Okun,
University of Florida, United States

Reviewed by:
Avi Mendelsohn,
University of Haifa, Israel
Bhavana Patel,
University of Florida, United States

***Correspondence:**
Robert E. Hampson
rhampson@wakehealth.edu

†Present address:
Alexander S. Dakos,
The Scotts Miracle-Gro Company,
Marysville, OH, United States
Brian S. Robinson,
The Johns Hopkins University Applied Physics Laboratory, Laurel, MD, United States

‡These authors have contributed equally to this work and share first authorship

§These authors have contributed equally to this work and share senior authorship

Specialty section:
This article was submitted to Brain Imaging and Stimulation, a section of the journal Frontiers in Human Neuroscience

Received: 30 April 2022
Accepted: 13 June 2022
Published: 25 July 2022

Citation:
Roeder BM, Riley MR, She X, Dakos AS, Robinson BS, Moore BJ, Couture DE, Laxton AW, Popli G, Munger Clary HM, Sam M, Heck C, Nune G, Lee B, Liu C, Shaw S, Gong H, Marmarelis VZ, Berger TW, Deadwyler SA, Song D and Hampson RE (2022) Patterned Hippocampal Stimulation Facilitates Memory in Patients With a History of Head Impact and/or Brain Injury. Front. Hum. Neurosci. 16:933401. doi: 10.3389/fnhum.2022.933401

MIMO and MDM-based hippocampal stimulation. Furthermore, effects of stimulation were also greater in subjects who were evaluated as having pre-existing mild-to-moderate memory impairment. Conclusion: These results show that hippocampal stimulation for memory facilitation was more beneficial for subjects who had previously suffered a brain injury (other than epilepsy), compared to control (epilepsy) subjects who had not suffered a brain injury. This study demonstrates that the epilepsy/intracranial recording model can be extended to test the ability of DBS to restore memory function in subjects who previously suffered a brain injury other than epilepsy, and support further investigation into the beneficial effect of DBS in TBI patients.

Keywords: deep brain stimulation, hippocampus, memory, non-linear dynamics, traumatic brain injury, epilepsy, memory encoding, memory decoding

INTRODUCTION

If brain stimulation is to be of use to treat memory disorders, or develop a prosthetic for memory disorders, it is indispensable to address some of the limitations of the various approaches. We are aware that deep brain stimulation (DBS) can affect brain networks associated with memory, even if it is not clear precisely how that effect is produced (Reinhart and Nguyen, 2019). However, as cellular pathology progresses from injury or illness, those networks may not be intact or differ anatomically compared to patients without injury or illness. On the other hand, multi-site stimulation can restore memory function by "bypassing" damaged brain areas (Mohan et al., 2020), enhancing synaptic activity (Gondard et al., 2019), or promoting cellular repair and neurogenesis (Jones et al., 2020). Even in these cases, it is possible that a point can be reached where network-dependent stimulation is simply not effective. Thus, a true neuroprosthetic must function to replace lost cognitive function by not only bypassing, but replacing the output of hippocampus and associated memory regions (Berger and Glanzman, 2005; Deadwyler et al., 2017).

Our laboratories have demonstrated that a non-linear multi-input, multi-output model of hippocampal CA3–CA1 neuron interactions can be used to restore and even enhance hippocampal memory processing in rodents (Berger et al., 2011), non-human primates (Hampson et al., 2013), and even humans (Hampson et al., 2018b). This model extracts cell–cell interactions of the hippocampus (Berger et al., 2005), resulting in a prosthetic design that mimics the memory encoding function of the hippocampal CA3 and CA1 cell fields (Song et al., 2018). However, even this may be insufficient when both the encoding and recall functions of memory are already compromised before "normal" hippocampal neural activity can be recorded. Thus, a true memory prosthetic needs to be able to replace the patterned neural responses or "codes" associated with specific memory items regardless of brain state.

Prior research from these laboratories have demonstrated that the hippocampus (Hampson et al., 1999, 2004, 2005) and prefrontal cortex (Marmarelis et al., 2014; Opris et al., 2015) encode task-relevant information necessary for memory encoding and retrieval. Moreover, that information can be extracted and "transferred" between subjects in a limited manner (Deadwyler et al., 2013). Ongoing studies have focused on determining whether neural codes that represent memory instances can also be identified and facilitated with stimulation, by means of a MIMO-derived model (Roeder, 2021a,b). A memory decoding model (MDM) has been built for decoding memory information from hippocampal spiking data (She et al., 2021). The MDM provides signature functions representing the spatio-temporal characteristic of spike patterns most relevant to the memory. Such signature functions can be used to derive neural code-base stimulation patterns for each memory categories. Tests have demonstrated facilitation of memory encoding and recall with a duration of up to 75 min after stimulation, with preliminary indications of facilitated retention up to 24 h after stimulation (manuscripts in preparation).

With an understanding that the encoding of memory-relevant items by the hippocampus can be facilitated by a model of a neural prosthetic for human memory (Hampson et al., 2018b), we now turn our attention to neurological disorders and diseases that potentially impair memory to determine the utility of the neural prosthetic design for different medical cases. We show here the first demonstration of MIMO-derived model stimulation in subjects with normal intact memory, subjects with impaired memory but no history of head injury, and in subjects with a medical history of head impact of varying degrees.

MATERIALS AND METHODS

Subjects

Twenty-five subjects were analyzed from the same pool of patients selected for the 2018 study (Hampson et al., 2018b). Subjects had medically-refractory focal epilepsy and were undergoing seizure monitoring and localization through the use of implanted intracranial depth electrodes, including surgical procedures, post-operative monitoring, and neurocognitive testing at one of the three sites participating in this study: Wake Forest Baptist Medical Center, Keck Hospital of USC, and Rancho Los Amigo National Rehabilitation Hospital. This study is part of the DARPA Restoring Active Memory (RAM) project. All procedures were reviewed and approved by each locations, Institutional Review Board (WFU IRB00023148, USC IRB#: HS-16-00068, RLANRH IRB#: 221) in accordance with

the National Institutes of Health. Subjects provided voluntary written informed consent prior to participation separate from their consent for surgery.

Memory Task

All memory testing utilized the two-part delayed-match-to-sample with delayed recognition (DMS-DR) assessment developed for the 2018 study (Hampson et al., 2018b). The DMS task consisted of 100–150 trials where each trial consisted of a single Sample phase image presented on a computer screen, a Sample response phase requiring a touch-screen response to the Sample image, a variable delay, a Match phase in which the Sample and 1–7 other images are displayed on-screen, and a Match response phase consisting of a touch-screen response to one of the images. Selection of the same image as the Sample was scored as a correct trial, while selection of any other image was scored as an error trial. DMS trials were separated by a 5 s intertrial interval.

The DR portion of testing commenced at minimum 15 min after completion of the DMS session. The total duration from start of DMS to completion of DR was 90 min or less. DR sessions always followed DMS stimulation sessions, but were not necessary when DMS results were recorded strictly for model generation. A DR trial consisted of presentation of three images at a time with a requirement that subjects rank the familiarity of each image. Each trial presented a Sample image from a prior DMS trial, a Non-match image (i.e., one of the other Match phase images) from the same DMS trial, and a Novel image that had not previously been seen by the subject. DR trials were presented in a randomized order compared to the sequence of DMS trials, and the locations of Sample, Non-match, and Novel images were also randomized to prevent the subject from memorizing sequence or position. Subjects ranked the familiarity of each image on a 0–5 scale, with 0 = not recognized, 1 = familiar escalating to 5 = certainty that the image had been seen in the prior DMS trials. Correct responses were scored as a trial in which the Sample image was ranked $\geq$3, and $\geq$the Non-matching image as well as the Novel image not being ranked at 5. Error trials were those trials in which Sample was ranked <3, Non-match images were ranked higher than the Sample, or if the Novel image was ranked =5.

Subjects were tested in two sessions; the first was 2 days after electrode implant and the second was 1 day before explant. These test days were selected because the patient would be on at least a partial dose of anti-seizure drugs and testing would not interfere with clinical seizure collection. The first test day collected data for model generation (see below) and consisted of a DMS session only. The second day consisted of 1 or 2 DMS-DR sessions. As only the second day utilized a DR session, we report only the analyses performed on these data sets.

Hippocampal Neural Recording, Modeling and Stimulation

Neuronal recording procedure and submission of the recordings to USC for modeling were as reported previously (Hampson et al., 2018b). Two variations of the non-linear multi-input, multi-output MIMO model were generated: (1) A sparse dynamic model with continuous prediction of CA1 outputs from CA3 inputs (Song et al., 2009, 2018), and (2) a MDM decodes memory labels of images shown in DMS tasks based on both CA3 and CA1 neuronal spikes (She et al., 2021). Irrespective of the model used, DMS-DR testing remained the same, and results were not segregated into image categories or content except as follows: an upcoming publication (Roeder, 2021a) shows that one category (Building) was incorrectly designed (see Section "Memory Decoding and Stimulus Categories," below), and the MDM stimulation always resulted in reduced performance on trials in which the category appeared. This category was omitted from analysis for the purpose of this report only.

Neuronal stimulation was controlled by a Matlab (Mathworks, Natick, MA, United States) script preprogrammed to emulate the MIMO and MDM models. Model-derived stimulation was applied to approximately two-third of all DMS trials, equally balanced between "positive" and "negative" stimulation trials. We specify that no stimulation was delivered during DR trials. All stimulation consisted of a 4 s multi-channel, spatio-temporally asynchronous biphasic square-wave pulse trains with a maximum continuous frequency of 20 Hz (Hampson et al., 2018b) commencing with Sample presentation. Positive stimulation-trains were derived from either the continuous MIMO model or the discrete MDM model corresponding to the category of the Sample image. Negative stimulation-trains consisted of either a random spatial–temporal pattern (counterbalancing the MIMO model), or were derived from the discrete MDM model for a different category from the Sample image. The remaining one-third of DMS trials received no stimulation.

Memory Decoding and Stimulus Categories

In human memory decoding, we used image labels to represent visual memory information. Such image labels were obtained from normal volunteers giving scores to DMS stimulus images through an online survey system. Five main categories (i.e., Animal, Building, Plant, Tool, and Vehicle) were selected as the main decoding target categories. The MDM (She et al., 2021) takes hippocampal CA3 and CA1 spiking activities as model inputs and labels of the five image categories as output. It has been proved to be able to identify spatio-temporal characteristics of spike patterns most relevant to the memory categories from ensemble spike patterns. Furthermore, model-based stimulation patterns can be derived based on MDM coefficients to elicit specific memories. In addition, parallel computing strategies were utilized to accelerate model estimation to ensure such model-based stimulation patterns can be calculated on time (She et al., 2022).

Note that survey respondents selected the features that best fit the image, but were not necessarily feature descriptions normally be associated with an image. Thus, there were some deviations from strict categories – Building category included houses, churches, office buildings, arenas, bridges, and architectural features. The Tool category is made up of items best described as "arts and crafts consumables." In the former case, the category

was quite broad, and less defined, and in the latter case, the category was narrow and quite coherent.

Images corresponding to a given category were used for the Sample and Match image within DMS trials, while images from other categories were used for Non-match images. The actual categories used did not affect the MIMO model tests, nor were categories treated separately for the MDM results reported here. A preliminary analysis of MDM stimulation revealed inconsistency with respect to effects of the Building category (Roeder, 2021a), suggesting that the "Building" category may not necessarily be a coherent category or it may be one for which "building" is not a good descriptor—merely the closest available from the survey. For that reason, "Building" trials were omitted from this analysis; the other four categories were combined into a single indication for comparison with similar results from MIMO stimulation.

Brain Injury and Memory Impairment

Since all subjects in this study had a history of epilepsy, it was expected that nearly all would show some form of memory impairment or brain injury. Medical records for all subjects were examined to determine whether a prior history of brain injury was reported, or whether pre-surgical neuropsychological assessment revealed memory impairment. For the purposes of this study, a classification of traumatic brain injury (TBI) was reserved for subjects whose epilepsy diagnosis commenced with a report of a serious fall, a severe head impact or motor vehicle accident. A classification of RMBI was applied to subjects with a history of head-impact through sports, falls or whose MRI showed evidence of prior impact trauma. Control subjects were those whose medical history ruled out TBI or RMBI. Furthermore, subjects were rated as Normal Memory if pre-surgical neuropsychological assessment observed no performance deficit in standardized memory assessments. Subjects with a diagnosis of mild-to-moderate memory, irrespective of spatial, verbal, or lateralization, were rated as Impaired Memory. No subjects in this study received a diagnosis of greater than moderate memory impairment.

RESULTS

A total of 25 Phase II (intracranial monitoring) epilepsy patients were tested as subjects in this study (**Table 1**). A total of 24 subjects were tested with either MIMO or MDM stimulation computed from a recording day at least 3 days prior to the stimulation day. Of those subjects, nine subjects were tested exclusively with stimulation derived from the MIMO model, eleven were tested exclusively with stimulation derived from MDM, and four were tested (separately) with stimulation derived from both models.

As a preliminary statistical screen, an ANOVA (SAS GLM, SAS Institute, Cary, NC, United States) of control DMS performance was performed to assess whether there were baseline differences with respect to age or sex (as provided in **Table 1**). Since subject sex was a binary classification, subject age was converted to a classification variable as well by grouping subjects into ages $<$35 years of age, 35–49 and $\geq$50 years of age. While not a perfectly uniform distribution, this grouping yielded 12 females: 5 @ $<$ 35, 3 @ 35–49 and 4 @ $\geq$ 50; and 13 males: 4 @ $<$ 35, 7 @ 35–49 and 2 @ $\geq$ 50. The ANOVA yielded a significant effect of the model [$F(5,63) = 3.22$, $p < 0.01$], and the main effect of age [$F(2,63) = 5$, $p < 0.01$], with non-significant main effects of sex [$F(1,63) = 0.59$, $p > 0.4$] and non-significant interaction [$F(2,63) = 2.75$, $p > 0.05$] term. The graph of the interaction plot shows considerable overlap in the main subject groups (**Figure 1**). Despite some non-significant differences in DMS-DR performance by age, the overlap in distribution of scores at all ages allowed us to proceed with analysis of TBI and memory impairment without an age subset.

During stimulation testing sessions, DMS trials received: (1) Positive stimulation, consisting of model-derived stimulation patterns that matched either the MIMO model prediction of CA1 firing from continuous CA3 input or MDM prediction of CA1 firing from CA3 input for a given trial type (image category); (2) Negative stimulation, consisting of either random patterns to mimic a non-specific MIMO CA1 spatio-temporal firing or MDM stimulation from a different trial type; or (3) No stimulation (NoStim). The three stimulation conditions were balanced within a session to provide one third of DMS trials meeting each stimulation condition. The Positive stimulation patterns were modeled to produce CA1 ensemble firing with the highest probability of correlation with correct DMS-DR performance. Negative stimulation patterns were intended to counter-balance the Positive stimulation but providing a spatio-temporal pattern that was either randomized or not correlated with the trial type. NoStim trials captured the normal range of subject performance without the influence of the hippocampal stimulation. All subjects performed at least 100 DMS-DR trials, with some subjects performing as many as 150 trials in a single ninety-minute test session. Subjects that were tested with more than one model were tested on the same day with at least one hour between test sessions.

Facilitation as a Function of Brain Injury Status

Mean ($\pm$SEM) DMS-DR performance sorted by TBI status is shown in **Table 2**. Due to the low "n" in several categories, a "Combined" model performance group (top rows in **Table 2**) shows DMS-DR performance for model-stimulated sessions irrespective of whether the model was MIMO or MDM-based. For the four subjects who received both MIMO and MDM-based stimulation, the performance for Positive, Negative, and NoStim trials was averaged across models. Note that for purposes of comparison between models, the MDM model results are averaged across performance of four trial image-type categories (see Section "Materials and Methods"). Instances in which only one subject's data was available do not report SEM.

The two columns at the right compare Positive stimulation trials to NoStim trials, and Negative stimulation trials to NoStim trials, respectively. The increase (positive values) or decrease (negative value) compared to absence of stimulation indicates the effectiveness of Model-based stimulation to alter memory

retention in the DMS-DR task. From these results, the MIMO and MDM models had varying degrees of effectiveness, but the combined results show effective facilitation of memory retention across control, RMBI, and TBI conditions. Effects of MIMO stimulation on Control subjects are consistent with the prior peer-reviewed report (Hampson et al., 2018b); while reduced from MIMO, the effectiveness of MDM-based stimulation is consistent with non-peer-reviewed results reported by this laboratory (Hampson et al., 2018a, 2019). While RMBI results were similar to Control for MDM and MIMO, TBI subjects appeared to obtain greater facilitation from MDM-based than MIMO-based stimulation.

Facilitation as a Function of Pre-existing Memory Status

Our prior study (Hampson et al., 2018b) suggested that baseline memory status did not significantly alter the effectiveness of memory facilitation by MIMO model-based stimulation. Since the earlier study utilized fewer subjects, and the influence of pre-existing memory status was not evaluated with either MDM-based stimulation, or with TBI status, subject results were sorted according to baseline memory function as reported by the pre-surgical neuropsychological assessment. **Table 3** shows that baseline memory performance does in fact appear to influence effects of both MIMO and MDM-based stimulation, with the MIMO model producing almost twice the facilitation of memory in subjects who already exhibit memory impairment. While the differential between impaired and normal subjects is less for MDM-based stimulation, it is nonetheless increased, and this differential carries through to the combined performance across models. It is worth noting the magnitude of the differential between Positive MIMO stimulation and Negative (randomized) stimulation for impaired subjects. Statistical analysis via ANOVA testing main effects of TBI status (RMBI, TBI, Control), memory status (Impaired, Normal) and the interaction of TBI and memory yielded a highly significant overall effect [$F(5,180) = 10.70$, $p < 0.001$], the main effect of memory status [$F(1,180) = 24.11$, $p < 0.001$] and the interaction of TBI*memory [$F(2,180) = 13.57$, $p < 0.001$], but non-significant main effects of TBI [$F(2,180) = 1.12$, $p > 0.3$]. These results confirm the trends listed in **Tables 2**, **3**.

TABLE 1 | Patient demographics.

Patient	Test site	TBI type	Memory	Sex	Age	MIMO	MDM
KECK06	KHUSC	TBI	Normal	M	42	√	
KECK08	KHUSC	Control	Impaired	M	26	√	√
KECK15	KHUSC	Control	Impaired	F	20		√
RANCHO01	RLANRH	RMBI	Impaired	M	35		√
RANCHO07	RLANRH	Control	Normal	M	35		√
WAKE14	WFSM	RMBI	Impaired	M	35	√	
WAKE15	WFSM	TBI	Impaired	M	45	√	
WAKE16	WFSM	Control	Normal	M	21	√	
WAKE17	WFSM	TBI	Impaired	F	31	√	
WAKE18	WFSM	Control	Normal	F	55	√	
WAKE19	WFSM	TBI	Normal	F	33	√	
WAKE20	WFSM	Control	Normal	F	31	√	√
WAKE21	WFSM	TBI	Impaired	F	26	√	√
WAKE22	WFSM	RMBI	Impaired	M	48		√
WAKE23	WFSM	RMBI	Normal	F	51		√
WAKE24	WFSM	Control	Normal	F	33		√
WAKE25	WFSM	Control	Impaired	F	67		√
WAKE26	WFSM	Control	Impaired	M	23		
WAKE28	WFSM	RMBI	Impaired	F	55		√
WAKE29	WFSM	Control	Normal	F	38		√
WAKE30	WFSM	RMBI	Normal	M	55		√
WAKE34	WFSM	TBI	Normal	F	40		√
WAKE35	WFSM	RMBI	Impaired	M	20	√	
WAKE36	WFSM	TBI	Normal	M	42	√	
WAKE37	WFSM	Control	Impaired	F	41	√	√

Subjects tested in the report. TEST SITE: KHUSC = Keck Hospital / School of Medicine, University of Southern California; RLANRH = Rancho Los Amigos National Rehabilitation Hospital; WFSM – Wake Forest School of Medicine (Atrium Health Wake Forest Baptist). TBI TYPE – TBI = Traumatic Brain Injury, subject has history of serious head injury (may include loss of consciousness); RMBI = Repeated Mild-Moderate Brain Injury, subject history indicates falls, sports injuries, or head impacts with no loss of consciousness; Control = no history of head impact. MEMORY - Normal = no evaluation of memory impairment in pre-surgical neuropsychological evaluation; Impaired = pre-surgical neuropsychological evaluation included an assessment of mild-to-moderate memory impairment. MIMO = subject was tested with hippocampal stimulation derived from non-linear multi-input, multi-output (MIMO) model of hippocampal CA1 neural ensemble activity. MDM = subject was tested with hippocampal stimulation derived from non-linear Memory Decoding Model (MDM) of hippocampal CA1 neural ensemble activity.

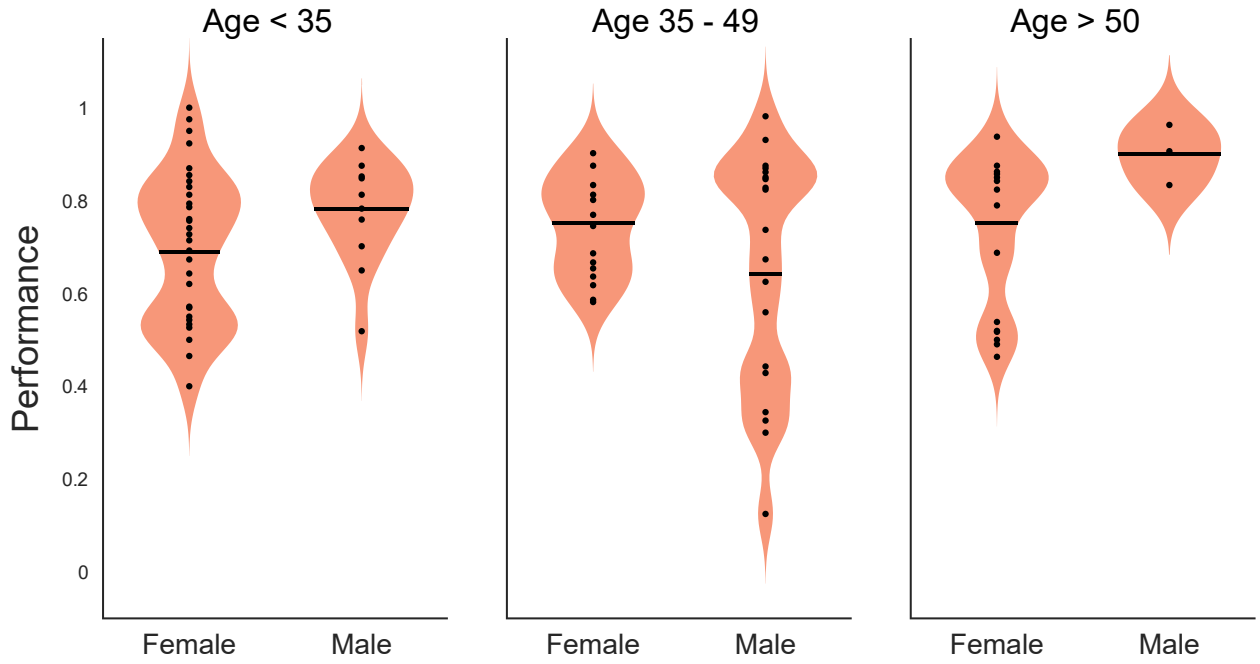

FIGURE 1 | Statistical interaction plot for the ANOVA. An ANOVA (SAS GLM, SAS Institute, Cary, NC, United States) of control (Non-stimulated) delayed-match-to-sample with delayed recognition (DMS-DR) test performance per subject sorted according to age (<35, 35–49, >50 years of age) and sex (Male, Female). DMS-DR performance was the dependent variable, subject was a continuous variable, while sex and age were independent discrete classification variables. The statistical interaction plot for the two-way ANOVA is shown.

TABLE 2 | Delayed-match-to-sample – delayed recognition (DMS-DR) performance by TBI status.

	#Subjects	Positive stim	NoStim	Negative stim	%Change positive stim	%Change negative stim
ALL STIM						
Control	11	81.1% ± 3.8%	70.6% ± 4.1%	71.9% ± 5.4%	14.8%	1.8%
RMBI	7	75.4% ± 7.2%	65.1% ± 8.3%	61.8% ± 11.6%	15.8%	–5.0%
TBI	7	80.5% ± 3.1%	70.6% ± 7.9%	60.2% ± 7.8%	14.1%	–14.8%
MDM STIM						
Control	10	79.9% ± 3.7%	70.2% ± 4.9%	71.7% ± 5.5%	13.8%	2.2%
RMBI	5	79.1% ± 9.3%	70.2% ± 9.5%	71.7% ± 9.4%	12.7%	2.2%
TBI	4	78.6% ± 3.2%	61.8% ± 9.7%	58.5% ± 7.6%	27.3%	–5.4%
MIMO STIM						
CONTROL	4	89.7% ± 3.9%	66.0% ± 6.5%	67.5% ± 8.5%	36.0%	2.4%
RMBI	2	65.9% ± 10.0%	52.3% ± 17.9%	12.5% ± .0%	26.1%	–76.1%
TBI	5	80.8% ± 4.1%	73.6% ± 9.2%	59.8% ± 11.0%	9.8%	–18.8%

Stimulated and non-stimulated task performance by TBI Status for subjects receiving CA1 stimulation based on MDM and MIMO models. Positive stim = stimulation patterns derived from modeling correct DMS trials (MIMO) or from MDM patterns that were congruent with the content classification of the Sample/Match image. NoStim = trials with no stimulation delivered. Negative stim = trials with random stimulation patterns (MIMO) or from MDM that were not specific to the content classification of the Sample/Match image). Stimulation was only delivered during the Sample phase of DMS trials, and not delivered during Match phase, nor during the DR assessment. %Change = percentage of increase (+, no symbol) or decrease (–) compared to NoStim.

Combined Brain Injury Plus Memory Status

Based on the indications of variable effectiveness due to pre-existing memory function, the subjects were further sorted according to TBI status and memory function. The results of the sorting are shown in **Table 4**. There were no RMBI+Normal subjects tested with MIMO-based stimulation; therefore that row was omitted from **Table 4**. There were also several conditions under which only one subject was tested. Those values are included in the table, but any interpretation of those results is premature. Highlighted cells in the columns for percentage change in DMS-DR performance due to model-based stimulation

TABLE 3 | Delayed-match-to-sample – delayed recognition performance by baseline memory function.

	#Subjects	Positive stim	NoStim	Negative stim	%Change positive stim	%Change negative stim
ALL STIM						
Impaired	12	75.5% ± 3.9%	61.9% ± 5.1%	56.4% ± 6.4%	22.0%	–8.8%
Normal	12	83.0% ± 3.5%	76.1% ± 4.3%	75.9% ± 5.2%	9.1%	–0.3%
MDM STIM						
Impaired	9	77.8% ± 4.6%	65.2% ± 5.9%	63.7% ± 4.9%	19.3%	–2.4%
Normal	10	80.9% ± 4.1%	71.4% ± 5.5%	73.9% ± 6.4%	13.4%	3.6%
MIMO STIM						
Impaired	5	73.1% ± 5.2%	54.9% ± 6.8%	40.3% ± 10.9%	33.2%	–26.6%
Normal	6	88.2% ± 3.2%	77.1% ± 6.4%	73.3% ± 6.6%	14.5%	–4.9%

Stimulated and non-stimulated task performance by baseline memory function for subjects receiving CA1 stimulation based on MDM and MIMO models. Positive stim = stimulation patterns derived from modeling correct DMS trials (MIMO) or from MDM patterns that were congruent with the content classification of the Sample/Match image. NoStim = trials with no stimulation delivered. Negative stim = trials with random stimulation patterns (MIMO) or from MDM that were not specific to the content classification of the Sample/Match image). Stimulation was only delivered during the Sample phase of DMS trials, and not delivered during Match phase, nor during the DR assessment. %Change = percentage of increase (+, no symbol) or decrease (–) compared to NoStim.

TABLE 4 | Delayed-match-to-sample – delayed recognition performance by TBI and memory.

		#Subjects	Positive stim	NoStim	Negative stim	%Change positive stim	%Change negative stim
ALL STIM							
Control	Impaired	4	83.9% ± 1.6%	73.6% ± 5.0%	75.3% ± 5.5%	13.9%**	2.2%
	Normal	6	79.2% ± 6.3%	68.6% ± 6.1%	69.2% ± 8.9%	15.4%	0.9%
RMBI	Impaired	5	69.0% ± 8.5%	58.6% ± 10.5%	46.7% ± 11.3%	17.6%	–20.4%
	Normal	2	91.3% ± 5.0%	81.1% ± 2.2%	92.2% ± 1.6%	12.5%*	13.6%**
TBI	Impaired	3	75.1% ± 3.9%	51.5% ± 3.8%	44.2% ± 7.1%	45.8%**	–14.2%
	Normal	4	84.6% ± 3.7%	84.9% ± 7.3%	76.1% ± 6.2%	–0.3%	–10.4%
MDM STIM							
Control	Impaired	4	83.1% ± 2.3%	74.6% ± 4.3%	74.0% ± 6.4%	11.5%*	–0.7%
	Normal	6	77.8% ± 6.0%	67.3% ± 7.8%	69.9% ± 8.9%	15.6%	3.9%
RMBI	Impaired	3	71.0% ± 14.2%	62.9% ± 15.3%	58.0% ± 7.8%	13.0%	–7.7%
	Normal	2	91.3% ± 5.0%	81.1% ± 2.2%	92.2% ± 1.6%	12.5%*	13.6%**
TBI	Impaired	2	77.2% ± 1.4%	49.9% ± 3.4%	51.3% ± 1.3%	54.6%**	2.8%
	Normal	2	80.1% ± 7.4%	73.7% ± 16.5%	65.6% ± 15.6%	8.7%	–10.9%
MIMO STIM							
Control	Impaired	1	83.3%	58.1%	68.6%	43.3%	18.0%
	Normal	3	91.8% ± 4.6%	68.6% ± 8.5%	67.0% ± 13.9%	33.9%**	–2.3%
RMBI	Impaired	2	65.9% ± 10.0%	52.3% ± 17.9%		26.1%	–76.1%
	Normal	0					
TBI	Impaired	2	75.1% ± 7.8%	55.8% ± 11.5%	40.0% ± 10.0%	34.7%*	–28.3%
	Normal	3	84.7% ± 4.3%	85.5% ± 7.7%	79.5% ± 4.5%	–1.0%	–7.0%

Stimulated and non-stimulated task performance sorted by TBI and memory for subjects receiving CA1 stimulation based on MDM and MIMO models. Positive stim = stimulation patterns derived from modeling correct DMS trials (MIMO) or from MDM patterns that were congruent with the content classification of the Sample/Match image. NoStim = trials with no stimulation delivered. Negative stim = trials with random stimulation patterns (MIMO) or from MDM that were not specific to the content classification of the Sample/Match image). Stimulation was only delivered during the Sample phase of DMS trials, and not delivered during Match phase, nor during the DR assessment. %Change = percentage of increase (+, no symbol) or decrease (–) compared to NoStim. Conditions with significant increase or decrease in DR performance relative to NoStim ($p < 0.01$, **$p < 0.001$ by pairwise linear contrasts) are indicated by asterisks. Note, there were no Normal Memory RMBI subjects tested with MIMO stimulation.*

indicate conditions with at least two subjects, and at least 2.25 × SEM differences (approx. $p < 0.01$) from NoStim.

In support of the stim effects in **Table 4**, we can confirm significant effects of memory and the interactions between TBI status and memory for individual stimulation models for the *Combined* task performance: main effect of memory [$F(2,63) = 11.24$, $p < 0.001$] and interaction TBI*memory [$F(1,63) = 8.38$, $p < 0.001$]; and for *MDM* task performance:

main effect of memory [$F(1,50) = 5.89$, $p < 0.01$], and interaction TBI*memory [$F(2,50) = 4.88$, $p < 0.01$]. Interestingly, for the MIMO model, there was no significant interaction, but significant main effects of TBI [$F(2,25) = 3.88$, $p < 0.05$] and memory [$F(1,25) = 6.59$, $p < 0.01$]. The interaction plots in **Figure 2** depict the performance changes associated with each of these analyses.

Comparisons highlighted in **Table 4**, right (%Change) are supported by ANOVA and linear contrasts of the derived measures of percent change from NoStim for positive and negative stim. The overall ANOVA was significant [$F(5,59) = 3.44$, $p < 0.01$]. Again, there was not a significant main effect of TBI [$F(2,59) = 0.42$, $p > 0.6$] but there were significant main effects of memory [$F(1,59) = 4.9$, $p < 0.05$] and interaction TBI*memory [$F(2,59) = 5.74$, $p < 0.01$]. Orthogonal pairwise contrasts were computed using this model. Asterisks in **Table 4** indicate conditions in which positive or negative stim results differed from NoStim with $p < 0.001$.

Summary of Stimulation-Induced Changes in Memory

To compute statistical comparisons of the effects of stimulation, normalized difference scores were calculated by subtracting the mean Control-NoStim DMS-DR performance and dividing by within-subject standard deviation to yield standardized scores with mean = 0 and SD = 1. Two additional derived factors – (1) the difference between NoStim performance for a given subject and the overall mean of NoStim Control trial DMS-DR performance, and (2) Delta – the difference between No-Stim trial DMS-DR performance and the Positive (or Negative) stim trial DMS-DR performance for a given subject.

The overall multi-factor ANOVA on effects of the stim model, TBI status, memory status and stimulation type yields a significant effect of the model, where [$F(50,104) = 2.59$, $p < 0.001$]. Main effects analyses for individual factors and interaction yielded Model type [$F(2,104) = 0.36$, $p = 0.70$]; TBI status [$F(2,104) = 2.58$, $p = 0.08$]; Memory status [$F(1,104) = 22.85$, $p < 0.001$]; and Stim type [$F(2,104) = 21.87$, $p < 0.001$]. The only significant interaction term (of all 2-way, 3-way, and 4-way interactions) was TBI status × Memory status [$F(2, 104) = 16.46$, $p < 0.001$].

Figure 3 shows the summary bargraph of Normalized change in DMS-DR Percent Correct for NoStim trials sorted by TBI status and Memory status. The normalization baseline was composed of non-stim trials specifically gathered from the Control/Normal subjects, supplying mean and standard deviation for computation of normalized values (e.g. standard scores). Performance for all memory-Impaired subjects (irrespective of stimulation model) was below the control mean for NoStim trials. Moreover, performance for Normal memory subjects was slightly elevated for the TBI and RMBI groups. Compared to baseline non-stimulated DMS-DR performance, memory-impaired subjects performed *all* DMS-DR trials at a performance level below that of normal memory subjects.

Figure 4 shows the summary of interactions between TBI and Memory status for each of the stimulation models. To identify individual effects of Positive stimulation of DMS-DR performance, orthogonal pairwise linear contrasts (Neter and Wasserman, 1974) were computed between Positive and NoStim for each condition. Asterisks (*) in **Figure 4** indicate those conditions under which there is a significant difference between positive stimulation and the normalized NoStim DMS-DR performance. To identify differential effects of stimulation, orthogonal pairwise linear contrasts were computed between Positive and Negative stimulation for each condition. Daggers (†) indicate significant differences between Positive and Negative stim conditions, indicating modulation of memory via stimulation even when that positive stim does not significantly increase DMS-DR performance. All comparisons are [$F(1,104) > 15.09$, $p < 0.001$] via orthogonal linear contrasts adjusted for multiple comparisons. (Neter and Wasserman, 1974)

DISCUSSION

The question of whether human memory can be modulated via intracranial stimulation of hippocampus (or entorhinal cortex) is one that suffers slightly from comparison with DBS fixed stimulation techniques (Mohan et al., 2020). Jacobs et al. (Jacobs et al., 2016; Goyal et al., 2018) stimulated hippocampus with high, fixed-frequency stimulation and noted impairment in working and episodic memory. Other studies by Aghajan et al. (2017), Titiz et al. (2017), Mankin et al. (2021) have stressed that the stimulation pulse-train frequency is essential to whether or not hippocampal/entorhinal stimulation is effective or not.

Theta-like activity in the 3.5–7 Hz band has been shown to be an important contributor to hippocampal-dependent memory processing (Kota et al., 2020; Kragel et al., 2020; Nicolas et al., 2021). Theta-burst stimulation of hippocampus improves memory (Titiz et al., 2017; Tambini et al., 2018; Jun et al., 2020), possibly by synchronizing theta power (Karakas, 2020), theta-gamma coupling (Jones et al., 2020), or via synaptic plasticity based on theta frequency activation of neuronal circuits in the temporal lobe (Tsanov and Manahan-Vaughan, 2009; Larson and Munkácsy, 2015).

Given that DBS-like high-frequency stimulation is most effective in facilitating memory when applied outside hippocampus (Ezzyat et al., 2018; Kucewicz et al., 2018), but not when applied to hippocampus (Jacobs et al., 2016), it is therefore possible that the MIMO model-based hippocampal stimulation applied here and previously (Hampson et al., 2018b; Roeder, 2021a) is effective at facilitating human short-term memory precisely because the stimulation frequency is capped at ≤20 Hz. Moreover, the stimulation is also based on a closed-loop approach that models the stimulation pattern on existing neural ensemble firing patterns associated with successful memory function (Song et al., 2016, 2018; She et al., 2021). Overall, the results presented here indicate that both MIMO or MDM-based stimulation can be effective in facilitating memory retention (up to 75 min) across all subjects irrespective of TBI status or pre-existing memory function. Irrespective of baseline memory function (impaired vs. normal), the MIMO model produces at least double the facilitation compared to the MDM model

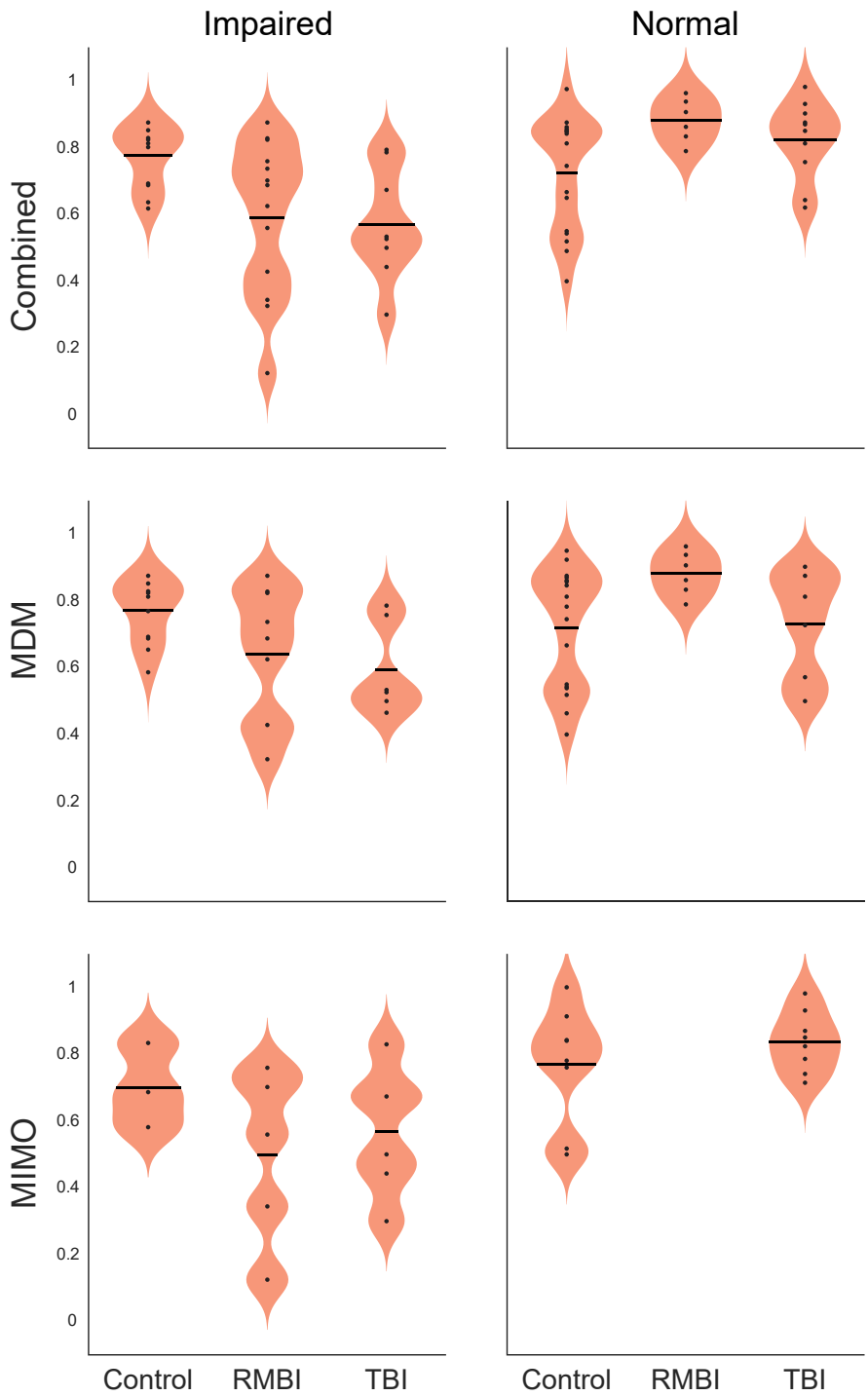

FIGURE 2 | Statistical interaction plot for the ANOVA by model. Performance by interaction traumatic brain injury (TBI)*memory plots for ANOVAs performed for each of the stimulation models. DMS-DR performance per subject (dependent variable) was modeled with independent variables of TBI-type [(Control, TBI, repeated and/or mild-to-moderate brain injury (RMBI)] and memory status (Normal, Impaired).

(**Table 4**). In all likelihood, this is due to the nature of the MDM model which is segmented into individually-specific discrete codes according to the categorization of the Sample image presented in DMS trials. It is possible, that the smaller effect of MDM-based stimulation is due to variability between categories within a subject, rather than variability between subjects.

The 2018 report from this laboratory did not reveal a significant effect of MIMO-based stimulation on subjects with

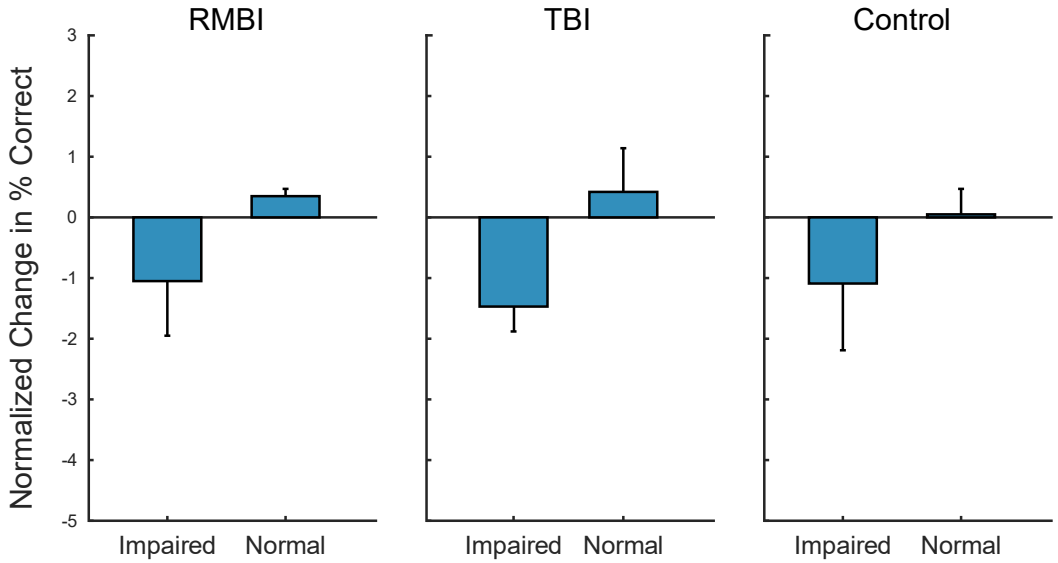

FIGURE 3 | Subject–Condition differences in non-stimulated DMS-DR performance. Individual subject DMS-DR results were normalized by subtracting overall non-stimulated trial performance from control performance (i.e., non-stim DMS-DR from Control/Normal subjects), and dividing by individual subject standard deviation. The resulting differences in performance for the RMBI/TBI by Impaired/Normal memory status is plotted as mean (±intersubject SEM) normalized difference from baseline, control performance in the absence of stimulation. As expected, memory impaired subject performance the DMS-DR task worse than non-impaired subjects. (Note, since control performance was aggregated from all Control/Normal subjects, the bar and SEM for Control/Normal indicate individual subject variability.)

impaired memory function (Hampson et al., 2018b), but concluded that at minimum, MIMO-model based stimulation was at least as effective across categories of pre-existing memory function. The present study includes more than three times as many subjects, and **Table 3** shows that the MIMO was at least twice as effective in memory-impaired subjects, while the MDM-based stimulation was at least one standard error (SEM) more effective in impaired subjects compared to subjects with normal memory function.

The collation of subjects by TBI status and memory function in **Table 4** shows that across subjects, the combined stimulation models were most effective in Impaired Controls, *Normal* RMBI and Impaired TBI subjects. Normal RMBI subjects also benefitted from Negative or non-category-specific MDM stimulation. This improvement overshadowed the decline in performance from the memory-impaired RMBI subjects and led to an overall increase with Negative MDM stimulation. This was the only case in which stimulation not specific to the model was facilitatory, and of course it raises the question of whether simply any low-frequency stimulation could be facilitatory in these subjects. However, it is quite subject specific (i.e. only Normal-memory, RMBI subjects). We are aware that there are some issues with respect to the composition of the categories used to generate that model (see Section "Materials and Methods") and it is possible that these results indicate cross-category similarities. On the other hand, Mankin and Fried (2020) suggest that a key component of the MIMO success derives from underlying low frequency and sparsity of the stimulation (Mankin and Fried, 2020). As mentioned above, theta-band stimulation has been significantly involved with hippocampal memory processing and our MDM stimulation has a significant theta-component. Therefore, we theorize that even non-specific stimulation likely creates an improvement if a patient does not have impaired memory. This is a subject of ongoing investigation.

Figure 3 demonstrates that, as expected, subjects with a neuropsych evaluation that included mild-to-moderate memory impairment scored lower on DMS-DR task performance. Normalizing the data to evaluate effects of stimulation irrespective of baseline DMS-DR performance (**Figure 4**) shows that the MIMO model significantly improved DMS-DR performance in TBI and Control (No-TBI) subjects, while the MDM stimulation was most effective in RMBI subjects (asterisks, **Figure 4**). The MIMO model was most effective in all RMBI, TBI and Control subjects, irrespective of memory impairment. In TBI subjects, both models were quite effective, particularly in memory-impaired subjects (daggers, **Figure 4**). One possibility why MIMO stimulation produces more of a differential in memory performance is because MIMO negative stimulation consisted of randomized stim patterns, while for MDM the negative stim was not random, but a pattern associated with a different category, which might have some cross-over benefit (see top graph in **Figure 4**, MDM-Normal) (Roeder, 2021a). Future studies will explicitly examine difference in possible partial benefit of out-of-category stimulation vs. randomized stimulation patterns.

Summary

These results suggest that controls and subjects with a diagnosis of TBI receive equal benefit from memory-facilitating stimulation. Biomimetic MIMO based stimulation is more effective than MDM based stimulation. Model-based stimulation

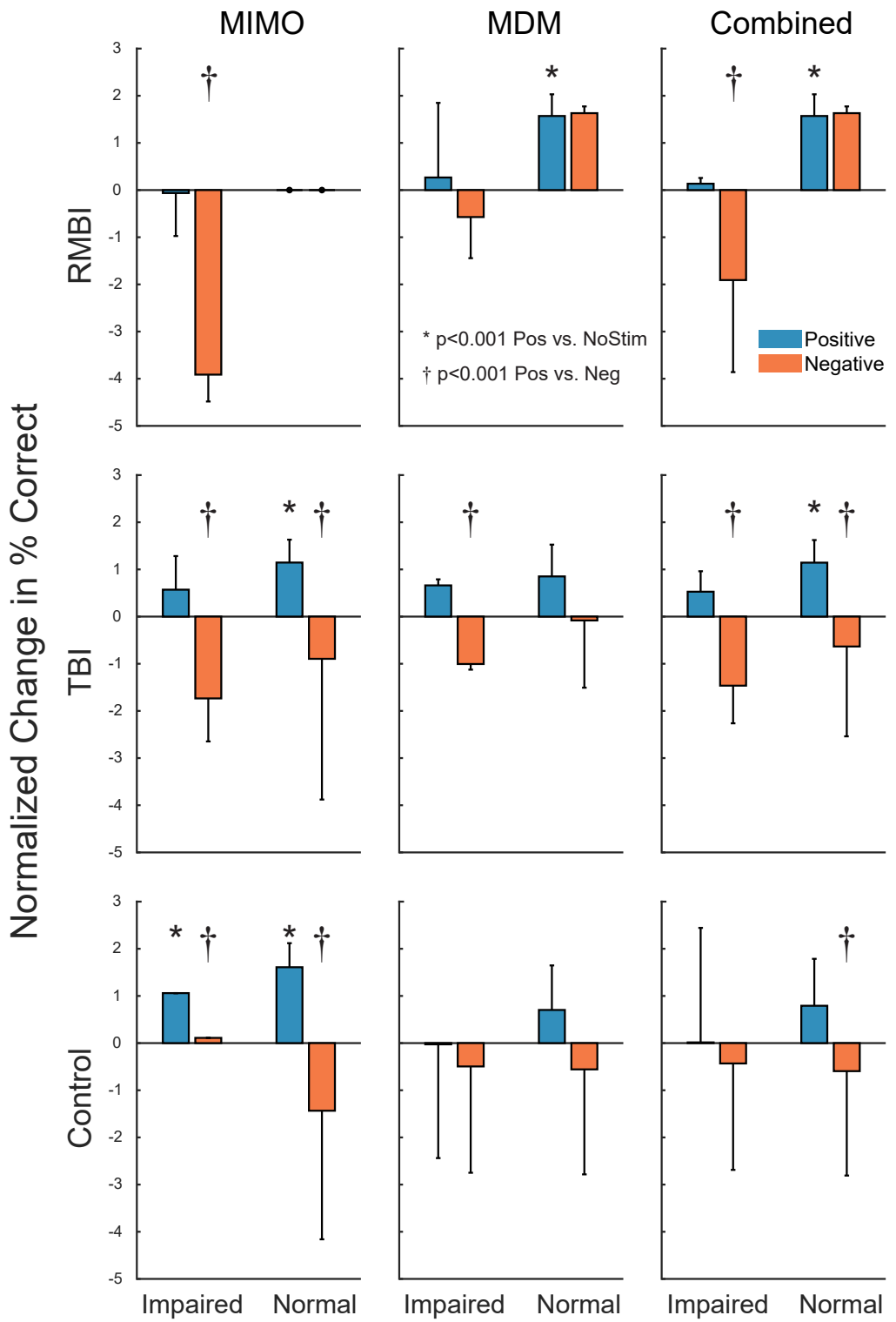

FIGURE 4 | Subject–Condition differences in stimulated DMS-DR performance. Individual subject DMS-DR results were normalized by subtracting mean within-subject NoStim positive and negative pattern stimulated trial performance, and dividing by individual subject standard deviation to produce standard scores. Scores were then sorted by TBI status, stimulation model and presence or absence of memory impairment, and plotted as normalized mean (±inter-subject SEM) differences in DMS-DR performance. Individual linear contrasts were computed using paired-differences and mean standard error (MSE) from the overall multi-factor ANOVA. Asterisks (*) indicate conditions with significant differences between positive stim and NoStim conditions. Daggers (†) indicate statistically significant differences between positive and negative stim conditions.

is more effective in subjects with a prior medical history of memory impairment, leading to maximal benefit in TBI subjects with memory impairment.

Effects of stimulation designed to emulate a neural prosthetic are different in subjects with a diagnosis of Repeated Mild-to-Moderate Brain Injury (RMBI, i.e., falls, concussions, sports injuries). Non-memory-impaired RMBI subjects received the most benefit from the model-based stimulation, while impaired RMBI subjects received benefit from the non-specific stimulation from the MDM.

These results suggest that both models have the potential to improve memory function in patients with neurological impairments caused by disease or injury.

DATA AVAILABILITY STATEMENT

The raw data supporting the conclusions of this article will be made available by the authors, without undue reservation.

ETHICS STATEMENT

The studies involving human participants were reviewed and approved by Wake Forest School of Medicine IRB (IRB00023148), Keck Hospital of the University of Southern California IRB (S-16-00068), and Rancho Los Amigos National rehabilitation Hospital IRB (IRB#221). The patients/participants provided their written informed consent to participate in this study.

AUTHOR CONTRIBUTIONS

RH was project PI and supervised all aspects of design, data collection, data analysis, and manuscript preparation. DS was co-PI of the overall clinical project, and shares senior authorship with RH. BMR, MR, and AD participated in study design, experimental control software, data collection (at WFSM), analysis, and manuscript preparation. BMR, XS, BM, and DS participated in data collection at KHUSC and RLANRH. XS, BR, BM, VM, TB, and DS participated in MIMO and MDM model development. DC, AL, BL, and CL provided IRB and study design, performed neurosurgical procedures at their respective institutions. GP, HMC, MS, CH, GN, SS, and HG provided IRB & study design, diagnostic, patient monitoring, supervised data collection, and neurological care for the subjects at their respective institutions. VM, TB, DS, SD, and RH participated in project management and study design. TB and DS were subcontract PIs for USC; SD was originating PI (now emeritus) for the study. Portions of this work appeared in BR's Ph.D. dissertation. All authors agree to be accountable for the content of this work.

FUNDING

This research was supported by DARPA Restoring Active Memory, contract #N66001-14-C-4016, the Wake Forest Clinical and Translational Sciences Institute (NIH CTSA UL1TR001420) COVID-19 Assistance grant, and intramural institutional funding.

ACKNOWLEDGMENTS

The authors acknowledge the incredible assistance and participation of the Epilepsy Monitoring Units and comprehensive epilepsy programs at Wake Forest School of Medicine/Atrium Health Wake Forest Baptist (AHWFB), Keck Hospital of the University of Southern California (KHUSC), and Rancho Los Amigos National Rehabilitation Hospital (RLANRH). We could not have done this work without the team of neurologists, neurosurgeons, nurses, and technicians of these units. We particularly thank Frances Miller, Christina Dyson, Joseph Noto, Valerie Woodard, Wendy Jenkins, Cassandra Cornell, Melissa Brown, Jennifer Neville, and Angelica Nguyen. Portions of this work were performed as partial fulfilment of the requirement for Brent M. Roeder's doctorate. We also thank his committee members: Joost Maier, Christos Constantinidis, Mark Ferris, and Ken Kishida for helpful comments.

SUPPLEMENTARY MATERIAL

The Supplementary Material for this article can be found online at: https://www.frontiersin.org/articles/10.3389/fnhum.2022.933401/full#supplementary-material

REFERENCES

Aghajan, Z. M., Schuette, P., Fields, T. A., Tran, M. E., Siddiqui, S. M., Hasulak, N. R., et al. (2017). Theta Oscillations in the Human Medial Temporal Lobe during Real-World Ambulatory Movement. *Curr. Biol.* 27, 3743–3751.e3.

Berger, T. W., Ahuja, A., Courellis, S. H., Deadwyler, S. A., Erinjippurath, G., Gerhardt, G. A., et al. (2005). Restoring lost cognitive function. *IEEE Eng. Med. Biol. Mag.* 24, 30–44.

Berger, T. W., and Glanzman, D. L. (2005). *Toward Replacement Parts for the Brain*. Cambridge, MA: MIT Press.

Berger, T. W., Hampson, R. E., Song, D., Goonawardena, A., Marmarelis, V. Z., and Deadwyler, S. A. (2011). A cortical neural prosthesis for restoring and enhancing memory. *J. Neural Eng.* 8:046017.

Deadwyler, S. A., Berger, T. W., Sweatt, A. J., Song, D., Chan, R. H., Opris, I., et al. (2013). Donor/recipient enhancement of memory in rat hippocampus. *Front. Syst. Neurosci.* 7:120. doi: 10.3389/fnsys.2013.00120

Deadwyler, S. A., Hampson, R. E., Song, D., Opris, I., Gerhardt, G. A., Marmarelis, V. Z., et al. (2017). A cognitive prosthesis for memory facilitation by closed-loop functional ensemble stimulation of hippocampal neurons in primate brain. *Exp. Neurol.* 287, 452–460. doi: 10.1016/j.expneurol.2016.05.031

Ezzyat, Y., Wanda, P. A., Levy, D. F., Kadel, A., Aka, A., Pedisich, I., et al. (2018). Closed-loop stimulation of temporal cortex rescues functional networks and improves memory. *Nat. Commun.* 9:365. doi: 10.1038/s41467-017-02753-0

Gondard, E., Teves, L., Wang, L., McKinnon, C., Hamani, C., Kalia, S. K., et al. (2019). Deep Brain Stimulation Rescues Memory and Synaptic Activity in

a Rat Model of Global Ischemia. *J. Neurosci.* 39, 2430–2440. doi: 10.1523/JNEUROSCI.1222-18.2019

Goyal, A., Miller, J., Watrous, A. J., Lee, S. A., Coffey, T., Sperling, M. R., et al. (2018). Electrical Stimulation in Hippocampus and Entorhinal Cortex Impairs Spatial and Temporal Memory. *J. Neurosci.* 38, 4471–4481.

Hampson, R. E., Pons, T. P., Stanford, T. R., and Deadwyler, S. A. (2004). Categorization in the monkey hippocampus: a possible mechanism for encoding information into memory. *Proc. Natl. Acad. Sci. U. S. A.* 101, 3184–3189.

Hampson, R. E., Roeder, B. M., Dakos, A. S., She, X., Moore, B., Song, D., et al. (2019). Decoding memory - Memory facilitation of category information for up to 75 minutes using hippocampal stimulation via a memory decoding model. *Soc. Neurosci. Abstr.* 2019:698.604.

Hampson, R. E., Roeder, B. M., Johnson, C. A., Dakos, A. S., She, X., Song, D., et al. (2018a). Facilitating memory: individualized prosthetic stimulation for memory categories. *Soc. Neurosci. Abstr.* 2018:335.326.

Hampson, R. E., Simeral, J. D., and Deadwyler, S. A. (1999). Distribution of Spatial and Nonspatial Information in Dorsal Hippocampus. *Nature* 402, 610–614.

Hampson, R. E., Simeral, J. D., and Deadwyler, S. A. (2005). "Cognitive processes in replacement brain parts: A code for all reasons," in *Toward Replacement Parts for the Brain. Implantable Biomimetic Electronics as Neural Prosthesis*, eds T. W. Berger and D. L. Glanzman (Cambridge, MA: MIT Press), 111–128.

Hampson, R. E., Song, D., Opris, I., Santos, L. M., Shin, D. C., Gerhardt, G. A., et al. (2013). Facilitation of memory encoding in primate hippocampus by a neuroprosthesis that promotes task-specific neural firing. *J. Neural. Eng.* 10:066013. doi: 10.1088/1741-2560/10/6/066013

Hampson, R. E., Song, D., Robinson, B. S., Fetterhoff, D., Dakos, A. S., Roeder, B. M., et al. (2018b). Developing a hippocampal neural prosthetic to facilitate human memory encoding and recall. *J. Neural. Eng.* 15:036014.

Jacobs, J., Miller, J., Lee, S. A., Coffey, T., Watrous, A. J., Sperling, M. R., et al. (2016). Direct Electrical Stimulation of the Human Entorhinal Region and Hippocampus Impairs Memory. *Neuron* 92, 983–990.

Jones, K. T., Johnson, E. L., and Berryhill, M. E. (2020). Frontoparietal theta-gamma interactions track working memory enhancement with training and tDCS. *Neuroimage* 211:116615. doi: 10.1016/j.neuroimage.2020.116615

Jun, S., Lee, S. A., Kim, J. S., Jeong, W., and Chung, C. K. (2020). Task-dependent effects of intracranial hippocampal stimulation on human memory and hippocampal theta power. *Brain Stimul.* 13, 603–613.

Karakas, S. (2020). A review of theta oscillation and its functional correlates. *Int. J. Psychophysiol.* 157, 82–99. doi: 10.1016/j.ijpsycho.2020.04.008

Kota, S., Rugg, M. D., and Lega, B. C. (2020). Hippocampal Theta Oscillations Support Successful Associative Memory Formation. *J. Neurosci.* 40, 9507–9518. doi: 10.1523/jneurosci.0767-20.2020

Kragel, J. E., VanHaerents, S., Templer, J. W., Schuele, S., Rosenow, J. M., Nilakantan, A. S., et al. (2020). Hippocampal theta coordinates memory processing during visual exploration. *Elife* 9:e52108. doi: 10.7554/eLife.52108

Kucewicz, M. T., Berry, B. M., Kremen, V., Miller, L. R., Khadjevand, F., Ezzyat, Y., et al. (2018). Electrical Stimulation Modulates High γ Activity and Human Memory Performance. *eNeuro* 5:ENEURO.0369-17.2018. doi: 10.1523/eneuro.0369-17.2018

Larson, J., and Munkácsy, E. (2015). Theta-burst LTP. *Brain Res.* 1621, 38–50. doi: 10.1016/j.brainres.2014.10.034

Mankin, E. A., Aghajan, Z. M., Schuette, P., Tran, M. E., Tchemodanov, N., Titiz, A., et al. (2021). Stimulation of the right entorhinal white matter enhances visual memory encoding in humans. *Brain Stimul.* 14, 131–140. doi: 10.1016/j.brs.2020.11.015

Mankin, E. A., and Fried, I. (2020). Modulation of Human Memory by Deep Brain Stimulation of the Entorhinal-Hippocampal Circuitry. *Neuron* 106, 218–235. doi: 10.1016/j.neuron.2020.02.024

Marmarelis, V. Z., Shin, D. C., Song, D., Hampson, R. E., Deadwyler, S. A., and Berger, T. W. (2014). On parsing the neural code in the prefrontal cortex of primates using principal dynamic modes. *J. Comput. Neurosci.* 36, 321–337. doi: 10.1007/s10827-013-0475-3

Mohan, U. R., Watrous, A. J., Miller, J. F., Lega, B. C., Sperling, M. R., Worrell, G. A., et al. (2020). The effects of direct brain stimulation in humans depend on frequency, amplitude, and white-matter proximity. *Brain Stimul.* 13, 1183–1195. doi: 10.1016/j.brs.2020.05.009

Neter, J., and Wasserman, W. (1974). *Applied Linear Statistical Models*. Homewood, IL: Richard D. Irwin, Inc.

Nicolas, B., Sala-Padro, J., Cucurell, D., Santurino, M., Falip, M., and Fuentemilla, L. (2021). Theta rhythm supports hippocampus-dependent integrative encoding in schematic/semantic memory networks. *Neuroimage* 226:117558. doi: 10.1016/j.neuroimage.2020.117558

Opris, I., Santos, L. M., Gerhardt, G. A., Song, D., Berger, T. W., Hampson, R. E., et al. (2015). Distributed encoding of spatial and object categories in primate hippocampal microcircuits. *Front. Neurosci.* 9:317. doi: 10.3389/fnins.2015.00317

Reinhart, R. M. G., and Nguyen, J. A. (2019). Working memory revived in older adults by synchronizing rhythmic brain circuits. *Nat. Neurosci.* 22, 820–827. doi: 10.1038/s41593-019-0371-x

Roeder, B. M. (2021a). *Chapter 2: Developing a Hippocampal Neural Prosthetic to Facilitate Human Memory Encoding and Recall of Stimulus Features and Categories*. Ph.D.thesis. North Carolina: Wake Forest University Graduate School of Arts and Sciences.

Roeder, B. M. (2021b). *Chapter 3: Shared Memory Codes for Specific Information Content Across Subjects Facilitate Encoding and Recall of Stimulus Features and Categories*. Ph.D.thesis. North Carolina: Wake Forest University Graduate School of Arts and Sciences.

She, X., Berger, T. W., and Song, D. (2021). A Double-Layer Multi-Resolution Classification Model for Decoding Spatiotemporal Patterns of Spikes With Small Sample Size. *Neural. Comput.* 34, 219–254. doi: 10.1162/neco_a_01459

She, X., Robinson, B., Flynn, G., Berger, T. W., and Song, D. (2022). Accelerating input-output model estimation with parallel computing for testing hippocampal memory prostheses in human. *J. Neurosci. Methods* 370:109492. doi: 10.1016/j.jneumeth.2022.109492

Song, D., Chan, R. H., Marmarelis, V. Z., Hampson, R. E., Deadwyler, S. A., and Berger, T. W. (2009). Nonlinear modeling of neural population dynamics for hippocampal prostheses. *Neural. Netw.* 22, 1340–1351.

Song, D., Hampson, R. E., Robinson, B. S., Marmarelis, V. Z., Deadwyler, S. A., and Berger, T. W. (2016). Decoding memory features from hippocampal spiking activities using sparse classification models. *Conf. Proc. IEEE Eng. Med. Biol. Soc.* 2016, 1620–1623. doi: 10.1109/EMBC.2016.7591023

Song, D., Robinson, B. S., Hampson, R. E., Marmarelis, V. Z., Deadwyler, S. A., and Berger, T. W. (2018). Sparse Large-Scale Nonlinear Dynamical Modeling of Human Hippocampus for Memory Prostheses. *IEEE Trans. Neural. Syst. Rehabil. Eng.* 26, 272–280. doi: 10.1109/TNSRE.2016.2604423

Tambini, A., Nee, D. E., and D'Esposito, M. (2018). Hippocampal-targeted Theta-burst Stimulation Enhances Associative Memory Formation. *J. Cogn. Neurosci.* 30, 1452–1472. doi: 10.1162/jocn_a_01300

Titiz, A. S., Hill, M. R. H., Mankin, E. A., Aghajan, M. Z., Eliashiv, D., Tchemodanov, N., et al. (2017). Theta-burst microstimulation in the human entorhinal area improves memory specificity. *Elife* 6:e29515. doi: 10.7554/eLife.29515

Tsanov, M., and Manahan-Vaughan, D. (2009). Long-term plasticity is proportional to theta-activity. *PLoS One* 4:e5850. doi: 10.1371/journal.pone.0005850

Conflict of Interest: RH discloses a current consulting and advisory relationship with Braingrade, Inc., a component of Engram (Holding), Inc., a Delaware C-Corporation. This relationship was not in effect at the time of the study.

The remaining authors declare that the research was otherwise conducted in the absence of any other commercial or financial relationships that could be construed as a potential conflict of interest.

Publisher's Note: All claims expressed in this article are solely those of the authors and do not necessarily represent those of their affiliated organizations, or those of the publisher, the editors and the reviewers. Any product that may be evaluated in this article, or claim that may be made by its manufacturer, is not guaranteed or endorsed by the publisher.

frontiers | Frontiers in Human Neuroscience

TYPE Perspective
PUBLISHED 29 July 2022
DOI 10.3389/fnhum.2022.983226

OPEN ACCESS

EDITED BY
Michael S. Okun,
University of Florida, United States

REVIEWED BY
Jun Yu,
University of Florida, United States

*CORRESPONDENCE
Andreas Schönau
schoenau@uw.edu

SPECIALTY SECTION
This article was submitted to Brain Imaging and Stimulation, a section of the journal Frontiers in Human Neuroscience

RECEIVED 30 June 2022
ACCEPTED 15 July 2022
PUBLISHED 29 July 2022

CITATION
Schönau A, Goering S, Versalovic E, Montes N, Brown T, Dasgupta I and Klein E (2022) Asking questions that matter – Question prompt lists as tools for improving the consent process for neurotechnology clinical trials. *Front. Hum. Neurosci.* 16:983226. doi: 10.3389/fnhum.2022.983226

Asking questions that matter – Question prompt lists as tools for improving the consent process for neurotechnology clinical trials

Andreas Schönau[1]*, Sara Goering[1], Erika Versalovic[1], Natalia Montes[1], Tim Brown[1], Ishan Dasgupta[2] and Eran Klein[3]

[1]Department of Philosophy, University of Washington, Seattle, WA, United States, [2]Dana Foundation, New York, NY, United States, [3]Department of Neurology, Oregon Health & Science University, Portland, OR, United States

Implantable neurotechnology devices such as Brain Computer Interfaces (BCIs) and Deep Brain Stimulators (DBS) are an increasing part of treating or exploring potential treatments for neurological and psychiatric disorders. While only a few devices are approved, many promising prospects for future devices are under investigation. The decision to participate in a clinical trial can be challenging, given a variety of risks to be taken into consideration. During the consent process, prospective participants might lack the language to consider those risks, feel unprepared, or simply not know what questions to ask. One tool to help empower participants to play a more active role during the consent process is a Question Prompt List (QPL). QPLs are communication tools that can prompt participants and patients to articulate potential concerns. They offer a structured list of disease, treatment, or research intervention-specific questions that research participants can use as support for question asking. While QPLs have been studied as tools for improving the consent process during cancer treatment, in this paper, we suggest they would be helpful in neurotechnology research, and offer an example of a QPL as a template for an informed consent tool in neurotechnology device trials.

KEYWORDS

BCI (brain computer interface), DBS (deep brain stimulation), QPL (question prompt list), neurotechnology, participant perspective

Introduction

Implantable neurotechnology devices such as Brain Computer Interfaces (BCIs) and Deep Brain Stimulators (DBS) are an increasing part of treating or exploring potential treatments for neurological and psychiatric disorders. While only a few devices are approved, many promising prospects for future devices are under investigation.

The decision to participate in a clinical trial can be challenging. Among other things, potential participants face a variety of challenges, including surgical risks (Fenoy and Simpson, 2014) and uncertainty about post-trial care (Hendriks et al., 2019; Sankary et al., 2021).

Over the last 10 years, our group gained experience working with people with amyotrophic lateral sclerosis (ALS) (Versalovic et al., 2020; Versalovic and Klein, 2020), Parkinson's Disease (Wexler et al., 2022), essential tremor (Brown et al., 2016), and obsessive compulsive disorder (OCD)/depression (Klein et al., 2016). During this time, we have found that neurotechnology device trials raise a number of issues for informed consent that are not traditionally included in existing informed consent discussions or are not fully appreciated in the process. These include issues such as agential changes in the ethical dimensions of privacy, authenticity, responsibility, trust (Schönau et al., 2021), as well as relational effects (Goering et al., 2017). Quotes from two participants from our prior work illustrate the difficulty of understanding those and others challenges before entering the trial:

Participant A "I think I understood as much as I was going to understand without being a part of it. I tried to ask all the questions that I could, but I don't think anything prepares you... I don't think you can ask the right questions without being a part of it. I learned the science whilst I was a part of it."

Participant B "I probably would have wanted to talk to somebody that was already involved to see what their experience was like. But as it turned out, there's not that many people doing this."

When it comes to communicating the challenges of a neurotechnology study during the informed consent process, it is important to recognize that potential participants might not consider – or have the language to consider – potential issues prior to enrolling in a clinical trial. At the same time, researchers themselves may struggle to identify and talk about them. Participants' expectations of a research trial during the consent process might be very different from the actual experience they have while being in the research trial. In hindsight, they might feel unprepared or wish that certain insights of what it feels like to use a device would have been shared with them before enrollment. At the same time, there are only a few participants in studies that are usually small and spread across institutions, which makes it hard for them to share their experience with others. There is a risk that topics that might be important to future participants' informed decision-making are not being addressed. This is why it is crucial to have practices in place that allow potential participants to engage in a more active role during the consent process for enrolling in a clinical trial.

One tool to help empower participants to play this more active role is a Question Prompt List (QPL). QPLs are communication tools that help participants and patients to articulate difficult concerns within the informed consent process (Dimoska et al., 2008). They offer a structured list of disease, treatment, or research intervention-specific questions that patients or prospective research participants can use as prompts for question-asking during the informed consent process. While QPLs have been used and tested in cancer treatment and clinical trials, their potential benefit for patients and research participants using novel neural devices has not been explored.

In this brief perspective paper, we present QPLs as a promising informed consent tool in clinical trials for neural devices. In see section "current research on question prompt lists," we review recent research on QPLs. See section "the potential of question prompt lists in neurotechnology research" explores the potential of QPLs as an informed consent tool for non-standard issues in neurotechnological studies, specifically BCI and DBS studies. In see section "example of question prompt list tool for implanted neurotechnology studies," we offer an example of a QPL that could serve as a template for an informed consent tool in neurotechnology device trials.

Current research on question prompt lists

The process of making a decision for or against treatment of a disease or whether to enroll in a clinical study is a difficult one. The lack of clinical knowledge, individual hopes and fears, as well as the uncertain nature of the whole endeavor can make the process of coming to a decision burdensome. Before patients enroll in clinical studies, they engage with researchers (who may also be their clinicians) who explain and answer questions about the trial that they might enter. However, potential participants may not know what to ask or might lack the language for expressing emerging concerns.

Question prompt lists offer research intervention specific questions that can help participants to identify and talk about those concerns during the informed consent process. Over the last two decades, QPLs have primarily been studied as tools for improving the consent process during cancer treatment. QPLs have been found to increase the total number of questions asked (Butow et al., 1994; Brown et al., 1999, 2001; Clayton et al., 2003, 2007). Most patients describe QPLs as helpful and useful to help them ask more questions (McJannett et al., 2003; Langbecker et al., 2012), value them to gather new trial information (Brown et al., 2011a), and generally endorse their early implementation into the consent process of active cancer treatment (Sato et al., 2021). In relation to cancer research, QPLs have been shown to increase treatment-related knowledge and reduce patient's decisional conflict (Jayasekera et al., 2020). They allow the patient to play a more active role during the consent process

through creating an environment conducive to shared decision making (Hoffmann et al., 2014).

Such studies strongly indicate that QPLs hold promise for empowering participants in the consent process. Due to their capacity to model what can be asked, QPLs may allow participants to have a better understanding of what it is like to be treated, develop a set of reasonable expectations of their future role, and allow them to play an active role during the consent process.

The potential of question prompt lists in neurotechnology research

One field that is particularly promising for the employment of QPLs as a tool for clinical trials is the field of neurotechnology research. Agreeing to take on an implantable neural device (such as a BCI or DBS) is momentous, given the significance of the brain for our sense of self, identity and agency (Schönau et al., 2021). In addition, making an informed decision to participate in a clinical trial with an implantable neural device can be challenging due to the range of other considerations involved, such as surgical risks (Fenoy and Simpson, 2014), or uncertainties about post-trial care (Hendriks et al., 2019). Recently, there is increased academic awareness about the need for better informed consent to get at issues of exit from a research study (Lázaro-Muñoz et al., 2018; Sankary et al., 2021). While details about those issues might already be in current informed consent documents, they might not be well understood or appreciated by potential participants. Encouraging them to play a more active role by asking questions could make those discussions easier. QPLs could help to prompt prospective participants about issues in the informed consent document that were unclear or are in need of clarification.

Beyond those concerns that are mostly addressed during the informed consent process but might need a better approach to be fully understood, neurotechnology studies provide another layer of potential issues that are not traditionally included in standard informed consent discussions. Among others, worries that go beyond that scope involve several dimensions of agency that can be impacted when participants are using a neurotechnological device. In the neuroethical literature, agential disruptions end users might experience are discussed as issues of responsibility, privacy, authenticity, trust (Schönau et al., 2021) and as relational effects (Klein et al., 2016). Responsibility is discussed under the framing of the responsibility gap, i.e., the unclarity of who is responsible for the unintended outcome of a BCI mediated movement (see, among others Grübler, 2011; Kellmeyer et al., 2016; Steinert et al., 2018; Schönau, 2021). Privacy is discussed as protecting brain data from unwanted access and establishing and negotiating boundaries (see, among others, Allen, 2014; Pyrrho et al., 2022). Authenticity is discussed as the risk of unintended changes of the self through neurostimulation (see, among others, Schüpbach et al., 2006; Kraemer, 2013; Pugh et al., 2017; Gilbert and Viaña, 2018). Trust denotes the difficulty to gain ownership or a sense of embodiment over a neurotechnological device (see, among others, Heersmink, 2011; Collins et al., 2017; Tbalvandany et al., 2019). Those non-standard issues of neurotechnology trials are wide ranging and might vary widely across studies.

People who are considering enrolling in a research trial with a BCI or a DBS might be unaware of the debate over those ethical dimensions and the agential changes they might experience after the device is implanted. And yet, during the deliberation phase for or against trial participation, they are confronted with the difficult task of imagining what it is like to have a device implanted in their head and what it feels like to actually live and act with it. Due to the novelty of the study and the limitations regarding relevant personal experience, they might lack not only the knowledge but also the language for asking about issues that are related to potential changes in their agency before enrolling in the trial.

This knowledge gap could be diminished by offering a QPL as a tool for the potential participant to ask questions informed by changes and experiences others have reported before them. While a QPL is not on par with the experience of what it is like to participate in the actual study, it can help prospective participants to know what to ask when entering the study. A well implemented QPL has the potential to facilitate enrollment of better informed participants who are more motivated throughout the trial, feel confident about what lies ahead of them, and have a better understanding about what happens when the trial ends. As such, QPLs can function as tools that help participants to imagine themselves during those trials in a more robust way.

Example of question prompt list tool for implanted neurotechnology studies

In order to improve the consent process for people who consider enrolling in a BCI or DBS trial, we advocate for creating a QPL that encourages them to ask clarifying questions about risks introduced in the informed consent form as well as about non-standard ethical issues and experiences others might have reported while being in a similar clinical trial. As a starting point for discussion, we developed a preliminary QPL that can be used during the informed consent process of BCI/DBS trials. We directly modeled our pilot based on a QPL by Brown et al. (2011b) that has been used to improve the decision making process for enrolling in cancer clinical trials. We then modified that QPL based on qualitative interviews we conducted over

the last 10 years, attending to different kinds of experiences participants report having.

This set of questions is not intended to be settled or comprehensive, but should be taken as illustrative of the kind of tool researchers could develop for neural device trials. We kept the QPL general because relevant issues to consider might vary widely across studies. From this initial model, we aim to gather feedback from and encourage discussion with participants, researchers, and stakeholders to continue revising and refining this QPL template.

Question prompt list for person considering sensorimotor brain computer interface study participation

Understanding the study's purpose and background

1. What is the purpose of this study?
2. What is already known about the technology/device being used in this study?
3. How experienced are you and your team with this device? With running this kind of study?

Understanding the alternatives

4. What makes me eligible (or not) for this study?
5. Are there other studies that I am eligible for?
6. If I participate in this study, will I not be eligible for studies involving future (next generation) BCIs?
7. Is access to the device only available through joining the study?

Understanding the possible benefits

8. What benefits could I possibly get if I join the study?
9. If I join this study, how might others benefit?
10. Have others like me benefited from participating in similar studies? If so, how?

Understanding the possible risks and burdens

11. Are there any long-term or permanent side effects from the surgery or from using the technology/device?
12. Are there any serious or rare side effects that I should know about?
13. Who can I call if something goes wrong?
14. If I get a side effect or injury because of being in the study, will I get compensation?
15. Will I have control over who has access to brain data collected by the device?

Learning from the experiences of others

16. How do participants of this and similar studies describe the experience of using the device?
17. Have other participants described what it feels like to control or struggle to control devices using the BCI?
18. Have participants in such studies talked about feeling unlike themselves, or somehow less authentic? Has this affected how individuals view/understand themselves or are viewed by others?
19. Have other participants described how the study has affected their family members?
20. Have participants in this study (or similar ones) noted any new or surprising burdens or benefits? What are these?
21. Have other people in this study (or similar ones) felt that, on balance, their participation was worthwhile? What seemed to make it feel worthwhile?

Understanding how the study is being carried out

22. How will I use this device in this study?
23. How often will I need to come in for the study?
24. Do people in the study find the experiments interesting and/or fun, or are they sometimes a bit boring?
25. Who will I interact with as part of the study and how often? How have other participants described their relationship with the research team?
26. How long has the trial been going on? How many people have been enrolled and how many are you planning to enroll? Are there any concerns about the study so far?
27. Who will have access to my medical records? How will my confidentiality be protected?
28. If I enter the study, will it require me to have extra tests, to attend more clinics and will it cost me extra money? (extra parking, extra medication?)
29. What happens if I am unable to come to or complete a study visit on a particular day (too tired, unable to find transportation, etc.)?

Understanding what happens after the study ends

30. At the end of the study, can I have the implant removed from my brain? Can I leave it in? What are the risks to either choice?
31. If the technology/device is successful, will I have access to it after the study is finished?
32. If the technology is successful for me, but the study is discontinued will I have access to it after the study is finished?
33. How will the results of the study be used?

Will I have access to the results of the study? If so, how and in what form?

Understanding possible conflicts of interest

34. Are you in charge of the study (the principal investigator)? If not, what's your role in the study?
35. Who is funding the study? Who is providing the devices for the study?

36. Is there a payment by the technology company to the university/hospital or to you if I go on this study? Could you tell me how much money and is this usual? How is the money spent?

Understanding my right to join or not to join the study

37. Will I get treatment if I decide not to go into the study?

38. Do I have time to think about whether to join the study (a day or two, or a week)?

39. If I join the study, but later change my mind, how can I stop? Will I be penalized in any way?

40. Will participating in this study change my brain in ways that will prevent me or make me ineligible to participate in future studies or use future devices?

Concluding questions

41. Can I speak to someone who is already participating in this study or who has participated in a similar study in the past?

42. Are there other sources of information I can access? How can I learn more about the study? Who else could I speak with?

Your own questions: (Please write down any questions not listed).

Data availability statement

The original contributions presented in this study are included in the article/supplementary material, further inquiries can be directed to the corresponding author.

Ethics statement

The studies involving human participants were reviewed and approved by the University of Washington Human Subjects Division (HSD) who determined that the study qualifies for exempt status. The patients/participants provided their written informed consent to participate in this study.

Author contributions

AS: conceptualization, original draft, review, and editing. SG and EK: conceptualization, review, editing, and supervision. NM, TB, ID, and EV: conceptualization, review, and editing. All authors approved the submitted version.

Funding

This work was supported by the National Institutes of Health (MH117800-01) and National Science Foundation (EEC-1028725).

Conflict of interest

The authors declare that the research was conducted in the absence of any commercial or financial relationships that could be construed as a potential conflict of interest.

Publisher's note

All claims expressed in this article are solely those of the authors and do not necessarily represent those of their affiliated organizations, or those of the publisher, the editors and the reviewers. Any product that may be evaluated in this article, or claim that may be made by its manufacturer, is not guaranteed or endorsed by the publisher.

References

Allen, A. (2014). "Privacy in health care," in *Encyclopedia Of Bioethics*, ed. J. Bruce (New York, NY: MacMillan Reference Books).

Brown, R. F., Butow, P. N., Dunn, S. M., and Tattersall, M. H. N. (2001). Promoting patient participation and shortening cancer consultations: a randomized trial. *Br. J. Cancer* 85, 1273–1279. doi: 10.1054/bjoc.2001.2073

Brown, R. F., Shuk, E., Butow, P., Edgerson, S., Tattersall, M. H. N., and Ostroff, J. S. (2011a). Identifying patient information needs about cancer clinical trials using a question prompt list. *Patient Educ. Couns.* 84, 69–77. doi: 10.1016/j.pec.2010.07.005

Brown, R. F., Shuk, E., Leighl, N., Butow, P., Ostroff, J., Edgerson, S., et al. (2011b). Enhancing decision making about participation in cancer clinical trials: development of a question prompt list. *Support. Care Cancer* 19, 1227–1238. doi: 10.1007/s00520-010-0942-6

Brown, R., Butow, P. N., Boyer, M. J., and Tattersall, M. H. N. (1999). Promoting patient participation in the cancer consultation: evaluation of a prompt sheet and coaching in question-asking. *Br. J. Cancer* 80, 242–248. doi: 10.1038/sj.bjc.6690346

Brown, T., Thompson, M. C., Herron, J., Ko, A., Chizeck, H., and Goering, S. (2016). Controlling our brains – a case study on the implications of brain-computer interface-triggered deep brain stimulation for essential tremor. *Brain Comput. Interfaces* 3, 165–170. doi: 10.1080/2326263X.2016.1207494

Butow, P. N., Dunn, S. M., Tattersall, M. H. N., and Jones, Q. J. (1994). Patient participation in the cancer consultation: evaluation of a question prompt sheet. *Ann. Oncol.* 5, 199–204. doi: 10.1093/oxfordjournals.annonc.a058793

Clayton, J. M., Butow, P. N., Tattersall, M. H. N., Devine, R. J., Simpson, J. M., Aggarwal, G., et al. (2007). Randomized controlled trial of a prompt list to help advanced cancer patients and their caregivers to ask questions about prognosis and end-of-life care. *J. Clin. Oncol.* 25, 715–723. doi: 10.1200/JCO.2006.06.7827

Clayton, J., Butow, P., Tattersall, M., Chye, R., Noel, M., Davis, J. M., et al. (2003). Asking questions can help: development and preliminary evaluation of

a question prompt list for palliative care patients. *Br. J. Cancer* 89, 2069–2077. doi: 10.1038/sj.bjc.6601380

Collins, K. L., Guterstam, A., Cronin, J., Olson, J. D., Ehrsson, H. H., and Ojemann, J. G. (2017). Ownership of an artificial limb induced by electrical brain stimulation. *Proc. Natl. Acad. Sci. U.S.A.* 114, 166–171. doi: 10.1073/pnas.1616305114

Dimoska, A., Tattersall, M. H. N., Butow, P. N., Shepherd, H., and Kinnersley, P. (2008). Can a "prompt list" empower cancer patients to ask relevant questions? *Cancer* 113, 225–237. doi: 10.1002/cncr.23543

Fenoy, A. J., and Simpson, R. K. (2014). Risks of common complications in deep brain stimulation surgery: management and avoidance: clinical article. *J. Neurosurg.* 120, 132–139. doi: /10.3171/2013.10.JNS131225

Gilbert, F., and Viaña, J. N. M. (2018). A personal narrative on living and dealing with psychiatric symptoms after DBS surgery. *Narrat. Inq. Bioeth.* 8, 67–77. doi: 10.1353/nib.2018.0024

Goering, S., Klein, E., Dougherty, D. D., and Widge, A. S. (2017). Staying in the loop: relational agency and identity in next-generation dbs for psychiatry. *AJOB Neurosci.* 8, 59–70. doi: 10.1080/21507740.2017.1320320

Grübler, G. (2011). Beyond the responsibility gap. Discussion note on responsibility and liability in the use of brain-computer interfaces. *AI Soc.* 26, 377–382. doi: 10.1007/s00146-011-0321-y

Heersmink, R. (2011). "Epistemological and phenomenological issues in the use of brain-computer interfaces," in *Proceedings of the IACAP 2011: First International Conference of IACAP : The computational Turn : Past, Presents, Futures?*, Münster. 87–90.

Hendriks, S., Grady, C., Ramos, K. M., Chiong, W., Fins, J. J., Ford, P., et al. (2019). Ethical challenges of risk, informed consent, and posttrial responsibilities in human research with neural devices: a review. *JAMA Neurol.* 76:1506. doi: 10.1001/jamaneurol.2019.3523

Hoffmann, T. C., Légaré, F., Simmons, M. B., McNamara, K., McCaffery, K., Trevena, L. J., et al. (2014). Shared decision making: what do clinicians need to know and why should they bother? *Med. J. Aust.* 201, 35–39. doi: 10.5694/mja14.00002

Jayasekera, J., Vadaparampil, S. T., Eggly, S., Street, R. L., Foster Moore, T., Isaacs, C., et al. (2020). Question prompt list to support patient-provider communication in the use of the 21-gene recurrence test: feasibility, acceptability, and outcomes. *JCO Oncol. Pract.* 16, e1085–e1097. doi: 10.1200/JOP.19.00661

Kellmeyer, P., Cochrane, T., Müller, O., Mitchell, C., Ball, T., Fins, J. J., et al. (2016). The effects of closed-loop medical devices on the autonomy and accountability of persons and systems. *Camb. Q. Healthc. Ethics* 25, 623–633.

Klein, E., Goering, S., Gagne, J., Shea, C. V., Franklin, R., Zorowitz, S., et al. (2016). Brain-computer interface-based control of closed-loop brain stimulation: attitudes and ethical considerations. *Brain Comput. Interfaces* 3, 140–148.

Kraemer, F. (2013). Me, myself and my brain implant: deep brain stimulation raises questions of personal authenticity and alienation. *Neuroethics* 6, 483–497. doi: 10.1007/s12152-011-9115-7

Langbecker, D., Janda, M., and Yates, P. (2012). Development and piloting of a brain tumour-specific question prompt list: questions to ask for people with brain tumours. *Eur. J. Cancer Care* 21, 517–526. doi: 10.1111/j.1365-2354.2012.01328.x

Lázaro-Muñoz, G., Yoshor, D., Beauchamp, M. S., Goodman, W. K., and McGuire, A. L. (2018). Continued access to investigational brain implants. *Nat. Rev. Neurosci.* 19, 317–318. doi: 10.1038/s41583-018-0004-5

McJannett, M., Butow, P., Tattersall, M., and Thompson, J. F. (2003). Asking questions can help: development of a question prompt list for cancer patients seeing a surgeon. *Eur. J. Cancer Prevent.* 12, 397–405. doi: 10.1097/00008469-200310000-00009

Pugh, J., Maslen, H., and Savulescu, J. (2017). Deep brain stimulation, authenticity and value. *Camb. Q. Healthc. Ethics* 26, 640–657.

Pyrrho, M., Cambraia, L., and de Vasconcelos, V. F. (2022). Privacy and health practices in the digital age. *Am. J. Bioeth.* 22, 50–59.

Sankary, L. R., Zelinsky, M., Machado, A., Rush, T., White, A., and Ford, P. J. (2021). Exit from brain device research: a modified grounded theory study of researcher obligations and participant experiences. *AJOB Neurosci.* 1–12. doi: 10.1080/21507740.2021.1938293 [Epub ahead of print].

Sato, A., Fujimori, M., Shirai, Y., Umezawa, S., Mori, M., Jinno, S., et al. (2021). Assessing the need for a question prompt list that encourages end-of-life discussions between patients with advanced cancer and their physicians: a focus group interview study. *Palliat. Support. Care* 1–6. doi: 10.1017/S1478951522000153

Schönau, A. (2021). The spectrum of responsibility ascription for end users of neurotechnologies. *Neuroethics* 14, 423–435. doi: 10.1007/s12152-021-09460-0

Schönau, A., Dasgupta, I., Brown, T., Versalovic, E., Klein, E., and Goering, S. (2021). Mapping the dimensions of agency. *AJOB Neurosci.* 12, 172–186.

Schüpbach, M., Gargiulo, M., Welter, M. L., Mallet, L., Behar, C., Houeto, J. L., et al. (2006). Neurosurgery in parkinson disease a distressed mind in a repaired body? *Neurology* 66, 1811–1816.

Steinert, S., Bublitz, C., Jox, R., and Friedrich, O. (2018). doing things with thoughts: brain-computer interfaces and disembodied agency. *Philos. Technol.* 32, 457–482.

Tbalvandany, S. S., Harhangi, B. S., Prins, A. W., and Schermer, M. H. N. (2019). Embodiment in neuro-engineering endeavors: phenomenological considerations and practical implications. *Neuroethics* 12, 231–242.

Versalovic, E., and Klein, E. (2020). "Who will i be?": relational identity, living with amyotrophic lateral sclerosis, and future-oriented decisionmaking. *Camb. Q. Healthc. Ethics* 29, 617–629. doi: 10.1017/S0963180120000365

Versalovic, E., Diamond, M., and Klein, E. (2020). "Re-identifying yourself": a qualitative study of veteran views on implantable BCI for mobility and communication in ALS. *Disabil. Rehabil.* 1–8. doi: 10.1080/17483107.2020.1817991

Wexler, A., Choi, R. J., Ramayya, A. G., Sharma, N., McShane, B. J., Buch, L. Y., et al. (2022). Ethical issues in intraoperative neuroscience research: assessing subjects' recall of informed consent and motivations for participation. *AJOB Empir. Bioeth.* 13, 57–66. doi: 10.1080/23294515.2021.1941415

frontiers | Frontiers in Human Neuroscience

TYPE Brief Research Report
PUBLISHED 03 August 2022
DOI 10.3389/fnhum.2022.958703

OPEN ACCESS

EDITED BY
Michael S Okun,
University of Florida, United States

REVIEWED BY
Leonardo Almeida,
University of Florida, United States
Alessandro Stefani,
University of Rome Tor Vergata, Italy
Jun Yu,
University of Florida, United States

*CORRESPONDENCE
Harrison C. Walker
hcwalker@uabmc.edu

†These authors have contributed equally to this work and share first authorship

SPECIALTY SECTION
This article was submitted to Brain Imaging and Stimulation, a section of the journal Frontiers in Human Neuroscience

RECEIVED 31 May 2022
ACCEPTED 27 June 2022
PUBLISHED 03 August 2022

CITATION
Olson JW, Gonzalez CL, Brinkerhoff S, Boolos M, Wade MH, Hurt CP, Nakhmani A, Guthrie BL and Walker HC (2022) Local anatomy, stimulation site, and time alter directional deep brain stimulation impedances. *Front. Hum. Neurosci.* 16:958703. doi: 10.3389/fnhum.2022.958703

Local anatomy, stimulation site, and time alter directional deep brain stimulation impedances

Joseph W. Olson[1†], Christopher L. Gonzalez[1†], Sarah Brinkerhoff[1], Maria Boolos[2], Melissa H. Wade[1], Christopher P. Hurt[3], Arie Nakhmani[4], Bart L. Guthrie[5] and Harrison C. Walker[1*]

[1]Department of Neurology, The University of Alabama at Birmingham, Birmingham, AL, United States, [2]Brainlab, Inc., Westchester, IL, United States, [3]Department of Physical Therapy, The University of Alabama at Birmingham, Birmingham, AL, United States, [4]Department of Electrical Engineering, The University of Alabama at Birmingham, Birmingham, AL, United States, [5]Department of Neurosurgery, The University of Alabama at Birmingham, Birmingham, AL, United States

Directional deep brain stimulation (DBS) contacts provide greater spatial flexibility for therapy than traditional ring-shaped electrodes, but little is known about longitudinal changes of impedance and orientation. We measured monopolar and bipolar impedance of DBS contacts in 31 patients who underwent unilateral subthalamic nucleus deep brain stimulation as part of a randomized study (SUNDIAL, NCT03353688). At different follow-up visits, patients were assigned new stimulation configurations and impedance was measured. Additionally, we measured the orientation of the directional lead during surgery, immediately after surgery, and 1 year later. Here we contrast impedances in directional versus ring contacts with respect to local anatomy, active stimulation contact(s), and over time. Directional contacts display larger impedances than ring contacts. Impedances generally increase slightly over the first year of therapy, save for a transient decrease immediately post-surgery under general anesthesia during pulse generator placement. Local impedances decrease at active stimulation sites, and contacts in closest proximity to internal capsule display higher impedances than other anatomic sites. DBS leads rotate slightly in the immediate postoperative period (typically less than the angle of a single contact) but otherwise remain stable over the following year. These data provide useful information for setting clinical stimulation parameters over time.

KEYWORDS

Parkinson, deep brain stimualtion, impedance, directional DBS, orientation, subthalamic nucleus, anatomical localization, Brainlab

Introduction

Deep brain stimulation (DBS) is a remarkable therapy for neurological disorders, but the complexity of therapy is increasing with new device technologies such as directional leads. Implantable electrical stimulation represents a complementary tool to pharmaceutical treatments—very localized interaction with neural elements *via* a

surgically implanted electrode array. Tissue impedance is a key property of electrode contacts on the implanted array, as it confirms electrical integrity of the system and impacts stimulation parameters that are required for effective therapy. Impedance is effectively the resistance within a given tissue medium and is fundamentally related to both the voltage and amount of current that can be delivered through the circuit.

Device technologies increasingly utilize more complex lead designs with greater numbers of contacts, directional selectivity, and considerations for sensing with future adaptive stimulation devices. Many currently commercially available devices now consist of electrode arrays far larger in length than the span of target brain structures leaving electrodes in adjacent brain structures. While electrodes outside target structures may or may not be used for therapy chronically, previous investigations have found impedances to vary by brain structure and over time with gradual decreases in electrode impedances over relatively long time intervals (Satzer et al., 2014, 2015, 2020; Wong et al., 2018). Electrode impedance should vary significantly among different anatomic sites since gray matter conducts electricity better than white matter (Laitinen et al., 1966; Latikka et al., 2001; Satzer et al., 2015). However, one group has measured higher impedance in gray compared to white matter (Satzer et al., 2015). The surface area of both the DBS contact(s) and the implanted pulse generator (IPG) contribute to the measured impedance, as well (Butson et al., 2006). Finally, prior work contrasting impedances of active versus unused electrode contacts showed trends toward lower impedances for contacts being used to deliver therapy (Hemm et al., 2004; Sillay et al., 2010).

Here we investigate both anatomic and longitudinal effects on the impedance of directional leads in the subthalamic nucleus (STN) region during the first year of therapy following DBS surgery for Parkinson's disease. To determine anatomical properties of the leads, we localize the contacts in anatomical regions, and compare lead orientations during surgery, immediately after surgery, and one year later to measure potential directional rotation over time. We test four interrelated hypotheses. First, we hypothesize that directional contacts display higher impedance than ring contacts. Second, we hypothesize that impedances decrease over time. Third, we hypothesize that active stimulation decreases local tissue impedance. Lastly, we hypothesize that higher impedances are associated with closer proximity to white matter (internal capsule) compared to gray matter tissue.

Methods

Participants were recruited as part of the SUNDIAL (SUbthalamic Nucleus DIrectionAL stimulation) study, a randomized, double-blind crossover study contrasting directional versus ring unilateral STN DBS for PD. Participants signed written consent prior to participation, and the STN target was recommended for routine care prior to recruitment for entry. Each participant was implanted unilaterally in the most severely affected brain hemisphere with Boston Scientific's Vercise^{TM} Cartesia 8-contact directional lead and Vercise^{TM} PC IPG as part of the study under FDA Investigational Device Exemption G-170063. Surgical targeting was refined with awake multi-pass microelectrode recordings, macrostimulation, intraoperative imaging, and macrostimulation with the newly implanted DBS lead, as described previously (Bour et al., 2010). Based upon the final microelectrode recording trajectory, we set lead depth such that the dorsal STN border corresponded to the midpoint between the ventral and dorsal directional DBS rows (i.e., rows 2 and 3).

We measured lead positioning by co-registering pre-operative MAGNETOM Prisma MRI scans (Siemens Medical Solutions USA, Inc.) with intra-operative O-arm 2 CT (Medtronic, Inc.) and post-operative high-resolution CT (Koninklijke Philips N.V.) images in Brainlab (Munich, Germany). Brainlab software detects lead position and directional orientation and parcellates subcortical brain regions. Based upon CT artifact alone, lead orientation cannot be distinguished from the opposite orientation (180°). Following the approach of prior studies (Hellerbach et al., 2018; Dembek et al., 2019, 2021), we assumed the correct solution was the orientation closest to 0° (anterior facing), as intended by the implanting surgeon. However, one intra-op orientation of -85° was changed to +95°, which seemed more likely given that the subsequent post-op orientation measured +60°. A subset of participants elected to undergo staged DBS on the opposite side of the brain following their 12-month study exit visit. In these participants, additional CT images were obtained as part of routine care and exploited to remeasure lead orientation of the original DBS lead at longer follow-up intervals.

Standard triangular language (STL) files for each contact and anatomical region were exported from Brainlab. We loaded the STL files into MATLAB R2020a (MathWorks, Natick, MA, United States) to create 3D alpha shapes for each object (MATLAB functions "createpde," "importGeometry," "generateMesh," "alphaShape") (**Figure 2A**). We computed the percent of each contact's volume inside each brain region of interest (MATLAB functions "inShape," "volume"), and assigned each contact to the region with its most overlap. The regions of interest were subthalamic nucleus (STN), zona incerta (ZI), internal capsule (IC), thalamus (Th), and substantia nigra (SN). The percent volume of a bipolar pair of directional contacts in each region was computed as the average percent volume of the two contacts.

Electrode impedance (Ohms W) was measured for all DBS contacts during at least seven longitudinal encounters: stage 1 surgery after lead placement in the brain and prior to testing for efficacy, stage 2 surgery after implant of the extension wire and lead connection to the IPG, device activation

approximately 1 month after implant, and at 2-, 4-, 6- and 12-months study visits post activation. Boston Scientific's external trial stimulator and clinician programmer were used for all impedance measures. Only monopolar impedances were recorded during battery placement; otherwise monopolar and bipolar impedances were measured together. All measurements during DBS programming visits were performed prior to changes in DBS settings.

Statistical analysis

Paired *t*-tests contrasted directional lead orientations at different time points. Linear mixed models (LMMs) tested four hypotheses regarding monopolar and bipolar contact impedance, using the "lme4" package in R Studio (Bates et al., 2015; R Core Team, 2020; R Studio Team, 2021). We utilized impedance as the dependent variable and included a random intercept by participant in all LMMs. First, to test whether directional and ring contacts had different impedances, post-operative monopolar impedances were pooled across visits, and we utilized contact geometry as a fixed effect (directional versus ring). Second, to test if monopolar impedances changed over time, we modeled directional and ring contacts separately with time as a fixed effect, using stage 1 surgery (lead placement) as the reference category. Third, to test the effects of time and active stimulation contact(s) on impedance we estimated models separately for monopolar and bipolar contacts that included a fixed interaction between time (days) and whether a contact was active or inactive. These analyses begin at the time of device activation and continue throughout subsequent study visits. Fourth, to estimate whether local anatomic tissue composition modifies impedance, we estimated the bipolar impedance of directional contacts (pooled across 1-, 2-, 4-, 6-, 12- month post-operative visits) using the percent volume of each contact pair in each region as fixed effects. We estimated the effect of local tissue with the bipolar impedances opposed to monopolar impedances since they provide a more local measurement.

Results

Lead orientation and localization

Deep brain stimulation lead orientations in intra-operative and post-operative CT scans were measured at 2.7° ± 37.2° (n = 23) and −16.5° ± 43.2° (n = 27) respectively, where 0° is the anterior direction based on the midsagittal plane and positive/negative angles are degrees lateral right/left rotation (**Figure 1**). The change in orientation from intra-operative scan to post-operative scan is statistically significant (−20.5° [CI: −36.3°, −4.8°], p = 0.013, paired t-test, n = 19) but considerably smaller than the total angular extent of a single directional contact (90°). A subset of participants (n = 7) underwent staged surgery on the opposite side of the brain after study exit which allowed assessment of potential changes in DBS orientation over longer time intervals. Orientation did not change significantly at these later time points versus the first postoperative scan (−1.5° [CI: −7.7°, 4.7°], p = 0.578, paired t-test). Based on the majority anatomic constituency per contact, most directional contacts localized to either STN (36.3%) or ZI (27.4%), however the location/composition of the more distant ring contacts were more variable (**Figure 2B** and **Supplementary Figure 1**).

Impedance

We report four main results regarding impedance. First, directional contacts displayed significantly higher impedances than ring contacts, pooled across post-operative visits (2,559 and 1,242 W, respectively, $p < 0.001$, n = 32) (**Figure 3A**). Second, both ring and directional contacts had significantly lower impedances during stage 2 surgery (battery placement) than during stage 1 surgery (both $p < 0.001$, n = 32) (**Figures 3B,C**). However, impedances increased starting at 1-month versus stage 1 surgery for directional contacts ($p < 0.001$ for 1-, 2-, 4-, 6-, and 12-month follow-up visit each, n = 32, **Figure 3C**) and at 4-month for ring contacts (p = 0.004, $p < 0.001$, p = 0.001, at 4-, 6-, and 12-month follow-up, respectively, n = 32, **Figure 3B**).

Third, active stimulation decreased both monopolar and bipolar impedances by 2.4 and 2.1 W/day respectively (both $p < 0.001$, n = 28, **Figure 4**). Conversely, inactive contacts displayed modest increases in both monopolar and bipolar impedances by 1.0 and 1.5 W/day, respectively over the 1-year follow-up interval (both $p < 0.001$, n = 28, **Figure 4**). The distance between bipolar pairs did not affect the change in impedance within a pair over time (p = 0.241, n = 28).

Finally, the local anatomic composition of a given pair of directional contacts significantly altered the measured impedance, such that for every 1% by volume of a bipolar pairing within internal capsule, the impedance increased by 4.2 W (p = 0.023, n = 27). In contrast, non-capsular structures such as STN, ZI, Th, or SN did not alter tissue impedance at our level of statistical power. As expected, distance between bipolar pairs increased impedance as well, such that every 1 mm increase in the distance between contacts increased impedance by 369.6 W ($p < 0.001$, n = 27).

Discussion

While DBS lead orientations during surgery predominantly face anteriorly, a few leads displayed greater deviations than 60° rotation from the midline (17%), which is slightly higher than the 11% found in Dembek et al. (2019) Some additional rotation appears to be incurred between implant and immediately after

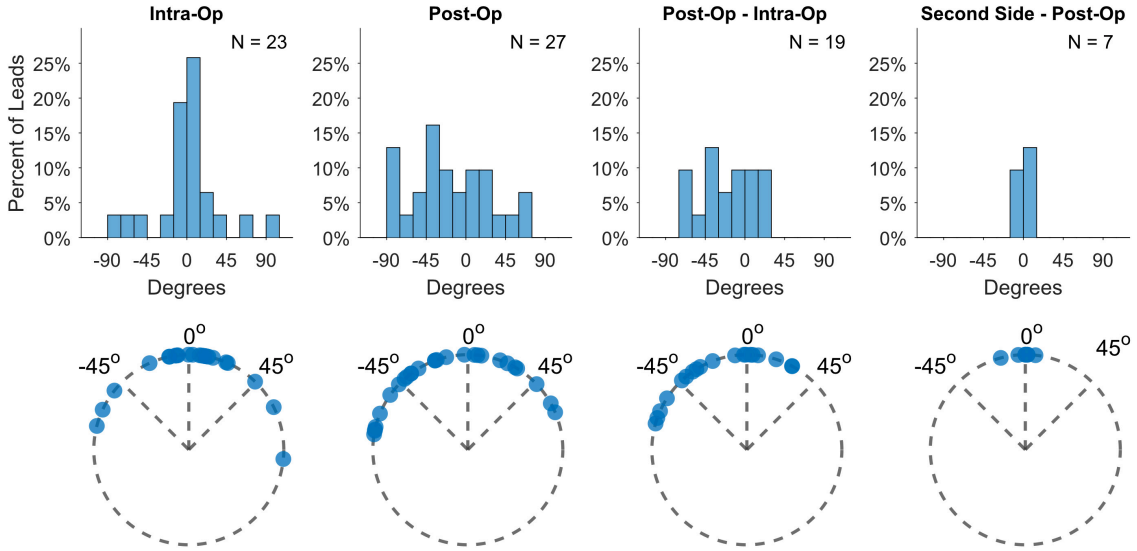

FIGURE 1
Lead orientation estimates during lead placement (intra-op) and immediately after surgery (post-op), as well as their differences and the differences from post-op to estimates derived from second-side surgery more than a year later.

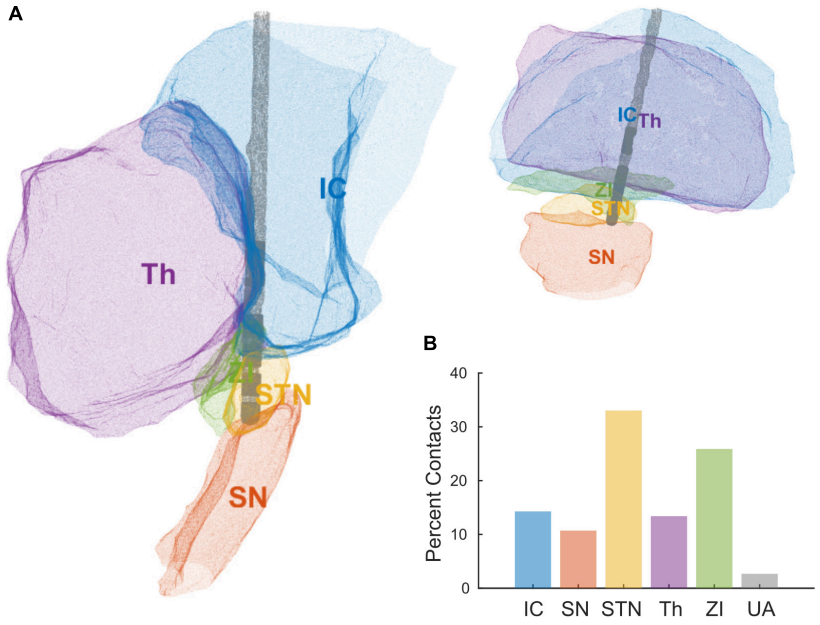

FIGURE 2
(A) Reconstruction of a single patient's DBS lead and local anatomical regions using STL files exported from Brainlab. **(B)** Percent of contacts' anatomical assignments, across all the patients, using the area of most overlap with a given a contact. Areas include internal capsule (IC), substantia nigra (SN), subthalamic nucleus (STN), thalamus (Th), zona incerta (ZI), and unaccounted (UA).

surgery, probably related to lead fixation as one study found no additional rotation from the orientation measured from X-rays immediately after lead fixation [cite Kruger]. Interestingly, we measured a left bias for lead rotation during this time, despite the push-button design of lead fixation device. Unintended residual torque might be transmitted to the lead based upon the handedness of the surgeon or other factors. Nevertheless, the total rotation magnitude is usually relatively small and only rarely was the degree of rotation larger than the width of an entire directional contact. We measured no further rotation when scans were available more than a year later, consistent with a few studies which have used various methods for measuring

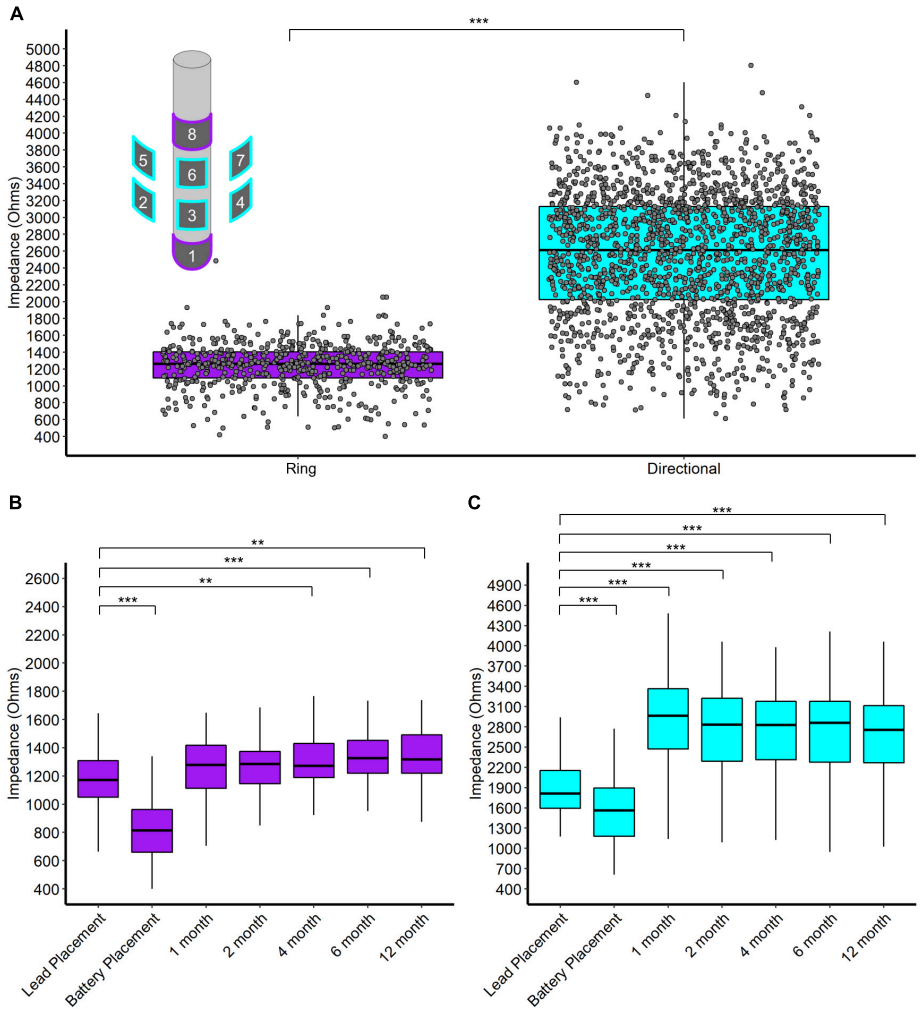

FIGURE 3
(A) Scatter and box plot of all monopolar impedance measurements (across patients, contacts, and visits) separated by ring and directional leads. Upper left contains a schema of the directional DBS lead. **(B)** Box plots of monopolar impedance for ring contacts across visits. **(C)** Box plots of monopolar impedance for directional contacts across visits. *$p < 0.05$, **$p < 0.01$, and ***$p < 0.001$.

orientation (Krüger et al., 2021; Lange et al., 2021) (**Figure 1**; Dembek et al., 2021).

Anatomic delineation of the local tissue environment in Brain lab and other related platforms appears to be useful in that DBS contacts can be linked more explicitly to local anatomy, without reliance on the ACPC coordinate system (**Figure 2**). These methods may prove useful for combining datasets across institutions in the future. Regardless, ACPC coordinates can be overlayed on the STL reconstructions if desired. This process is largely automated and provides greater anatomic specificity to guide targeting, postoperative programming, and analysis of intracranial electrophysiological signals. Of some interest, we measured greater tissue impedances in contacts most closely adjacent to the white matter of the internal capsule. Speculatively, the gradient of impedances within or across implant trajectories in an individual might be used as proxy for anatomic proximity to the internal capsule, a structure that can cause unwanted side effects in postoperative programming at the STN target in particular (Krack et al., 2002).

Directional DBS contacts showed higher impedances than ring contacts. The surface area of a directional contact is 1/4 of a ring contact's surface area so we naïvely expected directional contacts to have 4 times the impedance of ring contacts. However, we observe that directional contacts have about twice the impedance of ring contacts on average (**Figure 3**). Likely, local tissue properties contribute further differences since directional contacts are more likely to be located in the STN/ZI area. Interestingly, impedances decreased at the time of battery placement but then trended higher during the first year after surgery, somewhat contrary to our initial expectations. The initial decrease in impedance might relate to temporary edema or effects of general anesthesia, while later increases over the

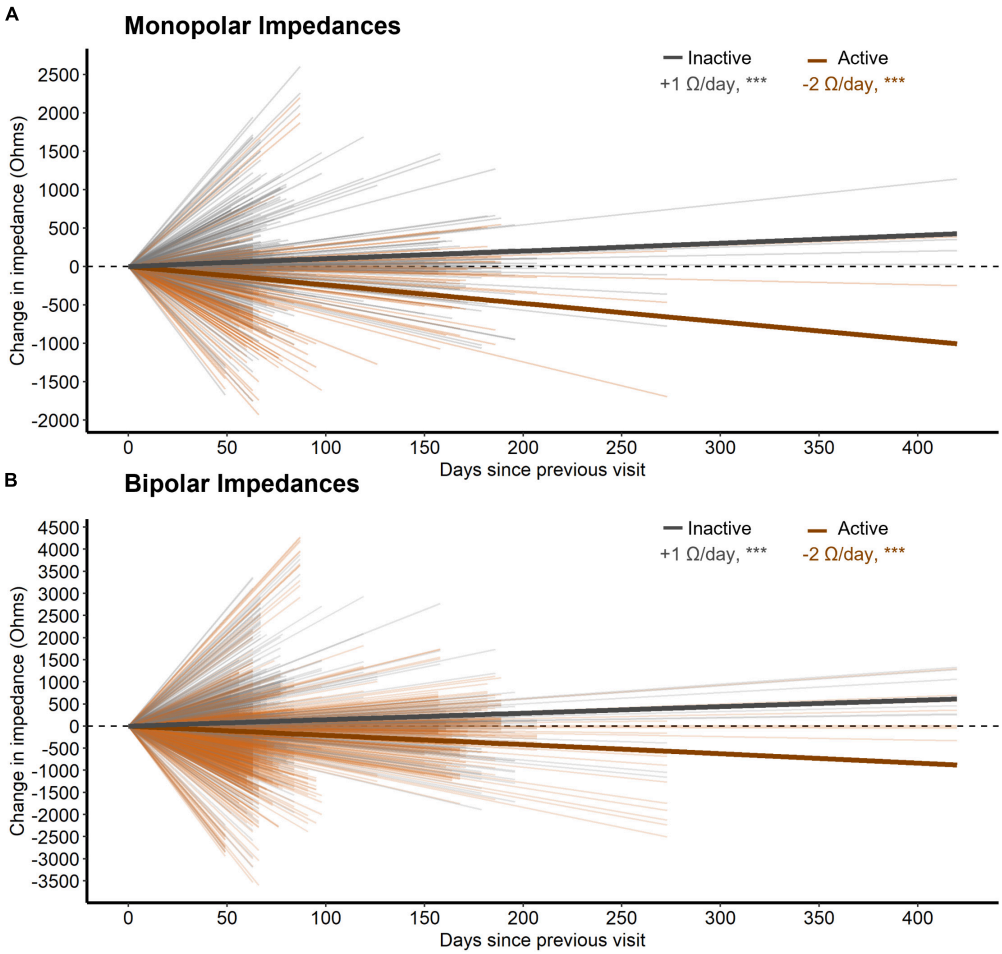

FIGURE 4
(A) The change in monopolar bipolar impedance per contact between subsequent post-operative visits as a function of time measured in days. Contacts are either inactive or active during this time. Thick lines represent the slope of impedance change for inactive and active contacts as determined by a LMM. **(B)** Same as **(A)** but for bipolar impedances. Here, a bipolar pair was labeled as active if either contact was active.

first year may reflect resolution of edema, tissue scarring, and/or glial encapsulation. Thus, the accumulated evidence suggests modest increases in average impedance over the first year of surgery, likely followed by slower declines over much longer time intervals (Wong et al., 2018).

Contacts involved in chronic stimulation displayed relative decreases in tissue impedance versus inactive contacts, as well. Although distance between contacts changes the measured impedance substantially (Almeida et al., 2016), we did not note any effects of distance on its rate of change. Better understanding changes in electrode impedance over time has implications for understanding how the DBS electrical field may change over time within an individual. Similarly, changes in local tissue impedance could conceivably alter the recording environment for control signals for future adaptive stimulation paradigms. We are unable to comment on the clinical relevance here because, due to the blinded nature of this study, active contacts were changed throughout the course of the year making it difficult to interpret any effect of impedance change on stimulation settings for an given contact.

Conclusion

Directional and ring contacts have different impedances but display similar longitudinal behaviors, with decreasing impedance immediately post-surgery followed by modest increases in over the first year. However, both active stimulation at a given site and longer follow intervals across all sites are associated with decreasing tissue impedances. Directional lead orientation can change modestly between intra-operative and post-operative scans, but otherwise appears to remain stable. Impedances within a given patient or recording site never completely stabilize, with different factors contributing to changes in the local tissue environment over time.

Data availability statement

The datasets presented in this study can be found in online repositories. The names of the repository/repositories and accession number(s) can be found below: Data Archive for the Brain Initiative (DABI) at https://dabi.loni.usc.edu/home.

Ethics statement

The studies involving human participants were reviewed and approved by University of Alabama at Birmingham IRB. The patients/participants provided their written informed consent to participate in this study.

Author contributions

CG and HW: experimental design, data collection, and writing and editing the manuscript. JO: data collection, data analysis and/or making figures, and writing and editing the manuscript. SB: data analysis and/or making figures and writing and editing the manuscript. MB: data collection and edits of manuscript. MW, CH, BG: experimental design, data collection, and edits of manuscript. AN: experimental design and edits of manuscript. All authors contributed to the article and approved the submitted version.

Funding

Funding for this work was provided by the National Institute of Neurological Disorders and Stroke BRAIN Initiative (UH3 NS100553) and the National Institute of Health (R01-NS119520).

Conflict of interest

MB is a paid full-time employee of Brainlab, Inc.

The remaining authors declare that the research was conducted in the absence of any commercial or financial relationships that could be construed as a potential conflict of interest.

Publisher's note

Supplementary material

The Supplementary Material for this article can be found online at: https://www.frontiersin.org/articles/10.3389/fnhum.2022.958703/full#supplementary-material

SUPPLEMENTARY FIGURE 1
(A) Percent of contacts' anatomical assignments, across all the patients, using the area of most overlap with a given a contact. Left and right bar plots are for directional and ring contacts, respectively. Panel **(B)** Similar to panel **(A)** but instead of the assigned region, plotted is the average percent volume of each contact contained in each region. Areas include internal capsule (IC), substantia nigra (SN), subthalamic nucleus (STN), thalamus (Th), zona incerta (ZI), and unaccounted (UA).

References

Almeida, L., Rawal, P. V., Ditty, B., Smelser, B. L., Huang, H., Okun, M. S., et al. (2016). Deep Brain Stimulation Battery Longevity; Comparison of Monopolar Versus Bipolar Stimulation Modes. *Mov. Disord. Clin. Pract.* 3, 359–366. doi: 10.1002/mdc3.12285

Bates, D., Maechler, M., Bolker, B., and Walker, S. (2015). Fitting linear mixed-effects models using lme4. *J. Stat. Softw.* 67, 1–48. doi: 10.18637/jss.v067.i01

Bour, L. J., Contarino, M. F., Foncke, E. M., de Bie, R. M., van den Munckhof, P., Speelman, J. D., et al. (2010). Long-term experience with intraoperative microrecording during DBS neurosurgery in STN and GPi. *Acta Neurochir.* 152, 2069–2077. doi: 10.1007/s00701-010-0835-y

Butson, C. R., Maks, C. B., and McIntyre, C. C. (2006). Sources and effects of electrode impedance during deep brain stimulation. *Clin. Neurophysiol.* 117, 447–454. doi: 10.1016/j.clinph.2005.10.007

Dembek, T. A., Asendorf, A. L., Wirths, J., Barbe, M. T., Visser-Vandewalle, V., and Treuer, H. (2021). Temporal Stablility of Lead Orientation in Directional Deep Brain Stimulation. *Stereotact. Funct. Neurosurg.* 99, 167–170. doi: 10.1159/000510883

Dembek, T. A., Hoevels, M., Hellerbach, A., Horn, A., Petry-Schmelzer, J. N., Borggrefe, J., et al. (2019). Leads show large deviations from their intended implantation orientation. *Parkinsonism Relat. Disord.* 67, 117–121. doi: 10.1016/j.parkreldis.2019.08.017

Hellerbach, A., Dembek, T. A., Hoevels, M., Holz, J. A., Gierich, A., Luyken, K., et al. (2018). DiODe: directional Orientation Detection of Segmented Deep Brain Stimulation Leads: a Sequential Algorithm Based on CT Imaging. *Stereotact. Funct. Neurosurg.* 96, 335–341. doi: 10.1159/000494738

Hemm, S., Vayssiere, N., Mennessier, G., Cif, L., Zanca, M., Ravel, P., et al. (2004). Evolution of brain impedance in dystonic patients treated by GPI electrical stimulation. *Neuromodulation* 7, 67–75. doi: 10.1111/j.1094-7159.2004.04009.x

Krack, P., Fraix, V., Mendes, A., Benabid, A. L., and Pollak, P. (2002). Postoperative management of subthalamic nucleus stimulation for parkinson's disease. *Mov. Disord.* 17(Suppl. 3), S188–S197. doi: 10.1002/mds.10163

Krüger, M. T., Naseri, Y., Cavalloni, F., Reinacher, P. C., Kägi, G., Weber, J., et al. (2021). Do directional deep brain stimulation leads rotate after implantation? *Acta Neurochir.* 163, 197–203.

Laitinen, L., Johansson, G. G., and Sipponen, P. (1966). Impedance and phase angle as a locating method in human stereotaxic surgery. *J. Neurosurg.* 25, 628–633. doi: 10.3171/jns.1966.25.6.0628

Lange, F., Steigerwald, F., Engel, D., Malzacher, T., Neun, T., Fricke, P., et al. (2021). Longitudinal Assessment of Rotation Angles after Implantation of Directional Deep Brain Stimulation Leads. *Stereotact. Funct. Neurosurg.* 99, 150–158. doi: 10.1159/000511202

Latikka, J., Kuurne, T., and Eskola, H. (2001). Conductivity of living intracranial tissues. *Phys. Med. Biol.* 46, 1611–1616. doi: 10.1088/0031-9155/46/6/302

R Core Team (2020). *R: A Language and Environment for Statistical Computing*.Vienna, AUS: R Foundation for Statistical Computing.

R Studio Team (2021). *RStudio: Integrated Development Environment for R. RStudio, PBC.* Vienna, AUS: R Studio Team.

Satzer, D., Lanctin, D., Eberly, L. E., and Abosch, A. (2014). Variation in deep brain stimulation electrode impedance over years following electrode implantation. *Stereotact. Funct. Neurosurg.* 92, 94–102. doi: 10.1159/000358014

Satzer, D., Maurer, E. W., Lanctin, D., Guan, W., and Abosch, A. (2015). Anatomic correlates of deep brain stimulation electrode impedance. *J. Neurol. Neurosurg. Psychiatry* 86, 398–403. doi: 10.1136/jnnp-2013-307284

Satzer, D., Yu, H., Wells, M., Padmanaban, M., Burns, M. R., Warnke, P. C., et al. (2020). Deep Brain Stimulation Impedance Decreases Over Time Even When Stimulation Settings Are Held Constant. *Front. Hum. Neurosci.* 14:584005. doi: 10.3389/fnhum.2020.584005

Sillay, K. A., Chen, J. C., and Montgomery, E. B. (2010). Long-term measurement of therapeutic electrode impedance in deep brain stimulation. *Neuromodulation* 13, 195–200. doi: 10.1111/j.1525-1403.2010.00275.x

Wong, J., Gunduz, A., Shute, J., Eisinger, R., Cernera, S., Ho, K. W. D., et al. (2018). Longitudinal Follow-up of Impedance Drift in Deep Brain Stimulation Cases. *Tremor Other Hyperkinet Mov.* 8:542. doi: 10.7916/D8M62XTC

frontiers | Frontiers in Human Neuroscience

TYPE Original Research
PUBLISHED 18 August 2022
DOI 10.3389/fnhum.2022.939258

OPEN ACCESS

EDITED BY
Adolfo Ramirez-Zamora,
University of Florida, United States

REVIEWED BY
Dong Song,
University of Southern California, United States
Wolf-Julian Neumann,
Charité Universitätsmedizin Berlin, Germany

*CORRESPONDENCE
Allison C. Waters
allison.waters@mssm.edu

SPECIALTY SECTION
This article was submitted to Brain Imaging and Stimulation, a section of the journal Frontiers in Human Neuroscience

RECEIVED 09 May 2022
ACCEPTED 25 July 2022
PUBLISHED 18 August 2022

CITATION
Smith EE, Choi KS, Veerakumar A, Obatusin M, Howell B, Smith AH, Tiruvadi V, Crowell AL, Riva-Posse P, Alagapan S, Rozell CJ, Mayberg HS and Waters AC (2022) Time-frequency signatures evoked by single-pulse deep brain stimulation to the subcallosal cingulate.
Front. Hum. Neurosci. 16:939258.
doi: 10.3389/fnhum.2022.939258

Time-frequency signatures evoked by single-pulse deep brain stimulation to the subcallosal cingulate

Ezra E. Smith[1], Ki Sueng Choi[2], Ashan Veerakumar[3], Mosadoluwa Obatusin[2], Bryan Howell[4], Andrew H. Smith[2], Vineet Tiruvadi[5,6], Andrea L. Crowell[7], Patricio Riva-Posse[7], Sankaraleengam Alagapan[8], Christopher J. Rozell[8], Helen S. Mayberg[2] and Allison C. Waters[2]*

[1]Private Practice, Tucson, AZ, Pima, [2]Departments of Psychiatry, Neuroscience, Neurology, Neurosurgery and Radiology, Nash Family Center for Advanced Circuit Therapeutics, Icahn School of Medicine at Mount Sinai, New York, NY, United States, [3]Department of Psychiatry, Schulich School of Medicine and Dentistry, London, ON, Canada, [4]Department of Biomedical Engineering, Duke University, Durham, NC, United States, [5]Emory University School of Medicine, Atlanta, GA, United States, [6]Department of Biomedical Engineering, Georgia Tech and Emory University, Atlanta, GA, United States, [7]Department of Psychiatry and Behavioral Sciences, Emory University School of Medicine, Atlanta, GA, United States, [8]School of Electrical and Computer Engineering, Georgia Institute of Technology, Atlanta, GA, United States

Precision targeting of specific white matter bundles that traverse the subcallosal cingulate (SCC) has been linked to efficacy of deep brain stimulation (DBS) for treatment resistant depression (TRD). Methods to confirm optimal target engagement in this heterogenous region are now critical to establish an objective treatment protocol. As yet unexamined are the time-frequency features of the SCC evoked potential (SCC-EP), including spectral power and phase-clustering. We examined these spectral features—evoked power and phase clustering—in a sample of TRD patients (n = 8) with implanted SCC stimulators. Electroencephalogram (EEG) was recorded during wakeful rest. Location of electrical stimulation in the SCC target region was the experimental manipulation. EEG was analyzed at the surface level with an average reference for a cluster of frontal sensors and at a time window identified by prior study (50–150 ms). Morlet wavelets generated indices of evoked power and inter-trial phase clustering. Enhanced phase clustering at theta frequency (4–7 Hz) was observed in every subject and was significantly correlated with SCC-EP magnitude, but only during left SCC stimulation. Stimulation to dorsal SCC evinced stronger phase clustering than ventral SCC. There was a weak correlation between phase clustering and white matter density. An increase in evoked delta power (2–4 Hz) was also coincident with SCC-EP, but was less consistent across participants. DBS evoked time-frequency features index mm-scale changes to the location of stimulation in the SCC target region and correlate with structural characteristics implicated in treatment optimization. Results also imply a shared generative mechanism (inter-trial phase clustering) between evoked potentials evinced by electrical

stimulation and evoked potentials evinced by auditory/visual stimuli and behavioral tasks. Understanding how current injection impacts downstream cortical activity is essential to building new technologies that adapt treatment parameters to individual differences in neurophysiology.

KEYWORDS

deep brain stimulation, subcallosal cingulate, single pulse electrical stimulation, time frequency analyses, treatment resistant depression (TRD), inter-trial phase clustering, stimulation evoked potential, perturbation mapping

Introduction

Background

There is growing scientific and clinical interest in the effect of single pulse electrical stimulation on the brain. This technique of perturbation mapping involves punctuated current injection to a circuit or cortical node using invasive (e.g., deep brain stimulation; DBS) or non-invasive methods (e.g., transcranial magnetic stimulation; TMS). Electrical perturbation of the living human brain elicits a temporal-spatial cascade of electrophysiological activity that appears sensitive to change in stimulation parameters, such as the precise location of stimulation in the brain. When this activity is averaged over repeated electrical pulses, a stereotyped series of spatial-temporal components are observed as an evoked potential. Importantly, DBS evoked potentials are coherent and reliable on the level of individuals (Waters et al., 2018), and are thus amenable to the development of patient-specific applications, such as confirmation of optimal surgical targeting. Precision targeting has been linked to the efficacy of subcallosal cingulate (SCC) DBS for treatment of depression (Riva-Posse et al., 2018). Understanding how the precise location of current injection impacts downstream cortical activity is essential to building new technologies that harness perturbation-based mapping approaches to confirm optimal therapeutic target engagement over the course of treatment.

A definitive biophysical explanation for evoked responses to single pulse stimulation is still unclear and may vary by scale (i.e., LFP, ECOG, EEG). Nevertheless, perturbation maps convey information that can be exploited to advance the clinical science of neuromodulation and to interrogate human brain networks (Fox et al., 2012; Entz et al., 2014; Sarasso et al., 2015; Borich et al., 2016; Solomon et al., 2018; Keller et al., 2018; Yu et al., 2019; Baker et al., 2002; Massimini et al., 2005). Stimulation-evoked brain responses are most frequently examined in the time domain (i.e., event related potentials, ERP) which ignores oscillatory features of neural activity like frequency, phase, and amplitude (Makeig et al., 2004). These spectral features are evident across spatial scales and species (Narayanan et al., 2013; Cohen, 2014; Robble et al., 2021), and a summation of spectral features—especially evoked power and phase consistency—contributes to manifest ERPs (Penny et al., 2002; Luu et al., 2004; Shah et al., 2004; Fuentemilla et al., 2006; Hanslmayr et al., 2007; Klimesch et al., 2007; Trujillo and Allen, 2007). Spectral metrics are also highly relevant to the study of depression pathophysiology because oscillation frequency and phase is critical to facilitating information multiplexing between and within brain networks. Spectral metrics also vary over time and examining dynamic frequency, phase, and amplitude is typically referred to as time-frequency analysis. This focus on examining brain activity in the time-frequency domain is also more compatible with the analytic techniques used with non-human animals, facilitating cross-species comparisons and interpretations (Cohen, 2011b; Basu et al., 2019). Amenability to cross-species comparisons is particularly relevant to understanding the effects of direct electrical stimulation to the brain since human trials are sparse and often costly. Altogether, applying time-frequency analysis to the investigation of stimulation-evoked responses can provide unique information that is obscured by conventional ERP analyses, facilitate cross-species comparisons and reveal biophysically plausible features relevant to functional brain networks.

Present study

In an effort to expand upon prior work examining SCC stimulation evoked potentials, we focus our analyses on the ERP, evoked power, and inter-trial phase consistency (ITPC) as our primary neural measures. This study aimed to discover time-frequency signatures evoked by SCC stimulation in eight patients undergoing DBS for treatment resistant depression (TRD). We test the hypothesis that time-frequency features of perturbation map will vary as a function of DBS location across a dorsal-ventral axis of the SCC target region, which may reflect mechanisms of neuronal communication that are disrupted with precise targeting of white matter elements in the SCC region.

Materials and methods

Participants

Subjects (n = 8; four males) were patients in a study of SCC DBS safety and efficacy for treatment of TRD (clinicaltrials.gov #NCT01984710) who underwent DBS surgery between 2015 and 2019. Inclusion and exclusion criteria for the parent study were identical to Holtzheimer et al. (2012) and Riva-Posse et al. (2018) and summarized in **Supplementary Materials**. Briefly, participants suffered from severe major depressive disorder and had failed multiple treatments, including medication, psychotherapy, and electroconvulsive therapy. Subjects ranged in age from 28 to 70 (mean: 53.1, *SD*: 14.3). One subject was left handed. All participants provided written informed consent to participate in this research, which was approved by the Emory University Institutional Review Board and the US Food and Drug Administration under an Investigational Device Exemption (IDE # G130107 held by H.S.M) and was monitored by the Emory University Department of Psychiatry and Behavioral Sciences Data Monitoring Board. Additional sample characteristics, including depression severity scores (Hamilton, 1960) at baseline and at the time of study participation, are provided in **Supplementary Material**.

Tractography guided implantation

Procedures for tractography guided surgical targeting and post-operative verification follow Riva-Posse et al. (2018). An Activa PC + S^{TM} pulse generator (Medtronic, Minneapolis, MNI) drove bilateral DBS leads (model 3387), each with 4 contacts (1.5 mm inter-contact spacing), which were implanted in the SCC region (**Figure 1A**) using a prospective connectomic approach and StimVision software (Noecker et al., 2017). This approach uses patient-specific deterministic tractography and anatomical images to optimize placement of the contact at the confluence point of four white matter fibers (Riva-Posse et al., 2014). In brief, magnetic resonance imaging data, (high-resolution T1 structural and diffusion-weighted) are acquired for each individual on a Siemens 3T Tim-Trio scanner (Siemens Medical Solution, Malvern, PA). Following surgery, high-resolution computed tomography (LightSpeed16, GE Medical System) images are used to verify that the contacts used for therapeutic stimulation respect to tractography.

Experimental procedures

Patients were fitted with a 256-channel Hydrocel Geodesic Sensor Net (MagStim-EGI, Eugene, OR) and seated in a climate controlled room. A chin rest was used to reduce motion artifacts. Patients were instructed to relax and allow their mind to wander. A series of eight conditions, each 2.5–3 min of stimulation, involved simultaneous EEG recording and unilateral stimulation from different locations in the SCC target region (i.e., ventral, mid-ventral, mid-dorsal or dorsal contacts on each lead). All conditions used a monopolar configuration for stimulation of 6 V with a 90 μs pulse width at 2 Hz (**Figure 1B**). Conditions were not randomized. In conditions 1–4, stimulation was delivered to the left hemisphere from the ventral-most to dorsal-most contact, respectively. Conditions 5–8 followed the same pattern with stimulation delivered to the right hemisphere. Patients were informed as to the start and end of each condition but were blind to parameter settings. Stimulation parameter changes were made by a physician team member using the Medtronic clinical programmer. For individual patients, testing was conducted at different times in treatment. Four patients participated after 4 weeks of therapeutic stimulation and four patients participated after 6 months of stimulation (**Supplementary Table 1**). For one participant (Patient 2), experimental procedures were interrupted resulting in one condition recorded on a subsequent day.

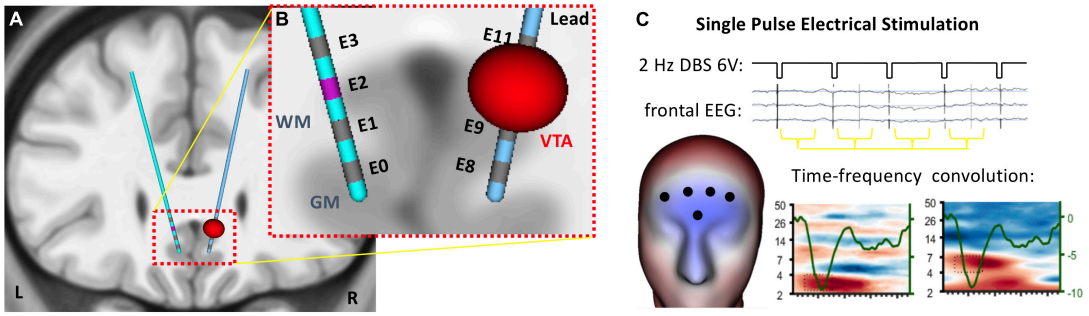

FIGURE 1
Single pulse electrical stimulation of the subcallosal cingulate (SCC) target for deep brain stimulation. **(A)** Four contacts span the SCC target region on bilateral DBS electrodes. **(B)** EEG was recorded on the head surface during single pulse electrical stimulation at each contact on the DBS leads. **(C)** Analytic window was coincident with the SCC-EP (~100 ms) detected in frontal channels.

EEG preprocessing

Recordings were from a NetAmps 400 amplifier (MagStim-EGI, Eugene, OR) with an online reference near the vertex (1,000 Hz sampling rate). In four of the eight recordings, 1–3 bad electrodes (of 256) were identified manually and spherically interpolated; none were in the frontal montage used for statistical analysis. One subject (Patient 3) had high impedance in one of the implanted electrodes (also throughout the parent study). That contact was excluded from the experimental procedures for that subject, only. Electroencephalogram (EEG) were then re-referenced to the average of all electrodes. A 2–50 Hz bandpass zero-phase shift FIR filter was applied. Hampel outlier rejection in the frequency domain was the primary correction for stimulator artifacts specifically. The spectral outlier rejection by Hampel filtering has the advantage of preserving phase-relationships in the signal, and has demonstrable efficacy for reducing stimulation artifacts (Allen et al., 2010). Briefly, Hampel filtering involves rejecting spectral outliers using a sliding window. The user selects the frequency window width ($N = 2$) and outlier criterion for rejection ($t = 5$), then spectral bins identified as outliers are replaced with the average of their neighbors. Manual rejection of artifactual independent components analysis was used for other non-neurogenic artifacts (Smith et al., 2017), and any residual stimulator artifacts. Artifact is a substantial concern in these recordings, and aggressive multistage processing aligns with the recommendations of a recent discussion on the topic (Lio et al., 2018).

EEG analyses

Average evoked-potentials. Epochs time-locked to the DBS pulse were cut and averaged to produce a mean time-series for each individual and in response to stimulation from each of eight contacts. A grand average is plotted for illustration in **Figure 2**.

Time-domain data were convolved with a family of Morlet wavelets to produce the time-frequency (TF) metrics of interest: ITPC and phase-locked TF power. The family of wavelets included 30 logarithmically spaced wavelets of varying frequency from 2 to 50 Hz, and with a varying number of cycles from 3 to 10 (higher frequencies with more cycles; e.g., Cohen, 2014). Time-frequency power was normalized (Z-score) relative to a -50 to -10 ms prestimulation baseline consistent with previous work (Waters et al., 2018).

Tissue activation and white matter density

The DBS contact location was identified in native T1 space based on a high-resolution postoperative CT image that

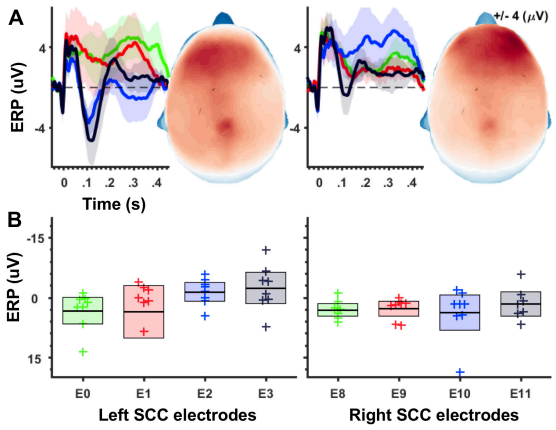

FIGURE 2
Magnitude of unilateral stimulation evoked potentials increases along the ventral-to-dorsal axis of the SCC target region. **(A)** Grand average waveforms for stimulation-evoked potentials. Shaded areas depict 95% confidence intervals after 1,000 bootstraps. Left panel shows ERPs following left SCC stimulation, and right panel shows ERPs following right SCC stimulation. Topographic plots show ERP magnitude integrated over 50–150 ms time window. **(B)** Boxplots depicting average ERP amplitudes (averaged across 50–150 ms, electrode montage shown in **Figure 1C**) separately for stimulation location. Left panel shows averages for left-SCC stimulation, right panel shows averages for right-SCC stimulation.

aligned to native T1 space using a linear registration toolbox (3dAllineate, AFNI: Analysis of Functional NeuroImages, Cox, 1996). The patient-specific volume of tissue activated (VTA) was then generated by electrical DBS field model on identified contact location for this study using the StimVision software toolbox with the following parameters: 130 Hz, 90 μs, and 6V (Noecker et al., 2018). The detailed methodology for DBS activation volume is described in Chaturvedi et al. (2013). Brain tissue segmentation was performed using a multichannel tissue classification algorithm (FAST, FMRIB)[1] to calculate the probability of gray matter, white matter, and cerebrospinal fluid. The activated WM volume of each contact was then computed by overlapped volume between the segmented WM tissue map and the patient-specific VTA.

Statistical analyses

Effect of target location in the SCC on stimulation evoked cortical electrophysiology. The effect of contact location within the SCC region on SCC-EP amplitude, spectral power and ITPC was assessed using a repeated measures analysis of variance (rmANOVA) with a four-level factor representing contact location along the dorsal to ventral axis of the implanted electrode and a two-level factor representing the

1 http://www.fmrib.ox.ac.uk/fsl

hemisphere that received unilateral DBS. Following Waters et al. (2018) data extracted for statistical analyses was an average across frontopolar channels (18, 25, 31, 32, 37) in a time-of-interest (TOI) coincident with the reported SCC-EP feature at its negative-going amplitude maxima (50–150 ms post-pulse). Analyses were conducted in IBM SPSS 26.0.0.2 (Mathworks, Armonk, NY).

To aid in the interpretation of results, we looked at the quantity of white matter (WM) activated by each deep brain electrode contact, and tested for a relationship with the magnitude of the evoked electrophysiological response. Our hypothesis was that greater activation of conductive brain tissue (i.e., WM) would lead to a more pronounced physiological effect being recorded at the head surface. The regression analysis was conducted using the *lme4* package in R.

Results

Electrophysiology

Using an averaged evoked-potential approach to analysis of the cortical response to single-pulse stimulation (**Figure 2A**), the effect of stimulation location in the SCC (dorsal-most to ventral most contracts labeled as E3 to E0) on the magnitude of the SCC-EP feature (maximal ∼100 ms) was statistically significant, $F(3, 18) = 4.868$, $p = 0.012$, partial eta^2 = 0.448, while the effect of hemisphere (which hemisphere received SCC DBS) was not, $p = 0.345$ (**Figure 2B**). The interaction of hemisphere and contact factors was below threshold for statistical significance, $p = 0.250$. Results of a within-subjects contrast indicated linear model fit to changes in mean amplitude, which decreased with stimulation along the dorsal to ventral axis of implanted contact, $F(1, 6) = 6.933$, $p = 0.039$, eta = 0.536. **Figure 2A** shows the topography of SCC-EP maxima averaged across all conditions. **Figure 2B** shows grand average SCC-EP traces at each of eight contacts, with 95% confidence intervals bootstrapped from 1,000 iterations.

ITPC in the theta band (4–7 Hz) was coincident with the SCC-EP following both right and left hemisphere stimulation (**Figure 3A**). The effect of stimulation location in the SCC region on the magnitude of theta ITPC was statistically significant, $F(3,18) = 7.902$, $p = 0.001$, partial eta^2 = 0.568, while the effect of hemisphere (which hemisphere received SCC DBS) was not, $p = 0.103$ (**Figure 3B**). The interaction of hemisphere and contact was significant, $F(3,18) = 3.3$, $p = 0.045$, eta^2 = 0.353. Mean ITPC magnitude decreased in response to stimulation along the dorsal-ventral axis of the DBS contact in the left hemisphere (E3 = 0.48, *SD* = 0.08; E2 = 0.32, *SD* = 0.11; E1 Mean = 0.30, *SD* = 0.08; E0 Mean = 0.27, *SD* = 0.05) and right hemisphere (E11 = 0.32, *SD* = 0.10; E10 = 0.28, *SD* = 0.07; E9 Mean = 0.29, *SD* = 0.13; E8 Mean = 0.25, *SD* = 0.07). Results of a within-subjects contrast indicated linear model fit to changes in mean amplitude across contacts, $F(1,6) = 16.804$, $p = 0.006$, eta = 0.737, with the interaction term below the significance threshold, $p = 0.059$. On the level of individual patients, theta ITPC coincident with the SCC-EP feature of the average evoked response was robust across the sample (**Figure 4**), including consistent spatial topography and effects of DBS location within the target region (**Figure 5**).

Using a time frequency approach to analysis of the cortical response to single-pulse stimulation, an increase in delta power (2–4 Hz) was observed in the study population average following both left and right stimulation but was inconsistently observed across individual subjects (**Supplementary Figure 1**) and thus excluded from additional analyses.

Regression results

ITPC across all stimulation locations was significantly correlated with EP amplitude Spearman's $r(64) = -0.41$, $p < 0.001$. Follow-up correlations showed that ITPC and EP were significantly correlated following left SCC perturbation $r(32) = -0.57$, $p < 0.001$, whereas ITPC and EP were unrelated following right SCC perturbation $r(32) = -0.002$.

When testing for a relationship between quantity of WM stimulated and Fpz theta ITPC, while accounting for contact position and non-independence of repeated ITPC measures in each subject, we found an association between activated WM (mm3) and ITPC, $R2 = 0.13$, $p < 0.01$ (**Supplementary Figure 2**).

Discussion

Findings

Using a perturbation-mapping approach, we investigated cortical time-frequency dynamics following stimulation applied to different locations of the SCC target region. Elaborating on the SCC DBS evoked potential described by Waters et al., 2018, pulse-wise perturbation was characterized by changes in delta band (2–4 Hz) power and theta band (4–7 Hz) phase alignment, coincident with the SCC-EP. Frontal theta phase alignment was observed after right or left hemisphere SCC stimulation with notable reliability; observed both at the group level and participant level. As hypothesized, millimeter scale changes in the location of stimulation also impacted cortical time-frequency dynamics: frontal theta phase clustering increased as the stimulation location was moved from ventral to dorsal contacts within the target region of the SCC, particularly when stimulation was initiated in the left hemisphere. ITPC evinced by left SCC stimulation was significantly correlated with SCC-EP magnitude. A *post hoc* correlation analysis demonstrated a

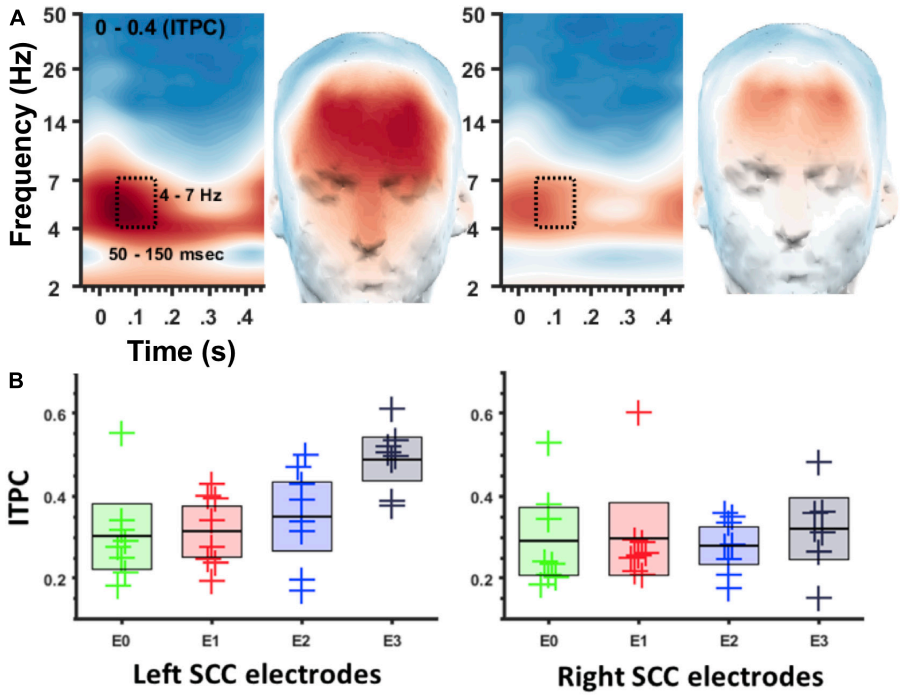

FIGURE 3
ITPC at 4–7 Hz depends on location of DBS in the SCC region. **(A)** Spectrogram of ITPC across time and frequency. Box denotes time-frequency region-of-interest used for topographic plots. Left panel for left SCC stimulation, right panel for right SCC stimulation. **(B)** Box plots showing ITPC (50–150 ms, 4–7 Hz) at different stimulation locations. Left panel for left SCC stimulation, right panel for right SCC stimulation. Green = E0/8, Red = E1/9, Blue = E2/10, Black = E3/11.

trend toward a positive correlations between theta ITPC and white matter volume.

Context/interpretation

In healthy control participants, oscillations at theta frequency (4–8 Hz) predict behavioral adaptation to errors, conflict, and novelty (Cavanagh et al., 2009; Cavanagh and Frank, 2014; Cooper et al., 2019; Duprez et al., 2020). Frontal theta oscillations are also a hypothesized mechanism of depression pathophysiology with relevance to recovery and responsivity to antidepressant medication (Arns et al., 2015; Pizzagalli et al., 2018; Whitton et al., 2019) and brain stimulation (Narushima et al., 2010; Broadway et al., 2012). Theta oscillations are pronounced across frontostriatal regions relevant to depression, especially midcingulate regions, striatum, ventral tegmental area, lateral prefrontal cortex, and hippocampus (Cavanagh et al., 2009; Cavanagh and Frank, 2014; Herweg et al., 2016; Marawar et al., 2017; Smith et al., 2020; Dede et al., 2021). The phase of theta oscillations specifically is believed to facilitate cross talk between nodes within this frontostriatal network (Cavanagh et al., 2009; Dede et al., 2021). For example, theta phase clustering is greatly enhanced across frontal regions in healthy participants after behavioral errors (Trujillo and Allen, 2007; Cavanagh and Frank, 2014), and theta phase predicts magnitude of participant's post-error behavioral adaptation (i.e., reaction time and accuracy; Cavanagh et al., 2009; Dede et al., 2021). Brain stimulation at theta frequencies targeted at the frontal lobes has also been successfully utilized as a treatment for depression (Berlim et al., 2017), and stimulation time-locked to the phase of a participant's frontal theta activity can enhance cognitive performance (Alagapan et al., 2019; Reinhart and Nguyen, 2019).

Enhancement of phase clustering is sometimes conceptualized as a "reset" in the timing of intrinsic brain rhythms. This phase "reset" is believed to facilitate a reorienting of attention, and/or the recruitment of brain regions important for modifying behavioral strategies (i.e., lateral prefrontal cortex; Cavanagh et al., 2009; Cavanagh and Frank, 2014). More specifically, the precise timing of a frontal theta rhythm is updated/(re)started, and this restart facilitates synchrony between brain regions demonstrating a propensity toward theta rhythm (e.g., frontostriatal regions noted above). Notably, cortical theta oscillations rely on structural pathways, and healthy participants with stronger theta tend toward larger pathway volumes across the PFC (Cohen, 2011a); conversely, reduced fractional anisotropy in individuals with head injury correlates with diminished theta-band synchrony (Cavanagh et al., 2020). Enhanced theta phase clustering can

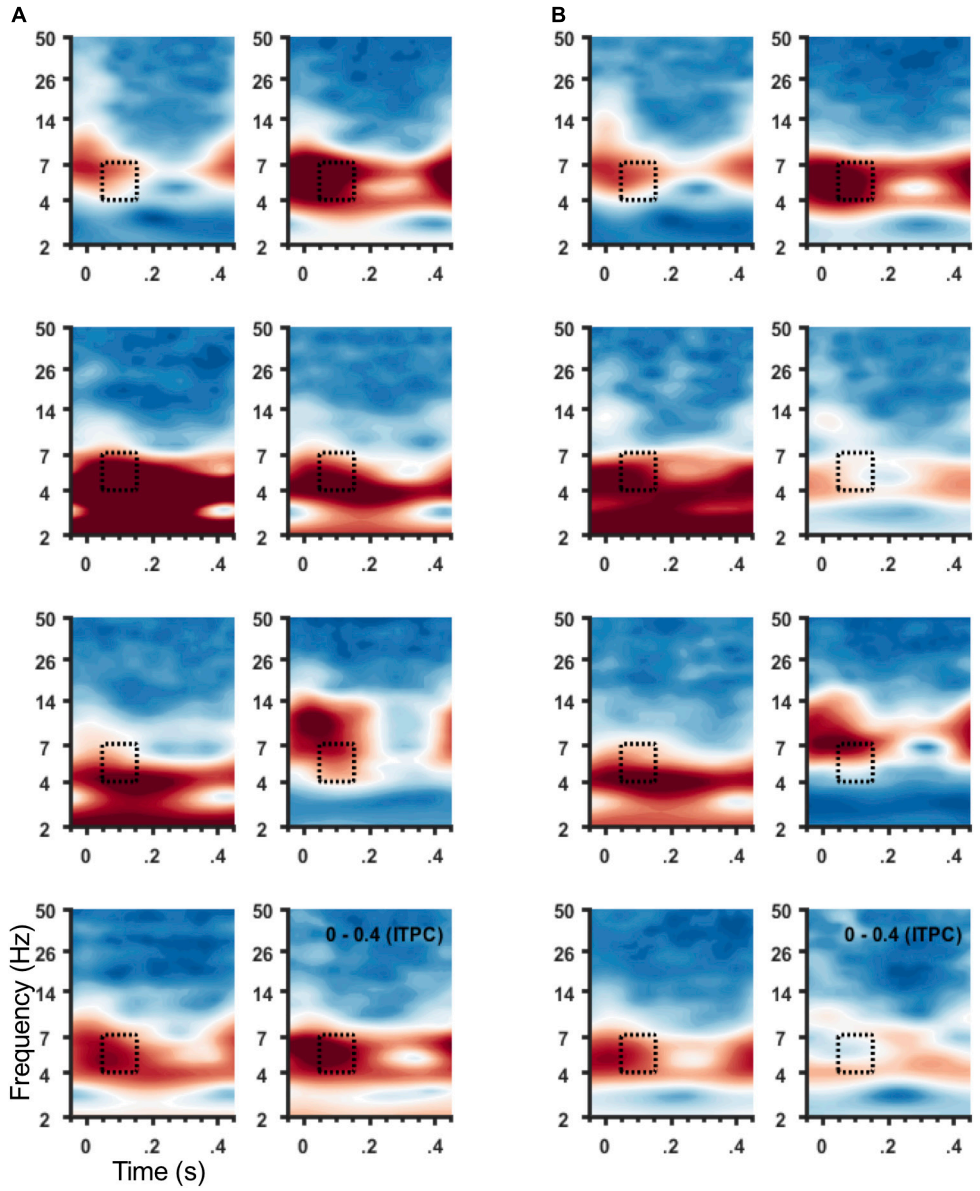

FIGURE 4
ITPC at 4–7 Hz for individual participants. Spectrograms of average ITPC across all stimulation locations from frontal sensors (**Figure 1C**) for individual participants. Subject order (1–8) shown within panel: right to left column then top to bottom row. **(A)** Spectrograms show ITPC time-locked to left hemisphere SCC DBS, and **(B)** to right hemisphere SCC DBS. Stippled box denotes time-frequency region of interest used for group analysis and topographic plots in **(B)**.

also produce ERP phenomenon (e.g., Trujillo and Allen, 2007), and present results imply ITPC contributes to the presentation of the SCC-EP. In fact, large positive correlations were observed between ITPC and EP measures in the present study, especially for left SCC stimulation. These results suggest ITPC contributes to generation of EP. This is consistent with the hypothesis that consistency in neural phase summates over experimental trials and helps generate ERPs (reviewed in Klimesch et al., 2007). Notably, prior studies examining generators of ERPs were in the context of visual/auditory stimuli or during behavioral tasks. In this regard, one speculative hypothesis is that ERPs evoked by electrical and non-electrical stimuli have overlapping biophysical (i.e., generative) mechanisms.

It has been hypothesized that electrical currents are less likely to flow through gray matter than electrically-shielded (i.e., myelin) white matter (Keller et al., 2014). Thus, it may be the case that electrical stimulation at DBS contacts near SCC gray matter (more ventral) produced a cortical response of smaller magnitude relative to DBS contacts near SCC white matter (more dorsal). A *post hoc* correlation was supportive of this

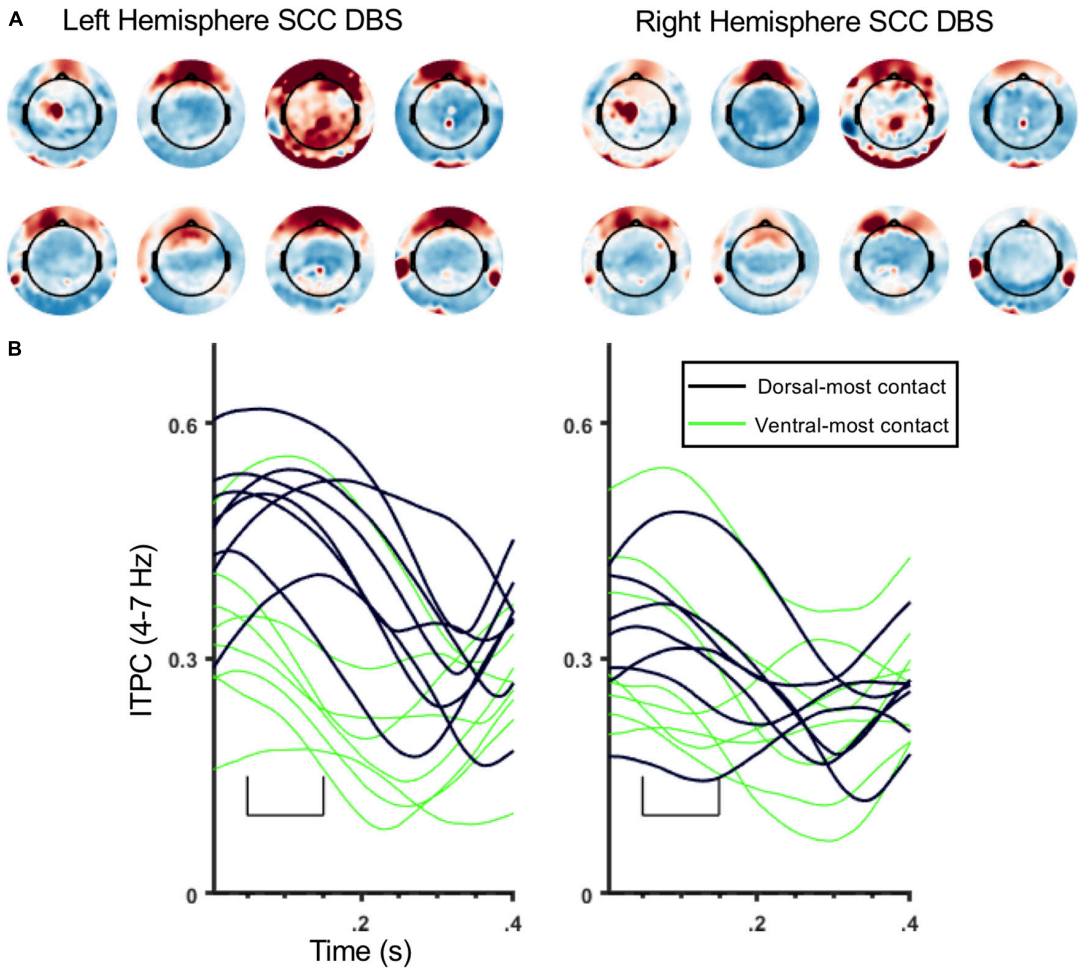

FIGURE 5
Topography and time course of ITPC at 4–7 Hz for individual participants. **(A)** ITPC topography for individual participants (4–7 Hz, 50–150 ms) averaged across all stimulation locations. The 8 topomaps on the left are from left SCC stimulation, and 8 topomaps on the right are from right SCC stimulation. Subject order (1–8) of topomaps: top rows (right to left) then bottom rows. **(B)** ITPC waveforms (4–7 Hz; frontal sensor montage, **Figure 1C**) from individual participants. Black lines are ITPC waveforms following stimulation at E3/11, green lines are ITPC waveforms following stimulation at E0/8. Left panel is from left SCC stimulation, and right panel is from right SCC stimulation.

possibility: ITPC amplitude showed a trend toward a positive correlation with white matter volume. Previous work has also demonstrated links between electrophysiological response magnitude and proximity of the stimulation location to white matter structures (Conner et al., 2011; Keller et al., 2014; Borich et al., 2016; Yamao et al., 2017; Nakae et al., 2019). Altogether, we are optimistic that changes in theta phase clustering represent differential activation of theta-sensitive pathways relevant for depression treatment and recovery. Future work is needed to see if features of the electrical perturbation map can further differentiate specific white matter bundles that define this therapeutic confluence point.

In the absence of acute and reliable behavioral responses to neuromodulation for psychiatric disorders, there is an urgent need for alternate methods to guide optimal parameter selection, including the position of the therapeutic contact in the target region. The SCC region is heterogeneous in terms of white matter crossing fibers (Vergani et al., 2016). Previous research demonstrated that treatment efficacy requires millimeter-scale precision of electrical stimulation at the confluence of four white matter bundles (Riva-Posse et al., 2014, 2018; Howell et al., 2019). Notably, similar approaches using stimulation pulses to guide targeting of DBS electrode placement have demonstrated promise for improved outcomes in patients with refractory conditions (Zumsteg et al., 2006; Fox et al., 2012; Entz et al., 2014; Van Gompel et al., 2015; Kimiskidis, 2016; Riva-Posse et al., 2018; Yamao et al., 2017). This line of inquiry opens new possibilities for brain mapping of structural elements in the living human brain, as well as a means to optimize and individualize the precision of brain stimulation for therapeutic purposes.

Limitations and future directions

Despite a clear rationale, analyses in the time-frequency (TF) domain have been underutilized to observe neural oscillations in the context of perturbation mapping. This may be in part due to the challenge of disentangling stimulation artifacts from the evoked response after pre-processing. The DBS artifact is significantly greater than neurogenic activity and may covary with phase-locked EP components, obscuring modifications in neural activity that result from stimulation. Moreover, the component-based artifact mitigation used here may have attenuated some phase-locked neurogenic activity that was temporally and statistically yoked to electrical stimulation (see Smith et al., 2020 for a discussion of component-based artifact correction). This might explain discrepant findings from a simpler rejection strategy. Similarly, the absence of a relationship between ITPC and EP for right SCC stimulation is not entirely clear. Notably, **Figure 2** suggests that the right SCC EP was relatively weak compared to the EP following left SCC stimulation. Research designs using symmetric biphasic pulses have the advantage of minimizing stimulator artifact on electrophysiological recordings (Liu et al., 2012) and should be considered in follow-up studies.

SCC stimulation was not randomized. This leaves open the possibility for confounding effects of stimulation location vs. stimulation sequence. This is an unfortunate consequence of experimental design, and future work will examine the influence of stimulation sequence on neural response to SCC perturbation. This confound significantly limits the conclusiveness of stimulation location effects regarding the SCC-EP. Importantly, the main findings of increased ITPC following SCC perturbation were observed regardless of SCC location.

Another important consideration in the present inquiry is the effect of current depression at time of testing: four subjects were studied after 4 weeks of treatment, and four participated after 6 months of treatment. All 8 participants were classified as responders at 6 months (HDRS depression scores reported in **Supplementary Materials**). A preliminary analysis suggested similar results irrespective of differences in treatment duration. Visual inspection of data from individual participants also suggests homogeneity in spatial-temporal-spectral pattern following SCC perturbation. Waters et al. (2018) also demonstrated high reliability for SCC-EP across 14 months, results arguing against a major interaction between treatment duration and response to single pulse SCC stimulation.

Conclusion

In a small sample of SCC-DBS patients, we demonstrate the potential utility of perturbation-mapping to observe the effect of mm-level changes in DBS locations at the cortical surface. This technique has the advantage of excellent spatial and temporal resolution and holds promise as an assay of causal neural mechanisms, and may be useful for optimizing electrode placement and directing DBS current flow(s). Moreover, a time-frequency approach to analysis of single pulse electrical stimulation EP provides a view of neural phenomena that is more directly relevant to endogenous neural dynamics. Here we show theta phase coherence as a likely constituent of the SCC-EP response to SCC stimulation. Inconsistent enhancement in evoked delta power was also observed for a few participants. Evidence for stimulation evoked EEG activity as a close proxy for white matter perturbation was modest in these findings, but the approach may be promising as a read out of individual differences in cortical activity relevant to depression and treatment. These findings are generally consistent with theories of MDD etiopathogenesis that point toward frontal-lobe processes important for cognitive control, and have profound implications for the evolution of MDD treatment with neurostimulation approaches.

Data availability statement

The data that support the findings of this study are available for research purposes upon request made to the corresponding author.

Ethics statement

The studies involving human participants were reviewed and approved by the Emory University Department of Psychiatry and Behavioral Sciences Data Monitoring Board. The patients/participants provided their written informed consent to participate in this study.

Author contributions

AW, ES, AV, and HM: design of inquiry. AW, AV, MO, VT, and AC: design and implementation of data collection. ES: time-frequency analyses. PR-P and AC: clinical management. KC: tractography mapping. ES, AW, BH, and AS: *post hoc* analyses. ES, AW, BH, AS, SA, CR, and HM: interpretation and preparation of the manuscript. All authors contributed to and approved the final version of the manuscript.

Funding

This work was supported by the NIH Brain Research through Advancing Innovative Neurotechnologies (BRAIN) Initiative (UH3NS103550; PI HM), the Hope for Depression

Research Foundation (PI HM), and the Howard Hughes Medical Institute Medical Research Fellows Program (AV).

Acknowledgments

The DBS Activa PC + S devices used in this research were donated by Medtronic (Minneapolis, MN). For their help with this project and report, we thank Martijn Figee, Kelly Bijanki, Sinead Quinn, Lydia Denison, Daniel Majarwitz, Shauna Bowes, and Nicole Webb. We thank the patients who participated in this research.

Conflict of interest

HM received consulting and intellectual property licensing fees from Abbott Labs. KC received consulting fees from Abbott Labs. The terms approved by Emory University and the Icahn School of Medicine in accordance with policies to manage conflict of interest.

The remaining authors declare that the research was conducted in the absence of any commercial or financial relationships that could be construed as a potential conflict of interest.

Publisher's note

All claims expressed in this article are solely those of the authors and do not necessarily represent those of their affiliated organizations, or those of the publisher, the editors and the reviewers. Any product that may be evaluated in this article, or claim that may be made by its manufacturer, is not guaranteed or endorsed by the publisher.

Supplementary material

The Supplementary Material for this article can be found online at: https://www.frontiersin.org/articles/10.3389/fnhum.2022.939258/full#supplementary-material

References

Alagapan, S., Lustenberger, C., Hadar, E., Shin, H. W., and Fröhlich, F. (2019). Low-frequency direct cortical stimulation of left superior frontal gyrus enhances working memory performance. *Neuroimage* 184, 697–706. doi: 10.1016/j.neuroimage.2018.09.064

Allen, D. P., Stegemoller, E. L., Zadikoff, C., Rosenow, J. M., and Mackinnon, C. D. (2010). Suppression of deep brain stimulation artifacts from the electroencephalogram by frequency-domain Hampel filtering. *Clin. Neurophysiol.* 121, 1227–1232. doi: 10.1016/j.clinph.2010.02.156

Arns, M., Etkin, A., Hegerl, U., Williams, L. M., DeBattista, C., Palmer, D. M., et al. (2015). Frontal and rostral anterior cingulate (rACC) theta EEG in depression: Implications for treatment outcome? *Eur. Neuropsychopharmacol.* 25, 1190–1200.

Baker, K. B., Montgomery, E. B., Rezai, A. R., Burgess, R., and Lüders, H. O. (2002). Subthalamic nucleus deep brain stimulus evoked potentials: Physiological and therapeutic implications. *Mov. Disord.* 17, 969–983. doi: 10.1002/mds.10206

Basu, I., Robertson, M. M., Crocker, B., Peled, N., Farnes, K., Vallejo-Lopez, D. I, et al. (2019). Consistent linear and non-linear responses to invasive electrical brain stimulation across individuals and primate species with implanted electrodes. *Brain Stimul.* 12, 877–892. doi: 10.1016/j.brs.2019.03.007

Berlim, M. T., McGirr, A., Dos Santos, N. R., Tremblay, S., and Martins, R. (2017). Efficacy of theta burst stimulation (TBS) for major depression: An exploratory meta-analysis of randomized and sham-controlled trials. *J. Psychiatr. Res.* 90, 102–109. doi: 10.1016/j.jpsychires.2017.02.015

Borich, M. R., Wheaton, L. A., Brodie, S. M., Lakhani, B., and Boyd, L. A. (2016). Evaluating interhemispheric cortical responses to transcranial magnetic stimulation in chronic stroke: A TMS-EEG investigation. *Neurosci. Lett.* 618, 25–30. doi: 10.1016/j.neulet.2016.02.047

Broadway, J. M., Holtzheimer, P. E., Hilimire, M. R., Parks, N. A., DeVylder, J. E., Mayberg, H. S., et al. (2012). Frontal theta cordance predicts 6-month antidepressant response to subcallosal cingulate deep brain stimulation for treatment-resistant depression: A pilot study. *Neuropsychopharmacology* 37:1764. doi: 10.1038/npp.2012.23

Cavanagh, J. F., and Frank, M. J. (2014). Frontal theta as a mechanism for cognitive control. *Trends Cogn. Sci.* 18, 414–421.

Cavanagh, J. F., Cohen, M. X., and Allen, J. J. (2009). Prelude to and resolution of an error: EEG phase synchrony reveals cognitive control dynamics during action monitoring. *J. Neurosci.* 29, 98–105. doi: 10.1523/JNEUROSCI.4137-08.2009

Cavanagh, J. F., Rieger, R. E., Wilson, J. K., Gill, D., Fullerton, L., Brandt, E., et al. (2020). Joint analysis of frontal theta synchrony and white matter following mild traumatic brain injury. *Brain Imaging Behav.* 14, 2210–2223. doi: 10.1007/s11682-019-00171-y

Chaturvedi, A., Luján, J. L., and McIntyre, C. C. (2013). Artificial neural network based characterization of the volume of tissue activated during deep brain stimulation. *J. Neural Eng.* 10:056023. doi: 10.1088/1741-2560/10/5/056023

Cohen, M. X. (2011a). Error-related medial frontal theta activity predicts cingulate-related structural connectivity. *Neuroimage* 55, 1373–1383. doi: 10.1016/j.neuroimage.2010.12.072

Cohen, M. X. (2011b). It's about time. *Front. Hum. Neurosci.* 5:2. doi: 10.3389/fnhum.2011.00002

Cohen, M. X. (2014). *Analyzing Neural Time Series Data: Theory and Practice*. Cambridge, MA:MIT press.

Conner, C. R., Ellmore, T. M., DiSano, M. A., Pieters, T. A., Potter, A. W., and Tandon, N. (2011). Anatomic and electro-physiologic connectivity of the language system: A combined DTI-CCEP study. *Comput. Biol. Med.* 41, 1100–1109. doi: 10.1016/j.compbiomed.2011.07.008

Cooper, P. S., Karayanidis, F., McKewen, M., McLellan-Hall, S., Wong, A. S. W., Skippen, P., et al. (2019). Frontal theta predicts specific cognitive control-induced behavioural changes beyond general reaction time slowing. *Neuroimage* 189, 130–140. doi: 10.1016/j.neuroimage.2019.01.022

Cox, R. W. (1996). AFNI: Software for analysis and visualization of functional magnetic resonance neuroimages. *Comput. Biomed. Res.* 29, 162–173. doi: 10.1006/cbmr.1996.0014

Dede, A. J., Marzban, N., Mishra, A., Reichert, R., Anderson, P. M., and Cohen, M. X. (2021). Prefrontal, striatal, and VTA subnetwork dynamics during novelty and exploration. *bioRxiv*[preprint]. doi: 10.1101/2021.11.24.469851

Duprez, J., Gulbinaite, R., and Cohen, M. X. (2020). Midfrontal theta phase coordinates behaviorally relevant brain computations during cognitive control. *NeuroImage* 207, 116340. doi: 10.1016/j.neuroimage.2019.116340

Entz, L., Tóth, E., Keller, C. J., Bickel, S., Groppe, D. M., Fabó, D., et al. (2014). Evoked effective connectivity of the human neocortex. *Hum. Brain Mapp.* 35, 5736–5753.

Fox, M. D., Buckner, R. L., White, M. P., Greicius, M. D., and Pascual-Leone, A. (2012). Efficacy of transcranial magnetic stimulation targets for depression is related to intrinsic functional connectivity with the subgenual cingulate. *Biol. Psychiatry* 72, 595–603.

Fuentemilla, L., Marco-Pallarés, J., and Grau, C. (2006). Modulation of spectral power and of phase resetting of EEG contributes differentially to the generation of auditory event-related potentials. *Neuroimage* 30, 909–916. doi: 10.1016/j.neuroimage.2005.10.036

Hamilton, M. (1960). A rating scale for depression. *J. Neurol. Neurosurg. Psychiatry* 23:56.

Hanslmayr, S., Klimesch, W., Sauseng, P., Gruber, W., Doppelmayr, M., Freunberger, R., et al. (2007). Alpha phase reset contributes to the generation of ERPs. *Cereb. Cortex* 17, 1–8. doi: 10.1093/cercor/bhj129

Herweg, N. A., Apitz, T., Leicht, G., Mulert, C., Fuentemilla, L., and Bunzeck, N. (2016). Theta-alpha oscillations bind the hippocampus, prefrontal cortex, and striatum during recollection: Evidence from simultaneous EEG–fMRI. *J. Neurosci.* 36, 3579–3587. doi: 10.1523/JNEUROSCI.3629-15.2016

Holtzheimer, P. E., Kelley, M. E., Gross, R. E., Filkowski, M. M., Garlow, S. J., Barrocas, A., et al. (2012). Subcallosal cingulate deep brain stimulation for treatment-resistant unipolar and bipolar depression. *Arch. Gene. Psychiatry* 69, 150–158.

Howell, B., Choi, K. S., Gunalan, K., Rajendra, J., Mayberg, H. S., and McIntyre, C. C. (2019). Quantifying the axonal pathways directly stimulated in therapeutic subcallosal cingulate deep brain stimulation. *Hum. Brain Mapp.* 40, 889–903. doi: 10.1002/hbm.24419

Keller, C. J., Honey, C. J., Mégevand, P., Entz, L., Ulbert, I., and Mehta, A. D. (2014). Mapping human brain networks with cortico-cortical evoked potentials. *Philos. Trans. R. Soc. B* 369:20130528

Keller, C. J., Huang, Y., Herrero, J. L., Fini, M. E., Du, V., Lado, F. A., et al. (2018). Induction and quantification of excitability changes in human cortical networks. *J. Neurosci.* 1088–1017.

Kimiskidis, V. K. (2016). Transcranial magnetic stimulation (TMS) coupled with electroencephalography (EEG): Biomarker of the future. *Revue Neurol.* 172, 123–126.

Klimesch, W., Sauseng, P., Hanslmayr, S., Gruber, W., and Freunberger, R. (2007). Event-related phase reorganization may explain evoked neural dynamics. *Neurosci. Biobehav. Rev.* 31, 1003–1016. doi: 10.1016/j.neubiorev.2007.03.005

Lio, G., Thobois, S., Ballanger, B., Lau, B., and Boulinguez, P. (2018). Removing deep brain stimulation artifacts from the electroencephalogram: Issues, recommendations and an open-source toolbox. *Clin. Neurophysiol.* 129, 2170–2185. doi: 10.1016/j.clinph.2018.07.023

Liu, L. D., Prescott, I. A., Dostrovsky, J. O., Hodaie, M., Lozano, A. M., and Hutchison, W. D. (2012). Frequency-dependent effects of electrical stimulation in the globus pallidus of dystonia patients. *J. Neurophysiol.* 108, 5–17. doi: 10.1152/jn.00527.2011

Luu, P., Tucker, D. M., and Makeig, S. (2004). Frontal midline theta and the error-related negativity: Neurophysiological mechanisms of action regulation. *Clin. Neurophysiol.* 115, 1821–1835.

Makeig, S., Debener, S., Onton, J., and Delorme, A. (2004). Mining event-related brain dynamics. *Trends Cogn. Sci.* 8, 204–210.

Marawar, R. A., Yeh, H. J., Carnabatu, C. J., and Stern, J. M. (2017). Functional MRI correlates of resting-state temporal theta and delta EEG rhythms. *J. Clin. Neurophysiol.* 34, 69–76.

Massimini, M., Ferrarelli, F., Huber, R., Esser, S. K., Singh, H., and Tononi, G. (2005). Breakdown of cortical effective connectivity during sleep. *Science* 309, 2228–2232.

Nakae, T., Matsumoto, R., Kunieda, T., Arakawa, Y., Kobayashi, K., Shimotake, A., et al. (2019). Connectivity Gradient in the Human Left Inferior Frontal Gyrus: Intraoperative Cortico-Cortical Evoked Potential Study. *Cereb. Cortex* 30, 4633–4650. doi: 10.1093/cercor/bhaa065

Narayanan, N. S., Cavanagh, J. F., Frank, M. J., and Laubach, M. (2013). Common medial frontal mechanisms of adaptive control in humans and rodents. *Nat. Neurosci.* 16, 1888–1895. doi: 10.1038/nn.3549

Narushima, K., McCormick, L. M., Yamada, T., Thatcher, R. W., and Robinson, R. G. (2010). Subgenual cingulate theta activity predicts treatment response of repetitive transcranial magnetic stimulation in participants with vascular depression. *J. Neuropsychiatry Clin. Neurosci.* 22, 75–84. doi: 10.1176/jnp.2010.22.1.75

Noecker, A. M., Choi, K. S., Riva-Posse, P., Gross, R. E., Mayberg, H. S., and McIntyre, C. C. (2018). StimVision software: Examples and applications in subcallosal cingulate deep brain stimulation for depression. *Neuromodulation* 21, 191–196. doi: 10.1111/ner.12625

Noecker, A. M., Choi, K. S., Riva-Posse, P., Gross, R. E., Mayberg, H. S., and McIntyre, C. C. (2017). StimVision Software: Examples and Applications in Subcallosal Cingulate Deep Brain Stimulation for Depression. *Neuromodulation* 21, 191–196.

Penny, W. D., Kiebel, S. J., Kilner, J. M., and Rugg, M. D. (2002). Event-related brain dynamics. *Trends Neurosci.* 25, 387–389.

Pizzagalli, D. A., Webb, C. A., Dillon, D. G., Tenke, C. E., Kayser, J., Goer, F., et al. (2018). Pretreatment rostral anterior cingulate cortex theta activity in relation to symptom improvement in depression: A randomized clinical trial. *JAMA Psychiatry* 75, 547–554. doi: 10.1001/jamapsychiatry.2018.0252

Reinhart, R. M. G., and Nguyen, J. A. (2019). Working memory revived in older adults by synchronizing rhythmic brain circuits. *Nat. Neurosci.* 22, 820–827. doi: 10.1038/s41593-019-0371-x

Riva-Posse, P., Choi, K. S., Holtzheimer, P. E., McIntyre, C. C., Gross, R. E., Chaturvedi, A., et al. (2014). Defining Critical White Matter Pathways Mediating Successful Subcallosal Cingulate Deep Brain Stimulation for Treatment-Resistant Depression. *Biological Psychiatry* 76, 963–9. doi: 10.1016/j.biopsych.2014.03.029

Riva-Posse, P., Choi, K., Holtzheimer, P. E., Crowell, A. L., Garlow, S. J., Rajendra, J. K., et al. (2018). A connectomic approach for subcallosal cingulate deep brain stimulation surgery: Prospective targeting in treatment-resistant depression. *Mol. Psychiatry* 23, 843–849. doi: 10.1038/mp.2017.59

Robble, M. A., Schroder, H. S., Kangas, B. D., Nickels, S., Breiger, M., Iturra-Mena, A. M., et al. (2021). Concordant neurophysiological signatures of cognitive control in humans and rats. *Neuropsychopharmacology* 46, 1252–1262. doi: 10.1038/s41386-021-00998-4

Sarasso, S., Boly, M., Napolitani, M., Gosseries, O., Charland-Verville, V., Casarotto, S., et al. (2015). Consciousness and complexity during unresponsiveness induced by propofol, xenon, and ketamine. *Curr. Biol.* 25, 3099–3105.

Shah, A. S., Bressler, S. L., Knuth, K. H., Ding, M., Mehta, A. D., Ulbert, I., et al. (2004). Neural dynamics and the fundamental mechanisms of event-related brain potentials. *Cereb. Cortex* 14, 476–483.

Smith, E. E., Reznik, S. J., Stewart, J. L., and Allen, J. J. (2017). Assessing and conceptualizing frontal EEG asymmetry: An updated primer on recording, processing, analyzing, and interpreting frontal alpha asymmetry. *Int. J. Psychophysiol.* 111, 98–114. doi: 10.1016/j.ijpsycho.2016.11.005

Smith, E. E., Tenke, C. E., Deldin, P. J., Trivedi, M. H., Weissman, M. M., Auerbach, R. P., et al. (2020). Frontal theta and posterior alpha in resting EEG: A critical examination of convergent and discriminant validity. *Psychophysiology* 57:e13483.

Solomon, E. A., Kragel, J. E., Gross, R., Lega, B., Sperling, M. R., Worrell, G., et al. (2018). Medial temporal lobe functional connectivity predicts stimulation-induced theta power. *Nat. Commun.* 9:4437. doi: 10.1038/s41467-018-06876-w

Trujillo, L. T., and Allen, J. J. (2007). Theta EEG dynamics of the error-related negativity. *Clin. Neurophysiol.* 118, 645–668.

Van Gompel, J. J., Klassen, B. T., Worrell, G. A., Lee, K. H., Shin, C., Zhao, C. Z., et al. (2015). Anterior nuclear deep brain stimulation guided by concordant hippocampal recording. *Neurosurg. Focus* 38:E9. doi: 10.3171/2015.3.FOCUS1541

Vergani, F., Martino, J., Morris, C., Attems, J., Ashkan, K., and Dell'Acqua, F. (2016). Anatomic connections of the subgenual cingulate region. *Neurosurgery* 79, 465–472.

Waters, A. C., Veerakumar, A., Choi, K. S., Howell, B., Tiruvadi, V., Bijanki, K. R., et al. (2018). Test-retest reliability of a stimulation-locked evoked response to deep brain stimulation in subcallosal cingulate for treatment resistant depression. *Hum. Brain Mapp.* 39, 4844–4856. doi: 10.1002/hbm.24327

Whitton, A. E., Webb, C. A., Dillon, D. G., Kayser, J., Rutherford, A., Goer, F., et al. (2019). Pretreatment Rostral Anterior Cingulate Cortex Connectivity With Salience Network Predicts Depression Recovery: Findings From the EMBARC Randomized Clinical Trial. *Biol. Psychiatry* 85, 872–880. doi: 10.1016/j.biopsych.2018.12.007

Yamao, Y., Suzuki, K., Kunieda, T., Matsumoto, R., Arakawa, Y., Nakae, T., et al. (2017). Clinical impact of intraoperative CCEP monitoring in evaluating the dorsal language white matter pathway. *Hum. Brain Mapp.* 38, 1977–1991. doi: 10.1002/hbm.23498

Yu, X., Ding, P., Yuan, L., Zhang, J., Liang, S., Zhang, S., et al. (2019). Cortico-cortical evoked potentials in tuberous sclerosis complex children using stereo-electroencephalography. *Front. Neurol.* 10:1093. doi: 10.3389/fneur.2019.01093

Zumsteg, D., Lozano, A. M., Wieser, H. G., and Wennberg, R. A. (2006). Cortical activation with deep brain stimulation of the anterior thalamus for epilepsy. *Clinical Neurophysiology* 117, 192–207.

frontiers | Frontiers in Human Neuroscience

TYPE Original Research
PUBLISHED 24 August 2022
DOI 10.3389/fnhum.2022.958247

OPEN ACCESS

EDITED BY
Michael S. Okun,
University of Florida, United States

REVIEWED BY
Takashi Morishita,
Fukuoka University, Japan
Jun Yu,
University of Florida, United States
Martijn Figee,
Icahn School of Medicine at Mount Sinai, United States

*CORRESPONDENCE
Pablo Andrade
pablo.andrade-montemayor@uk-koeln.de

SPECIALTY SECTION
This article was submitted to Brain Imaging and Stimulation, a section of the journal Frontiers in Human Neuroscience

RECEIVED 31 May 2022
ACCEPTED 01 August 2022
PUBLISHED 24 August 2022

CITATION
Heiden P, Weigel DT, Loução R, Hamisch C, Gündüz EM, Ruge MI, Kuhn J, Visser-Vandewalle V and Andrade P (2022) Connectivity in deep brain stimulation for self-injurious behavior: multiple targets for a common network?
Front. Hum. Neurosci. 16:958247.
doi: 10.3389/fnhum.2022.958247

Connectivity in deep brain stimulation for self-injurious behavior: multiple targets for a common network?

Petra Heiden[1,2], Daniel Tim Weigel[1], Ricardo Loução[1,2], Christina Hamisch[2], Enes M. Gündüz[1], Maximilian I. Ruge[1], Jens Kuhn[3,4], Veerle Visser-Vandewalle[1] and Pablo Andrade[1]*

[1]Department of Stereotactic and Functional Neurosurgery, Faculty of Medicine and University Hospital Cologne, University of Cologne, Cologne, Germany, [2]Department of Neurosurgery, Faculty of Medicine and University Hospital Cologne, University of Cologne, Cologne, Germany, [3]Department of Psychiatry and Psychotherapy, Faculty of Medicine and University Hospital Cologne, Cologne, Germany, [4]Department of Psychiatry, Psychotherapy and Psychosomatic, Johanniter Hospital Oberhausen, Oberhausen, Germany

Self-injurious behavior (SIB) is associated with diverse psychiatric conditions. Sometimes (e.g., in patients with autism spectrum disorder or acquired brain injuries), SIB is the most dominant symptom, severely restricting the psychosocial functioning and quality of life of the patients and inhibiting appropriate patient care. In severe cases, it can lead to permanent physical injuries or even death. Primary therapy consists of medical treatment and if implementable, behavioral therapy. For patients with severe SIB refractory to conventional therapy, neuromodulation can be considered as a last recourse. In scientific literature, several successful lesioning and deep brain stimulation targets have been described that can indicate a common underlying neuronal pathway. The objectives of this study were to evaluate the short- and long-term clinical outcome of patients with severe, therapy refractory SIB who underwent DBS with diverse underlying psychiatric disorders and to correlate these outcomes with the activated connectivity networks. We retrospectively analyzed 10 patients with SIB who underwent DBS surgery with diverse psychiatric conditions including autism spectrum disorder, organic personality disorder after hypoxic or traumatic brain injury or Tourette syndrome. DBS targets were chosen according to the underlying disorder, patients were either stimulated in the nucleus accumbens, amygdala, posterior hypothalamus, medial thalamus or ventrolateral thalamus. Clinical outcome was measured 6 months after surgery and at long-term follow-up after 10 or more years using the Early Rehabilitation Barthel index (ERBI) and time of restraint. Connectivity patterns were analyzed using normative connectome. Based on previous literature the orbitofrontal cortex, superior frontal gyrus, the anterior cingulate cortex, the amygdala and the hippocampus were chosen as regions of interest. This analysis showed a significant improvement in the functionality

of the patients with DBS in the short- and long-term follow-up. Good clinical outcome correlated with higher connectivity to the amygdala and hippocampus. These findings may suggest a common pathway, which can be relevant when planning a surgical procedure in patients with SIB.

KEYWORDS

self-injurious behavior, aggressiveness, deep brain stimulation, connectivity, psychosurgery

Introduction

Self-injurious behavior (SIB) is defined as a behavior where the affected individual inflicts physical injury upon him/herself (Minshawi et al., 2014). SIB is associated with diverse psychiatric disorders. In most cases it is part of the clinical appearance of the disease. In rare cases SIB is the most dominant symptom, almost solely limiting the patients' psychosociological functioning, reducing quality of life severely and inhibiting appropriate patient care. This mostly occurs in patients with advanced autism spectrum disorder, severe Tourette syndrome or in case of acquired brain injuries (Huisman et al., 2018). It is essential to differentiate SIB of these patients from non-suicidal self-injury in patients with borderline personality disorder or psychological distress (Brickman et al., 2014). Epidemiological studies have shown that about 4% to 9% of people with intellectual or developmental disabilities exhibit SIB; within the population of autism spectrum disorder this rate is 33% to 71% (Bradley et al., 2018) and within patients with Tourette syndrome 35% (Stafford and Cavanna, 2020). In severe cases, SIB can lead to serious permanent physical damages or even death and is frequently associated with social isolation and institutionalization. Further, it can entail a high psychological and financial burden for the social environment of the affected patient (Bradley et al., 2018).

Treatment should be focused on the underlying psychiatric diagnosis if a specific disorder is diagnosed (Antonacci et al., 2008). First-line treatment for SIB consists of pharmacological therapy. Mood stabilizers like valproate or carbamazepine have shown to be efficient in the treatment of aggression (Golden et al., 2006). Atypical antipsychotics are also used off-label, most frequently risperidone, aripiprazole or olanzapine. Behavioral therapies have been proven to be effective, however, severe symptoms may prohibit appropriate psychotherapeutic methods and only few have access to specialized centers (Antonacci et al., 2008). Also, several studies report a transient improvement of the symptoms after electroconvulsive therapy (Consoli et al., 2013).

Several stereotactic techniques have been introduced in the last decades with the aspiration to help patients with severe, otherwise therapy refractory SIB as a last resort. During the 1960s posteromedial hypothalamotomy and amygdalotomy emerged as treatment options for therapy refractory pathological aggressiveness (Narabayashi and Uno, 1966; Sano et al., 1966). Both procedures showed a significant improvement of the symptoms in more than half of the patients in the short- and long-term follow-up. However severe side effects were reported in studies with amygdalotomies, including Klüver-Bucy syndrome, seizures and hemiparesis (Narabayashi and Uno, 1966; Kiloh et al., 1974). Studies with hypothalamotomies only reported mild side effects (Sano et al., 1966). Further possible lesion targets described in subsequent literature are the anterior cingulate cortex (CC) and the anterior limb of the internal capsule (Jiménez et al., 2012). With the development of deep brain stimulation (DBS) it was reasonable to apply this possibly reversable method also for patients with severe pathological aggressiveness. The knowledge gained from studies using stereotactic lesioning was applied for the selection of possible target structures. The first DBS for pathological aggressiveness targeting the posteromedial hypothalamus was described by Franzini et al. (2005) in 2005. After that, Sturm et al. (2013) published the first case describing the efficacy of DBS of the amygdala for the treatment of pathological aggressiveness. Direct comparison of the reported cases is challenging due to the different clinical outcome measurements used, nonetheless most studies report satisfying results in most of the patients (Jiménez et al., 2012; Zhang et al., 2017; Torres et al., 2021; Yan et al., 2022). In summary, there are several possible target structures along the limbic system described in scientific literature for the treatment of pathological aggressiveness. It is believed that the neuronal circuits connecting the amygdala, the hippocampus and the periaqueductal gray, control reactive aggressiveness, moderated by the ventromedial frontal cortex, including the anterior CC (Rossel and Siever, 2015; Blair, 2016). Based on the functional and structural connections between the different stereotactic target regions and the observed beneficial outcome, this might indicate a common underlying neuronal network responsible for aggressive behavior.

The first objective of this study was to report the efficacy and safety of DBS in SIB patients treated at our clinic and their long-term clinical outcome. Our second objective was to analyze the connectivity patterns and the potentially identify common networks based on their clinical outcome.

Methods

Patient data

We retrospectively analyzed the data of 10 patients with SIB who underwent surgery for chronic DBS at the University Hospital Cologne between 2003 and 2009. All patients suffered from severe, continuous, therapy resistant SIB for a long time period, which was the dominant symptom of their disorder. All patients were evaluated by psychiatric experts from our hospital. Surgery was offered to these patients and their families or caregivers after individual evaluation by experienced neurosurgical and psychiatric specialists of the University Hospital Cologne. The performance of stereotactic surgery followed the premise of an individual attempt of healing in otherwise treatment refractory patients. The University Hospital of Cologne Medical Ethical Committee was informed and ethical approval was obtained before each intervention.

Five patients were diagnosed with therapy refractory Tourette syndrome, three patients developed SIB after hypoxic or traumatic brain injury and two patients suffered from SIB since childhood as part of their severe autism spectrum disorder. The target for DBS surgery was chosen according to the underlying psychiatric disorder, in all cases bilaterally. In three patients with Tourette syndrome the nucleus accumbens was targeted, in one patient the ventrolateral thalamus and in one further patient the posterolateral hypothalamus. In two patients with SIB after brain injury the posterolateral hypothalamus was targeted, in the third patient the medial thalamus. One patient with autism spectrum disorder received DBS in the nucleus accumbens, the second patient in the amygdala. Targets were identified using the Atlas of the Human Brain (Schaltenbrand and Wahren, 1977) and a preoperative MRI-scan. Stereotactic planning was performed using the STP 3.5 software (Howmedica Leibinger, Freiburg, Germany). Quadripolar electrodes (Medtronic 3389 or 3387, Medtronic Plc, Minneapolis, Minnesota, USA) were implanted stereotactically-guided, the accurate location of the electrodes was confirmed using intraoperative x-rays. Stimulation parameters were gradually adjusted individually during the follow-up visits.

Clinical outcome was measured using the Early Rehabilitation Barthel Index (ERBI) and percentage of time patients stay restrained, which was assessed prior to surgery, 6 months after the procedure and at the last follow-up appointment. On the ERBI each item measures the independency of the patient in daily activities. The final score ranges from −325 to +100 points, more positive values indicating higher independency (Rollnik, 2011). Patients were classified as responders with an improvement over 20 points on the ERBI (Quinn et al., 2011) 6 months after the surgery. Low-responders were defined as patients with an improvement between 20 and 100 points, patients were classified as good-responders with an improvement over 100 points.

Volume of activated tissue, connectivity and common activated fibers

In order to analyze the connectivity patterns, we estimated the volume of activated tissue using the following method. The preoperative T1 sequence of each patient was co-registered and normalized to ICBM 152 MNI 2009b space (Fonov et al., 2009) through a combination of linear and non-linear transformations, using Advanced Normalization Tools (ANTs[1], Avants et al., 2008; Tustison et al., 2019). The stereotactic AC/PC coordinates of the electrodes documented during surgery were transferred to MNI space and were projected using the open-source software Lead-DBS[2] (Horn and Kühn, 2015). Using the model described by Horn et al. (2017a), we estimated the volume stimulated by the active contacts (VTA, Volume of Tissue Activated) based on the stimulation parameters documented at the follow-up appointment 6 months past the surgery, with a general heuristic electrical field threshold of 0.2 V/mm.

Based on previous studies (Rossel and Siever, 2015; Blair, 2016; Rizzi et al., 2017) the medial and lateral orbitofrontal cortex (OFC), the superior frontal gyrus, the anterior CC, the amygdala, and the hippocampus were defined as regions of interest (ROIs). Subcortical nuclei were identified using the MNI PD25 (Xiao et al., 2017) atlas and cortical regions using the Desikan-Killiany atlas (Desikan et al., 2006). The connectivity of the VTAs to the ROIs was analyzed in a structural group connectome based on the diffusion spectrum imaging of 32 healthy adult subjects (Human Connectome Project, HCP; Setsomop et al., 2013; Horn et al., 2017b). Using TrackVis imaging software (Wang et al., 2007), we quantified the number of tracts passing through the VTAs and connecting each of them to each ROI. The VTAs for the left and right hemisphere were analyzed separately and only the connectivity to the ROI to the ipsilateral hemisphere was included in the analysis.

In a further analysis, we performed a whole-brain analysis identifying fibers associated with better clinical outcome. First, the tracts in the normative connectome which were hit by any VTA of the whole patient cohort were isolated. Then, for each tract of this subset, two groups of patients were defined: patients whose VTAs hit the tract in question, and patients whose VTAs did not hit the tract. The clinical outcomes of these two groups were then compared using Mann-Whitney-U test and an approximate z-value was calculated and attributed to the tract in question. Negative z-scores are associated with clinical worsening, while positive ones to clinical improvement. This analysis was performed iteratively on all tracts of the subset using custom-built MATLAB routines (version 2020b, The Mathworks Inc., Natick, Massachusetts, USA).

1 http://stnava.github.io/ANTs/
2 https://www.lead-dbs.org/

Statistical analysis

All data were analyzed using SPSS (IBM Corp. Released 2020. IBM SPSS Statistics for Macintosh, Version 28.0. Armonk, New York, USA). Each brain hemisphere was analyzed separately. In the absence of normal distribution determined using the Kolmogorov–Smirnov test, the Spearman rank's correlation was conducted between the connectivity parameters of each VTA with the individual ROIs and the clinical outcome. To compare clinical outcome at different time points the Wilcoxon test was conducted. p-values under 0.05 were considered significant. The data supporting the findings of this study, such as the DBS MRI datasets, are not publicly available due to data privacy regulations, but are available from the corresponding author upon reasonable request.

Results

Clinical outcome

Demographic and clinical data of the patients prior to surgery is summarized in Table 1. The mean age at the date of the surgery was 30.9 years (SD ± 11 years), ranging from 13 to 45 years. On average SIB persisted for 17.1 years prior to surgery (SD ± 14.7 years). Seven patients were males and three females. The mean ERBI at the time of the surgery

TABLE 1 Demographic table of the patients including stimulation parameters associated with the best clinical results 6 months past the surgery.

	Gender	Age at surgery (years)	Duration of symptoms (years)	Diagnosis	Target	Stimulation parameters
Patient 1	Male	45	40	Tourette syndrome	Posterior hypothalamus	3.5 V, 120 μs, 130 Hz C+, 1-, 2-
Patient 2	Male	24	6	Tourette syndrome	Nucleus accumbens	6.5 V, 120 μs, 130 Hz C+, 0-, 1-, 2-, 3-
Patient 3	Female	40	1	Hypoxic brain injury	Nucleus fasciculosus thalami	6.5 V, 90 μs, 130 Hz C+, 0-, 1-, 2-, 3-
Patient 4	Female	40	24	Tourette syndrome	Nucleus accumbens	4.5 V, 180 μs, 130 HZ C+, 0-, 1-
Patient 5	Male	47	32	Tourette syndrome	Nucleus accumbens	5.0 V, 150 μs, 60 Hz 1 +, 2-
Patient 6	Male	46	40	Autism spectrum disorder	Nucleus accumbens	6.0 V, 90 μs, 145 Hz C+, 1-, 2-, 3-
Patient 7	Male	25	22	Tourette syndrome	Ventrolateral thalamus	3.0 V, 120 μs, 130 Hz C+, 1-, 2-
Patient 8	Female	25	7	Traumatic brain injury	Posterior hypothalamus	2.8 V, 120 μs, 130 Hz C+, 0-, 1-
Patient 9	Male	24	0.5	Hypoxic brain injury	Posterior hypothalamus	5.5 V, 180 μs, 130 Hz C+, 1-, 2-, 3-
Patient 10	Male	13	10	Autism spectrum disorder	Amygdala	6.5 V, 90 μs, 130 Hz C+, 0-, 1-, 2-, 3-

Stimulation parameters were symmetrical in all patients.

TABLE 2 Summary of the clinical outcome and complications of each patient.

	Initial ERBI	Improvement in ERBI after 6 months	Comments
Patient 1	−30 points	0 points	No effect on SIB, discontinued the therapy after 7 years
Patient 2	−120 points	220 points	
Patient 3	−120 points	50 points	Discontinued follow up appointments
Patient 4	−65 points	165 points	Removal of the system after 1 month because of infection, reimplantation after 3 months. Discontinued the therapy after several years due to deterioration of health.
Patient 5	45 points	55 points	Multiple modifications in the stimulation parameters initially, including high frequency stimulation. Removal of the system after 5 years because of chronic infection. Reimplantation after 6 years for thalamic stimulation.
Patient 6	50 points	50 points	
Patient 7	45 points	55 points	
Patient 8	−105 points	120 points	Removal of the system after 3 months because of infection, reimplantation after 3 years
Patient 9	−135 points	125 points	
Patient 10	−110 points	160 points	Discontinued follow up appointments

was −54.5 points (SD ± 74.1). In all patients, there was a significant improvement 6 months after the surgery, with a mean ERBI of 38.5 points (SD ± 72.62; $z = -3.75$, $p < 0.001$). One patient was classified as a non-responder, four patients as low-responders and five as good-responders. There was also a significant reduction of the mean duration of restraint from 65% prior to surgery (SD ± 46.2%) to 11.5% (SD ± 15.9%) of the day 6 months after the intervention ($z = -3.09$, $p < 0.001$). The individual clinical course of each patient is displayed in **Table 2**.

Long-term follow-up after more than 10 years could be conducted in six patients. From the four patient who did not complete the long-term follow-up, two patients initially participated in follow-up appointments, however eventually did not visit our clinic anymore and could not be contacted *via* telephone or email. Two patients were excluded due to termination of the stimulation after several years because they did not benefit from the stimulation anymore. On average the last follow-up appointment was 14.7 years after the initial surgery (SD ± 2.3 years). The mean ERBI at the long-term follow-up was slightly lower than 6 months after the intervention, however the difference was not statistically significant (mean ERBI at long-term follow-up: 36.7, SD ± 74, $z = -1.86$, $p = 0.063$). Nonetheless, there was still a significant improvement when compared to the preoperative ERBI ($z = -2.87$, $p = 0.002$). The average time of restraint also increased in the long-term follow-up to 16.67% (SD ± 24.61%) of the day, however, there was still a significant difference to the pre-operative parameters ($z = -2.59$, $p = 0.01$).

Complications

Three patients had an infection of the DBS system, in one patient it occurred after 1 month, in the second patient after 3 months and in the third patient 5 years after the initial surgery. In all three cases a complete removal of the DBS system was performed. All three patients underwent additional surgery to reimplant the system at a later stage. Leads were placed at the same location in patients where the electrodes were removed after 1 and 3 months. For the third patient the target was changed from nucleus accumbens to the thalamus (centromedian nucleus/ventroralis internus). No further complications or permanent side effects were reported.

In both patients who underwent revision surgery within the first year, 6 months follow up data was collected 6 months after the reimplantation of the system.

Neuroimaging analysis

The proportion of tracts connecting the VTA to each ROI in all tracts activated by the VTA was calculated in the HCP normative connectome. There was a moderate correlation between the mean percentage of tracts connecting the VTAs to the medial OFC and the clinical improvement measured with the ERBI 6 months after the surgery (mean 5.21%, SD ± 8.72%, $r_s = 0.37$, $p = 0.109$; **Figure 1A**), however it was not statistically significant.

There was also no significant correlation between the proportion of tracts connecting to the lateral OFC (mean 3.89%, SD ± 4.91%, $r_s = 0.26$, $p = 0.26$; **Figure 1B**) or the superior frontal gyrus (mean 18.87%, SD ± 15.97, $r_s = -0.416$, $p = 0.068$; **Figure 1C**) and the clinical outcome.

The portion of tracts connecting the VTAs to the anterior CC moderately correlated with the clinical outcome, however this correlation was not statistically significant (mean 2.41%, SD ± 3.93%, $r_s = 0.383$, $p = 0.96$; **Figure 1D**).

Our data could show a significant moderate correlation between the clinical improvement measured on the ERBI and the percentage of tracts connecting to the amygdala (mean 12.04%, SD ± 14.19, $r_s = 0.478$, $p = 0.033$; **Figure 2**).

There was a stronger, also significant correlation between the clinical outcome and the proportion of tracts connecting to the hippocampus (mean 2.35%, SD ± 4.75, $r_s = 0.574$, $p = 0.008$; **Figure 3**).

Connectivity patterns of the VTAs to the whole brain weighted by clinical improvement of the patients are displayed in **Figures 4** and **5**. Tracts associated with better clinical improvement connected the VTAs to the amygdala, hippocampus and to the CC on both sides. Tracts associated with worse clinical outcome showed stronger connectivity to the superior frontal gyrus. In the OFC, activated fibers connecting to the medial part were associated with a greater clinical improvement, while fibers connecting to the lateral OFC were associated with less improvement measured on the ERBI.

Discussion

In this retrospective study we analyzed the clinical course of 10 patients with diverse psychiatric disorders under DBS, which all suffered from severe, chronic, therapy refractory SIB. Primary outcome was the improvement of functionality measured on the ERBI. As a further representative measurement for the psychosocial functionality of the patients we compared their time of restraint.

Our study showed a significant improvement in the functionality and time of restraint in SIB patients treated with DBS after 6 months as well as in a long-term follow-up with over 10 years of stimulation. In this retrospective analysis, 9 out of 10 patients reached satisfactory results with DBS, whereas one patient was a clear non-responder. A further patient was explanted due to loss of effect of the stimulation after several years of profiting from DBS. These results fall in line with the clinical outcome reported in the literature (Torres et al., 2021;

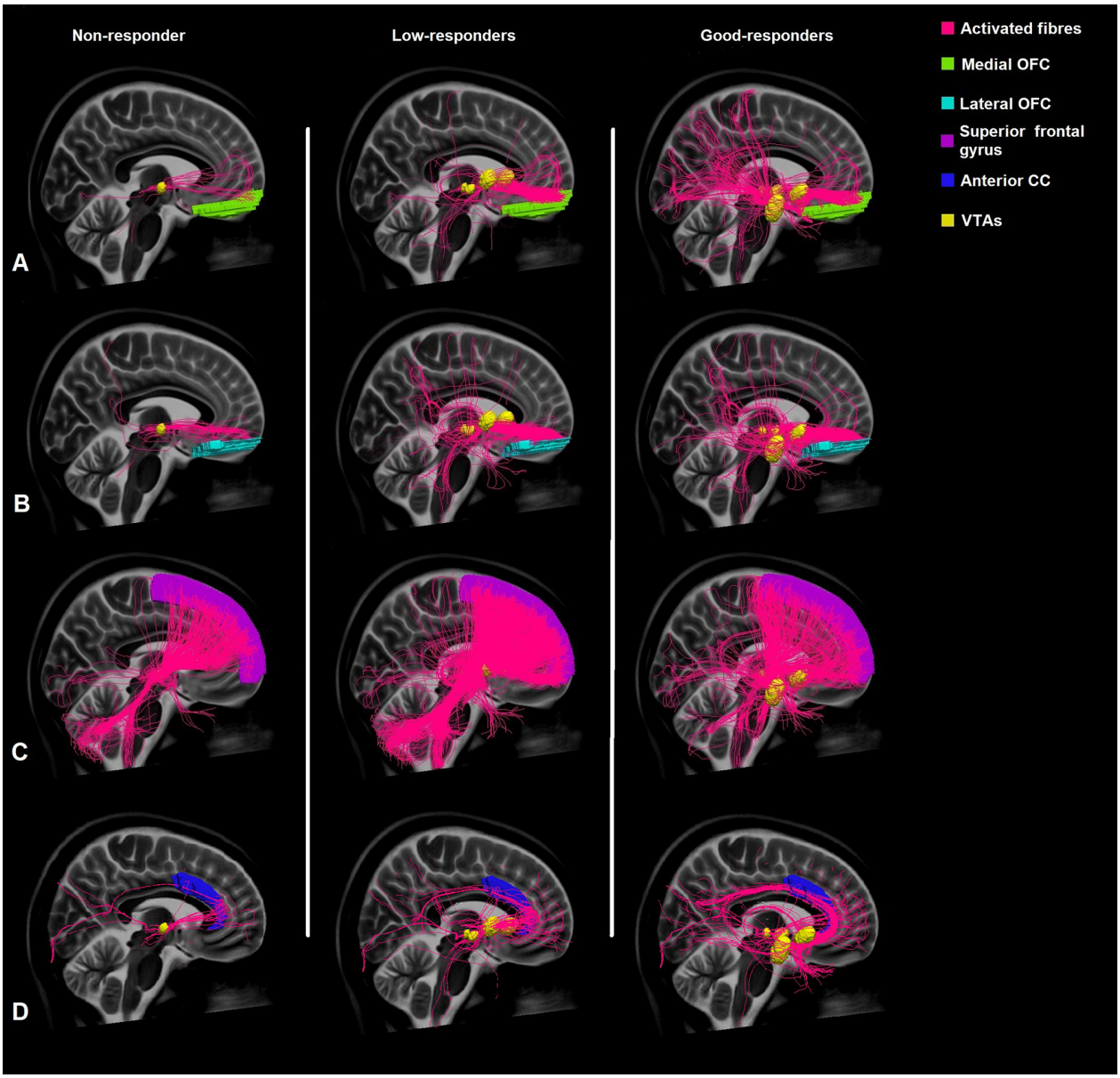

FIGURE 1
Comparison of the connectivity of the VTAs of non-responders, low-responders, and good-responders to the medial orbitofrontal cortex (medial OFC) **(A)**, lateral orbitofrontal cortex (lateral OFC) **(B)**, superior frontal gyrus **(C)**, and the anterior cingulate cortex (anterior CC) **(D)** based on normative connectome.

Yan et al., 2022), however direct comparison is not possible due to different outcome measures. In our patient group, there was no further improvement in the long-term follow-up, rather a slight deterioration compared to the follow-up 6 months after the intervention. There was still a significant improvement of the clinical status in the long-term follow-up in comparison to the baseline. Three out of 10 cases needed additional surgery because of an infection of the DBS-system were reported, which resulted in additional surgeries for the patients. All patients did well after re-implantation and suffered no permanent complications. This infection-rate is higher than in other DBS-studies, reporting a risk of infection of 5% (Kantzanou et al., 2021), probably due to the complex care and specific clinical status on account of skin wounds of patients suffering from SIB.

Analysis of the connectivity patterns using normative connectome showed a significant positive correlation between clinical improvement and the strength of connectivity to the hippocampus and the amygdala. Further, fibers associated

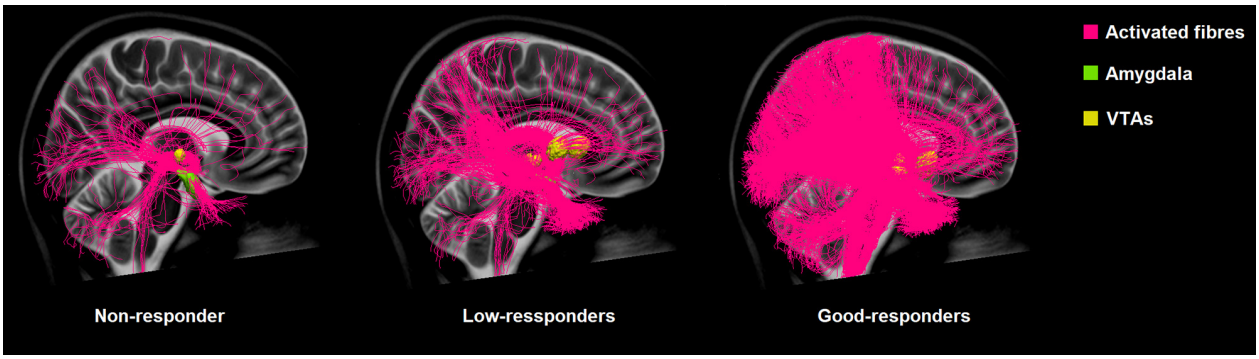

FIGURE 2
Comparison of the connectivity of the VTAs of non-responders, low-responders, and good-responders to the amygdala based on normative connectome.

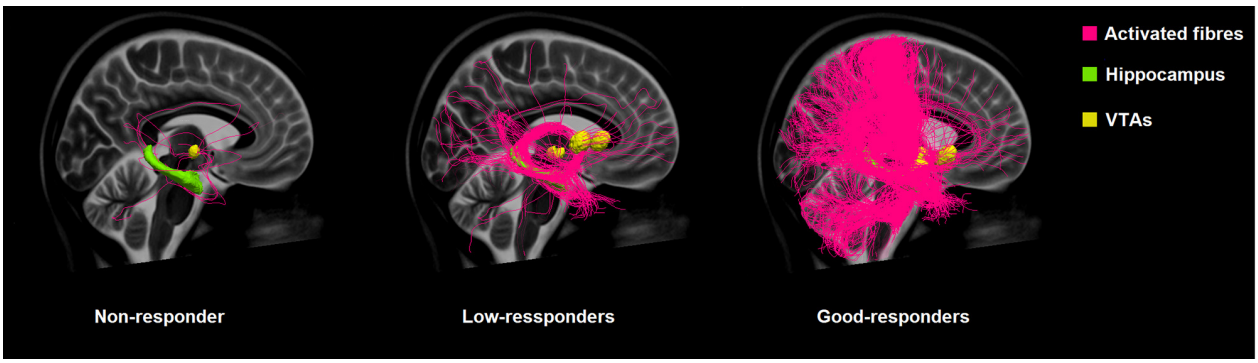

FIGURE 3
Comparison of the connectivity of the VTAs of non-responders, low-responders, and good-responders to the hippocampus based on normative connectome.

with better clinical outcome were shown to be connected to the amygdala and hippocampus and to the CC as well. Activated fibers projecting to the prefrontal cortex overlap the medial forebrain bundle as described by Coenen et al. (2018), these fibers are mostly associated with reward-associated behavior and motivation. Interestingly fibers associated with less improvement in the ERBI after 6 months organize in a more dorsal pathway which also overlaps the common pathway for deep-brain-stimulation in obsessive-compulsive disorder, as described by Li et al. (2020). Fibers which were associated with a better clinical outcome organize in a more ventral circuit and project more to the medial OFC.

Our results suggest a common underlying neuronal network which is stimulated at different areas in these patients, resulting in reduction of SIB. Whole-brain analysis also indicates a clear differentiation of this network from the common pathway previously identified for the treatment of obsessive-compulsive disorder. Identification of a common pathway would be especially helpful in these patients as they suffer from different underlying disorders, which should be also considered during the planning of a DBS procedure. For example, in patients with Tourette syndrome and SIB it might be beneficial to consider underlying pathways both in regard to the underlying neuropsychiatric condition and the auto-mutilative behavior. Previous studies showed that stronger connectivity to the supplementary motor area (SMA) and preSMA correlate with better tic-reduction (Andrade et al., 2020), thus a target affecting the motoric pathways and also with strong connectivity to the amygdala and hippocampus might be most beneficial for Tourette patients suffering from SIB.

Activated fibers associated with a worse clinical outcome projected to the superior frontal gyrus and the lateral OFC. However, it is important to note, that these fibers were not correlating with an increase of SIB, as none of the patients had a worse clinical outcome in compare to the baseline parameters at the follow-ups. Thus, these fibers probably have no association with the modulation of SIB.

An important limitation of this study is, that it analyses a symptom in a diversity of underlying psychiatric conditions, which makes the comparison and unification of these patients difficult.

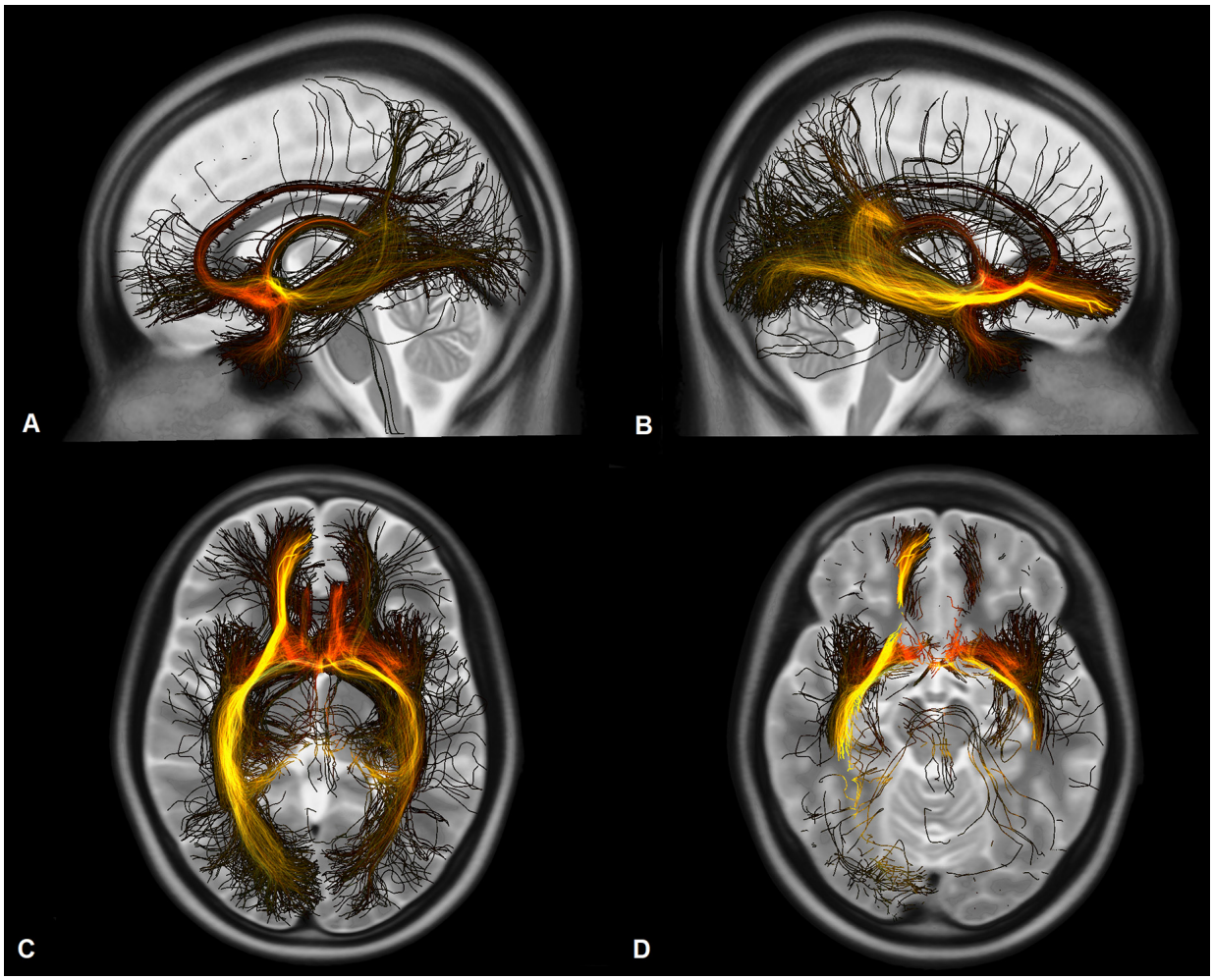

FIGURE 4
Fibers activated by the VTAs and associated with a better functional outcome of the patients measured on the ERBI in sagittal view from the left **(A)**, from the right **(B)**, in axial view on the level of the thalami **(C)**, and on the level of the hippocampus and the amygdala **(D)**. Darker colors represent a stronger correlation to the clinical outcome.

Regarding the method of neuroimage analysis, it is important to remark, that traumatic and hypoxic brain injuries are associated with altered structural and functional connectivity (Hayes et al., 2016; Smyser et al., 2019), therefore using a normative connectome when analyzing these patients might be misleading. Structural abnormalities have been also reported in the socio-emotional circuits of patients with autism spectrum disorder (Ameis et al., 2011) and studies also show an altered functional and structural connectivity in Tourette syndrome (Worbe et al., 2012; Cheng et al., 2014; Heiden et al., 2021). Analysis based on patient specific diffusion imaging data would be more suitable considering this patient collective. A further limitation is the low number of subjects in this study, which has a considerable effect on the interpretation of the clinical and neuroimaging results. A multi-center study involving larger patient groups would be necessary to further isolate neuronal networks which contribute to the reduction of SIB. However, the diversity of underlying psychiatric conditions and comorbidities of patients with SIB might complicate such an analysis. Randomized-controlled studies, although potentially of a high scientific value, are less likely to be successful in this particular patient group because of the complicated care, ethical issues related to informed consent, and lacking compliance of this patient population.

Conclusion

In this study, we reported an improvement of the psychosocial functionality in patients with diverse psychiatric

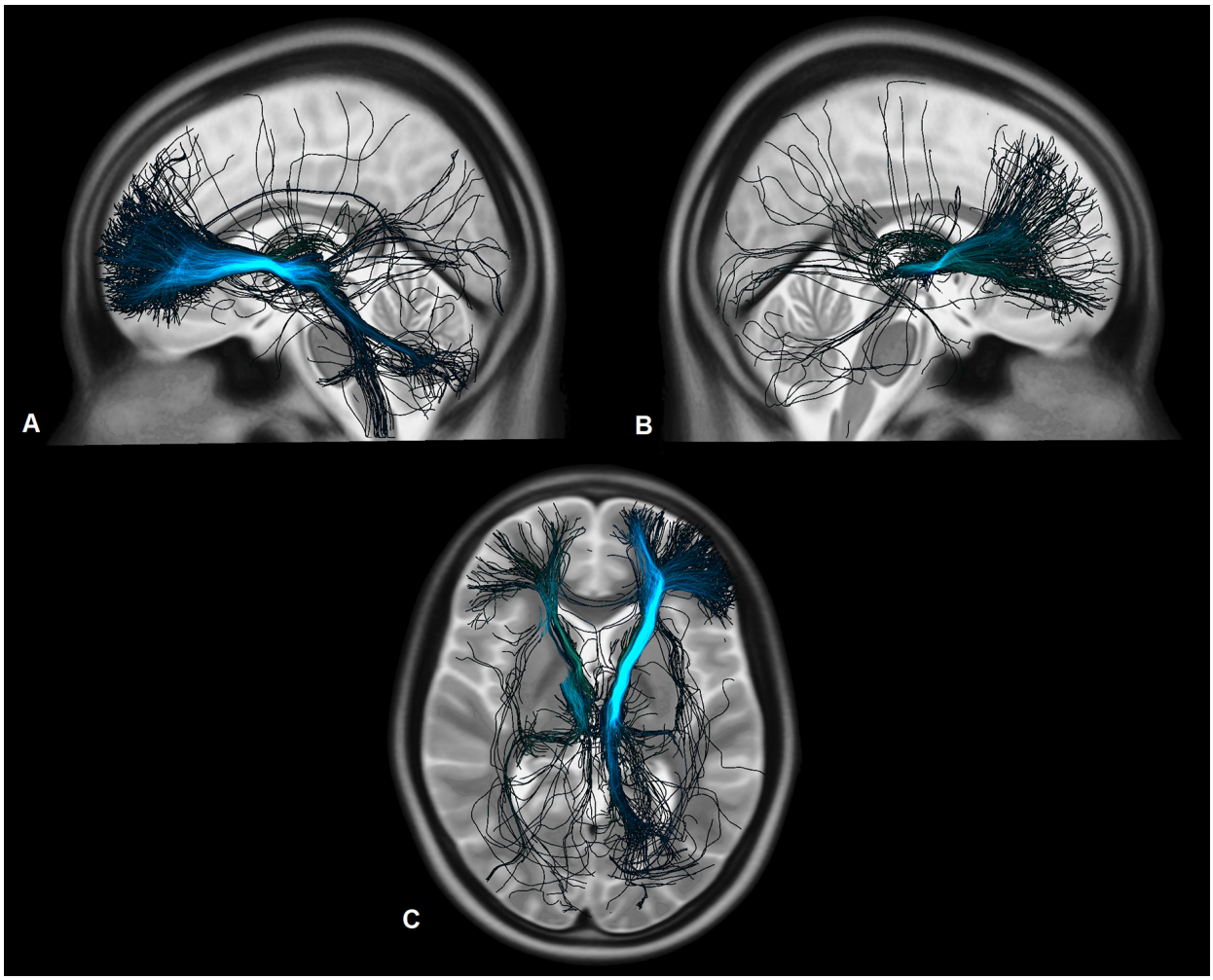

FIGURE 5
Fibers activated by the VTAs and associated with a worse functional outcome of the patients measured on the ERBI in sagittal view from the left **(A)**, from the right **(B)**, and in axial view on the level of the thalami **(C)**. Darker colors represent a stronger correlation to the clinical outcome.

conditions with severe SIB using DBS in diverse anatomical targets. We showed a significant correlation between the clinical improvement and connectivity patterns with higher number of activated tracts to the amygdala and the hippocampus bilaterally. These findings suggest the presence of a common underlying neuronal network for SIB between these targets, which can eventually assist when considering a surgical procedure for treatment refractory patients with diverse underlying conditions and comorbidities.

Data availability statement

The raw data supporting the conclusions of this article will be made available by the authors, without undue reservation.

Ethics statement

Ethical review and approval was not required for the study on human participants in accordance with the local legislation and institutional requirements. Written informed consent for participation was not required for this study in accordance with the national legislation and the institutional requirements.

Author contributions

PH, VV-V, and PA: conceptualization. PH, DW, RL, CH, EG, MR, JK, and PA: investigation. PH, DW, RL, and PA: methods. PH and PA: writing—original draft. PH, DW, RL, CH, EG, MR, JK, VV-V, and PA: writing—review and editing. All authors contributed to the article and approved the submitted version.

Funding

We acknowledge support for the Article Processing Charge from the DFG (German Research Foundation, 491454339).

Conflict of interest

The authors declare that the research was conducted in the absence of any commercial or financial relationships that could be construed as a potential conflict of interest.

Publisher's note

All claims expressed in this article are solely those of the authors and do not necessarily represent those of their affiliated organizations, or those of the publisher, the editors and the reviewers. Any product that may be evaluated in this article, or claim that may be made by its manufacturer, is not guaranteed or endorsed by the publisher.

References

Ameis, S. H., Fan, J., Rockel, C., Voineskos, A. N., Lobaugh, N. J., Soorya, L., et al. (2011). Impaired structural connectivity of socio-emotional circuits in autism spectrum disorders: a diffusion tensor imaging study. *PLoS One* 6:e28044. doi: 10.1371/journal.pone.0028044

Andrade, P., Heiden, P., Hoevels, M., Schlaman, M., Baldermann, J. C., Huys, D., et al. (2020). Modulation of fibers to motor cortex during thalamic DBS in Tourette patients correlates with tic reduction. *Brain Sci.* 10:302. doi: 10.3390/brainsci10050302

Antonacci, D. J., Manuel, C., and Davis, E. (2008). Diagnosis and treatment of aggression in individuals with developmental disabilities. *Psychiatr. Q.* 79, 225–247. doi: 10.1007/s11126-008-9080-4

Avants, B. B., Epstein, C. L., Grossmann, M., and Gee, J. C. (2008). Symmetric diffeomorphic image registration with cross-correlation: evaluating automated labeling of elderly and neurodegenerative brain. *Med. Image Anal.* 12, 26–41. doi: 10.1016/j.media.2007.06.004

Blair, J. R. (2016). The neurobiology of impulsive aggression. *J. Child Adolesc. Psychopharmacol.* 26, 4–9. doi: 10.1089/cap.2015.0088

Bradley, V., Hiersteiner, D., Rotholz, D., Maloney, J., Li, H., Bonardi, A., et al. (2018). Personal characteristics and outcomes of individuals with developmental disabilities who need support for self-injurious behavior. *J. Intellect. Disabil. Res.* 62, 1043–1057. doi: 10.1111/jir.12518

Brickman, L. J., Ammerman, B. A., Look, A. E., Berman, M. E., and McCloskey, M. S. (2014). The relationship between non-suicidal self-injury and borderline personality disorder symptoms in a college sample. *Borderline Pers. Disord. Emot. Dysregul.* 1:14. doi: 10.1186/2051-6673-1-14

Cheng, B., Braas, H., Ganos, C., Treszl, A., Biermann-Ruben, K., Hummel, F. C., et al. (2014). Altered intrahemispheric structural connectivity in Gilles de la Tourette syndrome. *Neuroimage Clin.* 4, 174–181. doi: 10.1016/j.nicl.2013.11.011

Coenen, V. A., Schuhmacher, L. V., Kaller, C., Schlaepfer, T. E., Reinacher, P. C., Egger, K., et al. (2018). The anatomy of the human medial forebrain bundle: ventral tegmental area connections to reward-associated subcortical and frontal lobe regions. *Neuroimage Clin.* 18, 770–783. doi: 10.1016/j.nicl.2018.03.019

Consoli, A., Cohen, J., Bodeau, N., Guinchat, V., Wachtel, L., and Cohen, D. (2013). Electroconvulsive therapy in adolescents with intellectual disability and severe self-injurious behavior and aggression: a retrospective study. *Eur. Child Adolesc. Psychiatry* 22, 55–62. doi: 10.1007/s00787-012-0320-7

Desikan, R. S., Ségonne, F., Fischl, B., Quinn, B. T., Dickerson, B. C., Blacker, D., et al. (2006). An automated labeling system for subdividing the human cerebral cortex on MRI scans into gyral based regions of interest. *Neuroimage* 31, 968–980. doi: 10.1016/j.neuroimage.2006.01.021

Fonov, V. S., Evans, A. C., McKinstry, R. C., Almli, C. R., and Collins, D. L. (2009). Unbiased nonlinear average age-appropiate brain templates from birth to adulthood. *Neuroimage* 47:S102. doi: 10.1016/S1053-8119(09)70884-5

Franzini, A., Marras, C., Ferroli, P., Bugiani, O., and Broggi, G. (2005). Stimulation of the posterior hypothalamus for medically intractable impulsive and violent behavior. *Stereotact. Funct. Neurosurg.* 83, 63–66. doi: 10.1159/000086675

Golden, A. S., Haut, S. R., and Moshé, S. L. (2006). Nonepileptic uses of antiepileptic drugs in children and adolescents. *Pediatr. Neurol.* 34, 421–432. doi: 10.1016/j.pediatrneurol.2005.08.017

Hayes, J. P., Bigler, E. D., and Verfaellie, M. (2016). Traumatic brain injury as a disorder of brain connectivity. *J. Int. Neuropsychol. Soc.* 22, 120–137. doi: 10.1017/S1355617715000740

Heiden, P., Hoevels, M., Bayram, D., Baldermann, J. C., Schüller, T., Huys, D., et al. (2021). Connectivity patterns of deep brain stimulation targets in patients with Gilles de la Tourette syndrome. *Brain Sci.* 11:87. doi: 10.3390/brainsci11010087

Horn, A., and Kühn, A. A. (2015). Lead-DBS: a toolbox for deep brain stimulation electrode localizations and visualizations. *Neuroimage* 107, 127–135. doi: 10.1016/j.neuroimage.2014.12.002

Horn, A., Kühn, A. A., Merkl, A., Shih, L., Alterman, R., and Fox, M. (2017a). Probabilistic conversion of neurosurgical DBS electrode coordinates into MNI space. *Neuroimage* 150, 395–404. doi: 10.1016/j.neuroimage.2017.02.004

Horn, A., Reich, M., Vorwerk, J., Li, N., Wenzel, G., Fang, Q., et al. (2017b). Connectivity Predicts deep brain stimulation outcome in Parkinson disease. *Ann. Neurol.* 82, 67–78. doi: 10.1002/ana.24974

Huisman, S., Mulder, P., Kuijk, J., Kerstholt, M., van Eeghen, A., Leenders, A., et al. (2018). Self-injurious behavior. *Neurosci. Biobehav. Rev.* 84, 483–491. doi: 10.1016/j.neubiorev.2017.02.027

Jiménez, F., Soto, J. E., Velasco, F., Andrade, P., Bustamante, J. J., Gómez, P., et al. (2012). Bilateral cingulotomy and anterior capsulotomy applied to patients with aggressiveness. *Stereotact. Funct. Neurosurg.* 90, 151–160. doi: 10.1159/000336746

Kantzanou, M., Korfias, S., Panourias, I., Sakas, E. D., and Karalexi, M. A. (2021). Deep brain stimulation-related surgical site infections: a systematic review and meta-analysis. *Neuromodulation* 24, 197–211. doi: 10.1111/ner.13354

Kiloh, L. G., Gye, R. S., Rusworth, R. G., Bell, D. S., and White, R. T. (1974). Stereotactic amygdalotomy for aggressive behavior. *J. Neurol. Neursurg. Psychiatry* 37, 437–444. doi: 10.1136/jnnp.37.4.437

Li, N., Baldermann, J. C., Kibleur, A., Treu, S., Akram, H., Elias, G. J. B., et al. (2020). A unified connectomic target for deep brain stimulation in obsessive-compulsive disorder. *Nat. Commun.* 11:3364. doi: 10.1038/s41467-020-16734-3

Minshawi, N. F., Hurwitz, S., Fodstad, J. C., Biebl, S., Morriss, D. H., and McDougle, C. J. (2014). The association between self-injurious behavior and autism spectrum disorders. *Psychol. Res. Behav. Manage.* 7, 125–136. doi: 10.2147/PRBM.S44635

Narabayashi, H., and Uno, M. J. S. (1966). Long range results of stereotaxic amygdalotomy for behavior disorders. *Confin. Neurol.* 27, 168–171. doi: 10.1159/000103950

Quinn, T. J., Langhorne, P., and Stott, D. J. (2011). Barthel Index for stroke trials: development, properties, and application. *Stroke* 42, 1146–1151. doi: 10.1161/STROKEAHA.110.598540

Rizzi, M., Trezza, A., Messina, G., De Benedictis, A., Franzini, A., and Marras, C. E. (2017). Exploring the brain through posterior hypothalamus surgery for aggressive behavior. *Neurosurg. Focus* 43:E14. doi: 10.3171/2017.6.FOCUS17231

Rollnik, J. D. (2011). The early rehabilitation barthel index. *Rehabilitation (Stuttg)* 50, 408–411. doi: 10.1055/s-0031-1273728

Rossel, D. R., and Siever, L. J. (2015). The neurobiology of aggression and violence. *CNS Spectr.* 20, 254–279. doi: 10.1017/S109285291500019X

Sano, K., Yoshioka, M., Ogashiwa, M., Ishijima, B., and Ohye, C. J. S. (1966). Postero-medial hypothalamotomy in the treatment of aggressive behaviors. *Confin. Neurol.* 27, 164–167. doi: 10.1159/000103949

Schaltenbrand, G., and Wahren, W. (1977). *Atlas for Stereotaxy of the Human Brain*. 2nd edn. Stuttgart: Thieme.

Setsomop, K., Kimmlingen, R., Eberlein, E., Witzel, T., Cohen-Adad, J., McNab, J. A., et al. (2013). Pushing the limits of *in vivo* diffusion MRI for the Human Connectome Project. *Neuroimage* 80, 220–233. doi: 10.1016/j.neuroimage.2013.05.078

Smyser, C. D., Wheelock, M. D., Limbrick, D. D., Jr., and Neil, J. J. (2019). Neonatal brain injury and aberrant connectivity. *Neuroimage* 185, 609–623. doi: 10.1016/j.neuroimage.2018.07.057

Stafford, M., and Cavanna, A. E. (2020). Prevalence and clinical correlates of self-injurious behavior in Tourette syndrome. *Neurosci. Biobehav. Rev.* 113, 299–307. doi: 10.1016/j.neubiorev.2020.03.022

Sturm, V., Fricke, O., Bührle, C. P., Lenartz, D., Maarouf, M., Treuer, H., et al. (2013). DBS in the basolateral amygdala improves symptoms of autism and related self-injurious behavior: a case report and hypothesis on the pathogenesis of the disorder. *Front. Hum. Neurosci.* 6:341. doi: 10.3389/fnhum.2012.00341

Torres, C. V., Blasco, G., Navas García, M., Ezquiaga, E., Pastor, J., Vega-Zelaya, L., et al. (2021). Deep brain stimulation for aggressiveness: long-term follow-up and tractography study of the stimulated brain areas. *J. Neurosurg.* 134, 366–375. doi: 10.3171/2019.11.JNS192608

Tustison, N. J., Avants, B. B., and Gee, J. C. (2019). Learning image-based spatial transformation via convolutional neural networks: a review. *Magn. Reson. Imaging* 64, 142–153. doi: 10.1016/j.mri.2019.05.037

Wang, R., Benner, T., Sorensen, A. G., and Wedeen, V. J. (2007). Diffusion toolkit: a software package for diffusion imaging data processing and tractography. *Proc. Int. Soc. Mag. Reson. Med.* 15:3720. Available online at: http://www.trackvis.org/faq/2007_ISMRM_diffusion_toolkit.pdf.

Worbe, Y., Malherbe, C., Hartmann, A., Pélégrini-Issac, M., Messé, A., Vidailhet, M., et al. (2012). Functional immaturity of cortico-basal ganglia networks in Gilles de la Tourette syndrome. *Brain* 135, 1937–1946. doi: 10.1093/brain/aws056

Xiao, Y., Fonov, V., Chakravarty, M. M., Bériault, S., Al-Subaie, F., Sadikot, A., et al. (2017). A dataset of multi-contrast population-averaged brain MRI atlases of a Parkinson's disease cohort. *Data Brief* 12, 370–379. doi: 10.1016/j.dib.2017.04.013

Yan, H., Elkaim, L. M., Venetucci Gouveia, F., Huber, J. F., Germann, J., Loh, A., et al. (2022). Deep brain stimulation for extreme behaviors associated with autism spectrum disorder converges on a common pathway: a systematic review and connectomic analysis. *J. Neurosurg.* doi: 10.3171/2021.11.JNS21928. [Online ahead of print].

Zhang, S., Zhou, P., Jiang, S., Li, P., and Wang, W. (2017). Bilateral anterior capsulotomy and amygdalotomy for mental retardation with psychiatric symptoms and aggression. *Medicine (Baltimore)* 96:e5840. doi: 10.1097/MD.0000000000005840

frontiers | Frontiers in Human Neuroscience

TYPE Original Research
PUBLISHED 24 August 2022
DOI 10.3389/fnhum.2022.929509

OPEN ACCESS

EDITED BY
Vladimir Litvak,
University College London,
United Kingdom

REVIEWED BY
Madeleine Lowery,
University College Dublin, Ireland
Robert LeMoyne,
Northern Arizona University,
United States
Monika Pötter-Nerger,
University of Hamburg, Germany

*CORRESPONDENCE
Michael S. Okun
okun@neurology.ufl.edu

SPECIALTY SECTION
This article was submitted to
Brain Imaging and Stimulation,
a section of the journal
Frontiers in Human Neuroscience

RECEIVED 26 April 2022
ACCEPTED 27 July 2022
PUBLISHED 24 August 2022

CITATION
Okun MS, Hickey PT, Machado AG,
Kuncel AM and Grill WM (2022)
Temporally optimized patterned
stimulation (TOPS®) as a therapy
to personalize deep brain stimulation
treatment of Parkinson's disease.
Front. Hum. Neurosci. 16:929509.
doi: 10.3389/fnhum.2022.929509

Temporally optimized patterned stimulation (TOPS®) as a therapy to personalize deep brain stimulation treatment of Parkinson's disease

Michael S. Okun[1]*, Patrick T. Hickey[2], Andre G. Machado[3], Alexis M. Kuncel[4] and Warren M. Grill[4,5]

[1]Department of Neurology, Norman Fixel Institute for Neurological Diseases, University of Florida, Gainesville, FL, United States, [2]Department of Neurology, Movement Disorders Center, Duke University Medical Center, Durham, NC, United States, [3]Department of Neurology, Neurological Institute, Cleveland Clinic, Cleveland, OH, United States, [4]Deep Brain Innovations, Cleveland, OH, United States, [5]Department of Biomedical Engineering, Duke University, Durham, NC, United States

Deep brain stimulation (DBS) is a well-established therapy for the motor symptoms of Parkinson's disease (PD), but there remains an opportunity to improve symptom relief. The temporal pattern of stimulation is a new parameter to consider in DBS therapy, and we compared the effectiveness of Temporally Optimized Patterned Stimulation (TOPS) to standard DBS at reducing the motor symptoms of PD. Twenty-six subjects with DBS for PD received three different patterns of stimulation (two TOPS and standard) while on medication and using stimulation parameters optimized for standard DBS. Side effects and motor symptoms were assessed after 30 min of stimulation with each pattern. Subjects experienced similar types of side effects with TOPS and standard DBS, and TOPS were well-tolerated by a majority of the subjects. On average, the most effective TOPS was as effective as standard DBS at reducing the motor symptoms of PD. In some subjects a TOPS pattern was the most effective pattern. Finally, the TOPS pattern with low average frequency was found to be as effective or more effective in about half the subjects while substantially reducing estimated stimulation energy use. TOPS DBS may provide a new programing option to improve DBS therapy for PD by improving symptom reduction and/or increasing energy efficiency. Optimizing stimulation parameters specifically for TOPS DBS may demonstrate further clinical benefit of TOPS DBS in treating the motor symptoms of Parkinson's disease.

KEYWORDS

Parkinson's disease, deep brain stimulation, movement disorders, subthalamic nucleus, programming, stimulation parameters

Introduction

Deep brain stimulation (DBS) of the subthalamic nucleus (STN) is a well-established therapy for the treatment of Parkinson's disease (PD) (Benabid et al., 2009). The efficacy of DBS is highly dependent upon the programing of stimulation parameters, including the pulse amplitude, pulse duration, and pulse repetition frequency, and, the lack of understanding of the mechanisms of action has limited the optimization of this therapy.

High frequency (>100 Hz) stimulation has been overall more effective than low frequency DBS in treating tremor and most PD motor features (Rizzone et al., 2001; Moro et al., 2002; Kuncel et al., 2006). The basis for the frequency-dependent effects on symptoms was hypothesized to be related to the frequency-dependent regularization (or masking) of pathological neural activity (Birdno and Grill, 2008) and this is one of several hypothesized mechanisms of action of DBS (McIntyre et al., 2004; Herrington et al., 2016). In addition to the strong dependence on frequency, the effects of DBS on the motor symptoms of PD are also dependent upon the temporal pattern of stimulation (Grill, 2018). Random patterns of stimulation applied in PD patients, despite having the same high average frequency, were less effective at suppressing bradykinesia than regular patterns of stimulation (Dorval et al., 2010), and similar observations were made in patients with essential tremor (Birdno et al., 2008). The dependence of DBS efficacy on both the frequency and the temporal pattern of stimulation motivated the idea that the temporal pattern of DBS could be manipulated to increase the efficacy and efficiency of PD DBS. Indeed, acute, intraoperative assessment in subjects undergoing implanted pulse generator (IPG) replacement surgery (Swan et al., 2014) revealed that certain non-regular patterns of DBS treated bradykinesia more effectively than conventional high frequency DBS (Brocker et al., 2013) while a second pattern produced equivalent reductions in bradykinesia but greatly improved energy efficiency (Brocker et al., 2017).

A randomized prospective study was designed to determine the effects of Temporally Optimized Patterned Stimulation (TOPS®) on the motor symptoms of PD. This study was conducted across three centers for a longer duration than the intraoperative pilot studies. The study used custom firmware temporarily downloaded onto previously implanted IPGs to enable the delivery of novel stimulation patterns. A subject's clinically optimized DBS parameter settings were used whenever possible. We evaluated two of the most promising patterns identified in the previous acute intraoperative study–designated TOPS1 and TOPS2–and compared the most effective TOPS to standard DBS and no stimulation.

Abbreviations: DBS, deep brain stimulation; STN, subthalamic nucleus; PD, Parkinson's disease; IPG, implanted pulse generator; TOPS, temporally optimized patterned stimulation; WO19, wearing-off-19 QUICK questionnaire; UPDRS, unified Parkinson's disease rating scale; MCID, minimally clinically important difference; PIGD, postural instability and gait disturbance; ANOVA, analysis of variance; sDBS, standard DBS.

Materials and methods

This study was a prospective, randomized, cross-over, feasibility study. The effectiveness of two different non-regular temporal patterns of stimulation (TOPS1 and TOPS2) and standard DBS (sDBS) was compared with no stimulation (no stim).

Study subjects

Individuals were recruited to participate in this study from the movement disorders centers at three sites including the Cleveland Clinic Foundation (Cleveland, OH), Duke University Medical Center (Durham, NC), and the University of Florida (Gainesville, FL). Eligible subjects had unilateral or bilateral STN DBS for Parkinson's disease implanted at least 12 months prior and demonstrated DBS effectiveness.

The institutional review boards at the three sites approved the study protocol, and subjects enrolled after providing written informed consent and after verification of all eligibility requirements.

Twenty-six subjects (**Table 1**) with STN DBS (five unilateral, 21 bilateral) were enrolled. Motor data from 20 subjects, including 17 subjects with complete data sets (all outcome measures recorded for TOPS1, TOPS2, sDBS, and no stim) and three subjects with partial data sets (all outcome measures for sDBS, no stim, and either TOPS1 or TOPS2), were included in the statistical analysis of the effects of DBS on motor PD symptoms. For the three subjects with partial data sets, TOPS1 was not tested in one subject (A-02), and TOPS2 was not tested in two subjects (C-02, C-07) due to programing errors. Six of the 26 subjects were excluded from the motor symptom analysis due to missing motor response data for sDBS and/or both TOPS patterns. Missing motor response data were due to programing errors during testing (A-01, B-04, B-06, and C-04) or strong side effects experienced by the subjects (B-07, B-11).

The mean age of the subjects was 61 ± 8.3 years (range 41–77 years) and, with DBS ON and on Parkinson's medications, the mean Schwab and England Score was 86 ± 8.8 and the median modified Hoehn and Yahr Score was 2 (**Table 1**). Twenty-four of 26 subjects were taking Parkinson's medications at the time of the study, and those subjects continued taking their regular medication doses throughout the pattern testing. Daily Levodopa Equivalent Doses are listed in **Table 1**. Subjects B-06 and B-07 were not taking Parkinson's medications at the time of the study.

TABLE 1 Subject characteristics.

Subject	Age (years)	Gender	Time since diagnosis (years)	Schwab and England score*	Hoehn and Yahr score*	Daily Levodopa equivalent dose (mg)
A-01	54.3	m	4.1	80	3	870
A-02	71.4	m	10.7	90	2	300
A-03	69.1	m	12.8	80	2	860
A-04	57.2	m	8.9	90	2	800
A-05	68.4	m	8.9	90	2	660
A-06	77.6	m	9.9	85	2	430
A-07	59.2	m	6.2	85	2	900
B-01	69.2	m	1.5	90	2	580
B-03	45.6	f	6.8	80	2.5	250
B-04	63.2	m	10.6	80	2.5	525
B-05	59	f	8.9	70	2.5	1000
B-06	63.3	m	5.8	90	2	0
B-07	59	m	9.1	90	2	0
B-09	72.6	m	11.5	90	3	400
B-10	63.1	m	6.2	100	3	50
B-11	67.4	f	16.6	90	3	1162.5
B-12[a]	57.6	m	6.1	100	2	0
C-01	54.9	m	n/a	90	2.5	1800
C-02	54.7	m	8.9	90	3	800
C-03	49	m	5.7	90	2	1280
C-04	41.6	m	4	90	2	500
C-05	63	f	18.8	80	2.5	570
C-06	67.1	m	6.2	80	3	800
C-07	64.5	m	9.1	90	2	800
C-08	62.8	m	10.9	100	2	560
C-09	61	m	22	60	2.5	550

*Assessments made while the subject was ON DBS and ON Parkinson's medications.
[a]Subject took a Sinemet CR (25/100) as needed, on average once every 2–3-weeks.
n/a, data not available.

All subjects had a Medtronic Activa DBS system implanted with Medtonic electrodes (Model #3387 and Model #3389) at least 12 months prior to participation in this study with an average implant duration of 2.2 years at the time of the study (**Table 2**). Twenty-three of the 26 subjects demonstrated at least a 30% reduction in their UPDRS III motor score with DBS ON compared to no stim in the no medication state, and three subjects (A-03, A-05, and C-04) had reductions less than 30% (**Supplementary Table 1**). Six subjects (B-03, B-05, B-06, C-05, C-06, and C-08) had IPG replacements prior to study participation, ranging from 1.5 to 18 months prior. Clinical stimulation parameters are summarized in **Table 2**.

Study design

Subjects were assigned to receive a sequence of test patterns of stimulation, and the order was randomized for each subject. The test patterns, including TOPS1, TOPS2, sDBS, and no stim, were tested during the same day in the medication "ON" state, and subjects were blinded to the pattern. The following three steps were repeated for each pattern. First, prior to turning each pattern on, stimulation was turned off for a 20-min washout period. Second, the Medtronic Activa IPG (bilaterally, if applicable) was programed to deliver the pattern and stimulation was initiated. Third, after 30 min of stimulation, while stimulation was still active, subjects rated the intensity of and described any side effects experienced during the 30 min of stimulation, a blinded evaluator administered part III of the Unified Parkinson's Disease Rating Scale (UPDRS), and tremor (rest and postural) was recorded and quantified. These three steps were then repeated for each of the other three patterns.

The subject's clinical stimulation parameters (i.e., contact configuration, pulse duration, and pulse amplitude; frequency when delivering standard DBS) that had previously been clinically optimized for sDBS were used during testing whenever

TABLE 2 Deep brain stimulation (DBS) parameters.

Subject	Time since implant* (years)	Right brain				Left brain			
		Contact configuration	Pulse width (μs)	Frequency (Hz)	Amplitude (V)	Contact configuration	Pulse width (μs)	Frequency (Hz)	Amplitude (V)
A-01	1.3	9-11+	60	180	3.9	1+2-3-	90	180	4.5
A-02[a]	3.3	2-C+ (2-3+)	60	130	2.6 (2.9)	10-C+	60	130	2.6
A-03	2.5	10-11+	90	130	4.5	2-3+	90	130	4.5
A-04[a,b]	1.3	1-2-3+	90	185 (100)	3.6 (3.5)	—	—	—	—
A-05	1.0	—	—	—	—	2-C+	60	130	3.4
A-06	1.6	10-11+	60	130	4.1	1 + 3-	90	130	3.7
A-07	1.5	—	—	—	—	2-C+	90	130	3.7
B-01[a]	2.7	10-C+	60	180	3.2	1-C+ (2+3-)	60	180	3.2
B-03[a]	2.6	9-10-C+	60	180	3	1-2-C+ (1-2-3+)	60	180	3
B-04[a]	1.2	10-11-C+ (9+10-11-)	90	185	2.5	2-3-C+	90	185	2.5
B-05[d]	7.0	9-10-11+	60	180	2.1	1-2-3+	60	180	2.2
B-06	3.1	8-9-10+	70	185	1.9	2-3-C+	70	185	3.8
B-07	1.6	8-9-10-11 +	90	185	4	0-1-2-3+	90	185	4
B-09[a]	1.1	10-C+	70	180	2.2 (2.8)	2-C+ (2-1+)	70	180	2.3 (2.8)
B-10[a]	1.9	9-10-C+	80	185	2.4	1-2-C+	60 (90)	185	2.2
B-11[a]	1.2	9-C+	80	170	2.4	1-2-C+ (1-2-3+)	90	170	2.7
B-12[a]	1.2	8+9-10-11- (9-10-11+)	90 (110)	180	4.2	1-2-3-C+ (1-2-3+)	90	180	3.4
C-01[a,b]	1.3	1-2-3+	150	180 (100)	2.7	9-10-11+	150	180 (100)	3
C-02[c]	2.5	n/a	n/a	n/a	n/a	1-3+	120	180	2
C-03	1.6	2-C+	120	185	2.7	—	—	—	—
C-04	1.6	—	—	—	—	1-C+	120	135	2.6
C-05[a]	6.1	10-C+ (9-10+)	90	185	4 (4.5)	2-C+	90	185	4.1
C-06[a]	3.1	2-C+	120	135	2	0-C+ (0-1-C+)	90	200	3
C-07	1.9	1-C+	120	100	3	1-2+	90	130	3
C-08	1.0	2-C+	120	180	1.7	1-3-C+	60	135	1.6
C-09[a]	2.7	1-C+	90	180 (135)	2 (2.1)	1-C+	120	180	2.8 (2.5)

*If the subject had bilateral DBS with leads implanted on different dates, the time shown is from the second lead implant.
[a]Stimulation parameters changed from the clinical settings for pattern testing. The subject's clinical settings are listed along with the settings used for testing, shown in parentheses.
[b]Stimulation frequency mistakenly programed to 100 Hz during standard pattern testing. The subject's clinical stimulation frequency is listed.
[c]Receives bilateral stimulation clinically, but lead in right brain was connected to a Soletra IPG. Soletra IPG was turned OFF for study, and subject was tested unilaterally.
[d]Left lead was replaced 7 months prior to study participation, but stimulation parameters were steady at time of study.
n/a, data not available.

possible. Reprograming was necessary in seven of the 26 subjects because the Research Programmer was unable to deliver stimulation with the same IPG (case) selected as the anode (+) bilaterally in subjects with a dual-channel implanted pulse generator. In these subjects, where the IPG (case) was set as the anode (C +) bilaterally, the side clinically programed with the lowest stimulation amplitude was reprogramed with an electrode contact (rather than the IPG) as the anode. In some instances, (3/7), additional reprograming of stimulation amplitude was done when deemed necessary by the clinician to optimize therapy after the change in contact configuration. Any changes made to stimulation parameters were made before

testing began, were used during the testing of all patterns, and are listed in **Table 2**.

Subjects were evaluated while receiving a pattern while in the medication "ON" state. At the end of the 20-min washout from the previous stimulation, immediately before the next pattern was programed, the medication "ON" state was assessed by the clinician and by the subject completing the Wearing-Off-19 QUICK Questionnaire (WO19) (Martinez-Martin et al., 2008). "ON" state was defined as <2 symptoms on the WO19. If the results of either the WO19 or the clinician assessment suggested that the subject was in the "OFF" state, the clinician determined if the next dose of medication should be administered.

Stimulation patterns

Temporally Optimized Patterned Stimulation (TOPS) are pulse trains with a repeating sequence of non-regular and non-random intervals between the stimulus pulses. TOPS1 was designed using model-based optimization with computational evolution and is a 9-pulse sequence with inter-pulse intervals of varying duration ranging from 2 to 52 ms. It has a lower average frequency (∼45 Hz) than the typical clinical frequency range of standard DBS (100–185 Hz), and therefore was hypothesized to be more efficient than standard DBS (Brocker et al., 2013). TOPS2 is a burst sequence composed of a long inter-burst interval (∼50 ms) followed by a burst with short IPIs (∼5 ms). TOPS2 has an average frequency (∼158 Hz) within the range of standard DBS, and prior intraoperative testing and computational analysis suggested TOPS2 to be more effective than standard DBS (Swan et al., 2014). The TOPS1 pattern may be found in Brocker et al. (2017) ("Genetic Algorithm Pattern"), and the TOPS2 pattern may be found in Brocker et al. (2013) ("Absence").

To enable delivery of TOPS1, TOPS2, and sDBS, custom firmware was developed and temporarily downloaded to the IPG (Medtronic, Neuromodulation, Minneapolis, MN, United States). The firmware was compatible with Medtronic Activa PC, SC, and RC IPGs. Stimulation patterns were programmed by a trained clinician using a Microsoft Windows-based user interface running on a PC laptop connected to the IPG *via* a telemetry head (Medtronic, Neuromodulation). Due to the research programmer design, stimulation trains were delivered simultaneously to both hemispheres in subjects with bilateral electrodes and an Activa PC. Because of this, the research system only allowed one hemisphere to use the IPG as the anode (C +). All stimulation settings followed charge-balanced guidelines at or below standard clinical amplitudes and within all FDA safety guidelines (30 $\mu C/cm^2$). At the conclusion of the testing session, temporary firmware was removed from all subject's IPGs, and stimulation was restored to original clinically-optimal therapeutic settings.

Outcome measures

Subjects rated the intensity of and described any side effects experienced during the 30 min of stimulation for each test pattern. Side effects were rated on a scale of 0–10, where a rating of 0 was no side effect and a rating of 10 was intolerable.

A blinded evaluator administered part III of the Unified Parkinson's Disease Rating Scale (UPDRS III), and the assessment was video recorded. Scoring was completed by three independent raters, including the on-site blinded evaluator (Rater 1) and two remote raters (Raters 2 and 3) who provided scores after watching the video recordings of the assessments. Raters 2 and 3 imputed the rigidity scores recorded by Rater 1 since rigidity could not be assessed from the video. Motor symptoms were rated on a 0 to 4-point scale where 0 indicated "none" and 4 indicated "severe" symptom. The maximum total score for UPDRS III is 108, and the Minimally Clinically Important Difference (MCID) in UPDRS III is approximately 5.0 points (Hauser et al., 2014; Horvath et al., 2015). Motor subscores for tremor (Items 20–21), rigidity (Item 22), bradykinesia subscores (Items 23–26, and 31), and postural instability and gait disturbance (PIGD) subscores (Items 27–30) were calculated and analyzed.

Tremor was also quantified using a system of hand-mounted accelerometers and gyroscopes (Kinesia One System, Great Lakes Neurotechnology, Cleveland, OH, United States). The system quantified resting and postural tremor for the left and right upper limb, and the kinematic data were transformed into a score, ranging from 0 (no tremor) to 4 (severe tremor), using a validated algorithm (Giuffrida et al., 2009). Six subjects (A-04, A-05, A-07, C-02, C-03, and C-04) received unilateral stimulation during testing, and the tremor data from the upper limb opposite stimulation were included in the tremor analysis. In the remaining 14 subjects, data from the subjects' more-affected side (assessed in the no stimulation condition) were included in the analysis. If the tremor with no stimulation was <0.05 (resting tremor $n = 5$, postural tremor $n = 4$), the subject was excluded from the analysis.

Estimated battery life was calculated according to the equations provided in Medtronic's *System Eligibility, Battery Longevity* Manual (Medtronic, 2018) using the subject's clinical settings at the time of the study. First, the clinical stimulation amplitude was rounded to the nearest volt, and Energy Usage was read from the "Activa PC and Activa SC IPG energy use for voltage mode" table. If the clinical stimulation frequency or pulse width was not listed in the table, the Energy Usage was interpolated for the clinical stimulation setting. For TOPS1, the Energy Usage for a frequency of 45 Hz was extrapolated from the data available in the table. Impedance was assumed to be 1,000 Ohms for all IPGs resulting in an impedance correction factor of one. The Adjusted Energy Use was calculated as Energy Use × the Impedance Correction Factor, and this number was doubled for subjects with an Activa PC. Finally, the longevity

estimate was estimated from the Activa SC or PC IPG "longevity estimates (years) for energy use" figures.

Data analysis and statistics

In some subjects, patterns were tested more than one time due to programing errors. In cases where test patterns were tested more than one time, the error was made in the testing sequence; the pattern testing was otherwise conducted according to protocol, and the evaluator remained blinded to the test pattern. In these cases, the repeated outcome measures were averaged. Motor response data were averaged for no stim in three subjects (A-02, B-09, and C-02) included in the motor analysis. Also, side effect intensity was averaged for no stim in five subjects (A-02, B-06, B-09, C-02, and C-04) and for TOPS1 in one subject (B-04) in the side effects results.

Side effects were recorded for each pattern tested (n = 26, No Stim; n = 23, standard DBS; n = 24, TOPS1; and n = 21, TOPS2). In some cases, side effect data were not recorded due to programing errors, due to missing data (A-05) or due to a pattern being skipped to avoid additional side effects (B-11).

Statistical analyses were conducted using JMP Pro 14 (SAS Institute, Inc., Cary, NC, United States). Motor outcome data for the most effective TOPS, sDBS, and no stim were analyzed using repeated measures analysis of variance (ANOVA) with UPDRS III scores or quantified tremor score as the repeated measure in each subject. *Post hoc* comparisons between stimulation patterns were made using Tukey's Honestly Significant Difference test. UPDRS III scores were normally distributed, confirmed using the Shapiro-Wilk test. Battery life data did not meet the normality assumptions and a paired comparison was made using the non-parametric Wilcoxon Signed Rank test. Statistical significance was defined as $\alpha = 0.05$.

Results

The effects of different temporal patterns of STN DBS on the motor symptoms of Parkinson's disease were quantified in a multi-center, randomized feasibility study conducted while patients were on their normal doses of Parkinson's medications.

Temporally optimized patterned stimulation reduced motor symptoms as effectively as clinically optimized standard deep brain stimulation

Unified Parkinson's disease rating scale III

Motor symptoms were quantified using UPDRS III scores during different patterns of DBS (**Supplementary Table 2**). Comparisons of UPDRS III scores between the most effective TOPS pattern (TOPS1 or TOPS2), sDBS, and no stim revealed that stimulation pattern had a significant effect on UPDRS III scores (One way ANOVA, F = 13.84, $p < 0.0001$) (**Figure 1**).

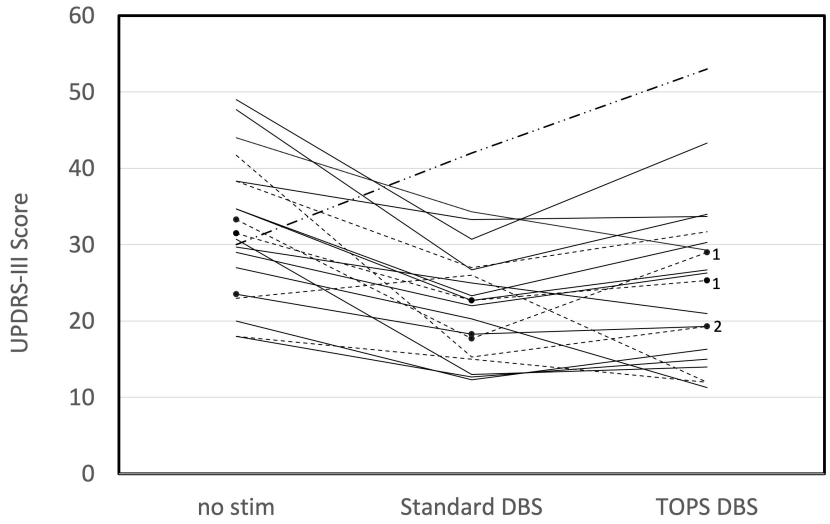

FIGURE 1
Motor symptoms, as measured using the UPDRS III in persons (n = 20) with PD and STN DBS while on their Parkinson's medications are dependent on the stimulation pattern (One way ANOVA, F = 13.84, $p < 0.0001$). UPDRS III scores are shown for no stim, standard DBS (sDBS) and the most effective TOPS pattern (TOPS1 or TOPS 2). Patterns were tested with each patient's stimulation parameters clinically optimized for sDBS. Dotted lines represent subjects in whom TOPS1 was the most effective TOPS pattern. Solid lines represent subjects in whom TOPS2 was the most effective TOPS. Note that TOPS1 and TOPS2 produced equal effects in one subject (B-05), for whom a dash-dot line is displayed. In three subjects, only one TOPS pattern was assessed, and these are marked with black dots and labeled with the pattern tested (TOPS1 = 1 or TOPS2 = 2).

UPDRS III scores were improved (reduced) compared to no stim with both sDBS (mean difference = 9.09, $p < 0.0001$) and the most effective TOPS (mean difference = 6.97, $p = 0.0012$). Also, UPDRS III scores in response to the most effective TOPS and sDBS were not significantly different (mean difference = −2.13, $p = 0.47$). Two subjects (A-05, B-05) had worsening of motor symptoms with sDBS compared to no stimulation, and this may be due to motor symptom fluctuation as a result of where they were in a medication cycle.

Comparison of the UPDRS III subscores for bradykinesia, tremor, and rigidity revealed stimulation pattern to have a significant effect on motor subscores (Table 3), with the exception of postural instability and gait disturbances. sDBS and the most effective TOPS produced equivalent reductions in UPDRS III subscores for tremor (mean difference = −0.8, p = 0.35), rigidity (mean difference = −0.5, $p = 0.58$), and bradykinesia (mean difference = 0.08, $p = 0.99$). Stimulation pattern did not have a significant effect on the PIGD subscores ($F = 0.33$, $p = 0.72$); neither sDBS nor TOPS DBS had a significant effect on the PGID motor subscores.

Tremor

Resting and postural tremors were quantified using a commercially available, objective, task-based motor assessment. Resting tremor was present (≥0.05) at baseline in 15/20 subjects and postural tremor in 16/20, and these subjects were included in the analysis. Comparisons of tremor scores between the most effective TOPS pattern (TOPS1 or TOPS2), sDBS, and no stim revealed that stimulation pattern had a significant effect on resting tremor (One-way ANOVA, $F = 9.64$, $p = 0.0007$) (Figure 2A) and postural tremor ($F = 11.64$, $p = 0.0002$) (Figure 2B).

Resting tremor scores were improved (reduced) compared to no stim with both sDBS (mean difference = −1.34, $p = 0.0006$) and the most effective TOPS (mean difference = −0.95, $p = 0.014$), and resting tremor scores in response to the most effective TOPS and sDBS were not significantly different (mean difference = −0.40, $p = 0.43$). Similarly, postural tremor scores were improved compared to no stim with both sDBS (mean difference = −1.27, $p = 0.0002$) and the most effective TOPS (mean difference = −0.96, $p = 0.004$). Postural tremor scores in response to the most effective TOPS and sDBS were not significantly different (mean difference = −0.30, $p = 0.52$).

TOPS deep brain stimulation was more effective than standard deep brain stimulation in a subset of subjects

Temporally optimized patterned stimulation DBS reduced the UPDRS III more than sDBS in 25% (5/20) of subjects (Figure 3). Further, in three of those five subjects, TOPS DBS reduced UPDRS III by at least five points more than sDBS. Conversely, sDBS reduced the UPDRS III more than TOPS DBS in 75% (15/20) of subjects. Further, in five of those 15 subjects, sDBS reduced UPRS III by at least five more points than TOPS.

Similarly, TOPS DBS was more effective than sDBS at reducing tremor in a subset of subjects. TOPS DBS improved the tremor score more than sDBS in 33% (5/15) of subjects for resting tremor and 38% (6/16) for postural tremor. Meanwhile, sDBS improved the tremor score more than TOPS DBS in 47% (7/15) subjects for resting tremor and in 46% (9/16) for postural tremor. When comparing no stim and the most effective TOPS, resting tremor increased with the TOPS DBS in three subjects. In two of these subjects (A05, C02), the resting tremor was rated less than 0.5 (out of 4) for both no stim and the most effective TOPS. In the third subject (C08) tremor increased from 1.1 with no stim to 2 with most effective TOPS.

TOPS1 deep brain stimulation was as effective as standard deep brain stimulation in a subset of subjects and used substantially less energy

TOPS1 was tested in 19 of the 20 subjects included in the motor symptom analysis, and TOPS1 was as effective (<5 point difference) or more effective at reducing the UPDRS motor score than sDBS in 47% (9/19) of subjects (Figure 4A). sDBS clinically improved (>5 point reduction) motor symptoms in 79% (15/19) of subjects and TOPS1 clinically improved motor symptoms in 42% (8/19) of the subjects. TOPS1 clinically

TABLE 3 Significance of stimulation patterns on UPDRS-III and motor subscores (D = mean difference).

	One-way ANOVA	*Post hoc* Tukey test results		
	Pattern significance	**No stim vs. Standard DBS**	**No stim vs. TOPS DBS**	**Standard DBS vs. TOPS DBS**
UPDRS-III Total	$F = 13.84$, $p < 0.0001$	$D = 9.09$, $p < 0.0001$	$D = 6.97$, $p = 0.0012$	$D = -2.13$, $p = 0.47$
Braykinesia	$F = 7.72$, $p = 0.0015$	$D = 2.60$, $p = 0.005$	$D = 2.69$, $p = 0.004$	$D = 0.083$, $p = 0.99$
Tremor	$F = 13.24$, $p < 0.0001$	$D = 2.85$, $p < 0.001$	$D = 2.05$, $p = 0.0026$	$D = -0.8$, $p = 0.35$
Rigidity	$F = 16.64$, $p < 0.0001$	$D = 2.98$, $p < 0.0001$	$D = 2.43$, $p = 0.0002$	$D = -0.55$, $p = 0.58$
PIGD	$F = 0.33$, $p = 0.72$	$D = 0.27$, $p = 0.72$	$D = 0.20$, $p = 0.83$	$D = -0.067$, $p = 0.98$

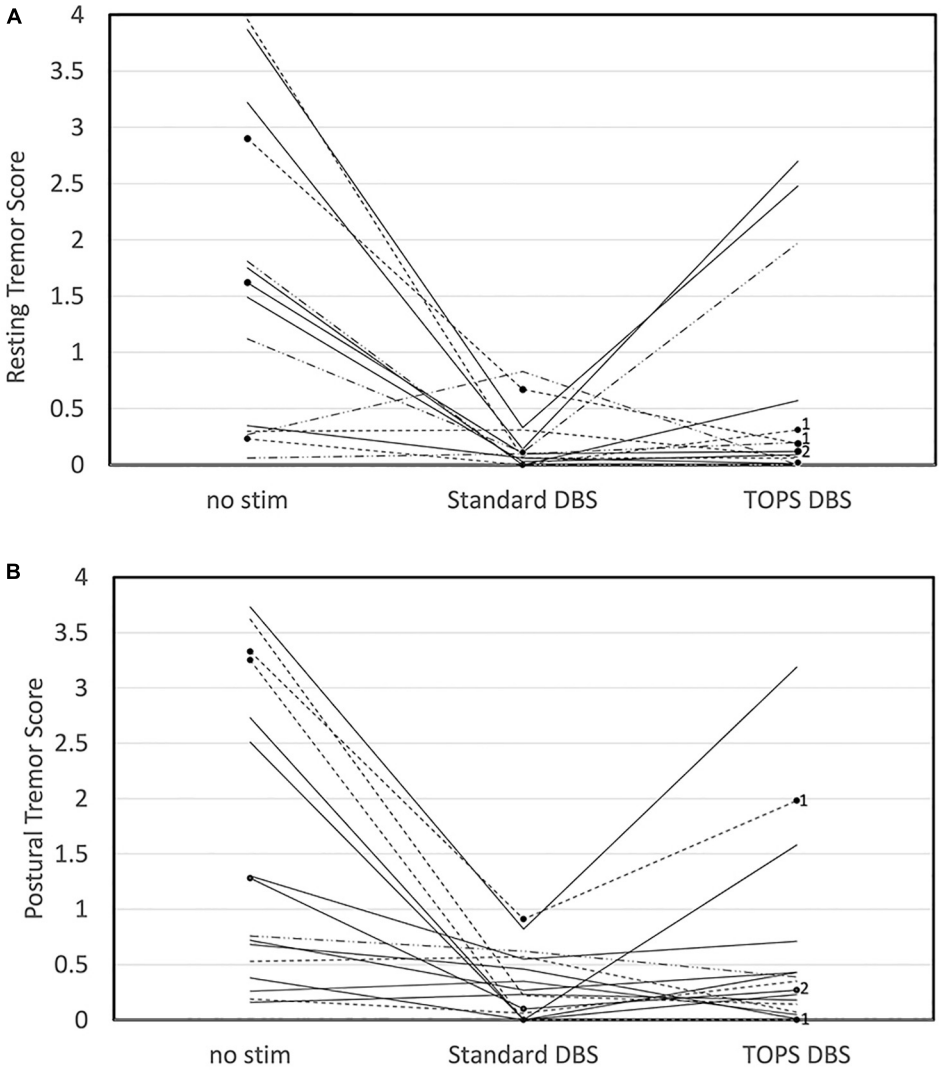

FIGURE 2
Tremor, quantified using the Kinesia One system, in persons with PD and STN DBS while on their Parkinson's medications was dependent on stimulation pattern. Resting **(A)** and Postural **(B)** tremor scores are shown for no stim, sDBS and the most effective TOPS pattern (TOPS1 or TOPS 2). Patterns were tested with each patient's stimulation parameters clinically optimized for sDBS. Scores varied across stimulation patterns for resting tremor ($F = 9.64$, $p = 0.0007$) and postural tremor ($F = 11.64$, $p = 0.0002$). Dotted lines represent subjects in whom TOPS1 was the most effective TOPS. Solid lines represent subjects in whom TOPS2 was the most effective TOPS. In three subjects, only one TOPS pattern was assessed, and these are marked with black dots and labeled with the pattern tested (TOPS1 = 1 or TOPS2 = 2).

improved motor symptoms in two subjects that sDBS did not; conversely, sDBS clinically improved motor symptoms in nine subjects that TOPS1 did not. When considering tremor, sDBS and TOPS1 reduced resting tremor in 71% (10/14) of subjects. sDBS and TOPS1 reduced postural tremor in 80% (12/15) and 67% (10/15) of subjects, respectively. TOPS1 was as effective as or more effective than sDBS at reducing tremor in 43% (6/14) of subjects for resting tremor and in 20% (3/15) of subjects for postural tremor. sDBS was as effective or more effective than TOPS1 at reducing rest tremor in 64% (9/14) of subjects and in 87% (13/15) of subjects for postural tremor.

In the nine subjects for which TOPS1 (average frequency = 45 Hz) was as effective or more effective than sDBS, at the battery life of each subject's IPG was estimated (Medtronic, 2018) for sDBS and TOPS1 using the subject's clinically optimized parameters for sDBS (**Figure 4B**). Median estimated IPG lifetime was significantly longer with TOPS1 (median = 8.2 years) than for sDBS (median = 3.0 years) (Wilcoxon Signed Rank Test, S = 27.5, $p = 0.002$). The median estimated IPG lifetime for TOPS2 (average frequency = 158 Hz) was 3.2 years.

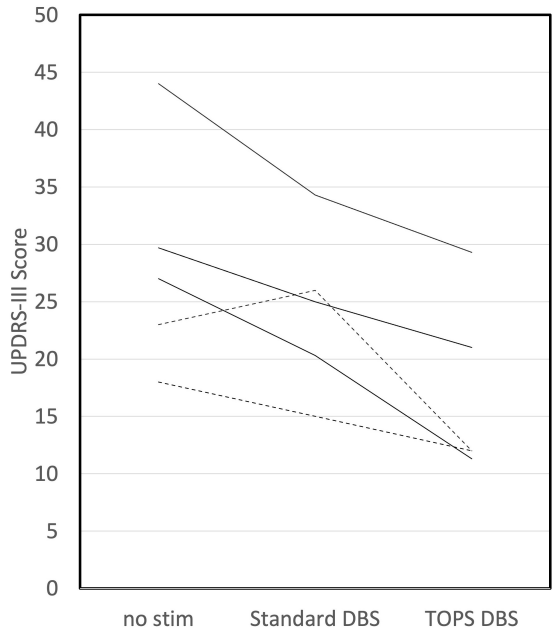

FIGURE 3
TOPS DBS reduced UPDRS III (improved symptoms) more than standard DBS in 25% (5/20) of subjects. Dotted lines represent subjects in which TOPS1 was the most effective TOPS. Solid lines represent subjects in which TOPS2 was the most effective TOPS.

Side effects elicited with temporally optimized patterned stimulation and standard deep brain stimulation were comparable

Eleven of the 26 subjects experienced a side effect during stimulation with one or more stimulation patterns. The types of side effects were similar across both TOPS patterns and sDBS and included paresthesias, difficulty speaking, involuntary muscle contractions, vision changes, and sensations of coldness, sweating, and anxiety. Side effects were reported 19 times across 11 subjects (**Figure 5**). There were 13 occurrences where the test patterns elicited mild and transient (rated < 8) side effects and six where strong and sustained (rated ≥ 8) side effects were elicited and required stimulation be turned off before the end of the 30-min test duration and precluded motor testing. TOPS1 ($n = 1$), TOPS2 ($n = 3$) and/or standard DBS ($n = 2$) elicited strong and sustained side effects in four subjects (**Table 4**).

Discussion

This multicenter study demonstrated the safety and feasibility of TOPS DBS as a novel approach to neuromodulation therapy. The data revealed a potential for TOPS DBS to improve the motor symptoms of PD more effectively and/or more efficiently than sDBS in a subset of patients. Patients with different Parkinson's disease subtypes may respond differently to TOPS DBS, but this study focused on feasibility and was not designed to evaluate effects on specific symptoms. Consistent with intra-operative testing of TOPS (Brocker et al., 2013, 2017), these novel patterns were well-tolerated by most subjects, and they were effective in alleviating the motor symptoms of PD. There were several key differences between this study and previous testing of TOPS DBS (Brocker et al., 2013, 2017): in the previous study testing was intraoperative, bradykinesia was estimated using a finger-tapping task on a computer mouse, the stimulation duration prior to completing a motor assessment was about 2–4 min of stimulation, and subjects were asked to withhold their Parkinson's medications. For the current study, TOPS settings were implemented in subjects with previously-implanted IPGs using a non-invasive firmware download. Firmware updates such as TOPS have the potential to provide a more personalized treatment for DBS patients, and device updates may enable such stimulation capabilities in the future.

Overall, TOPS reduced the motor symptoms of Parkinson's disease to the same degree as sDBS. The mean UPDRS III score for the most effective TOPS setting (either TOPS 1 or 2) was not significantly different than that with sDBS, and both TOPS and sDBS alleviated motor symptoms from the no stim condition. Similarly, the reduction in the bradykinesia, tremor, and rigidity subscores was similar between sDBS and the most effective TOPS. Further, the results of the quantitative measurement also demonstrated that sDBS and TOPS both reduced postural and resting tremor.

Temporally optimized patterned stimulation DBS reduced the UPDRS III more than sDBS in 25% (5/20) of subjects. TOPS1 DBS reduced UPDRS III maximally in two subjects and TOPS2 reduced UPDRS III maximally in three subjects. Importantly, TOPS2 reduced Parkinson's symptoms in one subject in which sDBS failed. Two subjects (A-05, B-05) had worsening of motor symptoms with sDBS compared to no stim, and this may be due to motor symptom fluctuation because of where they were in a medication cycle. Subjects A-05 and B-05 were taking frequent doses of medication (5×/day and 8×/day, respectively) and therefore likely had short ON/OFF cycles. TOPS DBS was also effective at reducing postural and resting tremor. Of note, the stimulation parameters used during testing of different stimulation patterns were optimized for sDBS. It is possible that optimization of contact configuration, pulse width, and pulse amplitude for TOPS would further increase the number of responders and the degree of symptom suppression relative to sDBS.

TOPS1 was as effective or more effective than sDBS at improving motor symptoms in almost half of subjects (9/19) and had the benefit of potentially doubling median IPG lifetime due to its lower average frequency. Current primary cell powered IPGs require surgical replacement every 3–5 years for standard stimulation settings (Medtronic, 2018), and increasing IPG lifetime will reduce the risks associated with device replacement including acute loss of symptomatic relief and infection as well

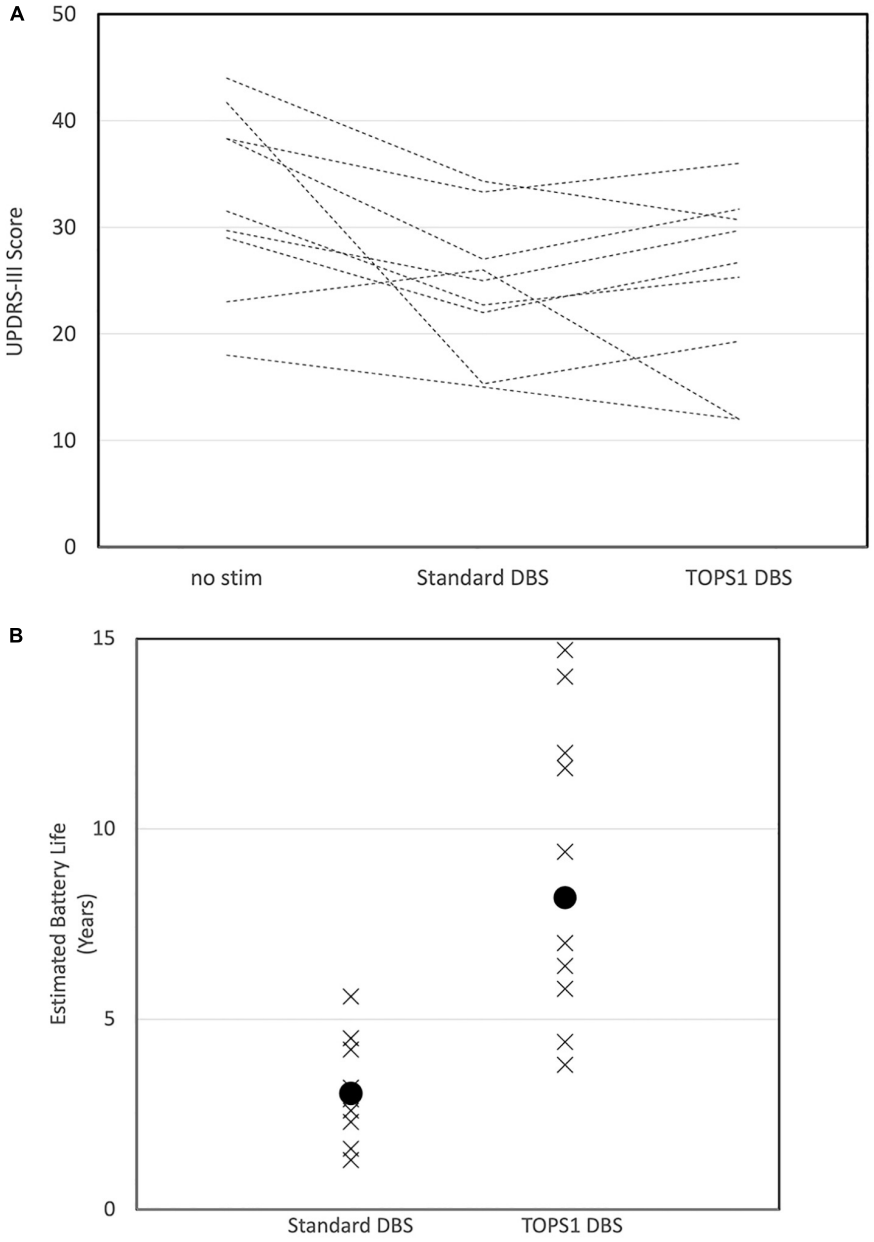

FIGURE 4
Motor scores (UPDRS III) in subjects (n = 9/19) for whom TOPS1 (average frequency = 45 Hz) was as effective or more effective than sDBS **(A)**. Subjects all have PD and STN DBS and were tested while on Parkinson's medications. Estimated implanted pulse generator battery life for sDBS and TOPS1 DBS **(B)** in nine subjects in which TOPS1 was as effective or more effective than sDBS. Median estimated battery life was significantly increased with TOPS1 DBS (S = 27.5, p = 0.002).

as reduce the overall cost of DBS therapy by reducing the number of required replacements during a patient's lifetime. In IPGs powered by rechargeable batteries, TOPS1 will increase the time between required recharging. The energy savings from TOPS1 could be most impactful for patients receiving DBS for applications requiring higher voltages (currents). Alternatively, the energy savings from TOPS1 could be directed to reduce the volume of IPGs and to maintain current device lifetime and recharge intervals.

The TOPS patterns were well-tolerated by a majority of the subjects and the types of side effects experienced were similar between sDBS and the TOPS patterns. Mild, transient side effects were experienced across all test patterns, including with the no stim condition. Four subjects rated the side effect intensity as strong, lasting, and intolerable (8, 9, or 10), but the intolerable side effects were not unique to TOPS. Two subjects (B-07, B-11) who rated TOPS patterns as intolerable also rated the side effects of sDBS as intolerable.

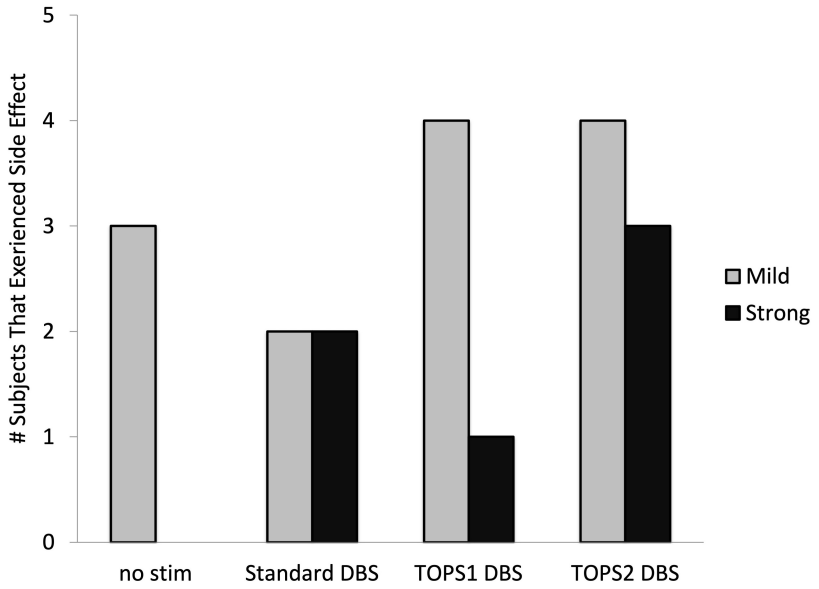

FIGURE 5
Number of subjects who experienced side effects with each stimulation pattern. Side effects with a mild intensity were rated less than an eight. Side effects with strong, sustained intensity and considered intolerable were rated 8, 9, or 10. Side effects were assessed in *n* = 26 (no stim), *n* = 23 (sDBS), *n* = 24 (TOPS1), and *n* = 21 (TOPS2) out of 26 subjects.

TABLE 4 Strong, sustained side effects were experienced by four subjects during at least one test pattern resulting in stimulation being turned OFF before the 30-min test period.

Subject	No stim	Standard	TOPS1	TOPS2
B-06	0	n/a	0	9
B-07	1	10	1	10
B-11	0	10	8	n/a
C-07	0	0	5	9

Strong side effects were defined as those rated 8–10 and are highlighted in gray.
n/a: data point not available; pattern was skipped to avoid side effect.

Both subjects were receiving bilateral stimulation from a single IPG. A possible explanation for strong side effects seen during sDBS is that for subjects with bilateral stimulation, pulses were delivered simultaneously to both hemispheres, instead of alternating pulses between hemispheres (interleaving) as standard for clinical therapy. Simultaneous bilateral stimulation may have also played a role in the intolerable side effects elicited by TOPS in one subject (B-06) in whom sDBS was not tested. The fourth subject who experienced intolerable side effects (C-07) was programed clinically to receive 100 Hz stimulation. The stronger side effects elicited with TOPS2 may have been caused by the increase in average frequency, and this may have been alleviated by a reduction in stimulation amplitude. Because this study was conducted as a clinical trial, stimulus parameter settings were not permitted to be adjusted during testing. Such adjustments usually can be used to increase tolerability.

This was a small feasibility study with a limited number of subjects meant to demonstrate tolerability and effectiveness of TOPS after a longer period (∼30 min) of stimulation and to inform the design and powering of a subsequent study. There were several important limitations to this study. Most important was that the patterns were not tested in a chronic state after several days on a particular setting. The effects of the different patterns on motor symptoms may change over a longer period of stimulation, and further adjustments to stimulation parameters or medications may be required. Assessments made at the 30-min mark are like those made during clinical programing, where the parameters are selected and determined to be appropriate to take home after a relatively short epoch of stimulation.

Also, an important purposeful design of this study was that subjects were tested while ON their Parkinson's medications, and this facilitated comparison of patterns in the subjects' best clinical state. This also allowed the testing session to be more tolerable for subjects and allowed us to determine whether switching to TOPS may be feasible for the many patients with pre-existing DBS devices. However, it is an important limitation that the timing of medication dosing was not consistent across subjects and that motor fluctuations due to medication status may have increased the variance in the assessments of the effects of stimulation patterns. The medication "ON" state was assessed by a clinician and also by the subject who completed the Wearing-Off-19 QUICK Questionnaire. The WO19 was used to screen for potential wearing off of medications, and the clinicians rendered a bedside decision if administering a next

dose of medication was appropriate to maintain the patient in an ON medication condition.

Another limitation of the study was the heterogeneous nature of the subjects' electrode configurations (bilateral vs. unilateral, monopolar vs. bipolar). Finally, and perhaps most importantly, the programmers in the study were not permitted to optimize the stimulation settings for TOPS. Based on our experience with DBS therapy, it would be likely that slight individual modifications could lead to even more benefits. It was assumed that subjects' standard DBS settings were reasonably optimized prior to the study.

This was the first test of TOPS in the clinical setting, and the results demonstrated that novel patterns of stimulation could provide a useful alternative to standard DBS. TOPS delivered a more efficient and for some patients a more effective option for DBS treatment. These patterns provide an entirely new parameter space for optimization of DBS for Parkinson's treatment and possibly could be used in other applications of DBS (Grill, 2018). Other recent studies have also demonstrated the feasibility of patterned DBS to improve DBS therapy by increasing the therapeutic window (Horn et al., 2020) or by improving axial symptoms in a subset of subjects (Sáenz-Farret et al., 2021). We posit that TOPS will be an important step for the personalization of the DBS experience which should be aimed at improving the outcome for individual patients with unique symptom profiles.

Data availability statement

The raw data supporting the conclusions of this article will be made available by the authors, without undue reservation.

Ethics statement

The studies involving human participants were reviewed and approved by Duke Health Institutional Review Board, Cleveland Clinic Institutional Review Board, and the WCG Institutional Review Board. The patients/participants provided their written informed consent to participate in this study.

Author contributions

MO: research project conception, study design and execution, and review of statistical analysis and the manuscript. PH and AM: study execution and review of the manuscript. AK: study design, project organization and execution, execution and review of statistical analysis, and writing first draft of manuscript. WG: research project conception, study design, and review of statistical analysis and manuscript. All authors contributed to the article and approved the submitted version.

Funding

This study received funding from the Deep Brain Innovations, LLC (DBI). DBI funding supported the design, data collection and analysis, decision to publish, and preparation of this manuscript.

Acknowledgments

We would like to acknowledge Chris Firestone at the Cleveland Clinic Foundation, Lisa Gauger at Duke University, and Julie Segura at the University of Florida for coordinating study activities. The testing was performed at the Parkinson's Foundation Centers of Excellence at the University of Florida, Duke University, and the Cleveland Clinic. We would like to acknowledge Medtronic, Robert Raike and Nicholas Buse for providing technical support and input on study design.

Conflict of interest

WG was Co-Founder, Chief Scientific Officer, and share owner in Deep Brain Innovations, LLC. He is an inventor on licensed patents on temporal patterns of brain stimulation and receives royalties therefrom. AK served as a consultant for Deep Brain Innovations, LLC and was the clinical project manager for this study. AM served as a consultant for St. Jude (Abbott), had distribution rights from IP for Enspire DBS and Cardionomics, and received fellowship support from Medtronic.

The remaining authors declare that the research was conducted in the absence of any commercial or financial relationships that could be construed as a potential conflict of interest.

Publisher's note

Supplementary material

The Supplementary Material for this article can be found online at: https://www.frontiersin.org/articles/10.3389/fnhum.2022.929509/full#supplementary-material

References

Benabid, A. L., Chabardes, S., Mitrofanis, J., and Pollak, P. (2009). Deep brain stimulation of the subthalamic nucleus for the treatment of Parkinson's disease. *Lancet Neurol.* 8, 67–81. doi: 10.1016/S1474-4422(08)70291-6

Birdno, M. J., and Grill, W. M. (2008). Mechanisms of deep brain stimulation in movement disorders as revealed by changes in stimulus frequency. *Neurotherapeutics* 5, 14–25. doi: 10.1016/j.nurt.2007.10.067

Birdno, M. J., Kuncel, A. M., Dorval, A. D., Turner, D. A., and Grill, W. M. (2008). Tremor varies as a function of the temporal regularity of deep brain stimulation. *Neuroreport* 19, 599–602. doi: 10.1097/WNR.0b013e3282f9e45e

Brocker, D. T., Swan, B. D., So, R. Q., Turner, D. A., Gross, R. E., and Grill, W. M. (2017). Optimized temporal pattern of brain stimulation designed by computational evolution. *Sci. Transl. Med.* 9:eaah3532. doi: 10.1126/scitranslmed.aah3532

Brocker, D. T., Swan, B. D., Turner, D. A., Gross, R. E., Tatter, S. B., Koop, M. M., et al. (2013). Improved efficacy of temporally non-regular deep brain stimulation in Parkinson's disease. *Exp. Neurol.* 239, 60–67. doi: 10.1016/j.expneurol.2012.09.008

Dorval, A. D., Kuncel, A. M., Birdno, M. J., Turner, D. A., and Grill, W. M. (2010). Deep brain stimulation alleviates parkinsonian bradykinesia by regularizing pallidal activity. *J. Neurophysiol.* 104, 911–921. doi: 10.1152/jn.00103.2010

Giuffrida, J. P., Riley, D. E., Maddux, B. N., and Heldman, D. A. (2009). Clinically Deployable Kinesia(TM) Technology for Automated Tremor Assessment. *Mov. Disord.* 24, 723–730. doi: 10.1002/mds.22445

Grill, W. M. (2018). Temporal pattern of electrical stimulation is a new dimension of therapeutic innovation. *Curr. Opin. Biomed. Eng.* 8, 1–6. doi: 10.1016/j.cobme.2018.08.007

Hauser, R. A., Gordon, M. F., Mizuno, Y., Poewe, W., Barone, P., Schapira, A. H., et al. (2014). Minimal clinically important difference in Parkinson's disease as assessed in pivotal trials of pramipexole extended release. *Park. Relat. Disord.* 2014:467131. doi: 10.1155/2014/467131

Herrington, T. M., Cheng, J. J., and Eskandar, E. N. (2016). Mechanisms of deep brain stimulation. *J. Neurophysiol.* 115, 19–38. doi: 10.1152/jn.00281.2015

Horn, M. A., Gulberti, A., Gülke, E., Buhmann, C., Gerloff, C., Moll, C. K. E., et al. (2020). New Stimulation Mode for Deep Brain Stimulation in Parkinson's Disease: Theta Burst Stimulation. *Mov. Disord.* 35, 1471–1475. doi: 10.1002/mds.28083

Horvath, K., Aschermann, Z., Ács, P., Deli, G., Janszky, J., Komoly, S., et al. (2015). Minimal clinically important difference on the Motor Examination part of UPDRS. *Park. Relat. Disord.* 21, 1421–1428. doi: 10.1016/j.parkreldis.2015.10.006

Kuncel, A. M., Cooper, S. E., Wolgamuth, B. A., Clyde, M. A., Snyder, S. A., Montgomery, E. B., et al. (2006). Clinical response to varying the stimulus parameters in deep brain stimulation for essential tremor. *Mov. Disord.* 21, 1920–1928. doi: 10.1002/mds.21087

Martinez-Martin, P., Tolosa, E., Hernandez, B., and Badia, X. (2008). Validation of the "QUICK" Questionnaire—A Tool for Diagnosis of "Wearing-Off" in Patients with Parkinson's Disease. *Mov. Disord.* 23, 830–836. doi: 10.1002/mds.21944

McIntyre, C. C., Savasta, M., Kerkerian-Le Goff, L., and Vitek, J. L. (2004). Uncovering the mechanism(s) of action of deep brain stimulation: Activation, inhibition, or both. *Clin. Neurophysiol.* 115, 1239–1248. doi: 10.1016/j.clinph.2003.12.024

Medtronic. (2018). *System Eligibility, Battery Longevity: Neurostimulation Systems For Deep Brain Stimulation*. Dublin: Medtronic.

Moro, E., Esselink, R. J. A., Xie, J., Hommel, M., Benabid, A. L., and Pollak, P. (2002). The impact on Parkinson's disease of electrical parameter settings in STN stimulation. *Neurology* 59, 706–713. doi: 10.1212/WNL.59.5.706

Rizzone, M., Lanotte, M., Bergamasco, B., Tavella, A., Torre, E., Faccani, G., et al. (2001). Deep brain stimulation of the subthalamic nucleus in Parkinson's disease: Effects of variation in stimulation parameters. *J. Neurol. Neurosurg. Psychiatry* 71, 215–219. doi: 10.1136/jnnp.71.2.215

Sáenz-Farret, M., Loh, A., Boutet, A., Germann, J., Elias, G. J. B., Kalia, S. K., et al. (2021). Theta Burst Deep Brain Stimulation in Movement Disorders. *Mov. Disord. Clin. Pract.* 8, 282–285. doi: 10.1002/mdc3.13130

Swan, B. D., Grill, W. M., and Turner, D. A. (2014). Investigation of deep brain stimulation mechanisms during implantable pulse generator replacement surgery. *Neuromodulation* 17, 419–424. doi: 10.1111/ner.12123

frontiers | Frontiers in Human Neuroscience

TYPE Systematic Review
PUBLISHED 29 September 2022
DOI 10.3389/fnhum.2022.997552

OPEN ACCESS

EDITED BY
Muthuraman Muthuraman,
Johannes Gutenberg University Mainz, Germany

REVIEWED BY
Nelleke van Wouwe,
University of Louisville, United States
Qichang Mei,
Ningbo University, China

*CORRESPONDENCE
Joshua K. Wong
Joshua.wong@neurology.ufl.edu

†These authors have contributed equally to this work and share first authorship

‡These authors share senior authorship

SPECIALTY SECTION
This article was submitted to Brain Imaging and Stimulation, a section of the journal Frontiers in Human Neuroscience

RECEIVED 19 July 2022
ACCEPTED 05 September 2022
PUBLISHED 29 September 2022

CITATION
King C, Parker TM, Roussos-Ross K, Ramirez-Zamora A, Smulian JC, Okun MS and Wong JK (2022) Safety of deep brain stimulation in pregnancy: A comprehensive review. *Front. Hum. Neurosci.* 16:997552. doi: 10.3389/fnhum.2022.997552

Safety of deep brain stimulation in pregnancy: A comprehensive review

Caroline King[1†], T. Maxwell Parker[2†], Kay Roussos-Ross[1,3], Adolfo Ramirez-Zamora[2], John C. Smulian[1,3‡], Michael S. Okun[2‡] and Joshua K. Wong[2*]

[1]Department of Obstetrics & Gynecology, University of Florida College of Medicine, Gainesville, FL, United States, [2]Department of Neurology, Norman Fixel Institute for Neurological Diseases, University of Florida College of Medicine, Gainesville, FL, United States, [3]Center for Research in Perinatal Outcomes, University of Florida College of Medicine, Gainesville, FL, United States

Introduction: Deep brain stimulation (DBS) is increasingly used to treat the symptoms of various neurologic and psychiatric conditions. People can undergo the procedure during reproductive years but the safety of DBS in pregnancy remains relatively unknown given the paucity of published cases. We thus conducted a review of the literature to determine the state of current knowledge about DBS in pregnancy and to determine how eligibility criteria are approached in clinical trials with respect to pregnancy and the potential for pregnancy.

Methods: A literature review was conducted in EMBASE to identify articles involving DBS and pregnancy. Two reviewers independently analyzed the articles to confirm inclusion. Data extracted for analysis included conditions treated, complications at all stages of pregnancy, neonatal/pediatric outcomes, and DBS target. A second search was then conducted using www.clinicaltrials.gov. The same two reviewers then assessed whether each trial excluded pregnant individuals, lactating individuals, or persons of childbearing age planning to conceive. Also assessed was whether contraception had to be deemed adequate prior to enrollment.

Results: The literature search returned 681 articles. Following independent analysis and agreement of two reviewers, 8 pregnancy related DBS articles were included for analysis. These articles described 27 subjects, 29 pregnancies (2 with subsequent pregnancies), and 31 infants (2 twin pregnancies). There was 1 preterm birth at 35 weeks, and 3 patients who experienced discomfort from the DBS battery (i.e., impulse generator) placement site. All 27 patients had a DBS device implanted before they became pregnant, which remained in use throughout their pregnancy. There was exclusion of pregnant individuals from 68% of 135 interventional trials involving DBS. Approximately 44% of these trials excluded persons of childbearing age not on "adequate contraception" or wishing to conceive in the coming years. Finally, 22% excluded breastfeeding persons.

Conclusion: The data from 29 pregnancies receiving DBS treatment during pregnancy was not associated with unexpected pregnancy or post-partum

complication patterns. Many clinical trials have excluded pregnant individuals. Documentation of outcomes in larger numbers of pregnancies will help clarify the safety profile and will help guide study designs that will safely include pregnant patients.

KEYWORDS

pregnancy, DBS, clinical trials, safety, ethics, deep brain stimulation, neuromodulation

Introduction

Deep brain stimulation (DBS) has been applied selectively for treatment of Parkinson's disease (PD), essential tremor (ET), dystonia, and many other neuropsychiatric disorders and symptoms (Denison and Morrell, 2022). The steadily improving safety profile has led to expansion into younger and healthier populations during reproductive ages, which raises important issues regarding DBS and pregnancy. Individuals with DBS may be interested in becoming pregnant or may unknowingly discover that they are pregnant after a DBS device has been implanted. Others may also be interested in the safety profile during lactation and whether or not they should consider enrollment in a clinical trial if pregnant or considering a future pregnancy.

There has been an increase in clinical trials utilizing DBS across 28 conditions, many of which are in the psychiatric or cognitive disease domains (Harmsen et al., 2020). Many focus on younger patients and thus pregnancy-related issues become more pertinent (Schrag and Schott, 2006; Louis and Dogu, 2008). With mean maternal age at first birth in the United States at 27 years, the use of DBS in pregnancy becomes an increasingly important topic (CDC, 2022). Additionally, many of the expanding indications for neuromodulation, such as major depressive disorder (MDD) and epilepsy, affect pregnant individuals. Each year, up to 20% of pregnant individuals suffer from a depressive disorder and over 1.1 million women of childbearing age have epilepsy (Sazgar, 2019; Van Niel and Payne, 2020). Uncontrolled and poorly controlled MDD and epilepsy in pregnancy pose significant threats to both mother and fetus, ranging from neurodevelopmental derangements to fetal hypoxia and growth restriction and even death (Battino and Tomson, 2007; Chan et al., 2014). In refractory cases of epilepsy (affecting 40% of all persons with the disease), seizures can increase in frequency during pregnancy (Kobau et al., 2008; Vitturi et al., 2019). Many first-line treatment modalities for these disorders, such as anti-epileptic pharmacotherapeutics, can cross the placenta and have known teratogenic effects on fetuses or neurodevelopmental delay during childhood, limiting the availability of safe and effective treatments in pregnancy (Artama et al., 2005). In these instances, the patient may benefit from alternative non-pharmacologic therapeutic approaches such as DBS.

It is thus an imperative to assess and analyze the data available surrounding DBS and the pregnant population with the most up to date evidence. Doing so will shed light on crucial areas of promise and progress, as well as better characterize considerations for each neurologist and obstetrician's own practice. In this comprehensive review we will address pregnancy-related DBS concerns including clinical trial enrollment using all available studies in the published literature. Our primary objective was to describe clinical outcomes of pregnancies in which DBS was used. Our secondary objective was to assess how clinical trials approached participation eligibility during pregnancy, lactation, and the reproductive years.

Methods

A comprehensive review of the literature for DBS in the childbearing and pregnant populations was conducted from March 2022 to June 2022 querying EMBASE for all cases reported to date. Our search criteria is available in Supplementary Data Sheet 1. Two independent raters (CK and MP) conducted a preliminary survey of the literature search results, evaluating both title and abstract for initial relevance. The two raters then reviewed the manuscripts of the screened publications for rigor prior to inclusion in the analysis. Inclusion criterion for manuscripts were: (1) an original research article, case report, case series, or trial of DBS co-occurring with pregnancy, (2) reporting on a DBS case in pregnancy that was carried out to completion (i.e., the subject had given birth). Exclusion criteria were: (1) duplicate publications, or conference proceeding of an eventual manuscript, (2) review articles or non-research articles or (3) did not include pregnancy information within the article. Published abstracts, letters to the editor or publications from conference proceedings were included in accordance with the recommendations put forth by Scherer and Saldanha (2019) if they met relevant pre-determined criteria. The inclusion and exclusion criteria used for manuscripts was applied to abstracts

and letters to the editor. The following data were extracted from each article: the condition to treat, DBS target structure, maternal complications, route of delivery, birth complications, neonatal complications, neurodevelopmental follow-up, and other pertinent information offered. This review was made in accordance with PRISMA guidelines as presented in **Figure 1** (Page et al., 2021).

A search of ClinicalTrials.gov for DBS studies involving dystonia, pain, epilepsy, MDD, obsessive-compulsive disorder (OCD), and Tourette syndrome (TS) was also conducted. The same two independent raters reviewed the results and included trials meeting the following criteria:(1) involved DBS of the relevant clinical condition and (2) offered DBS-based intervention. A trial was excluded if it (1) was a duplicate of another trial; (2) focused on another condition outside of the search; (3) did not involve DBS; or (4) was observational and not pertaining to a recently offered DBS based intervention. For all included trials, each rater reviewed the trial's inclusion and exclusion criteria. Three questions were addressed for each included trial. (1) Does the trial exclude subjects who are pregnant? (2) Does the trial exclude persons of childbearing age not on contraception deemed adequate by investigators and/or individuals intending to become pregnant? (3) Does the trial exclude breastfeeding individuals? Other data extracted from the clinical trial results included: enrollment status, regional location of trial, trial phase, date of trial start, and date of trial completion (if applicable).

Results

Deep brain stimulation

Results of the literature search are shown in **Table 1** and illustrated in **Figure 2**. Out of 681 publications, there were eight eligible publications reporting DBS in pregnancy that were included for analysis. All eight were full-length original research articles. These eight publications reported information on 27 patients with DBS who subsequently became pregnant and all received active neuromodulation treatment throughout their pregnancy (**Table 1**). Two individuals became pregnant twice with DBS for a total of 29 pregnancies. Another two persons conceived twin pregnancies, which brings the total to 31 infants. The most prevalent condition was dystonia (N = 17, 63%) followed by epilepsy (N = 4, 15%) and PD (N = 3, 11%). The most frequent target was the globus pallidus internus (N = 20, 74%) followed by the anterior nucleus of the thalamus (N = 4, 15%) and the subthalamic nucleus (N = 3, 11%).

Pregnancy complications for the 29 pregnancies were observed in three (12.9%) patients. Non-obstetric complications occurred in three individuals who had discomfort at the neurostimulator site (N = 2 subclavicular, N = 1 abdominal). One of these patients also had an obstetric complication of a preterm delivery at 35 weeks gestational age. The discomfort experienced by three subjects was mechanically induced from physiologic abdominal and breast changes as pregnancy progressed. One additional patient was reported to have experienced the spontaneous abortion of one fetus in the early weeks of a twin pregnancy (Scelzo et al., 2015). The authors, however, determined that this adverse event was not related to DBS, thus it was not included in our complication data. As noted by Ziman et al. (2016) a subject who experienced abdominal discomfort from the neurostimulator site was the same individual who experienced preterm birth at 35 weeks. This patient had a battery readjustment procedure following her first pregnancy, relocating the battery from the abdomen to the subcutaneous tissue of the chest. With her subsequent second pregnancy, she experienced less discomfort and had a term delivery. Three publications did not include any follow-up data on neonatal outcomes. The remaining publications (N = 5) followed subjects from 6 to 108 months. No negative neurodevelopmental outcomes were reported.

No articles were found focusing specifically on DBS's effects on lactation or future fertility; however all subjects had a DBS stimulator prior to conception and reported no issues with becoming pregnant. Additionally, five out of eight publications followed DBS subjects from initiation of DBS treatment, into a pregnancy, and then into the postpartum period. These studies did not report any issues related to fertility. One subject reported inability to breastfeed due to discomfort. Otherwise, there were no reports in the literature of DBS directly affecting lactation.

Out of a potential of 277 clinical trials for the secondary objective, 135 trials on DBS met criteria (**Figure 1**). In clinical trials offering DBS lead implantation across all conditions, 68% (N = 92) excluded actively pregnant subjects, 22% (N = 29) excluded breastfeeding individuals, and 44% (N = 59) excluded persons of childbearing age intending to conceive within the coming years and/or individuals not on "adequate" contraception. Details on which contraceptive methods were deemed adequate were not specified in the exclusion criteria. Trials examining DBS for MDD were most likely to exclude the populations of interest (91%). The trial indication least likely to exclude this population was dystonia (41%) (**Table 2**).

Discussion

Though our literature search for our primary objective to describe patients with DBS and pregnancy returned 681 potential articles, only eight met inclusion criteria for analysis. Data from these 8 reports of 29 pregnancies and 31 infants suggested reasonable safety profile for DBS in pregnancy. The 1 preterm birth (1 of 29 pregnancies, 4%) seems unlikely to be related to the DBS intervention since the expected rate of preterm birth in the general population would be approximately 10–12% (Walani, 2020). Discomfort at the battery site occurred

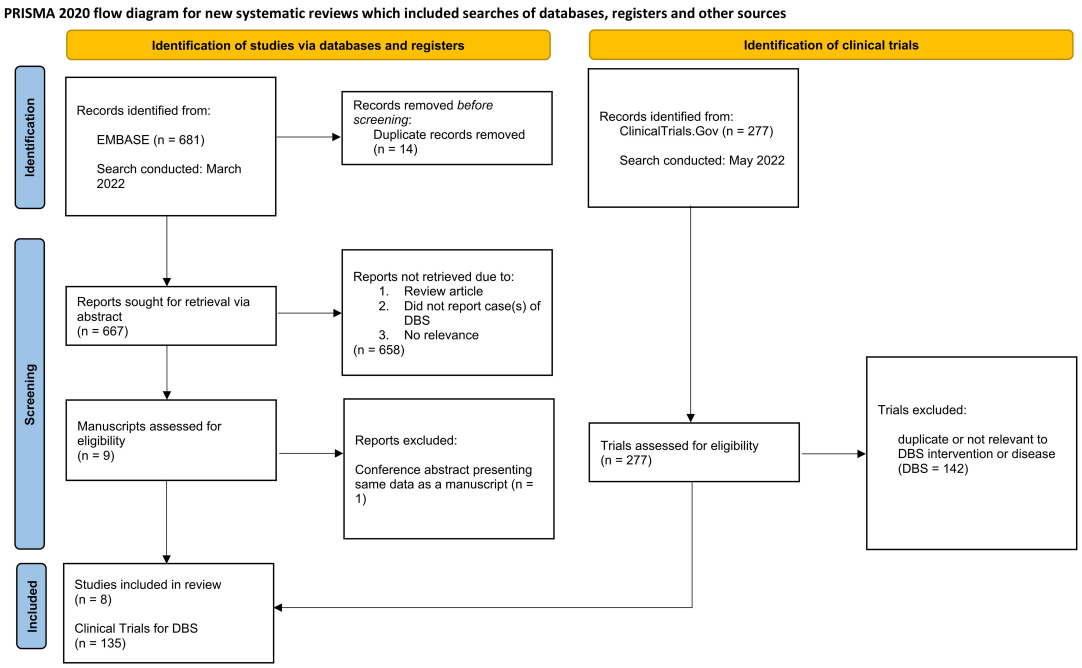

FIGURE 1
PRISMA 2020 flow diagram for systematic reviews detailing collection of data from EMBASE **(left)** and clinicaltrials.gov **(right)**.

TABLE 1 Deep brain stimulation (DBS) literature review data.

Study (Author)	Subjects (*N*)	Infants (N)	Conditions* (N, %)	Target structure (N, %)	Pregnancy complications (N)	Follow-up (months)
Scelzo et al., 2015	11[a,b]	13	PD (3), TS (2), OCD (1), dystonia (5)	Bilateral Gpi (8), STN (3)	Stimulator site discomfort (2)	24
Bóné et al., 2021	2	2	Epilepsy	ANT		40.5
Ziman et al., 2016	6[a]	7	Dystonia	Bilateral Gpi	PTD at 35 weeks (1) + stimulator site discomfort (1)	50.8
Ozturk and Kadiroğulları, 2022	1	1	Dystonia	Bilateral Gpi		N/a
Paluzzi et al., 2006	3[b]	4	Dystonia	Bilateral Gpi		N/a
Park et al., 2017	1	1	Dystonia	Bilateral Gpi		36
House et al., 2021	2	2	Epilepsy	ANT		15
Lefaucheur et al., 2015	1	1	Dystonia	Bilateral Gpi		N/a
Total	27	31[c]	PD (3, 11%), TS (2, 7%), OCD (1, 4%), dystonia (17, 63%), epilepsy (4, 15%)	Bilateral GPi (20, 74%), STN (3, 11%), ANT (4, 15%)		Average (months) = 33.26

The table displays the results of the literature review for DBS in pregnancy, outlining the number of subjects/infants, conditions, target structures, and pregnancy complications for each of the included studies.
*PD, Parkinson's disease; TS, Tourette's syndrome; OCD, obsessive-compulsive disorder; GPi, globus pallidus internus; STN, subthalamic nucleus; SAB, spontaneous abortion; ANT, anterior nucleus of thalamus; PTD, preterm delivery, [a]n = 1 subject became pregnant twice in this cohort, [b]n = 1 subject had a twin pregnancy in this cohort, [c]n = 1/31 fetus was spontaneously aborted in the first trimester determined to be unrelated to DBS.

in three pregnancies (10%) and may be a risk given the physiologic body changes related to pregnancy. Aside from the abdominal site, the nature of discomfort experienced by the patients with pulse generators in the subclavicular region is curious. This may suggest migration of the DBS pulse generator in response to pregnancy related body habitus changes. BMI

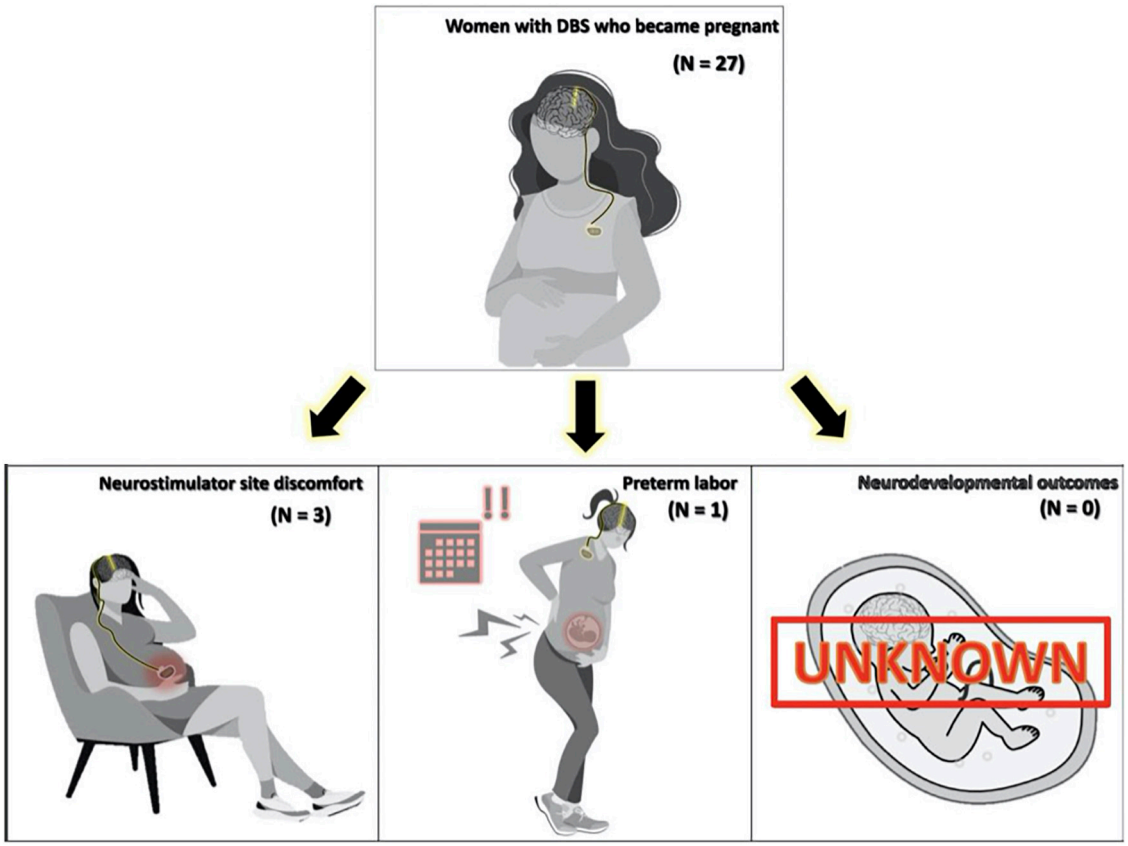

FIGURE 2
Figure displaying side effect profile found in a comprehensive literature review of pregnancy and Deep brain stimulation (DBS).

TABLE 2 Clinical trials review data.

	Condition	Included trials	Excludes pregnancy	Excludes POCBA*	Excludes breastfeeding
DBS					
	Pain	10	8 (80%)	6 (60%)	4 (40%)
	Dystonia	34	14 (41%)	4 (21%)	7 (21%)
	Tourette's	11	7 (64%)	3 (27%)	4 (36%)
	Epilepsy	15	11 (73%)	10 (67%)	2 (20%)
	Depression	35	32 (91%)	25 (71%)	6 (17%)
	Total (DBS)	**135**	**92 (68%)**	**59 (44%)**	**29 (22%)**

The table details the exclusion of various populations from clinical trials by modality of neuromodulation and the condition of interest for each trial.
*Persons of childbearing age (POCBA) planning to conceive or not on "adequate" contraception.

was not discussed in the studies reporting neurostimulator site discomfort. All 27 patients had DBS leads implanted prior to pregnancy with no reported fertility issues across a variety of subcortical targets.

The explicit exclusion of pregnant individuals from 68% of interventional trials involving DBS is somewhat problematic. It is a legitimate concern to proceed with caution when there are questions whether there is adequate equipoise for including this vulnerable population given the paucity of data. Based on our review, there were no trials, including observational, specifically designed to study the safety or efficacy of DBS in the pregnant population. This impairs the ability to determine whether DBS could be a reasonable and effective intervention in pregnancy. Nevertheless, our data are reassuring that there are no clear significant safety signals as of yet. Importantly, there are data from other treatments demonstrating relative safety and effectiveness of interventions that use electrical stimulation, such as

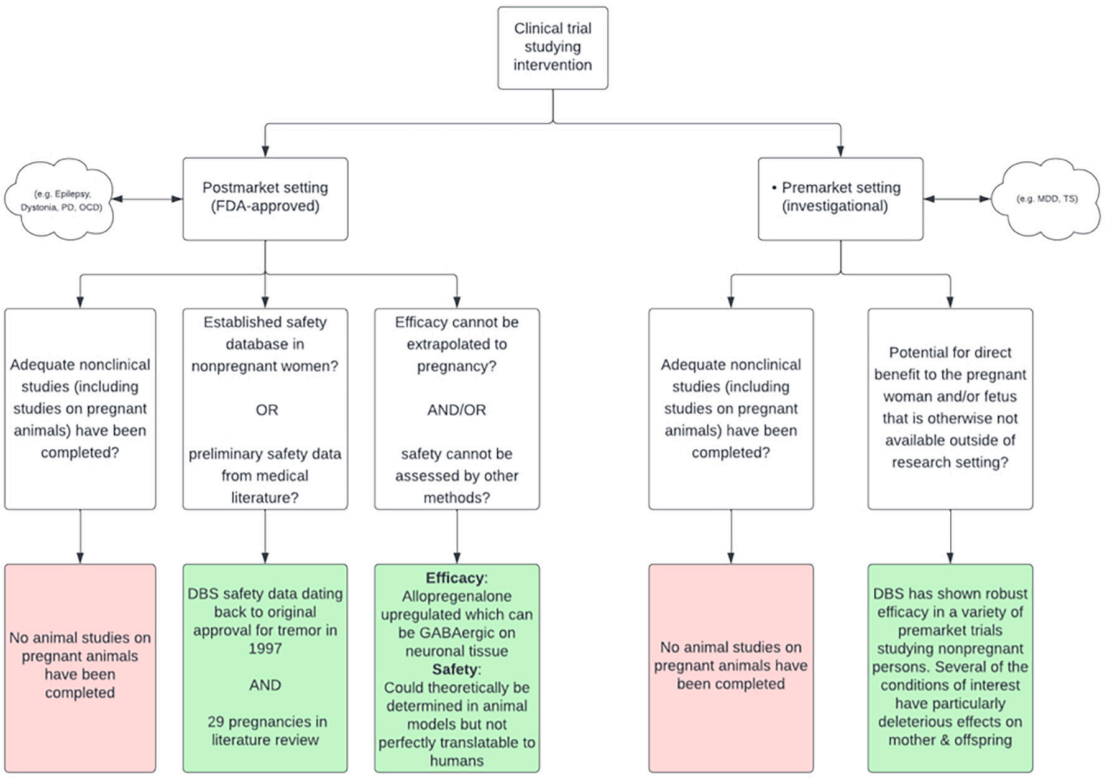

Research, C. for D.E. and (2020) *Pregnant Women: Scientific and Ethical Considerations for Inclusion in Clinical Trials, U.S. Food and Drug Administration*. FDA. Available at: https://www.fda.gov/regulatory-information/search-fda-guidance-documents/pregnant-women-scientific-and-ethical-considerations-inclusion-clinical-trials (Accessed: 30 June 2022).

FIGURE 3
Flow diagram describing 2018 draft by FDA on the inclusion of pregnant persons in clinical trials. PD, Parkinson's disease; OCD, obsessive-compulsive disorder; MDD, major depressive disorder; TS, Tourette's syndrome.

cardioversion for arrhythmias and electroconvulsive therapy (ECT) in pregnancy (Yonkers et al., 2009; Enriquez et al., 2014). Interestingly, when reviewing the clinical trials for DBS in MDD, very specific inclusion criteria were utilized such that the pregnant and post-partum populations, of which there is a significant incidence and prevalence, were excluded One possible explanation for this could be the attempt to limit confounding variables given the historically variable response after DBS in the already very specific treatment resistant depression population.

It is unlikely that experience with DBS in only 29 pregnancies is sufficient to offer guidance on DBS and pregnancy. For pharmacotherapeutics, the Food and Drug Administration (FDA) typically requires data from clinical trials adequately powered before offering clinical guidance. Because DBS trials are designed to treat a specific indication, the only way to learn whether DBS should be a treatment option in pregnancy is to include (not exclude) pregnancy in treatment trials for those indications. This is consistent with the FDA's stance on research and pregnancy. In 2018 the FDA issued a draft of a guidance communicating there were high exclusion rates of pregnant persons in clinical trials (Center for Drug Evaluation and Research, 2020). Guidance documents can be used to communicate regulatory hurdles and suggestions for industry to navigate the hurdles. This draft was revised in 2019, and has since seen no activity in revisions or suggestions. Specific medical devices were not mentioned in this document, which focused on pharmacologic agents. In the guidance, a framework was proposed by the FDA for inclusion of pregnant individuals in trials studying pharmacologic agents, which perhaps could be modeled to guide medical device trials in pregnancy. The FDA suggested the inclusion of pregnant individuals in clinical trials is ethically justifiable under specific criteria. These criteria, which differ slightly if the clinical trial is classified as pre- or post-market, are outlined in **Figure 3**.

There are several important issues to consider regarding potential for adverse effects of DBS in pregnancy. There are no animal models studying the safety of DBS in pregnancy and lactation or the effects of DBS on fertility. The first criterion for both pre-market and post-market studies from the FDA's draft for the inclusion of pregnant individuals

in clinical trials thus has not been met. Furthermore, the mechanism of action of DBS is not fully delineated, making it difficult to anticipate potential downstream effects on the reproductive cycle (Herrington et al., 2016). There is a paucity of evidence that DBS may affect second messengers involved with reproductive physiology. For example, DBS of the nucleus accumbens (not a target structure in any study in our review) has been shown to result in shifts in prolactin and cortisol levels (de Koning et al., 2013, 2016). Another DBS target with potential reproductive consequences is the hypothalamus. DBS targeting the lateral hypothalamic nuclei has been used to treat obesity, cluster headache, generalized anxiety disorder, and post-traumatic stress-disorder (May, 2008; Franco et al., 2018; Li et al., 2022). There is potential for off-target stimulation of other hypothalamic nuclei. These off target effects could theoretically impact fertility, pregnancy, and lactation. Finally, pregnancy induces the production of a large amount of allopregnanolone, a steroid hormone with gamma aminobutyric acid (GABA)-ergic effects on the central nervous system. Given higher levels of GABA-like activity during pregnancy, pregnant individuals may theoretically require pregnancy-specific stimulation settings to successfully achieve a therapeutic effect (Kim et al., 2011).

When considering these issues, it may be helpful to examine the status of ECT in pregnancy as it is relevant to the discussion about DBS. ECT has been approved for use in pregnancy and there is little ongoing debate regarding its safety in this population. No animal model studies were provided to support the use of ECT in pregnancy. This safety determination was made jointly by amassing case reports in 1994, and the American College of Obstetricians and Gynecologists (ACOG) and the American Psychiatric Association confirmed the evidence in 2009 (Miller, 1994; Yonkers et al., 2009). A review by Rose et al found four meta-analyses studying ECT, three of which found similar numbers of cases in the literature of over 300 (Rose et al., 2020). The most recent (fourth) meta-analysis in 2014 removed cases before 1975, which marked the transition to modern ECT anesthesia away from the insulin coma. This eliminated confounding adverse effects, and yielded only 76 cases (Pompili et al., 2014). This process could serve as a framework for determining the safety of neuromodulation in pregnant or lactating individuals. We encourage obstetricians, neurologists, psychiatrists, and neurosurgeons to continue publishing more cases of DBS in pregnancy to strengthen the body of evidence.

The results of this comprehensive review should be interpreted with caution. Included studies were retrospective case reports or case series. Heterogeneity of cases, sample size, limited follow up, outcome reporting bias, and publication bias could all have impacted the results. Additionally, the reported neonatal and infant outcome metrics were inconsistently reported. The data collected on child neurodevelopment was heterogenous, with some data collected up to 108 months and other studies failing to report any follow-up. Follow-up data, when available, varied from gross assessments to more specific milestone assessments conducted specifically by pediatricians. Further studies would be strengthened by uniform and detailed protocol assessments of neurodevelopmental progress. Nevertheless, the risk to the individual or fetus remains theoretical as the literature does not demonstrate evidence of harm beyond average obstetric risk. It is not theoretically feasible for electrical current from DBS stimulation to reach the uterus or developing fetus. There is little evidence to support the hypothetical risk of target stimulation leading to direct downstream effects on pregnancy, lactation, or fertility, similar to the use of ECT. The current clinical data for DBS in pregnancy are largely reassuring, demonstrate no clear adverse safety signals, and the sample size is large enough to justify inclusion of pregnant patients in well-designed clinical trials. Performing such trials is critically important to facilitate understanding of whether DBS has a role as an intervention in pregnancy and in reproductive age-patients. Without such studies, pregnant patients could be denied potentially effective treatment for serious conditions, which themselves could adversely impact obstetric and pediatric outcomes. Taking the complication rate of 12.9% in our cohort treated with DBS becomes particularly poignant when compared to, for example, a cohort of pregnant patients with dystonia without DBS experienced complications during pregnancy or delivery at a 45.26% rate (San Luciano et al., 2019). It is thus an imperative to find an inclusive set of criterion that allow for the access of a the latest treatment modalities to those most vulnerable.

Conclusion

The data from 29 pregnancies in 27 subjects suggest that DBS during pregnancy does not have a high perinatal complication profile. The most common reported concern was device discomfort, which should be considered when planning device placement in individuals considering pregnancy. Many but not all clinical trials exclude pregnant individuals and the documentation of safety in larger numbers of subjects may make more clinical trials available for pregnant individuals in the future. Increasing the number of pregnancy-related publications will clarify the safety profile for individuals with DBS interested in becoming pregnant and those who may find out they are pregnant following DBS implantation. Though the safety profile is emerging, the still small number of cases has hampered regulatory agencies from offering clear guidance on safety and on inclusion of this population in clinical trials. It will be interesting to observe whether the guidance will be similar to that for ECT. A roadmap guiding investigators toward safe neuromodulation in pregnant and lactating individuals will be of utmost importance, as DBS

continues to expand indications, and other neuromodulation techniques gain popularity (e.g., transcranial magnetic stimulation and transcranial direct current stimulation).

Data availability statement

The raw data supporting the conclusion of this article will be made available by the authors, without undue reservation.

Author contributions

CK and TP contributed to drafting the manuscript and data extraction. CK, TP, KR-R, AR-Z, JS, MO, and JW contributed to analysis and interpretation of the data in their respective expertise. AR-Z, KR-R, JS, MO, and JW critically revised the manuscript. All authors approved the manuscript as submitted.

Funding

JW's was supported by NIH R25NS108939. MO's was supported by: NIH R01 NR014852, R01NS096008, UH3NS119844, and U01NS119562 and also received the PI of the NIH R25NS108939 training grant.

Conflict of interest

MO serves as Medical Advisor the Parkinson's Foundation, and had received research grants from NIH, Parkinson's Foundation, the Michael J. Fox Foundation, the Parkinson Alliance, Smallwood Foundation, the Bachmann-Strauss Foundation, the Tourette Syndrome Association, and the UF Foundation. MO's research was supported by: NIH R01 NR014852, R01NS096008, UH3NS119844, and U01NS119562. MO had received royalties for publications with Demos, Manson, Amazon, Smashwords, Books4Patients, Perseus, Robert Rose, Oxford and Cambridge (movement disorders books). MO was an associate editor for New England Journal of Medicine Journal Watch Neurology and JAMA Neurology, and also participated in CME and educational activities (past 12–24 months) on movement disorders sponsored by WebMD/Medscape, RMEI Medical Education, American Academy of Neurology, Movement Disorders Society, and by Vanderbilt University. The institution and not MO receives grants from Medtronic, Abbvie, Boston Scientific, Abbott and Allergan, and the PI has no financial interest in these grants. MO had participated as a site PI and/or co-I for several NIH, foundation, and industry sponsored trials over the years but has not received honoraria. Research projects at the University of Florida receive device and drug donations.

The remaining authors declare that the research was conducted in the absence of any commercial or financial relationships that could be construed as a potential conflict of interest.

Publisher's note

Supplementary material

The Supplementary Material for this article can be found online at: https://www.frontiersin.org/articles/10.3389/fnhum.2022.997552/full#supplementary-material

References

Artama, M., Auvinen, A., Raudaskoski, T., Isojärvi, I., and Isojärvi, J. (2005). Antiepileptic drug use of women with epilepsy and congenital malformations in offspring. *Neurology* 64, 1874–1878. doi: 10.1212/01.WNL.0000163771.96962.1F

Battino, D., and Tomson, T. (2007). Management of epilepsy during pregnancy. *Drugs* 67, 2727–2746. doi: 10.2165/00003495-200767180-00007

Bóné, B., Kovács, N., Balás, I., Horváth, R. A., Dóczi, T., and Janszky, J. (2021). Pregnancy and deep brain stimulation therapy for epilepsy. *Epilept. Disord.* 23, 633–638. doi: 10.1684/epd.2021.1304

CDC (2022). *NVSS - Birth Data*. Available online at: https://www.cdc.gov/nchs/nvss/births.htm (accessed June 13, 2022).

Center for Drug Evaluation and Research (2020). *Pregnant women: Scientific and ethical considerations for inclusion in clinical trials, U.S. Food and Drug Administration*. FDA. Available online at: https://www.fda.gov/regulatory-information/search-fda-guidance-documents/pregnant-women-scientific-and-ethical-considerations-inclusion-clinical-trials (accessed June 30, 2022).

Chan, J., Natekar, A., Einarson, A., and Koren, G. (2014). Risks of untreated depression in pregnancy. *Can. Fam. Physician* 60, 242–243.

de Koning, P. P., Figee, M., Endert, E., Storosum, J. G., Fliers, E., and Denys, D. (2013). Deep brain stimulation for obsessive–compulsive disorder is associated with cortisol changes. *Psychoneuroendocrinology* 38, 1455–1459. doi: 10.1016/j.psyneuen.2012.12.006

de Koning, P. P., Figee, M., Endert, E., van den Munckhof, P., Schuurman, P. R., and Storosum, J. G. (2016). Rapid effects of deep brain stimulation reactivation on symptoms and neuroendocrine parameters in obsessive-compulsive disorder. *Transl. Psychiatry* 6:e722. doi: 10.1038/tp.2015.222

Denison, T., and Morrell, M. J. (2022). Neuromodulation in 2035: The neurology future forecasting series. *Neurology* 98, 65–72.

Enriquez, A. D., Economy, K. E., and Tedrow, U. B. (2014). Contemporary management of arrhythmias during pregnancy. *Circulation* 7, 961–967. doi: 10.1161/CIRCEP.114.001517

Franco, R. R., Fonoff, E. T., Alvarenga, P. G., Alho, E. J. L., Lopes, A. C., Hoexter, M. Q., et al. (2018). Assessment of safety and outcome of lateral hypothalamic deep brain stimulation for obesity in a small series of patients with prader-willi syndrome. *JAMA Netw. Open* 1:e185275. doi: 10.1001/jamanetworkopen.2018.5275

Harmsen, I. E., Elias, G. J. B., Beyn, M. E., Boutet, A., Pancholi, A., Germann, J., et al. (2020). Clinical trials for deep brain stimulation: Current state of affairs. *Brain Stimul.* 13, 378–385. doi: 10.1016/j.brs.2019.11.008

Herrington, T. M., Cheng, J. J., and Eskandar, E. N. (2016). Mechanisms of deep brain stimulation. *J. Neurophysiol.* 115, 19–38. doi: 10.1152/jn.00281.2015

House, P. M., Herzer, A., Lorenzi, I., Niedernhöfer, P., Voges, B., Stodieck, S., et al. (2021). Deep brain stimulation (DBS) of anterior nucleus thalami (ANT) in female epilepsy patients during pregnancy and delivery: Experience from two cases. *Epilept. Disord. Int. Epilepsy J. Videotape* 23, 933–936. doi: 10.1684/epd.2021.1330

Kim, D. R., Epperson, N., Paré, E., Gonzalez, J. M., Parry, S., Thase, M. E., et al. (2011). An open label pilot study of transcranial magnetic stimulation for pregnant women with major depressive disorder. *J. Womens Health (2002)* 20, 255–261. doi: 10.1089/jwh.2010.2353

Kobau, R., Zahran, H., Thurman, D. J., Zack, M. M., Henry, T. R., Schachter, S. C., et al. (2008). Epilepsy surveillance among adults–19 States, Behavioral Risk Factor Surveillance System, 2005. *MMWR Surveill. Summ.* 57, 1–20.

Lefaucheur, R., Derrey, S., Borden, A., Verspyck, E., Tourrel, F., and Maltête, D. (2015). Patient with perinatal brain injury dystonia treated by deep brain stimulation: Management during pregnancy. *Rev. Neurol.* 171, 90–91. doi: 10.1016/j.neurol.2014.08.005

Li, H.-T., Donegan, D. C., Peleg-Raibstein, D., and Burdakov, D. (2022). Hypothalamic deep brain stimulation as a strategy to manage anxiety disorders. *Proc. Natl. Acad. Sci. U.S.A.* 119:e2113518119. doi: 10.1073/pnas.2113518119

Louis, E. D., and Dogu, O. (2008). Does age of onset in essential tremor have a bimodal distribution? Data from a tertiary referral setting and a population-based study. *Neuroepidemiology* 29, 208–212. doi: 10.1159/000111584

May, A. (2008). Hypothalamic deep-brain stimulation: Target and potential mechanism for the treatment of cluster headache. *Cephalalgia* 28, 799–803. doi: 10.1111/j.1468-2982.2008.01629.x

Miller, L. J. (1994). Use of electroconvulsive therapy during pregnancy. *Hosp. Commun. Psychiatry* 45, 444–450. doi: 10.1176/ps.45.5.444

Ozturk, G., and Kadiroğulları, P. (2022). Management of pregnancy and childbirth in a cervical dystonia patient with an implanted deep brain stimulation system: A case report. *Ann. Indian Acad. Neurol.* 25, 121–123. doi: 10.4103/aian.AIAN_151_21

Page, M. J., McKenzie, J. E., Bossuyt, P. M., Boutron, I., Hoffmann, T. C., Mulrow, C. D., et al. (2021). The PRISMA 2020 statement: An updated guideline for reporting systematic reviews. *BMJ* 372:n71.

Paluzzi, A., Bain, P. G., Liu, X., Yianni, J., Kumarendran, K., and Aziz, T. Z. (2006). Pregnancy in dystonic women with in situ deep brain stimulators. *Mov. Disord.* 21, 695–698. doi: 10.1002/mds.20777

Park, H. R., Lee, J. M., Park, H., Shin, C. W., Kim, H. J., Park, H. P., et al. (2017). Pregnancy and delivery in a generalized dystonia patient treated with internal globus pallidal deep brain stimulation: A case report. *J. Korean Med. Sci.* 32, 155–159. doi: 10.3346/jkms.2017.32.1.155

Pompili, M., Dominici, G., Giordano, G., Longo, L., Serafini, G., Lester, D., et al. (2014). Electroconvulsive treatment during pregnancy: A systematic review. *Expert Rev. Neurother.* 14, 1377–1390. doi: 10.1586/14737175.2014.972373

Rose, S., Dotters-Katz, S. K., and Kuller, J. A. (2020). Electroconvulsive therapy in pregnancy: Safety, best practices, and barriers to care. *Obstet. Gynecol. Surv.* 75, 199–203. doi: 10.1097/OGX.0000000000000763

San Luciano, M., Shanker, V., Bressman, S., Raymond, D., and Saunders-Pullman, R. (2019). Pregnancy and delivery complications in women with inherited isolated dystonia [abstract]. *Mov. Disord.* 34(Suppl. 2).

Sazgar, M. (2019). Treatment of women with epilepsy. *Continuum (Minneapolis, Minn.)* 25, 408–430. doi: 10.1212/CON.0000000000000713

Scelzo, E., Mehrkens, J. H., Bötzel, K., Krack, P., Mendes, A., Chabardès, S., et al. (2015). Deep brain stimulation during pregnancy and delivery: Experience from a series of "DBS Babies". *Front. Neurol.* 6:191. doi: 10.3389/fneur.2015.00191

Scherer, R. W., and Saldanha, I. J. (2019). How should systematic reviewers handle conference abstracts? A view from the trenches. *Syst. Rev.* 8:264. doi: 10.1186/s13643-019-1188-0

Schrag, A., and Schott, J. M. (2006). Epidemiological, clinical, and genetic characteristics of early-onset parkinsonism. *Lancet Neurol.* 5, 355–363. doi: 10.1016/S1474-4422(06)70411-2

Van Niel, M. S., and Payne, J. L. (2020). Perinatal depression: A review. *Cleve. Clin. J. Med.* 87, 273–277. doi: 10.3949/ccjm.87a.19054

Vitturi, B. K., Cabral, F. B., and Cukiert, C. M. (2019). Outcomes of pregnant women with refractory epilepsy. *Seizure Eur. J. Epilepsy* 69, 251–257. doi: 10.1016/j.seizure.2019.05.009

Walani, S. R. (2020). Global burden of preterm birth. *Int. J. Gynaecol. Obstet.* 150, 31–33. doi: 10.1002/ijgo.13195

Yonkers, K. A., Wisner, K. L., Stewart, D. E., Oberlander, T. F., Dell, D. L., Stotland, N., et al. (2009). The management of depression during pregnancy: A report from the American Psychiatric Association and the American College of Obstetricians and Gynecologists. *Obstet. Gynecol.* 114, 703–713. doi: 10.1097/AOG.0b013e3181ba0632

Ziman, N., Coleman, R. R., Starr, P. A., Volz, M., Marks, W. J. Jr., Walker, H. C., et al. (2016). Pregnancy in a series of dystonia patients treated with deep brain stimulation: Outcomes and management recommendations. *Stereotact. Funct. Neurosurg.* 94, 60–65. doi: 10.1159/000444266

frontiers | Frontiers in Human Neuroscience

TYPE Original Research
PUBLISHED 19 October 2022
DOI 10.3389/fnhum.2022.1016379

OPEN ACCESS

EDITED BY
Joshua K. Wong,
University of Florida, United States

REVIEWED BY
Jackson N. Cagle,
University of Florida, United States
Stephanie Cernera,
University of California, San Francisco, United States

*CORRESPONDENCE
Wayne K. Goodman
Wayne.Goodman@bcm.edu

SPECIALTY SECTION
This article was submitted to Brain Imaging and Stimulation, a section of the journal Frontiers in Human Neuroscience

RECEIVED 10 August 2022
ACCEPTED 03 October 2022
PUBLISHED 19 October 2022

CITATION
Alarie ME, Provenza NR, Avendano-Ortega M, McKay SA, Waite AS, Mathura RK, Herron JA, Sheth SA, Borton DA and Goodman WK (2022) Artifact characterization and mitigation techniques during concurrent sensing and stimulation using bidirectional deep brain stimulation platforms. *Front. Hum. Neurosci.* 16:1016379. doi: 10.3389/fnhum.2022.1016379

Artifact characterization and mitigation techniques during concurrent sensing and stimulation using bidirectional deep brain stimulation platforms

Michaela E. Alarie[1], Nicole R. Provenza[2], Michelle Avendano-Ortega[3], Sarah A. McKay[3], Ayan S. Waite[1], Raissa K. Mathura[2], Jeffrey A. Herron[4], Sameer A. Sheth[2], David A. Borton[1,5] and Wayne K. Goodman[3]*

[1]Brown University School of Engineering, Providence, RI, United States, [2]Department of Neurosurgery, Baylor College of Medicine, Houston, TX, United States, [3]Menninger Department of Psychiatry and Behavioral Sciences, Baylor College of Medicine, Houston, TX, United States, [4]Department of Neurological Surgery, University of Washington, Seattle, WA, United States, [5]Department of Veterans Affairs, Center for Neurorestoration and Neurotechnology, Rehabilitation R&D Service, Providence, RI, United States

Bidirectional deep brain stimulation (DBS) platforms have enabled a surge in hours of recordings in naturalistic environments, allowing further insight into neurological and psychiatric disease states. However, high amplitude, high frequency stimulation generates artifacts that contaminate neural signals and hinder our ability to interpret the data. This is especially true in psychiatric disorders, for which high amplitude stimulation is commonly applied to deep brain structures where the native neural activity is miniscule in comparison. Here, we characterized artifact sources in recordings from a bidirectional DBS platform, the Medtronic Summit RC + S, with the goal of optimizing recording configurations to improve signal to noise ratio (SNR). Data were collected from three subjects in a clinical trial of DBS for obsessive-compulsive disorder. Stimulation was provided bilaterally to the ventral capsule/ventral striatum (VC/VS) using two independent implantable neurostimulators. We first manipulated DBS amplitude within safe limits (2–5.3 mA) to characterize the impact of stimulation artifacts on neural recordings. We found that high amplitude stimulation produces slew overflow, defined as exceeding the rate of change that the analog to digital converter can accurately measure. Overflow led to expanded spectral distortion of the stimulation artifact, with a six fold increase in the bandwidth of the 150.6 Hz stimulation artifact from 147–153 to 140–180 Hz. By increasing sense blank values during high amplitude stimulation, we reduced overflow by as much as 30% and improved artifact distortion, reducing the bandwidth from 140–180 Hz artifact to 147–153 Hz. We also identified artifacts that shifted in frequency through modulation of telemetry parameters. We found that telemetry ratio changes led to predictable shifts in the center-frequencies of the associated artifacts,

allowing us to proactively shift the artifacts outside of our frequency range of interest. Overall, the artifact characterization methods and results described here enable increased data interpretability and unconstrained biomarker exploration using data collected from bidirectional DBS devices.

KEYWORDS

deep brain stimulation, implantable devices, artifact characterization, bidirectional platforms, neuromodulation

Introduction

The recent expansion of deep brain stimulation (DBS) technologies has enabled unique opportunities to record intracranial neural activity during concurrent stimulation (Stanslaski et al., 2012; Gilron et al., 2021). One example of such an implantable neural stimulator (INS) is the Medtronic Summit RC + S (Herron et al., 2018; Stanslaski et al., 2018). The Summit RC + S has been used extensively to record neural activity in patients with neuropsychiatric disorders, enabling insights into DBS impact on symptom states (Johnson et al., 2021; Provenza et al., 2021). Not only do bidirectional systems provide opportunities for biomarker exploration in ecologically valid environments, a prerequisite for adaptive DBS, but they also allow us to better understand the underlying pathophysiology of neurological and psychiatric disorders (Gregg et al., 2021; Johnson et al., 2021; Pal Attia et al., 2021; Provenza et al., 2021). However, the artifacts introduced by high amplitude, high frequency stimulation present a challenge for analysis and interpretation of the relatively lower amplitude neural signals that we aim to measure (Zhou et al., 2018; Dastin-van Rijn et al., 2021). Therefore, it is important to identify potential artifact sources introduced by stimulation, developing techniques to mitigate these artifacts during data collection.

Previous studies have recommended optimal sense configurations for neural data collected during concurrent stimulation across several indications and stimulation targets (Ansó et al., 2022). Optimal configurations include sensing in a bipolar configuration where two contacts flank the monopolar stimulation channel, using active recharge, and blanking the amplifier during the stimulation pulse (Stanslaski et al., 2018). Additional recommendations revolve around wireless data transmission settings specific to the Summit RC + S: telemetry mode and telemetry ratio (Stanslaski et al., 2018). Telemetry mode determines the distance required between the INS and communication telemetry module to minimize data loss. Greater telemetry modes allow for increased data transmission at the expense of decreased telemetry range. Similarly, telemetry ratio values describe the proportion of uplink to downlink transmission timelines between the INS and tablet. Higher ratio values lead to slower transitions from uplink to downlink transmission, spending more time transmitting data from the INS before receiving instructions from the computer. Lower ratio values should be considered in implementation of "distributed" closed loop stimulation to decrease latency between symptom onset and stimulation changes (Herron et al., 2018).

Despite this guidance regarding the proper configuration of the Summit RC + S to collect neural data, stimulation and system-related artifacts can remain a significant problem, particularly when the SNR is very small. Furthermore, most of these artifact mitigation strategies have focused on movement disorders (e.g., Parkinson's disease and essential tremor) applications, for which neural activity in the DBS target region is relatively large (20–100 μVrms) and DBS amplitude is relatively small (less than 2 mA) (Koeglsperger et al., 2019; Ansó et al., 2022). For example, DBS for psychiatric disorders including OCD employ high amplitude (4.5–6 mA) stimulations to the VC/VS, whereas the amplitude of target neural features are reported between 1–20 μVrms (Provenza et al., 2021; Adkinson et al., 2022; Ansó et al., 2022). The injection of high amplitude stimulation leads to a decrease in SNR, making biomarker detection more difficult (Kopell et al., 2004; Greenberg et al., 2006; Ramasubbu et al., 2018). This injection of stimulation artifact, specifically at high stimulation amplitudes, can lead to "slew overflow," a form of signal distortion that occurs at the analog to digital converter (ADC), where the time-voltage signal changes too rapidly for the ADC to properly resolve the signal.

Here, we have characterized common artifacts that appear in response to high amplitude, high frequency stimulation for OCD. Specifically, we report data from a clinical trial for developing adaptive DBS in OCD using the Medtronic Summit RC + S (NCT04806516). First, we characterize stimulation artifact distortion due to slew overflow. Next, we identify low frequency artifacts (below the 150 Hz stimulation artifact) modulated by communication parameters. Lastly, we provide recommendations for sensing and telemetry configurations to optimize data quality, hence allowing for biomarker exploration in the entire frequency spectrum.

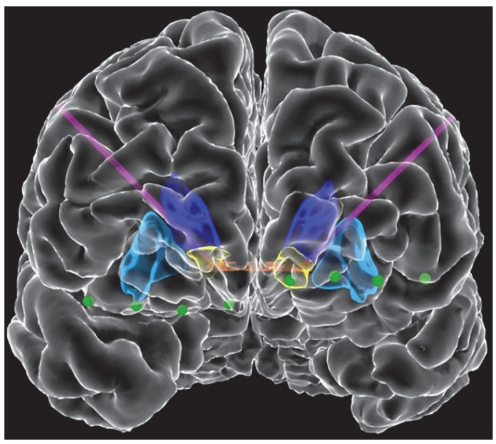

FIGURE 1
Front view of view of the reconstructed cortical surface and subcortical structures. Schematic includes DBS leads (purple) and electrocorticography contacts (green). Colored regions indicate the anterior commissure (orange), caudate (dark blue), putamen (light blue), and VS (yellow).

Materials and methods

Study participants and design

Three patients with medically refractory OCD were implanted with the Medtronic Summit RC + S as part of an IRB and IDE approved study. DBS leads were placed bilaterally in either ventral capsule/ventral striatum (VC/VS; **Figure 1**) or bed nucleus of the stria terminalis (BNST). Electrocorticography (ECoG) strips were also placed bilaterally in the orbitofrontal cortex (OFC; **Figure 1**), a brain region implicated in OCD symptoms of inflexibility and dysfunction of reward processing (Goodman et al., 2021). Analysis in this paper specifically highlights artifact characterization performed in P2, with a comprehensive list of artifacts and stimulation parameters for each participant listed in **Table 1**. Further, we include impedance measurements recorded from P2 in **Table 2**.

Stimulation of the VC/VS (or BNST; P3) was performed to treat OCD symptoms, using monopolar stimulation. Per optimal configurations previously described, we used active recharge and sensed in a bipolar configuration where two contacts flanked the monopolar stimulation channel (Stanslaski et al., 2018). Neural recordings were obtained from bilateral DBS electrodes targeted to VC/VS (or BNST; P3). Recordings were bipolar, such that recording contacts in each hemisphere (contact pair 0–2) flanked the monopolar stimulation contact (contact 1). The fourth contact (contact 3) was unused. Two bipolar recording channels were also obtained from the two pairs of contacts (contact pairs 8–9 and 10–11) on both ECoG strips. The DBS electrode (Medtronic Model 3387) and 4-contact flexible ECoG paddle (Medtronic Model 5387A) in each hemisphere were connected to an implantable neural stimulator (INS), such that each DBS electrode was connected to an independent INS (de Hemptinne et al., 2021). In total, there were three bipolar recording channels per hemisphere, one sensing VC/VS activity, and two sensing OFC activity.

Sending and transmitting neural signals

Recordings were performed at a sampling rate of 500 Hz with a high pass filter of 0.85 Hz. The low-pass filter stage 1 and 2 cutoff frequencies were both set to 100 Hz. Bidirectional communication between the INS and tablet is facilitated by the clinician telemetry module (CTM). Time-series voltage data collected onboard the device is assembled into packets and transmitted from the INS to a tablet via the Bluetooth connection established by the CTM. Similarly, stimulation parameter changes are sent from the tablet to the INS via the same CTM connection. The CTM facilitates either uplink (i.e., data sent from the INS to the tablet) or downlink transmission (i.e., data sent from the tablet to the INS), where transitioning from one direction to the other is referred to as the telemetry "ratio." Higher ratio values indicate that more time is spent transmitting packets of data from the INS before instructions are sent from the tablet to the INS. Lower ratio values reduce the time spent transmitting packets before sending a tablet instruction, leading to a faster rate of change between data collected and instructions relayed.

Telemetry "mode" is also a configurable parameter, which is related to the range in distance allowed between the CTM and INS. A greater telemetry mode requires a shorter range in distance but enables maximum data transmission rates. For this study, telemetry mode was set to the maximum value of 4.

Neural data analysis

Neural data analyses were performed offline, based on previous methods employed using the RC + S platform (Gilron et al., 2021; Provenza et al., 2021). LFP data were divided into 10-s segments. Any 10-s segments containing packet loss were excluded from analysis. Power spectral density estimates were calculated using pwelch in MATLAB. The mean of the entire recording was subtracted from each 10-s window to account for DC offset. A Hamming window was employed to divide each 10-s segment into 500-ms segments with 250 ms of overlap.

Stimulation amplitude modulation testing

Amplitude testing was performed to gain insight into how high (4.5–6 mA) vs. low (less than 2 mA) amplitude stimulation

TABLE 1 DBS surgery targets, stimulation contact, therapeutic stimulation amplitude and telemetry settings for each participant.

Participant	P1		P2		P3	
Stimulation target	VC/VS	VC/VS	VC/VS	VC/VS	BNST	BNST
Stimulation contact	1-/C +	1-/C +	1-/C +	1-/C +	2-/C +	1-/C +
Therapeutic stimulation amplitude	5 mA	5 mA	5.3 mA	5.5 mA	4 mA	4.5 mA
Telemetry ratio	32	32	32	32	32	32
Identified stimulation artifact distortion pre-sense blank change?	Yes	Yes	Yes	Yes	N/A	N/A
Existing modulation artifacts?	Yes	Yes	No	Yes	Yes	No
Location of modulation artifacts (Hz)	27, 54, 97, 124	27, 54, 97, 124	N/A	27, 54, 97, 124	27, 124	N/A

Stimulation artifact distortion was identified at default sense blank settings. Specific locations of modulation artifacts were identified when applicable.

TABLE 2 Impedances recorded on left and right hemispheres from P2 within 1 month of testing.

Hemisphere	Left						Right					
Contact pair	0–1 +	0–2 +	0–3 +	1–2 +	1–3 +	2–3 +	0–1 +	0–2 +	0–3 +	1–2 +	1–3 +	2–3 +
Impedance value (Ohms)	1,628	2,330	2,560	2,008	2,280	2,913	1,968	2,838	2,878	1,983	2,123	2,765

impacts the quality of neural recordings. Initially, stimulation amplitudes were set to 5 and 5.3 mA for the right and left hemispheres, respectively. Amplitude changes were made in each hemisphere independently, while holding the amplitude of the opposite hemisphere constant. For example, amplitude in the left hemisphere was kept constant at 5.3 mA while amplitudes in the right hemisphere were decreased in 0.5–0.8 mA increments. Once 2 mA was reached, amplitude was then increased in 0.5–0.8 mA increments. Neural data was recorded for 1 min at each increment. In total, there were 2 min of recordings at each amplitude increment in each hemisphere. The 2–5.3 mA range was used to represent therapeutic amplitudes used in both movement disorders (∼2 mA) and psychiatric disorders (over 4.5 mA). We focus specifically on contact pair 0–2 recordings (VC/VS; P2) due to their proximity to the stimulating contact. Prior to completing testing, each hemisphere was set back to the initial therapeutic stimulation parameter settings.

Measuring slew overflow

We quantified the percentage of neural data packets affected by slew overflow to understand the impact of high amplitude stimulation on our low amplitude recordings. Slew overflow specifically refers to when the slew rate, or the maximum rate of change over time, exceeds that measurable by the ADC. Slew overflow occurs when the stimulation amplitude is very high, such as in the case of psychiatric disorders where DBS amplitudes typically exceed 5 mA. Increasing the stimulation amplitude leads to larger rates of change in amplitude over time (larger delta). Increasing stimulation frequency also increases rate of change over time by producing more pulses per second and effectively decreasing the amount time permitted to reach the same stimulation amplitude. Therefore, surpassing the maximum delta permissible by the ADC limits its capacity to properly resolve the input signal, leading to distortion.

The Summit RC + S platform stores data in 11 JSON files, where data is transmitted as individual packets throughout a recording (Sellers et al., 2021). One of the JSON files represents the raw time domain data, where each packet contains a field called *DebugInfo*. This field indicates if slew overflow is occurring within an individual packet via a numeric value. The value refers to a binary representation (via 4 bits), indicating the sensing channel(s) for which overflow is occurring. A value of 0 indicates that there is no overflow occurring on any of the contacts for the duration of that packet whereas a value of 1 (binary representation 0001) indicates slew overflow on the first sensing channel. A value of 8 (binary representation 1000) indicates slew overflow on channel 3. Finally, when overflow is indicated on multiple channels, the *DebugInfo* field contains values above 3. For example, slew overflow on channels zero (binary representation 0001) and three (binary representation 1000) would result in binary representation 1001. This would present a numeric value "9" in the *DebugInfo* field, indicating both channel 0 and channel 3 have overflow.

Sense blank testing

We conducted sense blank testing to observe the impact of increased sense blank time on measured slew overflow. Sense blank time represents the time sensing is suspended during the stimulation pulse, measured between when the stimulation pulse is sent and the recording resumes (Hammer et al., 2022). The minimum sense blank value is automatically set based on pulse width, and the maximum is limited to 2.5 ms to minimize loss of meaningful data. During testing, sense blank

changes were made to both hemispheres simultaneously while maintaining a constant stimulation amplitude of 5 mA. Five sense blank values were tested: 0.755, 1.001, 1.5, 2, and 2.5 ms. We specifically focus on impacts of sense blank on VC/VS recordings (contact pair 0–2), recording for 1 min at each sense blank setting.

Modulation of low frequency artifacts and impacts from ratio changes

After identifying four consistent, focal spectral peaks in the 0–125 Hz during amplitude and sense blank testing, we analyzed impacts of stimulation frequency changes on artifact location. Specifically, we aimed to understand if these artifacts were aliases of the stimulation artifact at 150.6 Hz. We tested three different stimulation frequencies, 50, 100, and 149.3 Hz, recording for 1 min at each frequency.

To further characterize these artifacts, we tested the impact of telemetry ratio on artifact frequency. Telemetry ratio values can be configured within a range of 1–32. Prior to the artifact mitigation work described here, all recordings in this study were conducted using the maximum possible ratio value (32) to maximize the amount of data sent to the tablet during open loop DBS. Telemetry parameters were modified on both INS' simultaneously, such that data from both hemispheres was always recorded using the same ratio at any point in time. Recordings were captured for the entire 1–32 ratio range. Each recording lasted 30 s (16 min of data total).

Results

Increasing stimulation amplitude leads to distortion of stimulation artifact

We performed amplitude testing to understand the impact of high amplitude stimulation on the quality of neural recordings. Specifically, we conducted testing in the 2–5.3 mA range on both the left and right hemispheres, changing the amplitude in one hemisphere while keeping the amplitude in the contralateral hemisphere constant. At lower amplitudes, the left hemisphere artifact is localized to 150.6 Hz with small side lobes (**Figure 2A**). Further, the harmonic at ∼199 Hz is relatively small in amplitude. Increasing stimulation amplitude by ∼0.5 mA increments led to increased distortion of the stimulation artifact, producing a wider artifact bandwidth and larger side lobes. Increasing beyond 3.8 mA, the side lobes begin to subside as the artifact at 150.6 Hz becomes one large and unlocalized curve. For example, the frequency range of the localized stimulation artifact at 2 mA is ∼147–153 Hz. At the maximum amplitude of 5.3 mA, the bandwidth of the artifact itself increased by about sixfold to ∼140–180 Hz. Amplitude increases in the right hemisphere show a similar pattern where greater amplitudes lead to more stimulation artifact distortion (**Figure 2B**). Specifically, as amplitude is increased past ∼3.5 mA, side lobes dissipate as the stimulation artifact bandwidth increases (∼147–153 to 140–180 Hz). Contrastingly, amplitude testing in the right hemisphere showed distortion at all amplitudes, containing large side lobes around the stimulation artifact at 2 mA.

Increasing sense blank times reduces slew overflow and artifact distortion

To mitigate slew overflow in our neural recordings, we performed sense blank testing in the 0.755–2.5 ms range on both hemispheres, simultaneously (**Figures 2C,D**). Initially, a sense blank value of 0.755 ms demonstrated 60 and 80% overflow in the left and right hemispheres, respectively. This percentage represents the percent of overall packets during which overflow occurred. Increasing sense blank time led to mild decreases in overflow percentage in the left hemisphere (**Figure 2C**), with the lowest percentage being ∼40% overflow at a sense blank time of 2 ms. The right hemisphere (**Figure 2D**) showed larger changes in percent overflow, decreasing to ∼30% at 2.5 ms. The dashed red line in **Figures 2C,D** shows that amplitude was constant throughout this testing, ensuring overflow changes were not due to amplitude changes.

Next, we assessed how sense blank changes impacted artifact distortion (**Figures 2E,F**). We observed that increasing sense blank time led to decreases in peak power (dB) of both stimulation artifact (150.6 Hz) and harmonic artifact (199 Hz) in the left and right hemispheres. Further, increases in sense blank time led to decreases in stimulation artifact distortion. At a sense blank of 0.755 ms, peak (dB) of side lobes were approximately −70 to −60 dB and −60 to −50 dB on the left and right hemispheres, respectively. As sense blank increased from 0.755 to 2.5 ms stimulation artifact side lobes decreased in amplitude, leaving the artifact at 150.6 Hz with a localized bandwidth of 147–153 Hz.

Increasing amplitude increases low-frequency artifact amplitude

Throughout amplitude and sense blank testing, we observed four artifacts in the 0–125 Hz range localized at 27, 54, 97, and 124 Hz. We observed that amplitude increases led to larger artifact peaks at these frequencies (**Figure 3A**). From 2 to 3.5 mA, the artifacts at 54 and 97 Hz were not observed. Exceeding 3.5 mA, these two artifacts appear and increase in amplitude with each incremental ∼0.5 mA amplitude increase. Increasing sense blank time from 0.755 to 2.5 ms reduced stimulation artifact distortion, revealing a fourth

artifact at 124 Hz (**Figure 3B**). However, the sense blank changes themselves appear to have no impact on the artifact or the frequency it resides in.

Stimulation frequency changes demonstrate no impact on lower-frequency artifacts

To ensure the lower-frequency artifacts were not aliases of the stimulation artifact at 150.6 Hz, we altered stimulation frequency (**Figures 3C–E**). This testing was performed with the original sense blank value of 0.755 ms. Decreasing from 150.6 to 149.3 Hz showed no change in artifacts at 27 and 54 Hz, although 97 Hz was no longer apparent (**Figure 3C**). Similarly, decreasing frequency to 100 Hz still produced the artifact at 27 Hz (**Figure 3D**). The last frequency tested was 50 Hz, where no artifacts were distinguishable (**Figure 3E**). While the artifact at 54 Hz in **Figure 3D** and 27 Hz in **Figure 3E** are not as easily distinguishable due to the presence of stimulation artifact spectral lobes, some aspects of them remain (boxed in red). Therefore, it appears that stimulation artifact distortion due to slew overflow covered the 54 Hz artifact, reflecting similar mechanisms to those demonstrated with the 124 Hz artifact in **Figure 3B**. These do not seem to be the result of aliasing because stimulation changes result in no change to the artifact at 27 Hz. Although we tested a stimulation frequency of 100 Hz, it is clear the artifact at 54 Hz is not an alias since the expected alias would be at 50 Hz rather than 54 Hz. Overall, stimulation frequency changes have no impact on the frequency location of these lower-frequency artifacts.

Telemetry ratio changes shift lower-frequency artifacts

We next tested impacts of telemetry ratio changes on data quality, where we specifically report analysis from ratios 2, 6, 8, 10, 18, 26, and 32 on each hemisphere. Ratio had minimal impact on left hemisphere recordings, where no lower-frequency artifacts were observed (**Figure 3F**). Although changing ratio occasionally demonstrated decreases in stimulation artifact peak (dB) in the left hemisphere, these changes did not seem to be related to ratio increases or decreases. Contrastingly, ratio changes in the right hemisphere appeared to shift the center frequency of the lower-frequency artifacts (**Figure 3G**). As the ratio increases past a ratio of 2, two artifacts appear around roughly 60 and 90 Hz. From ratio 6 to 8, the center frequencies of the artifacts seem to move toward each other and cross paths as ratio increases. Exceeding ratio values of 10, the artifacts appear to diverge. Once a ratio of 32 is reached, two additional artifacts appear. At the final ratio tested of 32 two additional artifacts appear, making four in total: 27, 54, 97, and 124 Hz.

Amplitude, sense blank, and frequency testing shows modulation artifacts across subjects

Finally, we extensively analyzed two additional participants (P1 and P3) for both stimulation artifact distortion and lower-frequency, ratio modulated artifacts that we previously described. Results of this analysis are in **Table 1**, where we include information in each hemisphere on: stimulation target, stimulation contact, therapeutic amplitude of stimulation, telemetry mode and ratio, the presence of stimulation artifact distortion, pre-sense blank changes, and the appearance of lower-frequency artifacts. We define these lower-frequency artifacts as "modulation artifacts," as their center-frequency is modulated by ratio changes. In P1, we found stimulation artifact distortion in both hemispheres resulting from slew overflow. Stimulation artifact distortion pre-sense blank increases are not present in data collected from P3, as this was a later implanted patient in which sense blank mitigation strategies had already been implemented. We also assessed the presence of modulation artifacts in P1 and P3. In P1, we identified all four artifacts in the 0–125 Hz range on both hemispheres. For P3, we identified two artifacts at 27 and 124 Hz in the left hemisphere only.

Discussion

Evaluating and successfully mitigating all sources of artifact in neural data sensed from chronically implanted leads is a challenging task. This work builds upon our previous work on the removal of high amplitude stimulation artifacts from neural data collected onboard sensing-capable DBS devices (Dastin-van Rijn et al., 2021; Chen et al., 2022). In this study, our goal was to better understand the impact of high amplitude, high frequency stimulation on VC/VS recordings collected from bidirectional DBS platforms. The VC/VS local field potential (LFP) activity has lower peak-to-peak amplitude compared to other DBS targets used to treat movement disorders (such as STN and GPi), exacerbating already poor SNR during high amplitude stimulation. This lower peak-to-peak amplitude is common in white matter targets, which are increasingly being explored for psychiatric indications (Riva-Posse et al., 2014; Liebrand et al., 2019; Zhu et al., 2021). In this work, we characterized two previously undocumented types of artifacts in VC/VS LFP data collected in humans implanted with chronic, sensing-enabled DBS devices. We demonstrated that high amplitude stimulation leads to slew overflow and stimulation artifact distortion. Further, we discovered the presence of lower-frequency artifacts,

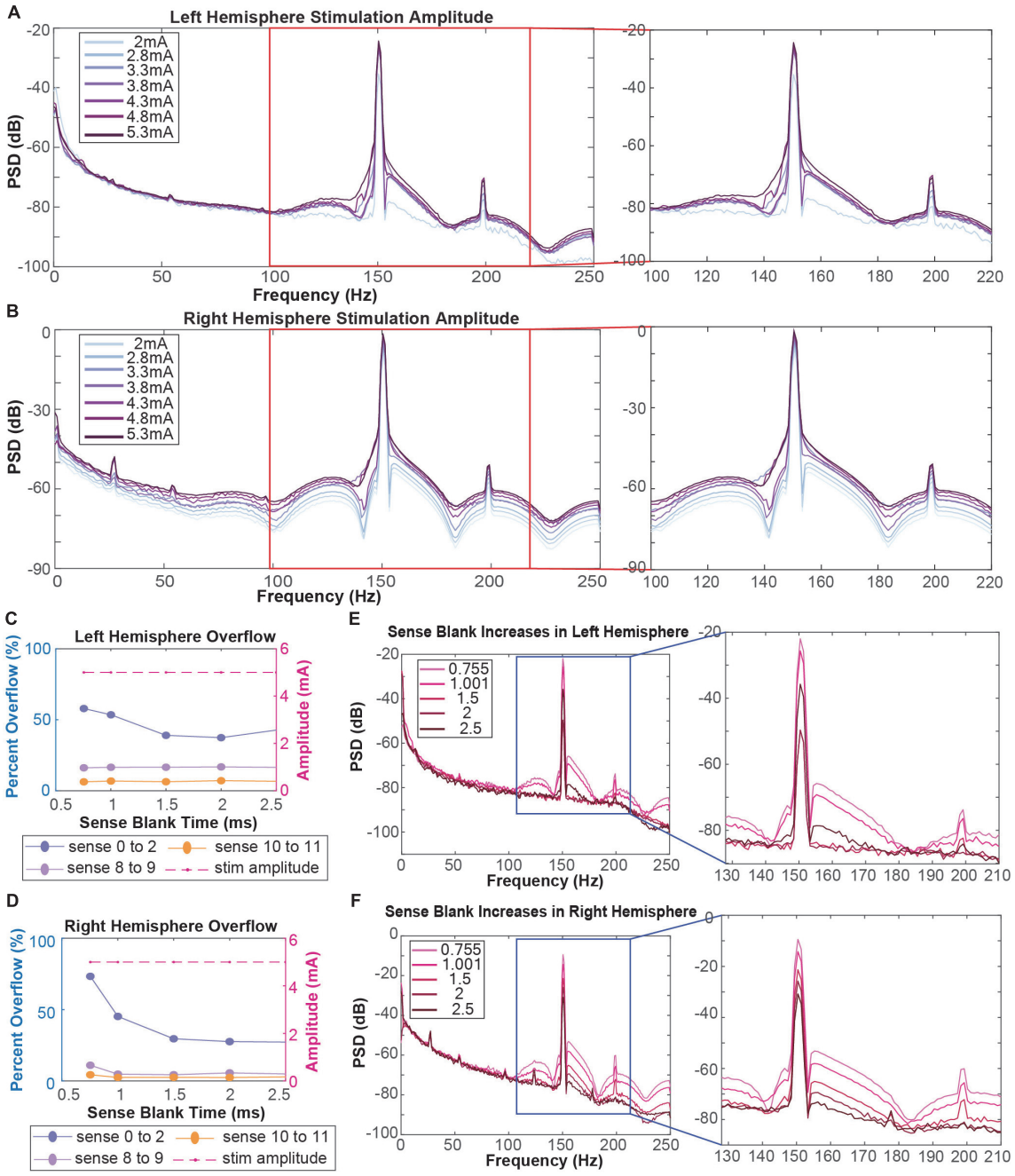

FIGURE 2
(A,B) Amplitude testing in the left **(A)** and right **(B)** hemispheres shows that increased amplitude leads to increased artifact distortion. Red boxes refer to stimulation artifacts and harmonics in the 130–220 Hz range. **(C,D)** Calculation of percentage of data packets with slew overflow in the left **(C)** and right **(D)** hemispheres at each sense blank value. Dotted purple lines represent data recorded in the ventral striatum. Dotted pink and orange lines represent data recorded in the orbitofrontal cortex. Dashed red line represents the stimulation amplitude at each sense blank value. **(E,F)** Sense blank impacts on left **(E)** and right **(F)** hemisphere spectral data. Blue boxes refer to stimulation artifacts and harmonics in the 130–210 Hz range.

termed "modulation artifacts," that responded to adjusting data transmission parameters.

We first evaluated the utility of sense blanking for mitigating stimulation artifact distortion and slew overflow. Stimulation was configured for this study using active recharge, where a negative pulse is actively delivered to tissue to quickly balance the charge at the implanted electrodes. Comparatively, passive recharge relies on the post-stimulation accumulated charge at

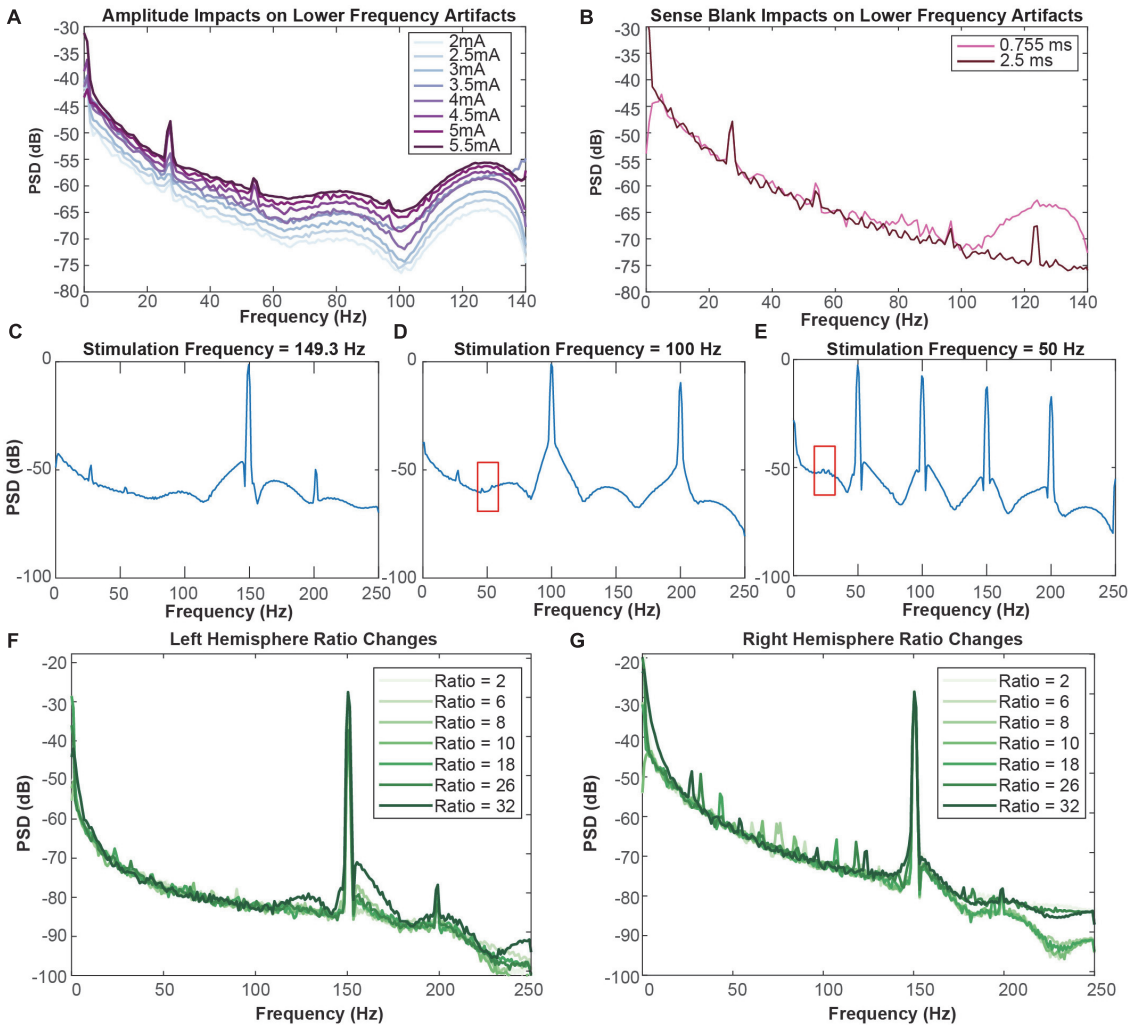

FIGURE 3

(A) Impact of amplitude increases on lower-frequency artifacts in the right hemisphere. The minimum amplitude tested was 2 mA (lightest) and the maximum amplitude tested was 5.5 mA (darkest). **(B)** Impact of sense blank increases on lower-frequency artifacts in the right hemisphere. The minimum sense blank tested was 0.755 ms (pink), and the maximum sense blank tested was 2.5 ms (dark pink). **(C)** 149.3 Hz, **(D)** 100 Hz, and **(E)** 50 Hz frequency testing to observe impacts on lower-frequency artifacts in the right hemisphere. Red boxes from C and E indicate areas where blockage of modulation artifacts occur due to slew overflow. **(F,G)** Representation of ratio change impacts on spectral plots (dB) across frequency (Hz). Ratio changes in the left **(F)** and right **(G)** hemispheres vary from 2 (lightest) to 32 (darkest). Blue arrows in **(G)** represent direction of artifact movement as ratio value is increased.

the electrode interface dissipating over time. While passive recharge was not tested in this study, it is possible that use of passive recharge would result in lower slew overflow events due to the lack of a secondary negative pulse and smaller change in charge over time as measured by the ADC. Future work should assess the potential trade-off presented by active vs. passive recharge, since the use of active recharge is promoted as a means of mitigating stimulation artifact by reducing the duration of the pulse. Overall, we found that increasing sense blank duration dramatically improved the integrity of the sensing data by reducing spectral side lobes and reducing the occurrence of logged slew overflow errors. Percentage of slew overflow and how it is represented in the neural data seemed to vary greatly, even within subject. However, it appears that certain sense blank values reflect a threshold for overflow to be represented in the neural data. Sense blank values at or exceeding 2 ms appear to minimize impacts of slew overflow on the neural data. Even though slew overflow was not observed to the same degree at these sense blank values, slew overflow was still measured at ∼40 and ∼30% for the left and right hemispheres, respectively. We recommend increasing sense blank duration to minimize stimulation artifact distortion; however, it is important to consider the tradeoff between sense blank duration and data distortion. As sense blank duration

increases, the amplifier is blanked for a greater percentage of the recording. When the amplifier is blanked, the analog front end of the Summit is disconnected. Although data itself is not lost, new data points are not effectively measured during the period of sense blanking, resulting in an artifact at the frequency of stimulation. Therefore, researchers should select the minimum sense blank duration required for adequate sensing performance to minimize data distortion. The amount of distortion would be estimated by multiplying the blanking time duration by the stimulation frequency. As an example, the maximum sense blank time permissible by the Summit RC + S is 2.5 ms, which if used with 150 Hz stimulation would result in a 37.5% data distortion due to blanking time. After calculating this percentage of data loss, it was confirmed with the Medtronic engineering team as being an accurate estimate of the system behavior during blanking. It should be noted however that this data loss is not always evident in the collected data, as transient activity in analog components of the temporarily disconnected analog front end of the Summit result in time-varying samples continuing to be collected throughout the blanking period.

We also observed and documented the presence of modulation artifacts that are unrelated to stimulation artifact distortion or previously documented artifacts. However, we observed that the center-frequency of the four modulation artifacts predictably shifted when adjusting telemetry ratio. Additionally, we observed that decreases in stimulation amplitude led to decreases in the peak of each individual modulation artifact (**Figure 3A**). Therefore, it appears that high amplitude stimulation in low peak-to-peak neural data results in lower SNR that manifests as artifacts such as the modulation artifacts observed here. It should be noted here that DBS OFF conditions were not tested. The clinical team did not support this testing due to lack of tolerability in patients when decreasing stimulation amplitude. To mitigate modulation artifacts caused by telemetry parameters, researchers can potentially adjust the telemetry ratio and mode such that artifact peaks are outside particular bands of interest. For example, to detect biomarkers in the 0–40 Hz range, a ratio value of 10 would place modulation artifacts above 50 Hz, outside of the frequency bands of interest. However, given the observed number of peaks at frequencies which are independently variable based on selected mode and ratio, this may prove to be a challenge in some protocols. Researchers interested in analyzing broad spectral bands may find that they must adjust their classifier designs to account for the presence of these artifacts. Splitting a larger frequency band into smaller sub-bands may be problematic if using the embedded linear discriminant classifier onboard the Summit RC + S that can only use a maximum of four configured power bands. Another concern is the case of adaptive PC-in-the-loop based stimulation experiments, where the telemetry mode and ratio parameters impact the round-trip time for sensing data and commands between the PC and INS. For example, if there is an identified biomarker that changes rather rapidly in time it would be important for ratio values to be as small as possible to allow more frequent updating of stimulation parameters as symptom state evolves over time. In this context, adjusting the mode and ratio to mitigate the artifacts described in this paper may result in reduced performance of the system. Overall, these findings demonstrate the value of configurable parameters within bidirectional DBS platforms, that previously were not expected to improve the quality of neural data or closed-loop system performance.

Given the proprietary nature of Summit RC + S hardware implementation, it is unclear how these modulation artifacts emerged. It is possible that the low peak-to-peak amplitude of native neural activity in VC/VS increases the likelihood that artifacts will be introduced due to the already low SNR compared to other gray matter DBS targets. As we previously discussed, increasing stimulation amplitude worsens SNR and exacerbates the modulation artifacts. As indicated in **Table 1**, we observed modulation artifacts and stimulation artifact distortion to varying extents across subjects and hemispheres that cannot be explained by differences in hardware or surgical procedures. The factors driving these differences are unclear and may be due to inherent device variability during high amplitude, high frequency stimulation. In future studies, stimulation artifact distortion and modulation artifacts should be explored in a larger cohort across multiple DBS target regions, as these artifacts are patient- and target-specific. We also emphasize that future device manufacturing needs to consider how artifacts present in different ranges of brain tissue, as current knowledge is mainly geared toward gray matter targets compared to quieter, white matter regions of the brain. Another mechanism that might be attributed to the artifacts observed in this paper is the relationship between impedance changes and poor common-mode rejection. Future studies should explore common-mode rejection and how it relates data quality, with specific consideration for slew overflow and modulation artifacts. Poor common-mode rejection can occur when sensing contacts have a mismatched electrode impedance (Stanslaski et al., 2012; Tiruvadi et al., 2022). Acceptable ranges of impedance mismatch across sensing electrodes are currently ill-defined and it is unclear how minute changes in impedance impact neural data, which calls for future work analyzing the degree to which these mismatches exacerbate stimulation artifact distortion at high amplitudes. Finally, while we examined modulation artifacts and stimulation artifacts independently, we do not fully understand any potential interactions between the two, calling for future studies on these potential relationships.

Distinguishing the artifacts described in this paper from possible neural signals of interest was in many ways only possible due to the sheer configurability of the Summit system. This may be difficult in future, less configurable systems to definitively determine the nature of a potential artifact. One example is Medtronic's Percept PC, a commercialized sensing-enabled device, where configuring sense blank values is not

possible and kept at constant values. Additionally, telemetry configurations of mode and ratio are non-configurable in the Percept PC platform, resulting in potential artifacts that cannot be tracked down the same way presented here. The key takeaway is that when interpreting results from neural data, researchers should take special note of all configurable and non-configurable parameters prior to making conclusionary ties between neural signatures and behavioral outcomes, and device manufacturers should consider enabling configuration of all parameters that are known to impact neural sensing data collection.

In recent years there has been great progress in identifying and mitigating sources of artifact in neural data collected onboard sensing-capable DBS devices. When interpreting neural data or designing adaptive algorithms, it is important to better understand all potential sources of artifact that contaminate neural signals onboard bidirectional DBS platforms. Beyond the stimulation artifact distortion and modulation artifacts described in this work, it is important for researchers to also be aware of additional sources of artifact, including stimulation (Dastin-van Rijn et al., 2021; Chen et al., 2022), electrocardiogram (Neumann et al., 2021), and body movement (Thenaisie et al., 2021; van Rheede et al., 2022). While some of these artifacts may be generalizable, many may only appear in certain contexts that are device, patient, or target specific. This work represents another step in the creation of a library of expected artifacts, which we hope to continue to expand upon as more artifacts are discovered.

Data availability statement

The raw data supporting the conclusions of this article will be made available by the authors, without undue reservation.

Ethics statement

The studies involving human participants were reviewed and approved by the Local Institutional Review Board at Baylor College of Medicine (H-40255 and H-44941 to Baylor College of Medicine, IAA 17–27 and IAA 19–51 to Brown University, and STUDY20110082 and STUDY20110084 to University of Pittsburgh) and the US Food and Drug Administration Center for Devices and Radiological Health. The patients/participants provided their written informed consent to participate in this study.

Author contributions

SS, DB, and WG conceived of the study. MA and NP conceptualized data analysis procedures and wrote the first draft of the manuscript. MA performed data analysis, interpreted data, and prepared figures and results with support from NP and JH. AW, MA-O, and SM performed data collection in the clinic. RM prepared the cortical reconstruction used in **Figure 1**. WG and SS performed clinical care aspects of the study. SS performed study surgical procedures. JH, NP, SS, DB, and WG oversaw collection of data, analysis, and manuscript completion. All authors contributed to the writing and revision of the manuscript.

Funding

This work was supported by NIH (1UH3NS100549-01) (WG and DB), the McNair Foundation (SS), and the National Science Foundation Graduate Research Fellowship (MA). This work was partially funded by U24NS113637 (JH and DB).

Acknowledgments

We thank the participants and their families for their involvement in the study. Additionally, we thank the Open Mind consortium for software resources and expert guidance (https://openmind-consortium.github.io/). Finally, we also thank Medtronic for donating Summit RC + S devices as part of the BRAIN Initiative Public-Private Partnership Program.

Conflict of interest

Medtronic donates devices as part of the NIH BRAIN Public-Private Partnership Program (WG and DB). SS was a consultant for Boston Scientific, Zimmer Biomet, and Neuropace. WG received royalties from Nview, LLC, and OCD scales, LLC for digitalized commercial use of the Y-BOCS.

The remaining authors declare that the research was conducted in the absence of any commercial or financial relationships that could be construed as a potential conflict of interest.

The handling editor JKW declared a past co-authorship with the several authors NP, WG and SS.

Publisher's note

References

Adkinson, J. A., Tsolaki, E., Sheth, S. A., Metzger, B. A., Robinson, M. E., Oswalt, D., et al. (2022). Imaging versus electrographic connectivity in human mood-related fronto-temporal networks. *Brain Stimul.* 15, 554–565. doi: 10.1016/j.brs.2022.03.002

Ansó, J., Benjaber, M., Parks, B., Parker, S., Oehrn, C. R., Petrucci, M., et al. (2022). Concurrent stimulation and sensing in bi-directional brain interfaces: A multi-site translational experience. *J. Neural Eng.* 19:026025. doi: 10.1088/1741-2552/ac59a3

Chen, P., Kim, T., Goodman, W. K., Borton, D. A., Harrison, M. T., and Darbon, J. (2022). Estimation of periodic signals with applications to deep brain stimulation. *bioRxiv* [Preprint]. doi: 10.1101/2022.05.23.493124

Dastin-van Rijn, E. M., Provenza, N. R., Calvert, J. S., Gilron, R., Allawala, A. B., Darie, R., et al. (2021). Uncovering biomarkers during therapeutic neuromodulation with PARRM: Period-based artifact reconstruction and removal method. *Cell Rep. Methods* 1:100010. doi: 10.1016/j.crmeth.2021.100010

de Hemptinne, C., Chen, W., Racine, C. A., Seritan, A. L., Miller, A. M., Yaroshinsky, M. S., et al. (2021). Prefrontal physiomarkers of anxiety and depression in Parkinson's disease. *Front. Neurosci.* 15:748165. doi: 10.3389/fnins.2021.748165

Gilron, R., Little, S., Perrone, R., Wilt, R., de Hemptinne, C., Yaroshinsky, M. S., et al. (2021). Long-term wireless streaming of neural recordings for circuit discovery and adaptive stimulation in individuals with Parkinson's disease. *Nat. Biotechnol.* 39, 1078–1085. doi: 10.1038/s41587-021-00897-5

Goodman, W. K., Storch, E. A., and Sheth, S. A. (2021). Harmonizing the Neurobiology and treatment of obsessive-compulsive disorder. *Am. J. Psychiatry* 178, 17–29.

Greenberg, B. D., Malone, D. A., Friehs, G. M., Rezai, A. R., Kubu, C. S., Malloy, P. F., et al. (2006). Three-year outcomes in deep brain stimulation for highly resistant obsessive–compulsive disorder. *Neuropsychopharmacology* 31, 2384–2393. doi: 10.1038/sj.npp.1301165

Gregg, N. M., Marks, V. S., Sladky, V., Lundstrom, B. N., Klassen, B., Messina, S. A., et al. (2021). Anterior nucleus of the thalamus seizure detection in ambulatory humans. *Epilepsia* 62, e158–e164. doi: 10.1111/epi.17047

Hammer, L. H., Kochanski, R. B., Starr, P. A., and Little, S. (2022). Artifact characterization and a multipurpose template-based offline removal solution for a sensing-enabled deep brain stimulation device. *Stereotact. Funct. Neurosurg.* 100, 168–183. doi: 10.1159/000521431

Herron, J., Stanslaski, S., Chouinard, T., Corey, R., Denison, T., and Orser, H. (2018). "Bi-directional brain interfacing instrumentation," in *Proceedings of the 2018 IEEE international instrumentation and measurement technology conference (I2MTC)* (Houston, TX: IEEE), 1–6.

Johnson, V., Wilt, R., Gilron, R., Anso, J., Perrone, R., Beudel, M., et al. (2021). Embedded adaptive deep brain stimulation for cervical dystonia controlled by motor cortex theta oscillations. *Exp. Neurol.* 345:113825. doi: 10.1016/j.expneurol.2021.113825

Koeglsperger, T., Palleis, C., Hell, F., Mehrkens, J. H., and Bötzel, K. (2019). Deep Brain stimulation programming for movement disorders: Current concepts and evidence-based strategies. *Front. Neurol.* 10:410. doi: 10.3389/fneur.2019.00410

Kopell, B. H., Greenberg, B., and Rezai, A. R. (2004). Deep brain stimulation for psychiatric disorders. *J. Clin. Neurophysiol.* 21, 51–67.

Liebrand, L. C., Caan, M. W. A., Schuurman, P. R., van den Munckhof, P., Figee, M., Denysad, D., et al. (2019). Individual white matter bundle trajectories are associated with deep brain stimulation response in obsessive-compulsive disorder. *Brain Stimul.* 12, 353–360. doi: 10.1016/j.brs.2018.11.014

Neumann, W.-J., Sorkhabi, M. M., Benjaber, M., Feldmann, L. K., Saryyeva, A., Krauss, J. K., et al. (2021). The sensitivity of ECG contamination to surgical implantation site in brain computer interfaces. *Brain Stimul.* 14, 1301–1306. doi: 10.1016/j.brs.2021.08.016

Pal Attia, T., Crepeau, D., Kremen, V., Nasseri, M., Guragain, H., Steele, S. W., et al. (2021). Epilepsy personal assistant device-a mobile platform for brain state, dense behavioral and physiology tracking and controlling adaptive stimulation. *Front. Neurol.* 12:704170. doi: 10.3389/fneur.2021.704170

Provenza, N. R., Sheth, S. A., Dastin-van Rijn, E. M., Mathura, R. K., Ding, Y., Vogt, G. S., et al. (2021). Long-term ecological assessment of intracranial electrophysiology synchronized to behavioral markers in obsessive-compulsive disorder. *Nat. Med.* 27, 2154–2164. doi: 10.1038/s41591-021-01550-z

Ramasubbu, R., Lang, S., and Kiss, Z. H. T. (2018). Dosing of Electrical parameters in deep brain stimulation (DBS) for intractable depression: A review of clinical studies. *Front. Psychiatry* 9:302. doi: 10.3389/fpsyt.2018.00302

Riva-Posse, P., Sueng Choi, K., Holtzheimer, P. E., McIntyre, C. C., Gross, R. E., Chaturvedi, A., et al. (2014). Defining critical white matter pathways mediating successful subcallosal cingulate deep brain stimulation for treatment-resistant depression. *Biol. Psychiatry* 76, 963–969. doi: 10.1016/j.biopsych.2014.03.029

Sellers, K. K., Gilron, R., Anso, J., Louie, K. H., Shirvalkar, P. R., Chang, E. F., et al. (2021). Analysis-rcs-data: Open-source toolbox for the ingestion, time-alignment, and visualization of sense and stimulation data from the medtronic summit RC+S system. *Front. Hum. Neurosci.* 15:714256. doi: 10.3389/fnhum.2021.714256

Stanslaski, S., Afshar, P., Cong, P., Giftakis, J., Stypulkowski, P., Carlson, D., et al. (2012). Design and validation of a fully implantable, chronic, closed-loop neuromodulation device with concurrent sensing and stimulation. *IEEE Trans. Neural Syst. Rehabil. Eng.* 20, 410–421. doi: 10.1109/TNSRE.2012.2183617

Stanslaski, S., Herron, J., Chouinard, T., Bourget, D., Isaacson, B., Kremen, V., et al. (2018). A chronically implantable neural coprocessor for investigating the treatment of neurological disorders. *IEEE Trans. Biomed. Circuits Syst.* 12, 1230–1245. doi: 10.1109/TBCAS.2018.2880148

Thenaisie, Y., Palmisano, C., Canessa, A., Keulen, B. J., Capetian, P., Jiménez, M. C., et al. (2021). Towards adaptive deep brain stimulation: Clinical and technical notes on a novel commercial device for chronic brain sensing. *J. Neural Eng.* 18:042002. doi: 10.1088/1741-2552/ac1d5b

Tiruvadi, V., James, S., Howell, B., Obatusin, M., Crowell, A., Riva-Posse, P., et al. (2022). Mitigating mismatch compression in differential local field potentials. *arXiv* [Preprint]. doi: 10.48550/arXiv.2204.03778

van Rheede, J. J., Feldmann, L. K., Busch, J. L., Fleming, J. E., Mathiopoulou, V., Denison, T., et al. (2022). Diurnal modulation of subthalamic beta oscillatory power in Parkinson's disease patients during deep brain stimulation. *Medrxiv* [Preprint]. doi: 10.1101/2022.02.09.22270606

Zhou, A., Johnson, B. C., and Muller, R. (2018). Toward true closed-loop neuromodulation: Artifact-free recording during stimulation. *Curr. Opin. Neurobiol.* 50, 119–127. doi: 10.1016/j.conb.2018.01.012

Zhu, Z., Hubbard, E., Guo, X., Barbosa, D. A. N., Popal, A. P., Cai, C., et al. (2021). A connectomic analysis of deep brain stimulation for treatment-resistant depression. *Brain Stimul.* 14, 1226–1233. doi: 10.1016/j.brs.2021.08.010

Frontiers in
Human Neuroscience

Bridges neuroscience and psychology to understand the human brain

The second most-cited journal in the field of psychology, that bridges research in psychology and neuroscience to advance our understanding of the human brain in both healthy and diseased states.

Discover the latest Research Topics

See more →

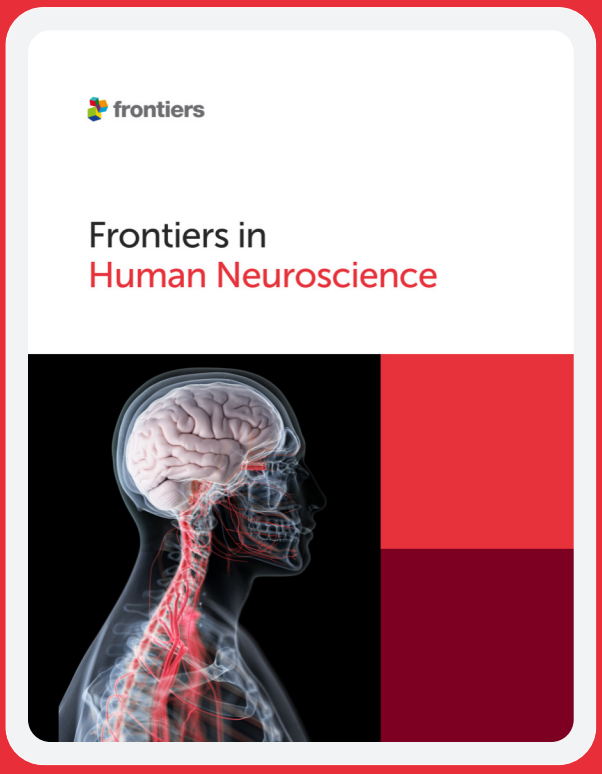

Frontiers

Avenue du Tribunal-Fédéral 34
1005 Lausanne, Switzerland
frontiersin.org

Contact us

+41 (0)21 510 17 00
frontiersin.org/about/contact